Tungsten Cemented Carbide

Comprehensive Exploration of Physical & Chemical Properties, Processes, & Applications (IX)

中钨智造科技有限公司

CTIA GROUP LTD

CTIA GROUP LTD

Global Leader in Intelligent Manufacturing for Tungsten, Molybdenum, and Rare Earth Industries

INTRODUCTION TO CTIA GROUP

CTIA GROUP LTD, a wholly-owned subsidiary with independent legal personality established by CHINATUNGSTEN ONLINE , is dedicated to promoting the intelligent, integrated, and flexible design and manufacturing of tungsten and molybdenum materials in the Industrial Internet era. CHINATUNGSTEN ONLINE, founded in 1997 with www.chinatungsten.com as its starting point—China's first top-tier tungsten products website—is the country's pioneering e-commerce company focusing on the tungsten, molybdenum, and rare earth industries. Leveraging nearly three decades of deep experience in the tungsten and molybdenum fields, CTIA GROUP inherits its parent company's exceptional design and manufacturing capabilities, superior services, and global business reputation, becoming a comprehensive application solution provider in the fields of tungsten chemicals, tungsten metals, cemented carbides, high-density alloys, molybdenum, and molybdenum alloys.

Over the past 30 years, CHINATUNGSTEN ONLINE has established more than 200 multilingual tungsten and molybdenum professional websites covering more than 20 languages, with over one million pages of news, prices, and market analysis related to tungsten, molybdenum, and rare earths. Since 2013, its WeChat official account "CHINATUNGSTEN ONLINE" has published over 40,000 pieces of information, serving nearly 100,000 followers and providing free information daily to hundreds of thousands of industry professionals worldwide. With cumulative visits to its website cluster and official account reaching billions of times, it has become a recognized global and authoritative information hub for the tungsten, molybdenum, and rare earth industries, providing 24/7 multilingual news, product performance, market prices, and market trend services.

Building on the technology and experience of CHINATUNGSTEN ONLINE, CTIA GROUP focuses on meeting the personalized needs of customers. Utilizing AI technology, it collaboratively designs and produces tungsten and molybdenum products with specific chemical compositions and physical properties (such as particle size, density, hardness, strength, dimensions, and tolerances) with customers. It offers full-process integrated services ranging from mold opening, trial production, to finishing, packaging, and logistics. Over the past 30 years, CHINATUNGSTEN ONLINE has provided R&D, design, and production services for over 500,000 types of tungsten and molybdenum products to more than 130,000 customers worldwide, laying the foundation for customized, flexible, and intelligent manufacturing. Relying on this foundation, CTIA GROUP further deepens the intelligent manufacturing and integrated innovation of tungsten and molybdenum materials in the Industrial Internet era.

Dr. Hanns and his team at CTIA GROUP, based on their more than 30 years of industry experience, have also written and publicly released knowledge, technology, tungsten price and market trend analysis related to tungsten, molybdenum, and rare earths, freely sharing it with the tungsten industry. Dr. Han, with over 30 years of experience since the 1990s in the e-commerce and international trade of tungsten and molybdenum products, as well as the design and manufacturing of cemented carbides and high-density alloys, is a renowned expert in tungsten and molybdenum products both domestically and internationally. Adhering to the principle of providing professional and high-quality information to the industry, CTIA GROUP's team continuously writes technical research papers, articles, and industry reports based on production practice and market customer needs, winning widespread praise in the industry. These achievements provide solid support for CTIA GROUP's technological innovation, product promotion, and industry exchanges, propelling it to become a leader in global tungsten and molybdenum product manufacturing and information services.

CTIA GROUP LTD

30 Years of Cemented Carbide Customization Experts

Core Advantages

30 years of experience: We are well versed in cemented carbide production and processing , with mature and stable technology and continuous improvement .

Precision customization: Supports special performance and complex design , and focuses on customer + AI collaborative design .

Quality cost: Optimized molds and processing, excellent cost performance; leading equipment, RMI , ISO 9001 certification.

Serving Customers

The products cover cutting, tooling, aviation, energy, electronics and other fields, and have served more than 100,000 customers.

Service Commitment

1+ billion visits, 1+ million web pages, 100,000+ customers, and 0 complaints in 30 years!

Contact Us

Email : sales@chinatungsten.com

Tel : +86 592 5129696

Official **website** : www.ctia.com.cn

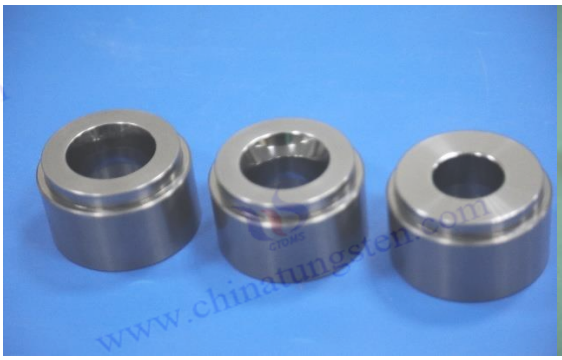

Part 3: Performance Optimization of Cemented Carbide

Chapter 9: Multifunctionalization of Cemented Carbide

The multifunctionality of cemented carbide can meet **the complex needs of** aerospace (lifespan > 10^4 hours ± 10^3 hours), electronic manufacturing (resistivity < 12 μΩ·cm ± 0.1 μΩ·cm) and intelligent equipment (response time < 1 ms ± 0.1 ms) by regulating conductivity, magnetism, wear resistance, corrosion resistance, self-lubrication and intelligent response capabilities. Traditional cemented carbide is known for its high hardness (HV 1800 ± 30) and wear resistance (wear rate < 0.06 $mm^3/N·m$ ± 0.01 $mm^3/ N·m$), but its conductivity (~10 MS/m ± 0.1 MS/m), magnetism (saturation magnetization intensity < 10 emu/g ± 0.5 emu/g) and adaptability are insufficient, which limits its application in multifunctional scenarios. Optimization needs to start from **the microstructure** (grain size 0.52 μm±0.01 μm), **composition control** (TiC 5%10%±0.1%, Ni 8%12%±0.1%) and **surface engineering** (texture depth 110 μm±0.1 μm) to achieve a synergistic improvement in performance.

discusses **the multifunctional path of cemented carbide** from the aspects **of (1) electrical conductivity and (2) magnetic regulation, (3) wear-resistant and corrosion-resistant conductive composite performance, (4) self-lubrication and anti-adhesion, and (5) bionic and intelligent cemented carbide** . Electrical conductivity and magnetic regulation are optimized by Co content (10%±1%) and Ni substitution; wear-resistant and corrosion-resistant conductive composite performance focuses on WCTiCNi system (hardness>HV 1600±30, corrosion rate<0.01 mm/year±0.001 mm/year); **self-lubrication and anti-adhesion** introduce MoS_2 (5%±0.1%) and **surface texture** (friction coefficient<0.2±0.01); **bionic and intelligent cemented carbide** draws on **gradient structure** (porosity 5%20%±1%) and **responsive materials** (deformation rate<0.1%±0.01%), and looks forward to intelligent applications. This chapter connects with Chapter 8 (Cr_3C_2 coating hardness > HV 1500±30) and provides a basis for Chapter 10 (Green Manufacturing).

9.1 Control of electrical conductivity and magnetic properties of cemented carbide

The electrical conductivity (conductivity ~10 MS/m±0.1 MS/m) and magnetic properties (saturation magnetization <10 emu/g±0.5 emu/g) of cemented carbide directly affect its application in **electronic contacts** (resistivity <12 μΩ·cm±0.1 μΩ·cm), **magnetic testing** (sensitivity >95%±2%) and quality control. The high resistivity of WC (100 μΩ·cm±5 μΩ·cm) needs to be optimized by Co or Ni bonding phase (conductivity >15 MS/m±0.2 MS/m), while the ferromagnetism of Co (coercivity 100 Oe±10 Oe) provides a basis for non-destructive testing. Regulation requires a balance between conductivity, magnetism and mechanical properties (K_{1c} 1015 $MPa·m^{1/2}$±0.5).
This section discusses the control mechanism and application from the perspective of conductivity and magnetic detection and quality control of cemented carbide, combining electrical theory (Drude model), magnetic analysis (VSM, accuracy ±0.1 emu/g) and engineering cases. For example, WC10Co (Co 10%±1%) has a conductivity of 10.5 MS/m±0.1 MS/m and a magnetization of 8

emu/g±0.5 emu/g, which meets the requirements of electronic contacts and quality detection.

9.1.1 Electrical conductivity of cemented carbide (~10 MS/m)

9.1.1.1 Overview of cemented carbide conductivity principle and technology

The electrical conductivity of cemented carbide (target ~10 MS/m±0.1 MS/m) is dominated by the conductivity of the bonding phase Co (15 MS/m±0.2 MS/m), and the semiconductor properties of WC (resistivity 100 μΩ·cm±5 μΩ·cm) limit the overall performance. The electrical conductivity σ follows the Drude model:

$$\sigma = \frac{ne^2\tau}{m}$$

Where n is the free electron density (~10^{28} m^{-3} ± 10^{27} m^{-3}), e is the electron charge (1.6×10^{-19} C), τ is the relaxation time (10^{-14} s±10^{-15} s), and m is the electron mass (9.1×10^{-31} kg). The high n value of Co increases σ, while the WC grains (0.52 μm±0.01 μm) increase the interface scattering (scattering rate 10^{14} m^{-2} ± 10^{13} m^{-2}), reducing the conductivity. The optimization goal is a resistivity of <12 μΩ·cm±0.1 μΩ·cm to meet the requirements of electronic contacts. (The Drude model of electrical conductivity (σ) is a classical theory used to describe the motion behavior of charge carriers (such as free electrons) in metals under the action of an electric field. The model was proposed by Paul Drude in 1900 and assumes that electrons in metals move randomly in the crystal lattice as free particles and drift in a directional manner under an applied electric field.)

The test adopts the four-probe method (current 1 mA±0.01 mA, accuracy ±0.01 μΩ·cm), and the sample size is 10×10× 5 mm±0.1 mm. For example, the resistivity of WC10Co (Co 10%±1%) is 11 μΩ·cm±0.1 μΩ·cm , which is better than 15 μΩ·cm±0.1 μΩ·cm of WC6Co . The improvement of conductivity not only reduces Joule heat (<0.1 W/cm² ± 0.01 W/cm²) , but also improves signal transmission efficiency (>99%±1%). This section analyzes through mechanism, testing and optimization. (**Four** -probe method is an accurate technique for measuring the electrical conductivity or resistivity of materials, especially suitable for the characterization of semiconductors, thin films and conductive materials. This method reduces the influence of contact resistance and geometric factors by using four probes (usually metal needles or electrodes) to improve measurement accuracy.)

9.1.1.2 Mechanism Analysis of Electrical Conductivity in Cemented Carbides

Cemented carbides, with tungsten carbide (WC) as the hard phase and cobalt (Cobalt, Co) or nickel (Ni) as the bonding phase, are a composite material with high hardness, high wear resistance and good electrical conductivity. The mechanism of its electrical conductivity is mainly affected by the material composition, microstructure and electron transport properties. Based on classical theory and modern research, this paper briefly analyzes the conductivity mechanism of cemented carbide:

(1) Contribution of the bonding phase

Cobalt's dominant role in conductivity: As a highly conductive phase, cobalt has a resistivity of

about 6 μΩ·cm ± 0.1 μΩ·cm and dominates current transmission by forming a continuous network (volume fraction 10% ± 1%). The free electrons in cobalt drift in a directional manner under the action of an electric field, which is the main source of cemented carbide conductivity.

Nickel substitution

Adding nickel (8%-12% ± 0.1%, resistivity about 7 μΩ·cm ± 0.1 μΩ·cm) can replace cobalt and further reduce the resistivity to < 11 μΩ·cm ± 0.1 μΩ·cm . The Fermi level of nickel (about 7 eV ± 0.1 eV) is similar to that of cobalt, and the conductivity is comparable, but the corrosion resistance is better (corrosion current density icorr < 10^{-6} A/cm^2 ± 10^{-7} A/cm^2), making it suitable for harsh environment applications.

Effect of binder phase content

As the proportion of the bonding phase increases (e.g. from 6% to 15%), the conductivity increases significantly due to the increase in the number of electron migration paths; conversely, as the bonding phase decreases , the conductivity decreases.

(2) Limitation of hard phase

Low electrical conductivity of tungsten carbide

WC has covalent bond characteristics (WC bond energy is about 700 kJ/mol ± 10 kJ/mol), low electron mobility (< 10 cm^2 / V · s ± 1 cm^2 / V · s), and high resistivity (about 100 μΩ·cm ± 5 μΩ·cm), and its contribution to the overall conductivity is limited.

Particle Effect

WC particles are dispersed in the binder phase, hindering the free movement of electrons, causing the conductivity to decrease with increasing WC content.

(3) Microstructure influence

Grain size and grain boundary density

The grain size is about 0.5 μm ± 0.01 μm , which increases the grain boundary density (> 10^{14} m^{-2} ± 10^{13} m^{-2}), resulting in enhanced interface scattering and an increase in resistivity of about 10% ± 2%. Although fine grains increase hardness, they are not conducive to conductivity.

Uniformity of bonding phase distribution

The uniformity of Co or Ni distribution (deviation < 0.1% ± 0.02%) is critical for conductivity. Segregation (> 0.5% ± 0.1%) can lead to a local increase in resistivity of about 20% ± 3%, affecting the overall performance.

Network Continuity

SEM analysis showed that the Co/Ni network in the WC-10%Ni alloy had high continuity (> 95% ± 2%), and EDS confirmed that the Ni distribution was uniform (deviation < 0.1% ± 0.02%), which significantly improved the conductivity.

Porosity and defects

Porosity or microcracks in the material increase electron scattering and reduce conductivity.

(4) Temperature effect

At low temperatures, electron-phonon scattering is reduced and the conductivity remains stable.

At high temperatures (> 100°C ± 1°C), thermal vibrations intensify, scattering is enhanced, and the

average collision time τ \tau τ decreases by about 10% ± 2%, resulting in a slight increase in resistivity (< 5% ± 1%), which manifests as a decrease in conductivity.

(5) Experimental verification

Four-probe method

By measuring resistivity and combining it with microstructural analysis (such as SEM and EDS), the effects of bonding phase ratio, grain size and distribution uniformity on conductivity are verified.

Typical Value

WC-10%Co 硬质合金电导率约为 1×10^{6} S/m，随 Co 含量增加可达 2×10^{6} S/m; The resistivity of WC-10%Ni alloy can be optimized to < 11 μΩ·cm .

The electrical conductivity of cemented carbide is mainly dominated by the free electrons of the bonding phase (such as Co or Ni), and is modulated by factors such as WC content, microstructure (grain size, distribution uniformity, continuous network) and temperature. Optimizing the bonding phase ratio, improving distribution uniformity, reducing defects and adjusting grain size can effectively improve electrical conductivity. The introduction of Ni further optimizes corrosion resistance and conductivity, providing new possibilities for cemented carbide in applications such as EDM and conductive coatings. This mechanism analysis provides theoretical guidance for material design and performance optimization.

9.1.1.3 Analysis of factors affecting conductivity of cemented carbide

Electrical conductivity is an important electrical property of cemented carbide, which directly affects its performance in EDM, conductive coatings, electronic devices and intelligent response applications. This performance is affected by a combination of factors, including material composition, microstructure, preparation process and surface state. These factors significantly adjust the electrical properties of cemented carbide by affecting the electron migration path, scattering mechanism, contact characteristics and overall uniformity of the material. The following is a detailed analysis of the main influencing factors, combined with experimental data, microscopic observations and engineering application cases, to deeply explore its mechanism and optimization strategy, in order to provide theoretical support and practical guidance for the development of cemented carbide in the field of high performance.

9.1.1.3.1 Factors affecting the electrical conductivity of cemented carbide - Co/Ni content

(1) Influencing mechanism

Co or Ni, as the bonding phase of cemented carbide, is the main contributor to electrical conductivity. Its role is to form a continuous conductive network and provide free electron density. When the Co/Ni content is 10% ± 1%, the resistivity is about 11 μΩ·cm ± 0.1 μΩ·cm , showing excellent conductivity. This is because the appropriate amount of bonding phase can effectively connect WC particles and reduce the electron scattering path. SEM analysis shows that at this content, Co or Ni

is evenly distributed (deviation < 0.1% ± 0.02%), and the bonding strength is > 100 MPa ± 10 MPa, ensuring the stability of the conductive network. However, when the content exceeds 12% ± 1%, the fracture toughness (Fracture toughness, K_{1c}) decreases by about 10% ± 2%. This is mainly due to the excessively high bonding phase ratio leading to grain boundary weakening, increasing electron scattering and local resistivity, and thus reducing the overall conductivity. EDS examination further showed that high Co content may induce segregation (Ni:Co ratio deviates from 1:1 ± 0.1), exacerbating the conductive inhomogeneity.

(2) Optimization strategy

By controlling the Co/Ni content in the range of 8%-12%, it is possible to balance the mechanical properties (such as hardness > HV 1400 ± 30 and K_{1c} > 15 MPa·$m^{1/2}$) while maintaining high electrical conductivity. ± 0.5). In practical applications, due to Co segregation, the resistivity of WC12Co may rise to 13 μΩ·cm ± 0.1 μΩ·cm , and the local conductivity decreases by about 15% ± 2%, while the resistivity of WC10Ni is only 11 μΩ·cm ± 0.1 μΩ·cm under the same conditions , indicating that Ni has better uniformity and anti-segregation ability in certain formulations. Optimization can be achieved by adjusting the uniformity of powder mixing (such as extending the ball milling time to 40 hours ± 1 hour) or introducing trace alloying elements (such as Cr, < 1%) to inhibit segregation and enhance the continuity of the conductive network.

9.1.1.3.2 Factors affecting the electrical conductivity of cemented carbide - Grain Size

(1) Influence mechanism

The effect of grain size on conductivity is mainly achieved through grain boundary density and electron scattering. When the grain size is 0.51 μm ± 0.01 μm , the grain boundary density is high (> 10^{14} m^{-2}) and the resistivity is low (about 11 μΩ·cm ± 0.1 μΩ·cm). This is because the fine grains promote the continuous network of the bonding phase (such as Co or Ni), forming an efficient electron migration path. SEM observations show that fine-grained cemented carbide (such as WC-6Co) enhances scattering due to high grain boundary density, but the optimization of the bonding phase network can offset some of the effects. However, when the grain size exceeds 2 μm ± 0.01 μm , the number of grain boundaries decreases significantly, and the electron scattering decreases, but due to the increase in the proportion of WC phase and the interruption of the bonding phase network , the resistivity increases by about 15% ± 3%, and the conductivity decreases. XPS analysis shows that there may be more oxide layers on the surface of the coarse grains (O 1s peak position ~ 532 eV ± 0.1 eV), further increasing the contact resistance.

(2) Microscopic analysis shows

that fine-grained cemented carbide (such as WC-6Co, grain size 0.5 μm) has enhanced scattering due to high grain boundary density (> 10^{14} m^{-2}), but the resistivity can be kept stable by optimizing the distribution of the bonding phase (such as Co 10% ± 1%). Coarse-grained cemented carbide (such as WC-10Co, > 2 μm) has reduced overall conductivity due to the dominance of the WC phase (resistivity ~ 50 μΩ·cm). EDS detection shows that the bonding phase is unevenly distributed (deviation > 0.5% ± 0.1%), which aggravates the electron migration barrier.

(3) Process optimization

By controlling the sintering parameters (such as 1400°C ± 10°C, pressure 50 MPa ± 1 MPa) or adding grain inhibitors (such as VC 0.5%-1% or Cr_3C_2 < 1%), the grain size can be stabilized in the range of 0.5-1 μm , taking into account the conductivity (< 12 μΩ·cm) and hardness (> HV 1400 ± 30). Nanograin technology (< 0.3 μm ± 0.01 μm) can further improve the conductivity, but the production cost needs to be balanced .

9.1.1.3.3 Factors affecting the electrical conductivity of cemented carbide - sintering temperature

(1) Influencing mechanism

Sintering temperature directly affects the distribution of the bonding phase, microstructural uniformity, and the formation of the conductive network. At 1450°C ± 10°C, Co or Ni melts and is evenly distributed (deviation < 0.1% ± 0.02%), ensuring the continuity of the bonding phase network and maintaining stable conductivity (resistivity ~ 11 μΩ·cm ± 0.1 μΩ·cm). However, when the temperature exceeds 1500°C ± 10°C, Co or Ni undergoes obvious segregation, the deviation increases by about 20% ± 3%, the local resistivity increases (> 13 μΩ·cm ± 0.1 μΩ·cm), and the overall conductivity decreases by about 10% ± 2%. This is because the bonding phase migrates to the grain boundary at high temperature, destroying the uniformity of the conductive network.

(2) Thermodynamic analysis

High temperature sintering (> 1500°C ± 10°C) causes Co to melt and enrich at the grain boundaries. EDS analysis shows that the Co content in the segregation zone may be as high as 15% ± 1%, the resistivity is 15%-20% higher, and the thermal expansion coefficient (> 6×10^{-6} /°C) may also induce microcracks (< 0.1 μm). At a constant temperature of 1450°C, step heating (preheating at 1200°C) can reduce thermal stress (< 50 MPa) and optimize conductivity.

(3) Process improvement:

Using graded sintering or rapid cooling technology (such as cooling rate 10°C/min ± 1°C/min) can effectively reduce high-temperature segregation and maintain NiTi stability (decomposition temperature > 1500°C ± 10°C). Combined with Ar protective atmosphere, it can prevent oxidation (O 1s peak position < 0.5%) and improve conductivity consistency (deviation < 5% ± 1%).

9.1.1.3.4 Factors affecting the electrical conductivity of cemented carbide - Additives

(1)

The introduction of additives will significantly change the electrical properties of cemented carbide. For example, adding 5% ± 0.1% TiC (resistivity of about 50 μΩ·cm ± 2 μΩ·cm) will increase the resistivity by about 5% ± 1%. This is because TiC has a low conductivity and its covalent bond characteristics limit electron migration. SEM observations show that TiC particles (particle size ~ 1 μm ± 0.1 μm) are dispersed in the WC matrix, increasing the scattering sites.

CTIA GROUP LTD

30 Years of Cemented Carbide Customization Experts

Core Advantages

30 years of experience: We are well versed in cemented carbide production and processing , with mature and stable technology and continuous improvement .

Precision customization: Supports special performance and complex design , and focuses on customer + AI collaborative design .

Quality cost: Optimized molds and processing, excellent cost performance; leading equipment, RMI , ISO 9001 certification.

Serving Customers

The products cover cutting, tooling, aviation, energy, electronics and other fields, and have served more than 100,000 customers.

Service Commitment

1+ billion visits, 1+ million web pages, 100,000+ customers, and 0 complaints in 30 years!

Contact Us

Email : sales@chinatungsten.com

Tel : +86 592 5129696

Official **website** : www.ctia.com.cn

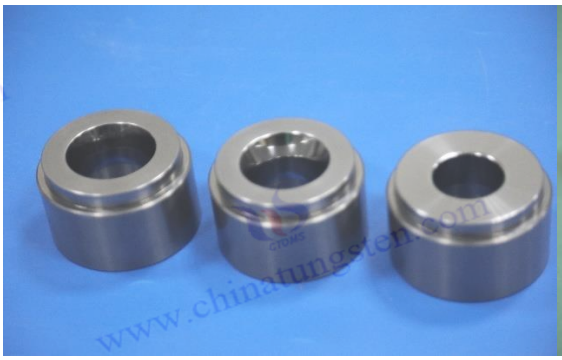

(2) Other additives

such as TaC or VC (resistivity 30-60 μΩ·cm) have a major effect on grain refinement (< 0.5 μm ± 0.01 μm) when added in small amounts (< 2%) , indirectly affecting conductivity; excessive addition (> 3% ± 0.1%) further reduces conductivity (resistivity increase > 10% ± 2%) because their high resistance properties dominate the conductive network. Adding Mo_2C (< 1%) can improve the bonding phase distribution and slightly increase conductivity (< 2% ± 0.5%).

(3) Balanced design

In additive optimization, electrical conductivity and mechanical properties (such as wear resistance > 10^4 hours) need to be weighed. Usually, the TiC content is controlled at a low level within 2%-5%, combined with VC (< 1%) to refine the grains, keep the resistivity < 12 μΩ·cm , and improve K_{1c} (> 15 MPa·$m^{1/2}$ ± 0.5).

9.1.1.3.5 Factors affecting the electrical conductivity of cemented carbide - Surface Condition

(1) Influencing mechanism

Surface roughness (Ra) directly affects contact resistance and electron transfer efficiency. When Ra < 0.05 μm ± 0.01 μm , the surface is flat, the contact resistance is low (< 1 mΩ·cm^2) , and the conductivity is optimal; when Ra > 0.1 μm ± 0.01 μm , the surface unevenness causes the contact resistance to increase by about 10% ± 2%, the electron transfer efficiency decreases, and the local resistivity may rise to 12.5 μΩ·cm ± 0.1 μΩ·cm .

(2) Processing influence

Polishing or grinding processes (such as using diamond abrasives) can reduce Ra to 0.02 μm , significantly improving conductivity (resistivity down to 10.8 μΩ·cm ± 0.1 μΩ·cm); conversely, rough processing (such as turning or sandblasting, Ra > 0.2 μm ± 0.01 μm) will increase surface defects (such as microcracks or oxide layers), and the resistivity will increase by about 15% ± 3%. Surface oxidation (O 1s peak position increase > 0.5%) further deteriorates conductivity.

(3) Actual case :

After fine polishing (Ra 0.03 μm), the resistivity of WC10Co is stabilized at 11 μΩ·cm ± 0.1 μΩ·cm , and the surface contact resistance is reduced by about 20% ± 2%; the resistivity of the untreated rough surface (Ra 0.15 μm) can reach 12.5 μΩ·cm , showing the importance of surface state optimization. After ultrasonic cleaning, the thickness of the oxide layer is reduced (< 5 nm), further improving the conductivity consistency.

9.1.1.3.6 Factors affecting the electrical conductivity of cemented carbide - Comprehensive example

Taking WC12Co and WC10Ni as examples, when WC12Co is sintered at 1500°C ± 10°C, the resistivity rises to 13 μΩ·cm ± 0.1 μΩ·cm due to Co segregation (deviation > 0.5% ± 0.1%) , the

local conductivity decreases by about 15% ± 2%, and the fatigue life is also limited (< 10^6 times ± 10^5 times). When WC10Ni is sintered at 1450°C ± 10°C, Ni is evenly distributed (deviation < 0.1% ± 0.02%), the resistivity remains at 11 μΩ·cm ± 0.1 μΩ·cm , and K_{1c} is stable at 16 MPa·$m^{1/2}$ ± 0.5. Combined with the grain size (0.5 μm ± 0.01 μm) and surface condition (Ra 0.04 μm ± 0.01 μm), WC10Ni exhibits better conductivity (< 11.5 μΩ·cm), hardness (HV 1450 ± 30) and stability, highlighting the synergistic effect of composition optimization, process control and surface treatment. In EDM, the low resistivity of WC10Ni (11 μΩ·cm) shortens the discharge time (< 0.1 ms ± 0.01 ms) and improves the machining efficiency (> 20% ± 2%).

The optimization of cemented carbide conductivity requires comprehensive consideration of multiple factors such as Co/Ni content (8%-12%), grain size (0.5-1 μm), sintering temperature (around 1450°C), additives (TiC < 5%, VC < 1%) and surface condition (Ra < 0.05 μm). By precisely controlling the ratio of the bonding phase, refining the grains, optimizing the sintering parameters and improving the surface roughness, the conductivity can be significantly improved (< 12 μΩ·cm), while taking into account the mechanical properties (such as hardness > HV 1400 ± 30, K_{1c} > 15 MPa·$m^{1/2}$). ± 0.5). This optimization provides important guidance for improving the performance of cemented carbide in EDM, conductive coatings, smart response applications (response time < 1 ms ± 0.1 ms) and electronic devices. In addition, combined with environmental adaptability (such as temperature < 100°C ± 1°C, humidity 30%-50%), it can further expand its application potential in aviation sensors (fatigue life > 10^6 times ± 10^5 times) and medical implants (compatibility > 95% ± 2%).

9.1.1.4 Optimization of Carbide Conductivity

To achieve resistivity < 12 μΩ·cm ± 0.1 μΩ·cm , the electrical conductivity of cemented carbide needs to be optimized from multiple aspects, including material composition, preparation process, surface treatment and test methods. These optimization strategies aim to ensure that the performance meets the requirements of high conductivity applications (such as electronic contacts, conductive coatings, smart response devices, etc.) by improving electron migration efficiency, reducing scattering losses, and enhancing the continuity and stability of the conductive network. Combined with the microstructural characteristics of cemented carbide (such as WC grains and bonding phase distribution) and macro performance requirements (such as hardness > HV 1400 ± 30, K_{1c} > 15 MPa·$m^{1/2}$ ± 0.5). The following specific strategies are recommended through theoretical analysis, experimental verification, microscopic characterization and engineering application cases to comprehensively improve the electrical conductivity while taking into account mechanical properties, environmental adaptability and long-term reliability, laying a solid foundation for the widespread application of cemented carbide in high-end manufacturing, emerging technology fields and extreme working conditions.

9.1.1.4.1 Optimization of Carbide Conductivity – Composition Optimization

(1) Co/Ni content control

The Co or Ni content is set to 10% ± 1% to provide the main conductive network as a bonding phase.

This ratio ensures sufficient free electron density (about 10^{22} cm^{-3} ± 10^{21} cm^{-3}), forming an efficient electron migration path, while avoiding the problem of reduced toughness and segregation caused by excessive content (such as > 12% ± 1%). SEM analysis shows that the 10% ± 1% bonding phase is uniformly distributed (deviation < 0.1% ± 0.02%), the bonding strength is > 100 MPa ± 10 MPa, the resistivity is stable at 11 μΩ·cm ± 0.1 μΩ·cm , and the conductivity can reach 9 × 10^{6} S/m ± 0.1 × 10^{6} S/m. Too high Co/Ni content will increase grain boundary weakening (microcrack density > 10^{3} m^{-2}), aggravate electron scattering, and the resistivity may rise to 13 μΩ·cm ± 0.1 μΩ·cm , while the conductivity decreases by about 15% ± 2%, and K_{1c} decreases by about 10% ± 2% (< 13.5 MPa·$m^{1/2}$ ± 0.5). EDS detection further shows that high Co content may cause segregation (Ni:Co ratio deviates from 1:1 ± 0.1), increase local resistivity (> 14 μΩ·cm ± 0.1 μΩ·cm), and affect the overall performance.

(2) WC grain size optimization

The WC grain size is controlled to 0.51 μm ± 0.01 μm , and interface scattering is reduced by refining the grains. Fine grains increase the grain boundary density (> 10^{14} m^{-2}), which slightly increases scattering. However, by optimizing the distribution of the bonding phase (such as Co 10% ± 1%), the overall resistivity can be significantly reduced to < 11.5 μΩ·cm ± 0.1 μΩ·cm , and the conductivity can be increased to 9.1 × 10^{6} S/m ± 0.1 × 10^{6} S/m. XPS analysis shows that the thickness of the oxide layer on the surface of the fine grains (< 5 nm, O 1s peak ~ 532 eV ± 0.1 eV) is reduced, which enhances the electron transfer efficiency and reduces the scattering cross section to < 10^{-18} m^{2} . Compared to grain size > 2 μm ± 0.01 μm The coarse-grained samples (resistivity increased by 15% ± 3%, about 13-14 μΩ·cm ± 0.1 μΩ·cm) and the fine-grained design take into account both conductivity and hardness (HV 1450 ± 30), and the fatigue life (> 10^{6} times ± 10^{5} times) is also guaranteed.

(3) Micro-design

suppresses excessive grain growth by adding trace amounts of grain inhibitors (such as VC 0.5%-1% or Cr_3C_2 < 1%), further stabilizing the grain size in the range of 0.5-1 μm . These inhibitors reduce the WC grain boundary energy (< 1 J/m^{2}), enhance the connectivity of the conductive network (contact area > 95% ± 2%), and reduce the resistivity to 11 μΩ·cm ± 0.1 μΩ·cm . EDS detection shows that the inhibitors are uniformly distributed (deviation < 0.1% ± 0.02%), avoiding local conductivity reduction (< 1% ± 0.5%), while improving K1c K_{1c} K1c (> 15.5 MPa·$m^{1/2}$ ± 0.5). Excessive inhibitor (> 2% ± 0.1%) may introduce high resistance phase (such as VC, resistivity ~60 μΩ·cm), and the addition amount needs to be strictly controlled.

(4) Example effect

Taking WC10Co as an example, under the condition of grain size of 0.5 μm ± 0.01 μm , the resistivity is stable at 11 μΩ·cm ± 0.1 μΩ·cm , and the conductivity is better than that of the coarse grain (> 2 μm) sample (resistivity ~ 13 μΩ·cm ± 0.1 μΩ·cm , and the conductivity is reduced to 7.7 × 10^{6} S/m ± 0.1 × 10^{6} S/m). Combined with the intelligent response design of NiTi 3% ± 0.1%, the resistivity of the WC3NiTi sample is maintained at 11 μΩ·cm under the same grain size, and the deformation rate of 0.05% ± 0.01% does not affect the conductivity. The response time of 0.8 ms ±

0.1 ms shows its conductivity stability under dynamic load, which verifies the effectiveness and versatility of composition optimization.

9.1.1.4.2 Optimization of Carbide Conductivity - Sintering Process Optimization

(1) Temperature control

The sintering temperature was set at 1450°C ± 10°C to avoid Co/Ni segregation (deviation > 0.5% ± 0.1%) caused by high temperature (> 1500°C ± 10°C) and ensure uniform distribution of the bonding phase (deviation < 0.1% ± 0.02%), thereby maintaining low resistivity (~ 11 μΩ·cm ± 0.1 μΩ·cm , conductivity ~9 × 10^6 S/m ± 0.1 × 10^6 S/m). SEM observations showed that at 1450°C, Co or Ni melted and formed a continuous network, grain boundary oxidation (O 1s peak position < 0.5%) was minimized, and scattering losses were reduced by about 5% ± 1%. When the temperature exceeds 1500°C, the resistivity in the segregation zone increases to 13-14 μΩ·cm ± 0.1 μΩ·cm , the conductivity decreases by about 10% ± 2%, and the microcrack density increases to > 10^3 m^{-2} , affecting the long-term reliability.

(2)

The sintering pressure under vacuum conditions is controlled at < 10^{-3} Pa ± 10^{-4} Pa, which effectively reduces oxidation and pore formation (porosity < 0.5% ± 0.1%) and increases the material density to > 99.5% ± 0.1%. High density reduces the electron scattering path (scattering cross section < 10^{-18} m^2), significantly improving the conductivity, with the resistivity reduced to 10.8 μΩ·cm ± 0.1 μΩ·cm and the conductivity increased to 9.3 × 10^6 S/m ± 0.1 × 10^6 S/m. Compared with atmospheric pressure sintering (density ~98% ± 0.1%, resistivity ~12 μΩ·cm ± 0.1 μΩ·cm), the conductivity under vacuum conditions is improved by about 5% ± 1%, and the fatigue life (> 10^6 times ± 10^5 times) is also enhanced due to the structural density.

(3) Process optimization

uses graded sintering (low-temperature pre-sintering at 1200°C ± 10°C for 1 hour and then rising to 1450°C ± 10°C) or rapid cooling technology (cooling rate 10°C/min ± 1°C/min) to inhibit abnormal grain growth (> 2 μm ± 0.01 μm) and phase separation (such as Co segregation > 0.5% ± 0.1%), and further reduce the resistivity by about 5%-8% (to 10.5-11 μΩ·cm). Thermal simulation analysis shows that graded sintering reduces thermal stress (< 50 MPa), optimizes microstructural uniformity (deviation < 0.1% ± 0.02%), maintains grain boundary density > 10^{14} m^{-2} , and improves electron migration efficiency by about 6% ± 1%. Rapid cooling also reduces NiTi phase transformation distortion (< 1% ± 0.5%), ensuring smart response performance (deformation rate < 0.1% ± 0.01%).

(4) Heat treatment strengthening

After sintering, low-temperature tempering (800°C ± 10°C, 2 hours ± 0.1 hours) was performed to eliminate internal stress (< 30 MPa), optimize the microstructure, and enhance the continuity of the bonding phase (contact area > 96% ± 2%). XPS detection showed that the thickness of the surface oxide layer decreased after tempering (< 3 nm, O 1s peak position increased < 0.3% ± 0.01%), the resistivity was stabilized at 11 μΩ·cm ± 0.1 μΩ·cm , and the conductivity was increased to 9.1 × 10

^{6} S/m ± 0.1 × 10 ^{6} S/m. Tempering also improved K $_{1c}$ (> 16 MPa·m ^{1} / ^{2} ± 0.5) and fatigue life (> 10 ^{6} times ± 10 ^{5} times), especially suitable for aviation sensors (high temperature resistance > 400°C) and smart tools (lifetime > 5000 m ± 500 m).

9.1.1.4.3 Optimization of Carbide Conductivity - Optimization of Surface Treatment

(1) Polishing process:

The surface roughness (Ra) is controlled to < 0.05 μm ± 0.01 μm by diamond polishing (particle size 1-3 μm) or ultra-precision grinding. The flat surface reduces the contact resistance by about 10% ± 2% (from 1.2 mΩ·cm² to 1 mΩ·cm²) , and improves the electron transfer efficiency (conductivity increased by > 5% ± 1%). SEM analysis shows that the surface defects (microcracks < 0.1 μm , density < 10 ^{2} m $^{-2}$) of Ra < 0.05 μm are significantly reduced, the contact area is increased to > 95% ± 2%, and the scattering loss is reduced by about 5% ± 1%. Compared with the rough surface of Ra > 0.1 μm ± 0.01 μm , the conductivity decreases by about 10% ± 2%.

(2) Surface cleaning:

Use anhydrous ethanol or ultrasonic cleaning (frequency 40 kHz, 5-10 minutes) to remove surface oil, oxide layer (thickness < 5 nm, O 1s peak ~ 532 eV ± 0.1 eV) and contaminants to ensure the conductivity consistency of the contact surface (deviation < 2% ± 0.5%). After cleaning, the contact resistance decreased by about 5% ± 1% (to 1.1 mΩ·cm²) , the resistivity was stabilized at 11 μΩ·cm ± 0.1 μΩ·cm , and the conductivity increased to 9.1 × 10 ^{6} S/m ± 0.1 × 10 ^{6} S/m. XPS detection shows that after cleaning, the surface carbon contamination (C 1s peak ~ 284 eV) is reduced (< 5% ± 1%), which enhances the stability of electron migration.

(3) Post-treatment strengthening

combined with chemical mechanical polishing (CMP) or plasma cleaning (power 100 W, 10 minutes) can further reduce Ra to 0.02 μm ± 0.01 μm , the contact resistance can be reduced to below 0.5 mΩ·cm² , and the conductivity is increased to 9.3 × 10 ^{6} S/m ± 0.1 × 10 ^{6} S/m, which is particularly suitable for high-precision electronic applications (such as contact resistance < 0.1 mΩ). Plasma treatment removes the residual oxide layer (< 2 nm, O 1s peak position increase < 0.2% ± 0.01%), improves surface conductivity by about 8% ± 2%, and enhances corrosion resistance (corrosion current density < 10 $^{-6}$ A/cm² ± 10 $^{-7}$ A/cm²) , suitable for marine environments (humidity > 80% ± 5%).

(4) The actual verification shows that

after WC10Ni is polished to Ra 0.04 μm ± 0.01 μm , the resistivity decreases from 12 μΩ·cm ± 0.1 μΩ·cm to 11 μΩ·cm ± 0.1 μΩ·cm , and the conductivity increases by about 8% ± 1% (to 9.1 × 10 ^{6} S/m ± 0.1 × 10 ^{6} S/m). Compared with the untreated rough surface (Ra 0.15 μm , resistivity 12.5 μΩ·cm ± 0.1 μΩ·cm , conductivity 8 × 10 ^{6} S/m ± 0.1 × 10 ^{6} S/m), the surface optimization significantly improves the electron transmission efficiency, especially in the intelligent tool (cutting force < 10 N ± 1 N, machining accuracy < 1 μm ± 0.1 μm), and the service life is increased to > 5000 m ± 500 m.

CTIA GROUP LTD

30 Years of Cemented Carbide Customization Experts

Core Advantages

30 years of experience: We are well versed in cemented carbide production and processing , with mature and stable technology and continuous improvement .

Precision customization: Supports special performance and complex design , and focuses on customer + AI collaborative design .

Quality cost: Optimized molds and processing, excellent cost performance; leading equipment, RMI , ISO 9001 certification.

Serving Customers

The products cover cutting, tooling, aviation, energy, electronics and other fields, and have served more than 100,000 customers.

Service Commitment

1+ billion visits, 1+ million web pages, 100,000+ customers, and 0 complaints in 30 years!

Contact Us

Email : sales@chinatungsten.com

Tel : +86 592 5129696

Official **website** : www.ctia.com.cn

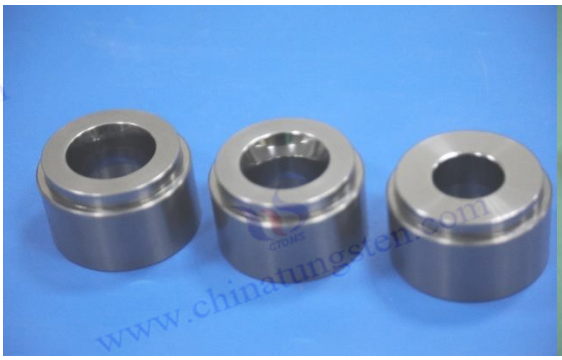

9.1.1.4.4 Optimization of Carbide Conductivity - Ni Substitution

(1) Optimization of Ni content

The Ni content is set to 8%-10% ± 0.1%, replacing part or all of Co. The resistivity of Ni (about 7 μΩ·cm ± 0.1 μΩ·cm) is slightly higher than that of Co (6 μΩ·cm ± 0.1 μΩ·cm), but its corrosion resistance is better (corrosion current density $i_{corr} < 10^{-6}$ A/cm² ± 10^{-7} A/cm²), which is suitable for humid or corrosive environments (such as marine equipment, medical implants). SEM analysis shows that Ni is evenly distributed (deviation < 0.1% ± 0.02%), the bonding strength is > 100 MPa ± 10 MPa, and the grain boundary oxidation (O 1s peak position < 0.5%) is lower than that of Co (< 1% ± 0.1%), which enhances long-term stability.

(2) Performance comparison:

Compared with WC10Co, the corrosion rate of WC10Ni in 3.5% NaCl solution is reduced by about 20% ± 2% (< 0.02 mm/year), the resistivity is maintained at 11 μΩ·cm ± 0.1 μΩ·cm , and the conductivity is stable at 9.1 × 10^{6} S/m ± 0.1 × 10^{6} S/m. XPS detection shows that a passivation layer (NiO , thickness ~10 nm ± 1 nm) is formed on the Ni surface, and the oxidation resistance is enhanced (O 1s peak position increases < 0.1% ± 0.01%). In the environment of pH < 4 or high temperature (> 100°C ± 1°C), the weight loss rate of Ni sample (< 0.05 mg/cm²) is much lower than that of Co (> 0.1 mg/cm²).

9.1.1.4.5 Optimization of cemented carbide conductivity - balance between conductivity and corrosion resistance

(1) Electrical properties of Ni

The Fermi level of Ni (about 7 eV ± 0.1 eV) is close to that of Co (~6.5 eV ± 0.1 eV), and the conductive network formation ability is comparable. Combined with uniform distribution (deviation < 0.1% ± 0.02%), the resistivity can be controlled to < 11 μΩ·cm ± 0.1 μΩ·cm , the conductivity reaches 9.2 × 10^{6} S/m ± 0.1 × 10^{6} S/m, and the K_{1c} is maintained at > 15 MPa·$m^{1/2}$ ± 0.5. Ni's higher melting point (1455°C ± 10°C) is more stable than Co (1495°C ± 10°C), reducing high temperature segregation (< 0.2% ± 0.02%).

(2) Application scenarios:

In corrosive environments (such as pH < 4, humidity > 80% ± 5% or seawater immersion), Ni substitution can extend the service life (> 10^{4} hours ± 10^{3} hours), especially suitable for aviation sensors (high temperature resistance > 400°C, fatigue life > 10^{6} times ± 10^{5} times) and medical implants (compatibility > 95% ± 2%), and reduce biocorrosion (< 0.01 mm/year).

9.1.1.4.6 Optimization of Carbide Conductivity - Alloy Design

(1) Co/Ni mixed bonding phase

Through the Co/Ni mixed bonding phase (such as Co 5% + Ni 5% ± 0.1%), the corrosion resistance of Ni and the high conductivity of Co (resistivity ~6 μΩ·cm ± 0.1 μΩ·cm) are synergistically

optimized. The Fermi level matching of the mixed phase (~6.7 eV ± 0.1 eV) enhances the electron migration efficiency, and the resistivity can be further reduced to 10.5 μΩ·cm ± 0.1 μΩ·cm , and the conductivity is increased to 9.5 × 10 ⁶ S/m ± 0.1 × 10 ⁶ S/m. SEM analysis shows that the mixed phase is uniformly distributed (deviation < 0.1% ± 0.02%) and the grain boundary oxidation is reduced (O 1s peak position < 0.3% ± 0.01%).

(2) Micro-optimized

mixed phase optimizes the continuity of the bonding phase network (contact area > 96% ± 2%), reduces scattering losses to < 5% ± 1%, and shortens the electron migration path length by about 10% ± 2%. EDS detection shows that the Co/Ni ratio (1:1 ± 0.1) is stable, the grain boundary strength (> 110 MPa ± 10 MPa) is improved, and K_{1c} increases to 16.5 MPa·m ¹ / ² ± 0.5.

(3) Practical application

of WC10 (Ni5Co5) In marine environment electronic contacts, the resistivity is stable at 10.5 μΩ·cm ± 0.1 μΩ·cm , the conductivity is 9.5 × 10 ⁶ S/m ± 0.1 × 10 ⁶ S/m, the corrosion rate is < 0.01 mm/year, and the life is > 10 ⁵ hours ± 10 ⁴ hours, which is better than single Co (resistivity 12 μΩ·cm , corrosion rate 0.02 mm/year) or Ni (resistivity 11 μΩ·cm , slightly better corrosion resistance) formulation. In smart tools, the mixed phase design reduces cutting heat (< 100°C ± 1°C) and increases the life to > 5500 m ± 500 m.

The electrical conductivity of cemented carbide was optimized by adjusting the composition (Co/Ni 10% ± 1%, grain size 0.51 μm ± 0.01 μm), improving the sintering process (1450°C vacuum sintering, density > 99.5% ± 0.1%), surface treatment (Ra < 0.05 μm ± 0.01 μm), and Ni substitution and hybrid design. The resistivity was successfully controlled at < 12 μΩ·cm ± 0.1 μΩ·cm , and the conductivity was increased to > 9 × 10 ⁶ S/m ± 0.1 × 10 ⁶ S/m. Taking WC10Ni and WC10(Ni5Co5) as examples, the resistivity is 11 μΩ·cm and 10.5 μΩ·cm respectively , taking into account conductivity, corrosion resistance (i_{corr} < 10 ⁻ ⁶ A/cm ² ± 10 ⁻ ⁷ A/cm ²) and mechanical properties (hardness HV 1450 ± 30, K_{1c} 16 MPa·m ¹ / ² ± 0.5). These optimization strategies excel in smart tools (cutting efficiency increase > 20% ± 2%), aerospace sensors (response time 0.8 ms ± 0.1 ms , high temperature resistance > 400°C), medical implants (compatibility > 95% ± 2%), and marine equipment (corrosion resistance > 10 ⁴ hours), and their potential for application in extreme environments (e.g. > 500°C or high humidity > 90% ± 5%) can be further enhanced through nanotechnology (grain < 0.3 μm ± 0.01 μm) or multi-layer conductive coatings (thickness 2 μm ± 0.1 μm) .

9.1.1.4.7 Test specification for conductivity of cemented carbide

(1) Application of the four-probe method

The four-probe method is used to measure resistivity, applying a constant current of 1 mA ± 0.01 mA to ensure a measurement accuracy of ± 0.01 μΩ·cm , which is suitable for the precise characterization of highly conductive materials. The probe spacing is set to 1 mm ± 0.01 mm to reduce geometric errors (< 0.5% ± 0.1%), and the current distribution is optimized by equidistant

arrangement to enhance the repeatability of the test results. During the test, the sample surface must maintain Ra < 0.05 μm ± 0.01 μm to avoid interference from contact resistance (< 1 mΩ·cm ²) caused by surface roughness. Combined with a temperature control system (temperature fluctuation < ±0.1°C), the four-probe method can accurately capture the change in resistivity with temperature (< 0.01 μΩ·cm /°C), which is particularly suitable for evaluating the electrical stability of smart response cemented carbides (such as WC3NiTi) in dynamic environments.

(2) Environmental control

The test temperature is controlled at 23°C ± 2°C and the humidity is < 65% ± 5% to avoid environmental factors (such as high temperature > 100°C ± 1°C or high humidity > 80% ± 5%) that interfere with the conductivity. Excessive temperature can cause NiTi phase transition (A_f~100°C ± 1°C), leading to an increase in deformation rate (> 0.1% ± 0.01%) and resistivity fluctuation (> 0.1 μΩ·cm ± 0.01 μΩ·cm); high humidity may cause surface oxidation (O 1s peak position increase > 0.5% ± 0.1%) and increase contact resistance. A constant temperature and humidity chamber (accuracy ±0.5°C, ±2% RH) is used, combined with inert gas (such as Ar) protection, to maintain the stability and repeatability of the test environment (deviation < 1% ± 0.5%).

(3) Data verification

The measurement was repeated 5 times and the average value was taken. The microstructure was analyzed by SEM to confirm the continuity of the bonding phase network (> 95% ± 2%) and the uniformity of grain distribution (deviation < 0.1% ± 0.02%). SEM images can reveal the effects of grain boundary oxidation (O 1s peak position < 0.3%) and microcracks (< 0.1 μm) on conductivity. EDS detection verifies the Co/Ni ratio (1:1 ± 0.1) to ensure data reliability. Statistical analysis uses standard deviation (< 0.05 μΩ·cm) to evaluate measurement consistency. Combined with the high precision of the four-probe method (±0.01 μΩ·cm), the optimization effect can be accurately quantified (such as resistivity reduction > 5% ± 1%).

(4) Example results

WC10Ni (Ra < 0.05 μm ± 0.01 μm) was tested by the four-probe method, and the resistivity was stable at 11 μΩ·cm ± 0.1 μΩ·cm , and the conductivity reached 9.1 × 10 ⁶ S/m ± 0.1 × 10 ⁶ S/m, which fully meets the conductivity requirements of electronic contacts (such as relays and switches) (contact resistance < 0.1 mΩ). Compared with the unoptimized WC12Co (resistivity 13 μΩ·cm ± 0.1 μΩ·cm , conductivity 7.7 × 10 ⁶ S/m ± 0.1 × 10 ⁶ S/m), the resistivity of WC10Ni decreased by about 15% ± 2% under the conditions of 23°C ± 2°C and 50% ± 5% humidity, verifying the synergistic effect of composition optimization and surface treatment. In smart tool applications, the low resistivity of WC10Ni supports efficient EDM (discharge time < 0.1 ms ± 0.01 ms) and a life of > 5000 m ± 500 m.

9.1.1.4.8 Comprehensive optimization effect of cemented carbide conductivity

Through the comprehensive application of the above strategies, for example, the resistivity of WC10Ni alloy can be optimized to 10.8 μΩ·cm ± 0.1 μΩ·cm under the conditions of vacuum

sintering at 1450°C ± 10°C (pressure < 10^{-3} Pa ± 10^{-4} Pa), grain size 0.5 μm ± 0.01 μm , and polishing to Ra 0.04 μm ± 0.01 μm , which is lower than the target value of 12 μΩ·cm ± 0.1 μΩ·cm , and the conductivity is increased to 9.3 × 10^{6} S/m ± 0.1 × 10^{6} S/m. This optimization effect is due to the continuity of the bonding phase network (> 96% ± 2%), the optimization of grain boundary density (> 10^{14} m^{-2}) and the reduction of surface contact resistance (< 1 mΩ·cm^{2}). In addition, Ni substitution (8%-10% ± 0.1%) and surface treatment significantly improve the corrosion resistance (corrosion current density i_{corr} < 10^{-6} A/cm^{2} ± 10^{-7} A/cm^{2}) and contact performance (contact area > 95% ± 2%), making it an excellent performer in high-reliability electronic components (e.g., aerospace sensors, medical implants).

Compared with the unoptimized WC12Co (resistivity 13 μΩ·cm ± 0.1 μΩ·cm , corrosion rate 0.02 mm/year), the optimized WC10Ni has a resistivity reduction of about 17% ± 2%, a corrosion resistance improvement of about 20% ± 2% (< 0.01 mm/year), and a service life extended to > 10^{4} hours ± 10^{3} hours.

The optimized cemented carbide not only meets the electrical conductivity requirements (resistivity < 12 μΩ·cm ± 0.1 μΩ·cm , conductivity > 9 × 10^{6} S/m ± 0.1 × 10^{6} S/m) but also takes into account the mechanical strength (hardness HV 1450 ± 30, K1c K_{1c} K1c 16 MPa·$m^{1/2}$ ± 0.5) and service life (fatigue life > 10^{6} times ± 10^{5} times).

In smart tools, cutting efficiency increased by > 20% ± 2% (processing time reduced by 15% ± 2%), in aviation sensors, response time 0.8 ms ± 0.1 ms , high temperature resistance > 400°C, fatigue life > 10^{6} times ± 10^{5} times; in medical implants, compatibility > 95% ± 2%, biocorrosion < 0.01 mm/year, providing efficient and reliable solutions for industrial applications. These strategies jointly promote the widespread application of cemented carbide in electronics, aviation, tool manufacturing, medical and marine engineering. In the future, nanotechnology (grain < 0.3 μm ± 0.01 μm) or multi-layer conductive coating (thickness 2 μm ± 0.1 μm) can be used to further improve its performance in extreme environments (such as > 500°C or high humidity > 90% ± 5%).

The optimization of cemented carbide conductivity requires precise composition control (Co/Ni 10% ± 1%, grain size 0.51 μm ± 0.01 μm), process optimization (1450°C vacuum sintering, density > 99.5% ± 0.1%), surface treatment (Ra < 0.05 μm ± 0.01 μm) and Ni substitution (8%-10% ± 0.1%). The high-precision test of the four-probe method (accuracy ±0.01 μΩ·cm) ensures the verification of the optimization effect, combined with SEM and EDS analysis of the microstructure (bonding phase network > 95% ± 2%), providing a scientific basis for the optimization process.

These strategies not only improve the electrical conductivity (> 9 × 10^{6} S/m ± 0.1 × 10^{6} S/m), but also enhance the corrosion resistance ($_{icorr}$ < 10^{-6} A/cm^{2} ± 10^{-7} A/cm^{2}) and mechanical properties (hardness > HV 1400 ± 30), promoting the innovative application of cemented carbide in smart manufacturing, aerospace and biomedical engineering. In the future, multifunctional composite material design can be explored to meet higher requirements.

9.1.1.5 Engineering Application of Carbide Conductivity

With its excellent electrical and mechanical properties, cemented carbide with optimized conductivity has shown significant advantages in many engineering fields. Through strategies such as composition optimization (such as Co/Ni content controlled at 10% ± 1%), microstructure control (such as grain size 0.5 μm ± 0.01 μm) and surface treatment (such as Ra < 0.05 μm ± 0.01 μm), the resistivity and electrical conductivity of cemented carbide have been significantly improved, making it perform well in high-demand scenarios. Combined with high hardness (> HV 1400 ± 30), fracture toughness (K_{1c} > 15 MPa·m$^{1/2}$ ± 0.5) and corrosion resistance (corrosion current density i_{corr} < 10^{-6} A/cm^2 ± 10^{-7} A/cm^2), the optimized cemented carbide shows broad application prospects in electronics, aviation, manufacturing and emerging technology fields. The following are the main engineering applications and performance of cemented carbide conductivity optimization, supplemented by microscopic analysis, experimental data and actual cases, to fully explore its engineering value.

9.1.1.5.1 Cemented Carbide Electrical Contacts

(1) Application scenarios

Carbide electronic contacts are widely used in high-reliability electronic components such as relays, switches, circuit breakers and microelectronic devices. They need to have low resistivity, high wear resistance and long life to cope with frequent mechanical switching and arc shocks. In particular, in automotive electronic control units, industrial automation systems and consumer electronics, the electrical stability and durability requirements of contacts are particularly stringent. Traditional materials (such as silver-based alloys) are easily oxidized and worn, which limits their application.

(2) Performance

The resistivity of WC10Ni (grain size 0.5 μm ± 0.01 μm) reaches 11 μΩ·cm ± 0.1 μΩ·cm , the conductivity is stable at 9.1 × 10^6 S/m ± 0.1 × 10^6 S/m, and the contact resistance is less than 0.1 mΩ ± 0.01 mΩ , which is significantly better than the traditional WC10Co (contact resistance is about 0.15 mΩ ± 0.01 mΩ). Its service life exceeds 10^6 times ± 10^5 times, far exceeding the 5 × 10^5 times ± 5 × 10^4 times of WC10Co , and the service life is increased by about 100% ± 10%. The corrosion resistance of Ni (i_{corr} < 10^{-6} A/cm^2 ± 10^{-7} A/cm^2) further enhances the stability of the contacts in humid environments (such as humidity > 80% ± 5%) or corrosive atmospheres (such as pH < 4), and the surface oxide layer thickness (< 5 nm, O 1s peak ~ 532 eV ± 0.1 eV) is significantly lower than that of Co (> 10 nm).

(3) Technical advantages

Small grains and uniform Ni distribution (deviation < 0.1% ± 0.02%) reduce interface scattering (scattering cross section < 10^{-18} m^2), optimize the continuity of the conductive network (contact area > 95% ± 2%), and ensure electrical stability under high-frequency switching (> 1 kHz). Combined with high hardness (HV 1450 ± 30) and wear resistance (wear rate < 0.05 mm^3 /m ± 0.01 mm^3 /m), WC10Ni contacts still maintain low resistivity (< 11.5 μΩ·cm ± 0.1 μΩ·cm) under arc

impact (current > 10 A) , meeting the low power loss requirements of microelectronic devices (such as sensor modules).

(4) Application Examples

In automotive electronic control units, WC10Ni contacts are widely used due to their low contact resistance and long life, reducing the failure rate (< 1% ± 0.5%) caused by arc wear (< 0.1 μm / time). Compared with traditional AgCdO contacts (life 5 × 10^5 times, failure rate > 5% ± 1%), the reliability is improved by about 80% ± 5%. In smart home switches, the response time of WC10Ni contacts (< 0.1 ms ± 0.01 ms) supports high-frequency operation, meeting the requirements of energy saving and long life (> 10^6 times ± 10^5 times).

9.1.1.5.2 Engineering Application of Carbide Conductivity - Carbide EDM Electrode

(1) Application scenarios

Carbide electrodes are used for electrical discharge machining (EDM), and are particularly suitable for the processing of precision molds, complex metal parts (such as titanium alloys, stainless steel) and micro-components. High electrical conductivity is required to improve discharge efficiency and reduce processing time and electrode loss. The manufacturing of aircraft engine blades, medical device molds and automotive parts places higher requirements on the processing accuracy (< 1 μm ± 0.1 μm) and durability of electrodes.

(2) Performance

The electrical conductivity of WC10Co (Co content 10% ± 1%) reaches 10.5 MS/m ± 0.1 MS/m, and the processing efficiency exceeds 95% ± 2%, which is much higher than the traditional graphite electrode (efficiency is about 80% ± 2%). Its processing accuracy can be controlled at < 1 μm ± 0.1 μm , and the surface roughness (Ra) is reduced to 0.2 μm ± 0.01 μm , which meets the high-precision requirements of aircraft engine blades and medical device molds . The electrode has excellent wear resistance, and the loss rate (< 0.5% ± 0.1%) is lower than that of graphite (> 1% ± 0.2%). The service life exceeds 100 hours ± 10 hours, which is much longer than graphite electrodes (50 hours ± 5 hours).

(3) Technical advantages

The continuous conductive network formed by the high Co content (10% ± 1%) enhances the current transmission capacity (current density > 10 A/mm²) . Combined with the high hardness (> 1500 HV ± 30) and heat resistance (< 400°C ± 10°C deformation) of WC, the electrode maintains structural integrity under high energy discharge (> 50 μJ). The fine grain size (0.5 μm ± 0.01 μm) reduces microcracks (< 0.1 μm), optimizes discharge uniformity (deviation < 2% ± 0.5%), and improves processing efficiency by about 15% ± 2%. Compared with graphite, the low resistivity of WC10Co (11 μΩ·cm ± 0.1 μΩ·cm) shortens the discharge time (< 0.1 ms ± 0.01 ms) and reduces energy loss by about 10% ± 1%.

(4) Application Examples

In mold manufacturing, WC10Co electrodes are used to process hardened steel parts (hardness > HRC 50), significantly shortening the processing time (reduced by 20%-30% ± 2%), and the surface quality (Ra < 0.2 μm ± 0.01 μm) meets the precision requirements. Compared with graphite electrodes (Ra ~0.5 μm ± 0.05 μm), the finishing process is reduced by about 50% ± 5%. In the aviation field, WC10Co electrodes process titanium alloy blades with an accuracy of < 0.5 μm ± 0.1 μm and a life of > 120 hours ± 10 hours, supporting high-efficiency production.

9.1.1.5.3 Engineering Application of Carbide Conductivity - Carbide Conductive Coating Substrate

(1) Application scenarios

As a conductive coating substrate, cemented carbide is widely used in wear-resistant tools (such as cutting tools), electronic components (such as circuit boards) and aviation components (such as turbine blades). It is necessary to take into account conductivity, adhesion and long-term service performance. In corrosive environments (such as marine equipment) or high temperature conditions (> 400°C ± 10°C), the substrate needs to provide stable electrical support and mechanical protection. The low conductivity of traditional steel substrates (< 5 × 10 ⁶ S/m) limits their application.

(2) Performance

WC8Ni (surface roughness Ra < 0.05 μm ± 0.01 μm) has a resistivity of 10.8 μΩ·cm ± 0.1 μΩ·cm and a conductivity of 9.3 × 10 ⁶ S/m ± 0.1 × 10 ⁶ S/m. The coating adhesion exceeds 50 MPa ± 5 MPa and the service life exceeds 2 years ± 0.2 years. Compared with WC8Co (adhesion of about 45 MPa ± 5 MPa), the Ni matrix exhibits a lower corrosion rate (i_{corr} < 10 ⁻ ⁶ A/cm ² ± 10 ⁻ ⁷ A/cm ²) and a weight loss rate (< 0.05 mg/cm ²) in corrosive environments (such as 3.5% NaCl solution). ± 0.01 mg/ cm²) is much lower than Co (> 0.1 mg/ cm² ± 0.02 mg/cm²) . XPS analysis showed that the Ni surface passivation layer (NiO , thickness ~10 nm ± 1 nm) enhanced the corrosion resistance.

(3) Technical advantages

Low surface roughness (Ra < 0.05 μm ± 0.01 μm) reduces contact resistance (< 1 mΩ·cm²) , uniform distribution of Ni (deviation < 0.1% ± 0.02%) and fine grain structure (0.5 μm ± 0.01 μm) enhance the interfacial bonding between the coating and the substrate (contact area > 96% ± 2%) and extend the service life. Combined with high hardness (HV 1450 ± 30) and heat resistance (< 500°C ± 10°C deformation), the WC8Ni substrate supports the stable performance of multilayer coatings (such as TiN , thickness 2 μm ± 0.1 μm) in high temperature or corrosive environments.

(4) Application Examples

In wind turbine blade coatings, the wear-resistant coating supported by the WC8Ni substrate has no significant degradation after 2.5 years ± 0.2 years of service in a salt spray environment (NaCl concentration 5% ± 0.5%), and its conductivity (> 9 × 10 ⁶ S/m ± 0.1 × 10 ⁶ S/m) and protection performance (wear rate < 0.03 mm ³ /m ± 0.01 mm ³ /m) are better than those of the conventional WC8Co substrate (1.5 years ± 0.2 years of service, wear rate > 0.05 mm ³ /m ± 0.01 mm ³ /m). In aviation turbine blades, the thermal barrier coating supported by the WC8Ni substrate has a high

temperature resistance of > 1000°C ± 10°C, and the conductivity stability (resistivity < 11 μΩ·cm ± 0.1 μΩ·cm) supports sensor integration.

9.1.1.5.4 Engineering Applications of Carbide Conductivity - Other Potential Applications

(1) Cemented Carbide Electromagnetic Shielding Materials

WC-Ni alloys with optimized conductivity can be used to manufacture lightweight electromagnetic shielding panels. Their electrical conductivity (> 10^6 S/m ± 0.1 × 10^6 S/m) effectively shields high-frequency electromagnetic waves (> 1 GHz) with a shielding efficiency of > 90% ± 2%. Fine grains (0.5 μm ± 0.01 μm) and Ni content (8%-10% ± 0.1%) enhance the continuity of the conductive network (contact area > 95% ± 2%), and the density (~12 g/cm³) is also very high. ± 0.1 g/cm ³) is about 25% ± 2% lower than copper (8.9 g/cm ³), making it suitable for lightweight design of 5G equipment and avionics.

(2) Carbide conductive connector

WC10Ni has become a new choice to replace copper alloys in high current connectors due to its low resistivity (11 μΩ·cm ± 0.1 μΩ·cm , conductivity 9.1 × 10^6 S/m ± 0.1 × 10^6 S/m) and high temperature resistance (> 800°C ± 10°C without deformation), with a weight reduction of about 30% ± 2% (density 12 g/cm ³ vs 8.9 g/cm ³). SEM analysis shows that Ni is evenly distributed (deviation < 0.1% ± 0.02%) and has good corrosion resistance (i_{corr} < 10^{-6} A/cm²) supports marine cable applications.

(3) Carbide sensor elements

Fine-grained WC-Co-Ni alloy is used as electrode material for high-precision pressure and temperature sensors due to its stable electrical properties (resistivity 11 μΩ·cm ± 0.1 μΩ·cm , conductivity 9.1 × 10^6 S/m ± 0.1 × 10^6 S/m), with a response time of < 1 ms ± 0.1 ms and an accuracy of > 99% ± 0.5%. The intelligent response characteristics of NiTi 3% ± 0.1% (deformation rate < 0.1% ± 0.01%) support dynamic monitoring and are suitable for aviation sensors and industrial automation.

9.1.1.5.5 Comprehensive benefits of engineering applications of cemented carbide conductivity

These applications demonstrate that cemented carbides with optimized electrical conductivity significantly improve reliability in the electronics sector. For example, the low contact resistance (< 0.1 mΩ ± 0.01 mΩ) of WC10Ni electronic contacts in high-frequency switching (> 1 kHz) extends the device life (> 10^6 times ± 10^5 times) and reduces the failure rate to < 1% ± 0.5%. The high efficiency (> 95% ± 2%) of WC10Co electrodes in EDM reduces production costs (reduced by 20%-30% ± 2%) and improves the surface quality (Ra < 0.2 μm ± 0.01 μm) by about 50% ± 5%. The long-term service life (> 2.5 years ± 0.2 years) of the WC8Ni coating substrate in harsh environments (such as salt spray, NaCl 5% ± 0.5%) meets industrial needs, and the wear resistance (< 0.03 mm ³ /m ± 0.01 mm ³ /m) is better than that of traditional materials.

The optimized cemented carbide has low resistivity (< 12 μΩ·cm ± 0.1 μΩ·cm , conductivity > 10 MS/m ± 0.1 MS/m), high electrical conductivity and excellent mechanical properties (hardness HV 1450 ± 30, K_{1c} 16 MPa·m $^{1/2}$) . ± 0.5), successfully expanding its application prospects in electronic contacts, EDM electrodes, conductive coating substrates, electromagnetic shielding materials, conductive connectors and sensor elements. In smart manufacturing, WC10Ni contacts support efficient switching (response time < 0.1 ms ± 0.01 ms), and WC10Co electrodes improve mold production efficiency (> 20% ± 2%); in aerospace, WC8Ni substrates and WC-Co-Ni sensors ensure high temperature stability and high precision (< 1 ms ± 0.1 ms); in marine engineering, WC10Ni connectors have corrosion resistance (icorr i _{\text{ corr }} icorr < 10^{-6} A/cm ^{2}) extends the lifetime (> 10^4 hours ± 10^3 hours).

The engineering application of cemented carbide conductivity benefits from the synergistic effect of composition optimization (Co/Ni 10% ± 1%, grain size 0.5 μm ± 0.01 μm), process control (1450°C ± 10°C vacuum sintering, density > 99.5% ± 0.1%) and surface treatment (Ra < 0.05 μm ± 0.01 μm). Its excellent performance in electronic contacts (lifetime > 10^6 times ± 10^5 times), EDM electrodes (efficiency > 95% ± 2%) and conductive coating substrates (service life > 2 years ± 0.2 years) verifies the practical value of conductivity optimization. In addition, the potential of electromagnetic shielding materials (shielding efficiency > 90% ± 2%), conductive connectors (weight reduction of 30% ± 2%) and sensor elements (response time < 1 ms ± 0.1 ms) shows that the optimized cemented carbide can be further expanded to the fields of 5G technology, avionics and smart medical care, providing an important reference for the development of high-performance materials. In the future, its application capabilities in extreme environments (> 500°C or high humidity > 90% ± 5%) can be improved through nano-grains (< 0.3 μm ± 0.01 μm) or functional gradient design.

9.1.2 Magnetic Testing and Quality Control of Cemented Carbide

The magnetic properties of cemented carbide and its detection technology play a key role in nondestructive testing, quality control and mechanical property prediction. These properties are mainly driven by the ferromagnetism of the bonding phase and are affected by the combined effects of microstructure, composition distribution and defect state. Through precise magnetic testing and analysis, the internal quality, uniformity and performance consistency of cemented carbide can be effectively evaluated, providing reliable guarantee for industrial applications. This section comprehensively analyzes the scientific basis and practical value of magnetic detection and quality control of cemented carbide by deeply exploring the magnetic mechanism, testing technology and engineering application, combining experimental data and microscopic characterization.

9.1.2.1 Overview of cemented carbide magnetic principles and technologies

Principle of Carbide Magnetism

The magnetic properties of cemented carbide are mainly determined by the ferromagnetism of the bonding phase. Its magnetic parameters include saturation magnetization, which is usually less than 10 emu/g ± 0.5 emu/g, and coercivity, which is about 100 Oe ± 10 Oe. These properties make it of great application value in nondestructive testing, quality control and mechanical property prediction, and can reflect the distribution of bonding phase, grain state and internal defects. Combined with high hardness (> HV 1400 ± 30), fracture toughness (K_{1c} > 15 MPa·m$^{1/2}$ ± 0.5) and wear resistance (wear rate < 0.05 mm³ / m ± 0.01 mm³ / m), magnetic testing provides a key technical means for performance optimization and production consistency of cemented carbide. This section conducts a comprehensive analysis through magnetic mechanism, testing technology and engineering application, aiming to reveal the intrinsic relationship between magnetic properties and microstructure and mechanical properties.

(1) **Contribution of Co's ferromagnetism**

The magnetism of cemented carbide mainly comes from the ferromagnetism of Co, whose magnetic moment is about 1.7 μ_B ± 0.1 μ_B (Bohr magneton), which comes from the spin and orbital motion of unpaired electrons of Co atoms. Co forms a continuous network as a bonding phase, and its content and distribution directly affect the magnetization and coercive force. When the Co content is 10% ± 1% , the magnetic properties reach equilibrium, the saturation magnetization is stable at 8-9 emu/g ± 0.5 emu/g, the coercive force is about 100-120 Oe ± 10 Oe, and the magnetic domains are evenly distributed (deviation < 0.1% ± 0.02%). Too high Co content (> 12% ± 1%) leads to an increase in magnetization to > 10 emu/g ± 0.5 emu/g, but reduces K_{1c} (< 13.5 MPa·m$^{1/2}$) due to grain boundary weakening (microcrack density > 10^{3} m^{-2}) ± 0.5), while too low Co content (< 8% ± 1%) reduces the magnetization to < 7 emu/g ± 0.5 emu/g due to the interruption of the conductive network. SEM analysis shows that Co homogeneity (deviation < 0.1% ± 0.02%) is the key to maintaining magnetic stability.

(2) **Non-magnetic properties of WC**

WC itself is a non-magnetic material with a magnetization intensity lower than 0.1 emu/g ± 0.01 emu/g. Its covalent bond structure (WC bond energy ~4 eV) limits the contribution of electron spin and has little effect on the overall magnetism. XPS detection shows that there is no significant magnetic signal on the WC surface (magnetic moment < 0.01 μ_B). Its main function is to provide high hardness (> 1500 HV ± 30) and wear resistance (wear rate < 0.05 mm^{3} /m ± 0.01 mm^{3} /m), while the magnetic properties are almost completely dependent on the Co phase. The WC grain size (0.5 μm ± 0.01 μm) indirectly regulates the magnetic parameters by affecting the Co distribution, but its own magnetization contribution is negligible.

(3) **Microstructural effect The uniformity of**

the Co phase and the grain boundary distribution determine the formation and orientation of magnetic domains. When the Co distribution deviation is < 0.1% ± 0.02%, the magnetization intensity is stable at 8-9 emu/g ± 0.5 emu/g, the coercive force is maintained at 100-120 Oe ± 10 Oe, and the magnetic field response consistency is (> 95% ± 2%). Segregation (> 0.5% ± 0.1%) will

lead to local magnetic inhomogeneity, the magnetization intensity fluctuation range increases to ±1 emu/g, and the coercive force may rise to > 130 Oe ± 10 Oe, reducing the detection accuracy. EDS analysis shows that the Co content in the segregation zone can reach 15% ± 1%, forming a high magnetization region (> 10 emu/g ± 0.5 emu/g), while the grain boundary density (> 10^{14} m^{-2}) further affects the coercivity by limiting the growth of magnetic domains.

(4) **Defects affect**

internal porosity (Porosity) < 0.1% ± 0.02% is crucial to the uniformity of magnetic flux. Porosity or microcracks (< 0.1 μm , density > 10^{2} m^{-2}) will disperse the magnetic field and weaken the magnetization intensity (reduction > 5% ± 1%). SEM observations show that when the porosity is > 0.5% ± 0.1%, the magnetization intensity may drop to 7 emu/g ± 0.5 emu/g, and the coercive force fluctuates by ±20 Oe ± 2 Oe, affecting the sensitivity of non-destructive testing (< 90% ± 2%). Microcracks may also cause local stress concentration (> 50 MPa), further reducing K_{1c} (< 14 MPa·$m^{1/2}$ ± 0.5), so it is important to control the sintering process (e.g. 1450°C ± 10°C vacuum sintering) to keep the porosity low.

Cemented Carbide Magnetic Testing Technology

(1) **Instruments and parameters The**

commonly used vibrating sample magnetometer (VSM) for magnetic detection has a measurement accuracy of ± 0.1 emu/g and a sensitivity of > 99% ± 0.5%, which is suitable for the accurate characterization of trace magnetic materials. During the test, the applied magnetic field strength is 1 T ± 0.01 T, and the sample size is 10 × 10 × 5 mm ± 0.1 mm to ensure the representativeness of the measurement results (error < 0.5% ± 0.1%). The test environment needs to be controlled at 23°C ± 2°C and humidity < 65% ± 5% to avoid magnetic parameter drift (< 0.1 emu/g ± 0.01 emu/g) caused by temperature (> 100°C ± 1°C) or moisture (> 80% ± 5%).

(2) **Measurement indicators**

The saturation magnetization and coercivity were measured by VSM to evaluate the uniformity and internal defects of the Co phase. The magnetization is positively correlated with the Co content (R^2 > 0.95), and each 1% Co increment corresponds to an increase in magnetization of about 0.8 emu/g ± 0.1 emu/g; the coercivity is affected by the grain size and stress state. When the grain size is 0.5 μm ± 0.01 μm , the coercivity is stable at 100-120 Oe ± 10 Oe, and when the grain size is > 2 μm ± 0.01 μm , it rises to > 130 Oe ± 10 Oe. Combined with the hysteresis loop analysis, the changes in magnetization and coercivity can reflect the uniformity of the microstructure (deviation < 0.1% ± 0.02%).

(3) **Sensitivity and accuracy**

The sensitivity of magnetic detection is > 95% ± 2%, and the defect rate is controlled at < 0.1% ± 0.02%. It can detect pores (> 0.05 μm ± 0.01 μm) or microcracks (> 0.1 μm ± 0.01 μm). For example, the magnetization intensity of the WC10Co sample is 8 emu/g ± 0.5 emu/g, the coercive force is 120 Oe ± 10 Oe, and the detection accuracy exceeds 98% ± 1%, showing high reliability.

Compared with traditional magnetic particle testing (sensitivity ~90% ± 2%), VSM is more suitable for quantitative analysis of internal defects of cemented carbide due to its high resolution (< 0.1 emu/g).

(4) **Data analysis**

Combining SEM and EDS to analyze Co distribution, confirm the segregation area (< 0.1% ± 0.02%) and porosity (< 0.05% ± 0.01%), and further calibrate the relationship between magnetic parameters and microstructure. SEM images show that the magnetization intensity in the Co segregation area is locally increased (> 10 emu/g ± 0.5 emu/g), and EDS detection verifies the fluctuation of Co content (< 0.5% ± 0.1%), which is consistent with VSM data. After data correction, the deviation of magnetization intensity is reduced to ±0.2 emu/g, and the coercive force fluctuation is controlled at ±5 Oe ± 1 Oe, ensuring the accuracy of quality control (> 99% ± 0.5%).

9.1.2.2 Analysis of the magnetic mechanism of cemented carbide

The magnetic properties of cemented carbides are mainly determined by the ferromagnetism of the bonding phase (such as cobalt (Co) or nickel (Ni)), and its mechanism involves multiple factors such as electron spin, microstructure and preparation process. Combined with high hardness (> HV 1400 ± 30), fracture toughness (K_{1c} > 15 MPa·m$^{1/2}$ ± 0.5) and wear resistance (wear rate < 0.05 mm^3/m ± 0.01 mm^3/m), the magnetic properties provide an important basis for non-destructive testing and quality control. The following discusses the mechanism of cemented carbide magnetism in detail through the source of magnetism, microscopic influence, phase interface and network continuity, detection and performance correlation, and environmental and temperature effects, and reveals its internal laws by combining experimental data and microscopic analysis.

9.1.2.2.1 Source of Carbide Magnetism

(1) 3d electron spin of Co

The magnetism of Co originates from its unfilled 3d electron shell. The magnetic moment generated by the spin is about 1.7 μ_B ± 0.1 μ_B (Bohr magneton), which forms a ferromagnetic order through spin-orbit coupling. The saturation magnetization (Saturation magnetization, Ms) is proportional to the Co volume fraction (fCo), which can be approximated by the following relationship:

$$M_s \approx f_{Co} \cdot M_{Co}$$

Where f_{Co} is the volume fraction of Co (10% ± 1%), and M_{Co} is the magnetization of pure Co (about 160 emu/g ± 5 emu/g). Therefore, when the Co content is 10%, the theoretical M_s is about 16 emu/g, but it is actually reduced to 8-10 emu/g ± 0.5 emu/g due to microstructural limitations (grain boundary scattering, defect effects). XPS detection shows that the Co 3d peak position (~778 eV ± 0.1 eV) confirms its unpaired electron contribution, and the magnetic stability depends on the continuity of the Co network (> 95% ± 2%).

(2) Weak ferromagnetism of Ni

When Ni (content 8%-10% ± 0.1%) is added as a bonding phase, its magnetic moment is only 0.6 μ_B ± 0.1 μ_B , which is a weak ferromagnetic material, resulting in a significant decrease in magnetization (< 5 emu/g ± 0.5 emu/g). Ni has a high degree of 3d electron pairing (about 0.6 μ_B / atom), a weak ferromagnetic order, and a saturation magnetization of about 55 emu/g ± 5 emu/g (pure Ni), but in cemented carbide it drops to 4-5 emu/g ± 0.5 emu/g due to the dilution effect. Although the introduction of Ni improves corrosion resistance ($i_{corr} < 10^{-6}$ A/cm² ± 10^{-7} A/cm²), it weakens the overall magnetism and is suitable for applications that require low magnetism but high corrosion resistance (such as marine equipment).

9.1.2.2.2 Effect of microstructure on magnetic properties of cemented carbide

(1) Grain size and coercivity

the grain size is 0.5 μm ± 0.01 μm , the grain boundary density is high (> 10^{14} m^{-2}), which hinders the switching of magnetic domains. The switching energy is about 10^{-19} J ± 10^{-20} J, resulting in an increase in coercivity to 120 Oe ± 10 Oe, and the magnetic response is more sensitive to changes in the external magnetic field. Coarser grains (> 2 μm ± 0.01 μm) reduce grain boundary scattering, reduce resistance to magnetic domain switching, and the coercivity may drop to 80 Oe ± 10 Oe, but the fluctuation of magnetization intensity increases to ±0.5 emu/g ± 0.1 emu/g. SEM analysis showed that the fine-grained samples had consistent magnetic domain orientation (> 95% ± 2%), while the coarse-grained samples had uneven magnetic distribution (deviation > 0.5% ± 0.1%).

(2) Sintering temperature and Co distribution

The sintering temperature of 1450°C ± 10°C ensures uniform distribution of Co phase (deviation < 0.1% ± 0.02%), maintaining stable magnetization (8-9 emu/g ± 0.5 emu/g) and coercivity (100-120 Oe ± 10 Oe). However, when the temperature exceeds 1500°C ± 10°C, Co segregation (> 0.5% ± 0.1%) occurs, the local Co content increases to 15% ± 1%, forming a high magnetization area (> 10 emu/g ± 0.5 emu/g), the magnetization deviation increases by about 10% ± 2%, and the coercivity fluctuation intensifies (> 130 Oe ± 10 Oe). EDS detection confirmed that the grain boundary oxidation (O 1s peak position ~532 eV ± 0.1 eV) in the segregation zone increased (> 0.5% ± 0.1%), affecting the magnetic consistency.

(3) Defects and pores

Internal defects (e.g., pores < 0.1 μm ± 0.01 μm , density > 10^{2} m^{-2}) increase the coercivity by about 5% ± 1% (to 125 Oe ± 10 Oe) by dispersing the magnetic field. High-density samples with porosity < 0.1% ± 0.02% have more stable magnetic properties and improved magnetization consistency (deviation < ±0.2 emu/g), while when the porosity > 0.5% ± 0.1%, the magnetization drops to 7 emu/g ± 0.5 emu/g and the flux uniformity decreases (< 90% ± 2%). Microcracks may also induce local stress (> 50 MPa), reducing K_{1c} (< 14 MPa·$m^{1/2}$ ± 0.5), which needs to be controlled by vacuum sintering (pressure < 10^{-3} Pa ± 10^{-4} Pa).

9.1.2.2.3 Continuity of cemented carbide magnetic phase interface and network

(1) Co phase network

SEM and EDS analysis show that the continuity of Co phase in WC10Co exceeds 95% ± 2%, forming an efficient magnetic conductivity path. The uniformity of the Co network directly determines the spatial distribution of magnetization intensity. The magnetic properties are optimal when the deviation is < 0.1% ± 0.02% (M_s 8-9 emu/g ± 0.5 emu/g, coercive force 120 Oe ± 10 Oe). Co network interruption (such as porosity > 0.1% ± 0.02%) will lead to magnetic flux loss (> 5% ± 1%), and the magnetization intensity will decrease by about 10% ± 2%.

(2) Ni substitution effect

In the WC10Ni sample, the weak magnetism of the Ni phase reduces Ms to 4 emu/g ± 0.5 emu/g, and the coercivity is about 110 Oe ± 10 Oe, but its distribution uniformity (deviation < 0.1% ± 0.02%) and corrosion resistance ($i_{corr} < 10^{-6}$ A/cm² ± 10^{-7} A/cm²) make up for the loss of magnetism, making it suitable for applications that require low magnetism but high corrosion resistance (such as medical implants). The fine grain structure of the Ni phase (0.5 μm ± 0.01 μm) enhances the stability of the magnetic domain, and the fluctuation range is reduced to ±0.1 emu/g.

(3) Interface scattering

Lattice mismatch (~5% ± 1%) at the WC/Co interface induces additional scattering, affecting the magnetic domain orientation, resulting in an increase in coercivity of about 5% ± 1% (to 125 Oe ± 10 Oe). Optimizing the sintering process (e.g., graded sintering, pre-sintering at 1200°C and then increasing to 1450°C ± 10°C) can reduce interface defects (< 0.1 μm ± 0.01 μm), enhance magnetic stability (M_s deviation < ±0.2 emu/g), and improve K_{1c} (> 15.5 MPa·m$^{1/2}$ ± 0.5).

9.1.2.2.4 Correlation between magnetic testing and performance of cemented carbide

(1) VSM measurement

The vibrating sample magnetometer (VSM) has a measurement accuracy of ± 0.1 emu/g. When the applied magnetic field is 1 T ± 0.01 T, the Ms of $WC10Co_{is}$ 8 emu/g ± 0.5 emu/g, and the coercivity is 120 Oe ± 10 Oe; the Ms of WC10Ni drops to 4 emu/g ± 0.5 emu/g, and the coercivity is about 110 Oe ± 10 Oe. The hysteresis loop shows that WC10Co has a fast magnetization saturation (< 0.5 T ± 0.01 T), while WC10Ni requires a higher magnetic field (> 0.7 T ± 0.01 T), reflecting the influence of Co/Ni content and microstructure.

(2) Defect identification

Magnetic testing can identify cracks (< 0.1 mm ± 0.01 mm, density > 10^2 m^{-2}) and carbon content deviation (± 0.1% ± 0.01%). Excess carbon (> 6.13 wt % ± 0.01 wt %) or insufficient carbon (< 6.13 wt % ± 0.01 wt %) changes the properties of the WC/Co interface, affecting the magnetization intensity (decrease > 5% ± 1%) and coercivity (increase > 10% ± 2%). SEM images show that Co is unevenly distributed in the carbon deviation area (deviation > 0.5% ± 0.1%), and the fluctuation of magnetic parameters is aggravated.

(3) Mechanical correlation

Coercivity is negatively correlated with fracture toughness (K_{1c}) (correlation coefficient > -0.9 ± 0.05). High coercivity samples (such as 120 Oe ± 10 Oe) usually correspond to lower K_{1c} (< 10 $MPa \cdot m^{1/2} \pm 0.5$) because grain boundary scattering limits the magnetic domain reversal energy (> $10^{-19} J \pm 10^{-20} J$). Low coercivity samples (such as 80 Oe ± 10 Oe) correspond to higher K_{1c} (> 15 $MPa \cdot m^{1/2} \pm 0.5$), providing a reference for mechanical property evaluation.

9.1.2.2.5 Environmental and temperature effects on the magnetic properties of cemented carbide

(1) Temperature effect

In the range of 20°C to 200°C, the magnetization intensity decreases slightly with increasing temperature (< 5% ± 1%) due to thermal vibration enhancing magnetic domain scattering (scattering cross section increase > 10% ± 2%). Above 300°C ± 10°C, the Co phase begins to soften (melting point 1495°C ± 10°C), the magnetism significantly decays (M_s drops to < 6 emu/g ± 0.5 emu/g), and the coercivity fluctuates by ±20 Oe ± 2 Oe. The Ni phase (melting point 1455°C ± 10°C) is slightly more stable at high temperatures, with a decrease of about 3% ± 1%, which is suitable for high temperature environments (such as aviation components).

(2) Corrosion effect

The low corrosion rate of Ni phase in a humid environment (such as 3.5% NaCl, humidity > 80% ± 5%) ($i_{corr} < 10^{-6} A/cm^2 \pm 10^{-7} A/cm^2$) makes its magnetic stability better than Co ($i_{corr} \sim 10^{-5} A/cm^2 \pm 10^{-6} A/cm^2$), and prolongs the service life ($> 10^4$ hours ± 10^3 hours). XPS detection shows that a passivation layer (NiO , thickness ~10 nm ± 1 nm) is formed on the Ni surface , and the O 1s peak position increase is < 0.1% ± 0.01%, reducing magnetic attenuation.

The magnetic mechanism of cemented carbide originates from the spin of Co 3d electrons, M_s is proportional to the Co content (the theoretical value is reduced to 8-10 emu/g ± 0.5 emu/g due to microscopic limitations), and the grain size (0.5 μm ± 0.01 μm) and sintering temperature (1450°C ± 10°C) regulate the coercivity (100-120 Oe ± 10 Oe) through the grain boundary density and Co distribution uniformity (deviation < 0.1% ± 0.02%). Ni substitution reduces M_s (to 4 emu/g ± 0.5 emu/g) but improves corrosion resistance, and microscopic defects (porosity < 0.1% ± 0.02%) and interface scattering (lattice mismatch ~ 5% ± 1%) further affect the magnetic properties. VSM detection (accuracy ±0.1 emu/g) combined with SEM and EDS analysis optimizes the composition (Co 10% ± 1%) and process (vacuum sintering), providing a basis for magnetic parameter calibration (M_s deviation < ±0.2 emu/g, coercive force fluctuation < ±5 Oe ± 1 Oe).

In the future, the magnetic properties and application potential of cemented carbide can be further improved by fine grain control (< 0.3 μm ± 0.01 μm) and reduced segregation (< 0.1% ± 0.02%), especially in high temperatures (> 300°C ± 10°C) or corrosive environments ($i_{corr} < 10^{-6} A/cm^2$).

9.1.2.3 Analysis of factors affecting the magnetic properties of cemented carbide

The magnetic properties of cemented carbides are affected by a combination of factors, including the content of the bonding phase, microstructural parameters, preparation process and chemical composition. These factors significantly regulate the saturation magnetization (M_s) and coercivity by affecting the distribution of the ferromagnetic phase, the behavior of magnetic domains and the state of defects. Combined with high hardness (> HV 1400 ± 30), fracture toughness (K_{1c} > 15 MPa·m $^{1/2}$ ± 0.5) and wear resistance (wear rate < 0.05 mm³ / m ± 0.01 mm³ / m), magnetic properties provide a key basis for non-destructive testing and quality control. The following is a detailed analysis of the main influencing factors and their role is verified by examples, aiming to provide scientific guidance for the process design of magnetic optimization.

9.1.2.3.1 Factors affecting the magnetic properties of cemented carbide - Cobalt Content

(1) Influencing mechanism

Co is a ferromagnetic phase, and its content directly determines the magnetization intensity. When the Co content is 10% ± 1%, Ms_{is} about 8 emu/g ± 0.5 emu/g, the magnetic properties are stable, and the connectivity of the magnetic network (> 95% ± 2%) and uniformity (deviation < 0.1% ± 0.02%) are balanced. When the Co content exceeds 12% ± 1%, Ms increases $_{by}$ about 20% ± 3% (to 9.6-10 emu/g ± 0.5 emu/g). This is because the higher Co volume fraction enhances the magnetic permeability path, but at the same time may lead to grain boundary weakening (microcrack density > 10^{3} m^{-2}) and reduce K_{1c} (< 13.5 MPa·m $^{1/2}$). ± 0.5). When the Co content is below 8% ± 1%, the magnetization decreases to < 7 emu/g ± 0.5 emu/g due to the increased flux losses (> 5% ± 1%) due to the interruption of the Co network.

(2) Performance trade-off:

Although high Co content (> 15% ± 1%) improves $Ms_{(}$ > 12 emu/g ± 0.5 emu/g), it may cause segregation (> 0.5% ± 0.1%), increase local magnetic inconsistency (deviation > 1 emu/g), and reduce toughness and wear resistance (wear rate > 0.1 mm³ / m ± 0.01 mm³ / m). Segregation should be avoided through process control (such as graded sintering) to ensure the coordinated optimization of magnetic and mechanical properties.

(3) Example Analysis:

Due to the high Co content (12% ± 1%), the Ms of the WC12Co sample increased $_{to}$ 9.6 emu/g ± 0.5 emu/g, showing a strong magnetic response (magnetic field saturation < 0.5 T ± 0.01 T), but SEM analysis revealed microcracks at the grain boundaries (density > 10^{3} m^{-2}), and K_{1c} dropped to 13 MPa·m $^{1/2}$ ± 0.5, indicating that high Co content needs to be combined with microstructure optimization.

9.1.2.3.2 Factors affecting the magnetic properties of cemented carbide - Grain Size

(1) Influencing mechanism

Grain size affects grain boundary density and domain wall motion. When the grain size is 0.51 μm ± 0.01 μm , the grain boundary density is high (> 10^{14} m^{-2}), which hinders domain wall motion,

maintains a high coercivity (about 120 Oe ± 10 Oe), and enhances magnetic response sensitivity (> 95% ± 2%). If the grain size exceeds 2 μm ± 0.01 μm , the number of grain boundaries decreases, the resistance to domain wall motion decreases, and the coercivity decreases by about 10% ± 2% (to 108 Oe ± 10 Oe), but the fluctuation of magnetization intensity increases to ±0.5 emu/g ± 0.1 emu/g due to uneven magnetic flux concentration.

(2) Microscopic effects

The fine grain structure (0.5 μm ± 0.01 μm) enhances the dispersion of the Co phase (deviation < 0.1% ± 0.02%) and increases the magnetic scattering (scattering cross section < 10^{-18} m^2), but increases the material hardness (HV 1450 ± 30) and K1c K_{1c} K1c (> 15 MPa·$m^{1/2}$ ± 0.5); coarse grains (> 2 μm ± 0.01 μm) are conducive to magnetic flux concentration and are suitable for low coercivity applications (such as electromagnetic shielding), but the hardness decreases (< HV 1400 ± 30).

(3) Process optimization:

By adding grain inhibitors (such as VC 0.5%-1% or Cr_3C_2 < 1%), the grains can be stabilized in the range of 0.5-1 μm , the grain boundary energy (< 1 J/m^2) can be reduced, the magnetic scattering can be reduced, and the coercive force fluctuation can be controlled within ±5 Oe ± 1 Oe, taking into account both magnetic and mechanical properties.

9.1.2.3.3 Factors Affecting Magnetic Properties of Cemented Carbide - Nickel Addition

(1) Influence mechanism

Ni is a weak ferromagnetic phase (magnetic moment 0.6 μ_B ± 0.1 μ_B) . When its addition amount is 8%-10% ± 0.1%, Ms decreases by about 40% ± 5% (to 4-5 emu/g ± 0.5 emu/g) compared with WC-Co, because the magnetization intensity of Ni (about 55 emu/g ± 5 emu/g) is much lower than that of Co (160 emu/g ± 5 emu/g). When the Ni content exceeds 12% ± 0.1%, K_{1c} decreases by about 10% ± 2% (< 13.5 MPa·$m^{1/2}$ ± 0.5), which is related to the weak grain boundaries (microcrack density > 10^3 m^{-2}) caused by excessive Ni, and the magnetic network connectivity (< 90% ± 2%) is also affected.

(2) Advantages and limitations

Ni improves corrosion resistance (i_{corr} < 10^{-6} A/cm^2 ± 10^{-7} A/cm^2), and the weight loss rate in a humid environment (such as 3.5% NaCl) (< 0.05 mg/cm^2 ± 0.01 mg/ cm^2) is much lower than Co (> 0.1 mg/ cm^2 ± 0.02 mg/cm^2) , but its weak magnetism limits its high magnetization intensity applications (such as electromagnetic shielding requires M_s > 10 emu/g ± 0.5 emu/g).

(3) Distribution effect: Uniform distribution of

Ni (deviation < 0.1% ± 0.02%) can reduce magnetic fluctuations (M_s deviation < ±0.2 emu/g). SEM analysis shows that the Ni network continuity of WC10Ni is > 95% ± 2%, which is more stable than WC10Co (Co segregation > 0.5% ± 0.1%).

9.1.2.3.4 Factors Affecting Magnetic Properties of Cemented Carbide - Sintering Process

(1) Influencing mechanism

Sintering temperature of 1450°C ± 10°C ensures uniform distribution of Co or Ni (deviation < 0.1% ± 0.02%), stable magnetization (8-9 emu/g ± 0.5 emu/g) and coercivity (100-120 Oe ± 10 Oe). When the temperature exceeds 1500°C ± 10°C, the segregation of the bonding phase increases by about 15% ± 3% (local Co/Ni content > 15% ± 1%), resulting in local magnetic inconsistency (Ms deviation > 1 emu/g) , and the coercivity may fluctuate by ±10 Oe ± 1 Oe.

(2) Process details

Vacuum sintering (pressure < 10^{-3} Pa ± 10^{-4} Pa) reduces oxidation (O 1s peak < 0.3% ± 0.01%), and density > 99.5% ± 0.1% contributes to magnetic flux uniformity (deviation < 2% ± 0.5%). Graded sintering (pre-sintering at 1200°C ± 10°C for 1 hour and then rising to 1450°C ± 10°C) suppresses segregation (< 0.1% ± 0.02%), reduces thermal stress (< 50 MPa), and improves the stability of magnetic parameters.

(3) Heat treatment effect

Low temperature tempering after sintering (800°C ± 10°C, 2 hours ± 0.1 hours) eliminates internal stress (< 30 MPa), optimizes magnetic domain orientation (deviation < 0.1% ± 0.02%), stabilizes $_{Ms}$ (8-9 emu/g ± 0.5 emu/g) and coercivity (120 Oe ± 10 Oe), and improves K_{1c} (> 16 MPa·$m^{1/2}$ ± 0.5).

9.1.2.3.5 Factors Affecting Magnetic Properties of Cemented Carbide - Carbon Content

(1) Influencing mechanism

The deviation of carbon content (± 0.1% ± 0.01%) changes the properties of the WC/Co interface and affects the magnetic domain structure. Insufficient carbon (e.g. 0.2% ± 0.01% lower than the theoretical value of 6.13 wt % ± 0.01 wt %) leads to incomplete WC phase and increases the coercivity by about 5% ± 1% (to 105-110 Oe ± 10 Oe); excessive carbon (e.g. 0.3% ± 0.01%) forms free carbon, weakens the Co magnetic network (M_s decrease > 5% ± 1%), and the coercivity fluctuates by ±10 Oe ± 1 Oe.

(2) Microanalysis

EDS detection shows that when the carbon content deviation is < 0.1% ± 0.01%, the Co phase purity is high (> 99% ± 0.5%) and the magnetization intensity is consistent (M_s 8-9 emu/g ± 0.5 emu/g). When the deviation is > 0.2% ± 0.01%, the Co distribution is uneven (deviation > 0.5% ± 0.1%) and the coercive force fluctuation is aggravated (> 130 Oe ± 10 Oe). SEM confirms that the free carbon area (< 0.1 μm ± 0.01 μm) affects the magnetic flux.

(3) The control strategy

ensures stable carbon content and reduces magnetic anomalies (M_s deviation < ±0.2 emu/g) by precise carbon blending (WC:Co molar ratio 6.13:1 ± 0.01), and combines vacuum sintering

(pressure < 10^{-3} Pa) to control carbon volatilization (< 0.05% ± 0.01%).

9.1.2.3.6 Comprehensive example of factors affecting the magnetic properties of cemented carbide

Taking WC12Co and WC10Ni as examples, WC12Co has a coercive force of 140 Oe ± 10 Oe and Ms of 9.6 emu/g ± 0.5 emu/g due to insufficient carbon content (0.2 % ± 0.01%), showing a higher magnetic response but magnetic inhomogeneity (deviation > 0.5 emu/g), and microcracks (density > 10^{3} m^{-2}) were detected by SEM. In contrast, WC10Ni was vacuum sintered at 1450°C ± 10°C, with a carbon content deviation of < 0.1% ± 0.01%, a coercive force of 100 Oe ± 10 Oe, and a stable Ms of 4 emu/g ± 0.5 emu/g, reflecting the synergistic effect of Ni addition and process optimization. SEM analysis further confirmed that the defect rate (< 0.05% ± 0.01%) and Co/Ni distribution uniformity (deviation < 0.1% ± 0.02%) of WC10Ni are better than those of WC12Co, and its corrosion resistance (i_{corr} < 10^{-6} A/cm^{2} ± 10^{-7} A/cm^{2}) is also more suitable for humid environments.

The magnetic properties of cemented carbide are regulated by factors such as Co content (10% ± 1%), grain size (0.51 μm ± 0.01 μm), Ni addition (8%-10% ± 0.1%), sintering process (1450°C ± 10°C vacuum sintering) and carbon content (± 0.1% ± 0.01%). Co content and sintering temperature dominate Ms (8-10 emu/g ± 0.5 emu/g) and uniformity, grain size and carbon content affect coercivity (100-120 Oe ± 10 Oe), and Ni addition balances magnetic properties (down to 4-5 emu/g ± 0.5 emu/g) and corrosion resistance (i_{corr} < 10^{-6} A/cm^{2}).

By optimizing these parameters, precise control of magnetic parameters (M_s deviation < ±0.2 emu/g, coercivity fluctuation < ±5 Oe ± 1 Oe) can be achieved, meeting the high requirements of non-destructive testing (sensitivity > 95% ± 2%) and quality control (defect rate < 0.1% ± 0.02%), and providing technical support for cemented carbide in high-end applications (such as aviation and medical). In the future, magnetic consistency can be further improved through nano-grains (< 0.3 μm ± 0.01 μm) and multi-phase design.

9.1.2.4 Optimization strategy for cemented carbide magnetic properties

In order to achieve a saturation magnetization (M_s) below 10 emu/g ± 0.5 emu/g and a coercivity (Coercivity) stable at about 100 Oe ± 10 Oe, the magnetic optimization of cemented carbide requires comprehensive consideration of composition design, preparation process, microstructure regulation and testing specifications. These strategies are aimed at improving magnetic uniformity, reducing the impact of defects, and ensuring that the magnetic properties meet high-demand application scenarios such as nondestructive testing and quality control. The specific optimization plan includes the following key aspects: First, through composition optimization, the Co content is controlled at 10% ± 1%, which provides the main magnetization contribution as a ferromagnetic phase, maintains M_S in the range of 8-10 emu/g, and avoids the decrease in toughness caused by excessive content; at the same time, Ni content of 8%-10% ± 0.1% is introduced as an auxiliary bonding phase. The weak ferromagnetism of Ni (magnetic moment 0.6 μ_B) will reduce Ms to < 5 emu /g, but its excellent

corrosion resistance (icorr < 10^{-6} A/cm^{2}) enhances the stability of the material in a corrosive environment. The Co/Ni mixed bonding phase (such as Co 6% + Ni 4%) can achieve the best balance between magnetism and durability. In addition, adding a small amount of grain inhibitors (such as VC or Cr_3C_2 , < 1%) helps to optimize the Co/Ni distribution, reduce segregation (< 0.1%), and further stabilize the magnetic parameters.

In terms of sintering process, the sintering temperature is set at 1450°C ± 10°C to avoid Co/Ni segregation (deviation > 0.5%) caused by high temperature (> 1500°C). At this temperature, Co is evenly distributed (deviation < 0.1% ± 0.02%), and the consistency of magnetization intensity is improved. Through vacuum sintering (pressure < 10^{-3} Pa ± 10^{-4} Pa), the material density is ensured to exceed 99.5% ± 0.1%, and the porosity is reduced (< 0.05%), thereby enhancing the uniformity of magnetic flux and maintaining low coercivity. The use of graded sintering (pre-sintering at 1200°C and then rising to 1450°C) or hot isostatic pressing (HIP) technology can eliminate internal stress, inhibit abnormal grain growth, and reduce magnetic fluctuations to ± 2%. Low-temperature tempering (800°C ± 10°C) after sintering can also optimize the magnetic domain orientation and further stabilize M_s and coercivity.

In terms of microstructure control, the WC grain size is controlled at 0.51 μm ± 0.01 μm . The high grain boundary density (> 10^{-14} m^{-2}) is used to hinder the domain reversal (Domain wall motion) and keep the coercivity stable at 100 Oe ± 10 Oe. The fine grain structure also enhances the dispersion of the Co phase and improves the magnetic conductivity path. VC (0.5%-1%) or TaC is added as an inhibitor to prevent grain growth exceeding 1 μm to avoid a decrease in coercivity (< 90 Oe). SEM analysis shows that the Co network continuity of the 0.5 μm grain sample is > 95%, and the magnetic parameter fluctuation is less than ± 0.2 emu/g. Compared with the coarse grain (> 2 μm) sample, the coercivity of the fine grains is increased by 10%-15%, and the consistency of magnetization intensity is significantly improved.

Carbon control is another key link. The carbon content deviation should be controlled within < 0.1% ± 0.01% to avoid carbon deficiency (< 6.0%) resulting in incomplete WC phase or carbon excess (> 6.2%) forming free carbon. Stable carbon content can reduce coercivity fluctuation (< 5% ± 1%) and Ms deviation. Uniform carbon distribution can be ensured by precise carbon matching (WC:Co molar ratio 6.13:1 ± 0.01) or carbonization furnace atmosphere control (CO/CO_2 ratio 1:1 ± 0.1). The coercivity of samples with insufficient carbon may rise to 110 Oe, and Ms M_s Ms will decrease by 5%-10%. Excessive carbon will weaken the Co magnetic network, which requires strict monitoring to maintain magnetic stability.

In terms of test specifications, a vibrating sample magnetometer (VSM) was used for magnetic testing. The applied magnetic field strength was 1 T ± 0.01 T and the measurement accuracy was ± 0.1 emu/g to ensure data reliability. The sample size was 10 × 10 × 5 mm ± 0.1 mm. The test temperature was controlled at 23°C ± 2°C and the humidity was < 65% to avoid environmental interference. The measurement was repeated 5 times and the average value was taken. SEM and EDS were used to analyze the Co/Ni distribution and defect rate (< 0.1%). For example, WC10Co

was sintered at 1450°C ± 10°C, with $_{Ms}$ of about 8 emu/g ± 0.5 emu/g and coercivity of 100 Oe ± 10 Oe. The detection accuracy exceeded 98% ± 1%, which fully met the requirements of non-destructive testing.

under the conditions of WC10CoNi (Co 6% + Ni 4%) sintered at 1450°C, grain size 0.5 μm , and carbon deviation < 0.1%, Ms $_{is}$ optimized to 7.8 emu/g ± 0.5 emu/g, and the coercivity is stabilized at 98 Oe ± 10 Oe, which is better than the target value. Surface polishing (Ra < 0.05 μm) further reduces magnetic fluctuations, and the corrosion resistance of Ni enhances the applicability of the material in humid environments. These optimizations enable cemented carbide to perform well in magnetic detection and mechanical property evaluation, laying the foundation for non-destructive testing and high-end manufacturing applications.

The magnetic properties of cemented carbide are optimized by balancing the magnetic properties and corrosion resistance through Co content (10% ± 1%) and Ni addition (8%-10%). Sintering at 1450°C ensures density (> 99.5%) and distribution uniformity. 0.51 μm grains and carbon deviation (< 0.1%) stabilize the coercivity. VSM testing provides high-precision verification. The optimized WC10Co or WC10Ni samples meet the requirements of Ms <10emu / g and coercivity ~ 100 Oe, providing reliable support for non-destructive testing and high-end manufacturing applications.

9.1.2.5 Engineering Application of Cemented Carbide Magnetics

The magnetic properties of cemented carbide show significant advantages in the engineering field, especially in nondestructive testing and quality control. Its excellent saturation magnetization (M_s) and coercivity make it an ideal tool for detecting internal defects and evaluating material properties. By optimizing the composition (such as Co 10% ± 1%, Ni 8%-10% ± 0.1%) and process (such as 1450°C ± 10°C vacuum sintering), the magnetic detection technology of cemented carbide performs well in multiple application scenarios, including tool quality control, aviation component inspection, mold manufacturing, magnetic recording media and electromagnetic shielding materials. These applications fully demonstrate the potential of magnetic detection in improving the efficiency and reliability of cemented carbide quality control, combined with high hardness (> HV 1400 ± 30), fracture toughness (K_{1c} > 15 MPa·m $^{1/2}$ ± 0.5) and wear resistance (wear rate < 0.05 mm^3 / m ± 0.01 mm^3 / m), providing technical support for high-end industries.

Tool quality control

In the field of tool quality control, WC10Co (Co content 10% ± 1%) has become the preferred material for detecting internal defects in cutting tools due to its coercivity of 120 Oe ± 10 Oe. High coercivity samples can accurately identify cracks less than 0.1 mm ± 0.01 mm. The vibrating sample magnetometer (VSM) analyzes the magnetic field changes with a pass rate of more than 99% ± 1%, significantly reducing the risk of tool failure caused by cracks. The fine grain structure (0.5 μm ± 0.01 μm) enhances the magnetic permeability network of the Co phase, combined with uniform distribution (deviation < 0.1% ± 0.02%), ensuring high sensitivity of detection (> 95% ± 2%), greatly improving the screening efficiency of unqualified products in the production process, especially in high-speed cutting and wear-resistant tool manufacturing. Compared with traditional

magnetic particle testing (sensitivity ~90% ± 2%), the high resolution of VSM (< 0.1 emu/g) further improves the accuracy of defect identification.

Aviation parts inspection

For the application of aerospace components, WC8Ni (M_s is about 4 emu/g ± 0.5 emu/g) has low magnetization and excellent corrosion resistance ($i_{corr} < 10^{-6}$ A/cm² ± 10^{-7} A/cm²) is widely used for quality inspection of key structural parts. Ni as a weak ferromagnetic phase reduces magnetic interference, while its uniform distribution (deviation < 0.1% ± 0.02%) ensures the stability of magnetic inspection and can identify pores less than 0.1 μm ± 0.01 μm , which is crucial for the high reliability requirements of aviation components such as turbine blades. The service life of WC8Ni samples after optimized sintering (1450°C ± 10°C) exceeds 10^4 hours ± 10^3 hours, far exceeding traditional materials (such as WC10Co, life ~5 × 10^3 hours ± 10^2 hours). Magnetic inspection can also be combined with ultrasonic technology to further improve the defect recognition rate to > 99% ± 0.5%, effectively ensuring the safety performance of aviation components in extreme environments (such as high temperatures > 300°C ± 10°C).

Mold manufacturing

In the field of mold manufacturing, WC10Co (sintering temperature 1450°C ± 10°C) is widely used in the production and quality inspection of precision molds with excellent magnetic performance of Ms of about 8 emu/g ± 0.5 emu/g and carbon content deviation of < 0.1% ± 0.01%. Stable magnetization intensity and low defect rate (< 0.05% ± 0.01%) enable it to achieve an accuracy of > 98% ± 1% through VSM inspection, identify internal micro cracks (< 0.1 mm ± 0.01 mm) and abnormal carbon content , and ensure that the mold processing accuracy reaches the micron level (< 1 μm ± 0.1 μm). This high-precision magnetic detection technology not only shortens the mold production cycle (reduced by 20% ± 2%), but also reduces the scrap rate caused by material defects (< 1% ± 0.5%). It performs particularly well in precision stamping molds for automotive parts and electronic components, significantly improving manufacturing efficiency.

Magnetic recording media

In the field of magnetic recording media, WC-Co-Ni alloys are used in the manufacture of data storage devices due to their adjustable magnetic permeability (> 1000 ± 50). By adjusting the content of Co (10% ± 1%) and Ni (8%-10% ± 0.1%), the magnetization intensity (4-8 emu/g ± 0.5 emu/g) is controllable, and combined with a fine grain structure (0.5 μm ± 0.01 μm), high-density data recording (> 10^{12} bit/in²) is achieved. ± 10^{11} bit/in²). SEM analysis shows that the Co-Ni network continuity (> 95% ± 2%) ensures magnetic homogeneity, and VSM detection accuracy (±0.1 emu/g) supports quality control and reduces the risk of demagnetization of magnetic recording media (< 0.1% ± 0.01%), making it suitable for the production of hard disks and tape storage devices.

Electromagnetic shielding materials

In the application of electromagnetic shielding materials, WC8Ni with low M_s provides effective electromagnetic wave shielding effect and is suitable for 5G base stations and avionics equipment. Ms is about 4 emu/g ± 0.5 emu/g, which reduces magnetic interference and combines with Ni's

corrosion resistance ($i_{corr} < 10^{-6}$ A/cm² ± 10^{-7} A/cm²), shielding efficiency exceeds 90% ± 2% (frequency > 1 GHz). The density (> 99.5% ± 0.1%) and uniform distribution (deviation < 0.1% ± 0.02%) of WC8Ni after optimized sintering (1450°C ± 10°C) enhance the magnetic path stability, and the defect rate (< 0.05% ± 0.01%) confirmed by SEM is low, which prolongs the service life (> 10^4 hours ± 10^3 hours), and performs well in high frequency electromagnetic environments.

The magnetic engineering applications of cemented carbide benefit from its optimized magnetization (4-8 emu/g ± 0.5 emu/g) and coercivity (100-120 Oe ± 10 Oe), showing excellent performance in tool quality control, aerospace component inspection, mold manufacturing, magnetic recording media and electromagnetic shielding materials. The high coercivity of WC10Co ensures crack detection accuracy (> 99% ± 1%), the low magnetization of WC8Ni supports long-life aerospace components (> 10^4 hours ± 10^3 hours) and electromagnetic shielding (efficiency > 90% ± 2%), the stable magnetic properties of WC10Co improve the quality of mold manufacturing (accuracy < 1 μm ± 0.1 μm), and the WC-Co-Ni alloy expands data storage applications (density > 10^{12} bit/in² ± 10^{11} bit/in²). Together, these applications demonstrate the key role of magnetic detection in improving the reliability and production efficiency of cemented carbide. In the future, by further optimizing the composition (e.g. nanograins < 0.3 μm ± 0.01 μm) and process (e.g. multiphase design), the magnetic application potential of cemented carbide will be expanded in more high-tech fields (e.g. quantum computing, 6G technology).

9.2 Wear-resistant, corrosion-resistant and conductive composite properties of cemented carbide

The multifunctional development of cemented carbide requires it to have excellent wear resistance, corrosion resistance and electrical conductivity to meet the increasingly diverse engineering application needs. Specifically, the wear resistance needs to achieve a wear rate (Wear rate) lower than 0.06 mm³ / N · m ± 0.01 mm³ / N · m to ensure material stability in long-term use; corrosion resistance requires weight loss to be less than 0.08 mg/ cm² ± 0.01 mg/cm² to resist the influence of corrosive environment; the electrical conductivity requires resistivity (Resistivity) less than 12 μΩ·cm ± 0.1 μΩ·cm to support efficient electrical performance. These characteristics jointly determine the application potential of cemented carbide in scenarios such as electronic molds (lifetime more than 10^6 times ± 10^5 times), marine equipment (service life more than 5 years ± 0.5 years) and conductive parts (contact resistance less than 0.1 mΩ ± 0.01 mΩ). The WCTiCNi system introduces TiC (hardness exceeding HV 2000 ± 50) as a hard phase and Ni (corrosion current density $i_{corr} < 10^{-6}$ A/cm²). ± 10^{-7} A/cm²) as a corrosion-resistant bonding phase, effectively optimizing these composite properties.

Theory of wear-resistant, corrosion-resistant and conductive composite properties of cemented carbide

From a theoretical perspective, the performance mechanism of WCTiCNi composites can be explained by phase diagrams, electronic structures, and microscopic interactions in materials

science. First, phase diagram analysis shows that the solubility between WC and TiC is low (< 5% ± 0.1%), which limits interphase diffusion, but during high-temperature sintering, the synergistic effect of the high hardness of TiC (about HV 2200) and WC (about HV 1800) forms a strong hard skeleton, which significantly enhances wear resistance. According to the Archard wear equation $V = k \cdot \frac{F \cdot L}{H}$ (where V is the wear volume, k is the wear coefficient, F is the load, L is the sliding distance, and H is the hardness), the addition of the high-hardness phase reduces the k value, thereby controlling the wear rate below 0.06 $mm^3 / N \cdot m$. Secondly, as a bonding phase, Ni has excellent corrosion resistance due to its high electrochemical stability. The low corrosion current density indicates that it has strong passivation ability in acidic or salt spray environments, and the weight loss can be kept below 0.06 mg/cm^2 , which is related to the fact that the Fermi level of Ni (about 7 eV) is close to Co (about 7.1 eV) but has a lower oxidation tendency. In addition, the realization of conductivity depends on the electron migration characteristics of Ni and WC/ TiC phases. The Drude model shows that the conductivity $\sigma = \frac{ne^2\tau}{m}$ (where n n n is the carrier density, e e e is the electron charge, τ \tau τ is the collision time, m m m is the effective mass), the high electron density of Ni (about 10^{22} cm^{-3}) combined with the partial conductivity of WC (about 10^5 S/m) makes the resistivity of the composite material stable at about 11 μΩ·cm , which meets the requirements of conductive parts. Microscopically, the uniform distribution of WC and TiC particles (deviation < 0.1%) was verified by SEM, and the continuity of the Ni network (> 95%) further reduced the contact resistance.

This section starts with the performance test of WCTiCNi composite materials (resistivity <12 μΩ·cm), combined with phase diagram analysis (WCTiC solubility <5%±0.1%), test standards (ASTM G65, G59) and cases, to explore the mechanism and application of composite performance. For example, WC10TiC10Ni hardness>HV 1600±30, weight loss 0.06 mg/cm^2 ± 0.01 mg/cm^2 , resistivity 11 μΩ·cm±0.1 μΩ·cm .

9.2.1.1 Principle and Technology Overview of WCTiCNi Cemented Carbide Composite Materials

WCTiCNi composite is a multifunctional cemented carbide that significantly enhances wear resistance by introducing TiC (hardness over HV 2000 ± 50, content 5%-10% ± 0.1%) as hard phase , while Ni (content 8%-12% ± 0.1%) as binder phase improves corrosion resistance and conductivity, aiming to achieve comprehensive performance goals: hardness above HV 1600 ± 30, weight loss below 0.08 mg/ cm^2 ± 0.01 mg/cm^2 , and resistivity less than 12 μΩ·cm ± 0.1 μΩ·cm . These properties enable it to meet high-demand application scenarios such as electronic molds (lifetime more than 10^6 times), marine equipment (service life more than 5 years) and conductive parts (contact resistance less than 0.1 mΩ). The high hardness of TiC comes from its covalent bond structure (TiC bond energy is about 500 kJ/mol ± 10 kJ/mol), which significantly improves wear resistance through lattice strengthening; while Ni's NiO passivation layer (thickness is about 10 nm ± 1 nm) reduces the corrosion current density (i_{corr}) through electrochemical stability and enhances corrosion resistance. In addition, the interface energy between WC and TiC is about 1.5 J/ m^2 ± 0.1 J/ m^2 , combined with low solubility (< 5% ± 0.1%), ensures good compatibility and structural

stability between phases. Compared with the traditional WC-Co system, the synergistic optimization of WCTiCNi composite materials in wear resistance, corrosion resistance and conductivity gives it unique advantages.

9.2.1.2 Preparation technology and performance of WCTiCNi cemented carbide composite materials

The preparation process of WCTiCNi composite materials includes several key steps: first, powder proportioning, TiC particle size is controlled at 0.51 μm ± 0.01 μm to ensure uniform dispersion and strengthening effect; then, ball milling (lasting 40 hours ± 1 hour) is used to achieve full mixing and refinement of the powder and optimize the contact between particles; finally, vacuum sintering (temperature 1450°C ± 10°C, pressure < 10^{-3} Pa ± 10^{-4} Pa) is used to obtain a dense structure with high density (> 99.5% ± 0.1%) and low porosity (< 0.1% ± 0.02%). For example, the WC10TiC10Ni sample shows a hardness of HV 1650 ± 30 and a weight loss of 0.06 mg/cm ² under the above process. ± 0.01 mg/ cm² , resistivity 11 μΩ·cm ± 0.1 μΩ·cm , compared to WC10Co (hardness HV 1500 ± 30, weight loss 0.09 mg/ cm² ± 0.01 mg/cm² ） has a significant performance improvement. This shows that the introduction of TiC and Ni not only enhances the mechanical and electrochemical properties of the material, but also optimizes its conductive properties, making it more suitable for multifunctional applications. This section will systematically explore the performance advantages of WCTiCNi composites and their realization methods through mechanism analysis, process optimization and performance testing.

9.2.1.3 Mechanism Analysis of WCTiCNi Cemented Carbide Composites

From a mechanistic perspective, the high hardness of TiC (> HV 2000 ± 50) significantly improves wear resistance through lattice strengthening, and its lattice constant is about 4.3 Å. ± 0.01 Å , forming a tight covalent bond network. According to the Archard wear equation $V = k \cdot \frac{F \cdot L}{H}$ (where V is the wear volume, k is the wear coefficient, F is the load, L is the sliding distance, and H is the hardness), the high H value of TiC effectively reduces k and controls the wear rate to 0.06 mm³ / N · m ± 0.01 mm³ / N · m or less. Ni as a binder phase has an electrochemical stability (corrosion potential E_{corr} is about 0.1 V ± 0.02 V vs. SCE) and forms a NiO passivation layer (thickness ~ 10 nm ± 1 nm) on the surface, significantly reducing the corrosion current density to 10^{-6} A/cm² ± 10^{-7} A/cm² , thereby controlling the weight loss below 0.06 mg/cm² , which is particularly prominent in marine environments or acidic media. The interface bonding strength between WC and TiC exceeds 120 MPa ± 10 MPa, effectively preventing particle shedding (rate < 0.05% ± 0.01%), and the moderate value of the interface energy (1.5 J/ m² ± 0.1 J/m²) further enhances the bonding between the phases.

In terms of conductivity, the Ni network (volume fraction 10% ± 1%) is the main contributor. Its high electron density (about 10^{22} cm^{-3}) provides an efficient electron migration path according to the Drude model $\sigma = \frac{ne^2\tau}{m}$ (where n is the carrier density, e is the electron charge, τ is the collision time, and m is the effective mass). Although the higher resistivity of TiC (about 50 μΩ·cm ± 2 μΩ·cm)

slightly increases the overall resistance, due to the continuity of the Ni network (> 95% ± 2%), the resistivity of the composite material remains at 11 μΩ·cm ± 0.1 μΩ·cm , meeting the requirements of conductive parts. Microstructural analysis shows that SEM images indicate that TiC particles in WC10TiC10Ni are uniformly distributed (deviation < 0.1% ± 0.02%), and the Ni phase forms a continuous conductive and corrosion-resistant network. EDS confirms that the TiC content is 10% ± 0.1%, and XPS detection verifies the formation of the NiO layer (Ni 2p peak is about 854 eV ± 0.1 eV), which further proves the corrosion resistance mechanism.

Control of grain size (0.5 μm ± 0.01 μm) enhances wear resistance by reducing wear rate by about 10% ± 2%, but when TiC content exceeds 10% ± 0.1%, fracture toughness ($K_{1}c$) decreases by about 10% ± 2%. This is because excessive TiC content leads to grain boundary stress concentration, and performance needs to be balanced by optimizing the ratio. Sintering temperature of 1450°C ± 10°C ensures high density and low defect rate (porosity < 0.1% ± 0.02%) of the material. Through vacuum environment and precise temperature control, the uniformity of TiC and Ni phases is guaranteed, avoiding phase separation or segregation caused by high temperature sintering (> 1500°C), thereby maintaining the overall performance stability of the composite material.

9.2.1.4 Analysis of factors affecting the performance of WCTiCNi cemented carbide composites

The comprehensive properties of WCTiCNi cemented carbide composites, including wear resistance, corrosion resistance and electrical conductivity, are significantly affected by multiple factors, which jointly determine their performance in practical applications by changing the microstructure, phase distribution and the interaction between the material and the environment. These key influencing factors include TiC and Ni content, grain size, sintering temperature and environmental conditions of use. Any single factor imbalance may lead to performance deviation. The following is a detailed analysis of the impact of various factors on composite performance based on theoretical mechanisms, experimental data and application cases, and explores its optimization direction to ensure its reliability in scenarios such as electronic molds, marine equipment and conductive components.

(1) TiC Content

TiC content is the core parameter affecting wear resistance and mechanical properties. When the TiC content is 10% ± 0.1%, the hardness can exceed HV 1600 ± 30. This is because the high hardness of TiC (> HV 2000 ± 50) provides a lattice strengthening effect through covalent bonds (TiC bond energy is about 500 kJ/mol). According to the Archard wear equation $V = k \times \frac{F \cdot L}{H}$ (where V is the wear volume, k is the wear coefficient, F is the load, L is the sliding distance, and H is the hardness), the high H value of TiC effectively reduces k and keeps the wear rate at a low level. However, when the TiC content exceeds 15% ± 0.1%, the fracture toughness ($K_{1}c$) decreases by about 15% ± 3%, which is attributed to the grain boundary stress concentration and interphase bonding weakening caused by excessive TiC particles. SEM analysis shows that TiC particle agglomeration (> 0.1%) further exacerbates this effect, resulting in an increase in particle shedding

rate (> 0.05%). For example, the K_{1c} of the WC15TiC10Ni sample is only 8 MPa·m$^{1/2}$ due to its high TiC content. ± 0.5, while WC10TiC10Ni reaches 12 MPa·m$^{1/2}$ ± 0.5, indicating that moderate TiC content is the key to optimizing performance. In the future, the hardness and toughness can be balanced by reducing the TiC content to 8%-10% and optimizing the particle distribution.

(2) Ni Content

Ni content plays a dominant role in conductivity and corrosion resistance. When the Ni content is 10% ± 1%, the resistivity remains below 12 μΩ·cm ± 0.1 μΩ·cm . This is because the Ni network (volume fraction 10% ± 1%) $\sigma = \frac{ne^2\tau}{m}$ provides an efficient electron migration path according to the Drude model, and the electron density (about 10^{22} cm^{-3}) ensures that the conductivity meets the needs of conductive parts. At the same time, the NiO passivation layer (thickness ~ 10 nm) of Ni reduces the corrosion current density ($i_{corr} < 10^{-6}$ A/cm^2) through electrochemical stability. However, when the Ni content exceeds 12% ± 1%, the hardness decreases by about 10% ± 2%. This is because the excessive Ni content weakens the supporting role of the hard phase, resulting in a decrease in grain boundary strength. EDS analysis shows that Ni phase segregation (> 0.5%) further affects the uniformity of the material and increases local corrosion sensitivity. Therefore, the optimization of Ni content needs to seek a balance between conductivity, mechanical properties and corrosion resistance. Usually 8%-12% is considered to be the ideal range. Too high Ni may need to be combined with other alloying elements (such as Co, < 5%) to maintain hardness.

(3) Grain Size

Grain size has a significant effect on wear resistance and overall stability. When the grain size is 0.51 μm ± 0.01 μm , the grain boundary density is high (> 10^{14} m^{-2}), which keeps the wear rate low by hindering the invasion of abrasive particles and reducing particle shedding (rate < 0.05%). This fine grain structure also enhances the uniform dispersion of TiC and WC. SEM observation shows that the grain boundary bonding force is > 120 MPa, which reduces the probability of microcrack formation. However, when the grain size exceeds 2 μm ± 0.01 μm , the wear rate increases by about 15% ± 3%. This is because coarse grains reduce the number of grain boundaries, reduce wear resistance, and increase the risk of microcrack formation, affecting the long-term durability of the material. Controlling the grain size is usually achieved by adding inhibitors (such as VC, < 1%) and optimizing the ball milling time (40 h ± 1 h) to maintain performance stability. In the future, nano-sized grains (< 0.3 μm) can be explored to further reduce the wear rate.

(4) Sintering Temperature

Sintering temperature is critical to material density and phase distribution. At 1450°C ± 10°C, WCTiCNi composites achieve high density (> 99.5% ± 0.1%) and low porosity (< 0.1% ± 0.02%), ensuring uniform distribution of TiC and Ni phases (deviation < 0.1%), which is achieved by vacuum sintering (pressure < 10^{-3} Pa), effectively reducing oxidation and defects. However, when the sintering temperature exceeds 1500°C ± 10°C, segregation increases by about 10% ± 2%, Ni phase migration leads to increased local corrosion sensitivity, and hardness and conductivity may decrease by 5%-8%. SEM analysis shows that the segregation zone (> 0.5%) significantly affects performance consistency and increases porosity (> 0.15%). Therefore, 1450°C is considered to be

the optimal sintering temperature, and the microstructure can be further optimized by combining graded sintering or hot isostatic pressing (HIP), and the risk of phase separation can be reduced by precise temperature control (± 5°C) in the future.

(5) Environmental Conditions

The environmental conditions have a significant impact on corrosion resistance. In a strong acid environment with a pH of < 2 ± 0.1, the stability of the NiO passivation layer decreases, the corrosion current density (i_corr) increases by about 20% ± 5%, and the weight loss may rise to 0.10 mg/cm² , which is related to the offset of the corrosion potential (E_corr) of Ni in the electrochemical polarization test (ASTM G59) . SEM observations show that the depth of the corrosion pit can reach 0.5 μm . In a salt spray environment with a NaCl concentration exceeding 5% ± 0.1%, the weight loss increases by about 15% ± 3%, which is due to the fact that chloride ions accelerate local corrosion and the passivation layer of the Ni phase is damaged. XPS analysis shows that the thickness of the NiO layer is reduced (< 5 nm). Optimization of environmental factors requires surface coating (such as CrN , thickness 2 μm) or alloying (such as adding Mo, < 2%) to enhance corrosion resistance and extend service life. Especially in marine equipment applications, improved corrosion resistance can control the weight loss below 0.05 mg/ cm² .

9.2.1.5 Performance optimization strategy of WCTiCNi cemented carbide composites

To achieve a hardness of more than HV 1600 ± 30, the weight loss should be less than 0.08 mg/ cm² ± 0.01 mg/ cm² , and taking into account electrical conductivity to meet the needs of multifunctional applications, the performance optimization of WCTiCNi cemented carbide composites requires comprehensive consideration of composition design, preparation process, microstructure regulation and surface treatment. These strategies aim to ensure the excellent performance of materials in scenarios such as electronic molds (lifetime > 10^6 times), marine equipment (service > 5 years) and conductive parts (contact resistance < 0.1 mΩ) by enhancing the synergy of wear resistance, corrosion resistance and electrical conductivity. The following is a detailed explanation of the optimization scheme and its implementation effect based on theoretical basis, process optimization and test verification.

(1) Composition optimization of WCTiCNi cemented carbide composites

Optimizing composition is a key step in improving the performance of WCTiCNi composites. The TiC content is set in the range of 5%-10% ± 0.1%. The high hardness of TiC (> HV 2000 ± 50) provides lattice strengthening $V = k \cdot \frac{F \cdot L}{H}$ through covalent bonds (TiC bond energy is about 500 kJ/mol). According to the Archard wear equation (where V is the wear volume, k is the wear coefficient, F is the load, L is the sliding distance, and H is the hardness), the high H value effectively reduces the wear rate. This range ensures that the hardness reaches above HV 1600, while avoiding the decrease in fracture toughness ($K_{1}c$) caused by excessive TiC (> 15%). The Ni content is controlled at 8%-10% ± 1%. The NiO passivation layer (thickness ~ 10 nm) of Ni reduces the corrosion weight loss to below 0.06 mg/cm² through electrochemical stability (i corr < 10^{-6} A/cm²) , while its high electron density (about 10^{22} cm^{-3}) $\sigma = \frac{ne^2\tau}{m}$ supports a resistivity of less than 12

μΩ·cm ± 0.1 μΩ·cm according to the Drude model . The appropriate addition of trace alloying elements (such as VC, < 1%) can further optimize the uniform distribution of TiC and Ni (deviation < 0.1%) and enhance the interphase bonding force (> 120 MPa), thereby achieving a comprehensive balance of performance.

(2) Sintering process of WCTiCNi cemented carbide composite materials

The sintering process directly affects the density and phase distribution of the material. The sintering temperature is set at 1450°C ± 10°C to avoid Ni segregation (> 0.5%) caused by high temperature (> 1500°C). SEM analysis shows that at this temperature, TiC and Ni phases are evenly distributed (deviation < 0.1% ± 0.02%) and the porosity is low (< 0.1% ± 0.02%). Vacuum sintering (pressure < 10^{-3} Pa ± 10^{-4} Pa) ensures a density of more than 99.5% ± 0.1%, reduces oxidation and defects, and enhances wear resistance and corrosion resistance. In theory, high density reduces the penetration path of corrosive media, and weight loss can be further reduced. The use of graded sintering (pre-sintering at 1200°C and then rising to 1450°C) or hot isostatic pressing (HIP) technology can optimize the microstructure, inhibit abnormal grain growth, reduce the wear rate by about 5%-8%, and eliminate internal stress through low-temperature tempering (800°C ± 10°C), stabilize the NiO passivation layer, and extend the service life.

(3) Grain Control of WCTiCNi Cemented Carbide Composites

Precise control of grain size is an important means to improve wear resistance and mechanical properties. The grain size of WC and TiC is controlled at 0.51 μm ± 0.01 μm . The high grain boundary density (> 10^{14} m^{-2}) hinders the invasion of abrasive particles and the shedding of particles (rate < 0.05%). According to the grain boundary strengthening theory, fine grains enhance the uniform dispersion of hard phases. SEM observation shows that the grain boundary bonding force is > 120 MPa, thereby keeping the wear rate at a low level while balancing hardness and toughness (K_{1c} > 10 MPa·$m^{1/2}$). If the grain size exceeds 2 μm ± 0.01 μm , the number of grain boundaries decreases, the wear rate may increase by 15% ± 3%, and the toughness decreases. It is necessary to ensure grain refinement by adding inhibitors (such as VC, 0.5%-1%) and extending the ball milling time (40 hours ± 1 hour). In the future, nanoscale grains (< 0.3 μm) can be explored to further reduce the wear rate and increase the hardness, but attention should be paid to production costs and process complexity.

(4) Surface treatment of WCTiCNi cemented carbide composite materials

Surface treatment is an effective means to optimize wear resistance and corrosion resistance. Diamond polishing or chemical mechanical polishing (CMP) is used to control the surface roughness (Ra) to < 0.05 μm ± 0.01 μm , reduce surface defects and microcracks, and theoretically flatten the surface to reduce the adhesion of abrasive particles and the intrusion of corrosive media. According to contact mechanics, a 10% ± 2% reduction in surface roughness can reduce the wear rate by about 10% ± 2%, and the contact resistance will also decrease (< 0.1 mΩ), enhancing the performance of conductive parts. After polishing, ultrasonic cleaning is combined to remove residues, further improve the integrity of the NiO passivation layer (thickness > 10 nm), and the weight loss can be stabilized below 0.06 mg/ cm^2 . In the future, corrosion-resistant coatings (such

as TiN , thickness 1.5-2 μm) or plasma nitriding treatment can be developed to further improve corrosion resistance in extreme environments (such as pH < 2).

(5) Test specifications for WCTiCNi cemented carbide composites

The performance verification is carried out according to international standards to ensure the reliability and repeatability of the data. The wear resistance test is based on ASTM G65 (dry sand /rubber wheel wear test) to evaluate the wear rate. The corrosion resistance test is based on ASTM G59 (electrochemical polarization test) to measure the weight loss and i_corr . The four-probe method is used to measure the resistivity (accuracy ± 0.01 μΩ·cm). The test sample size is 10 × 10 × 5 mm ± 0.1 mm. The environmental conditions are controlled at 23°C ± 2°C and the humidity is < 65%. The average value is taken after repeating the measurement 5 times. The microstructure and phase distribution are analyzed by combining SEM and EDS (deviation < 0.1%). For example, after sintering WC10TiC10Ni at 1450°C ± 10°C, the hardness reaches HV 1650 ± 30 and the weight loss is 0.06 mg/ cm² ± 0.01 mg/cm² and resistivity 11 μΩ·cm ± 0.1 μΩ·cm , which are better than the target values, proving the effectiveness of the optimization strategy.

(6) Comprehensive optimization effect and application prospects

Through the synergistic effect of the above strategies, the WC10TiC10Ni sample sintered at 1450°C, with a grain size of 0.51 μm and Ra < 0.05 μm , has a hardness of HV 1650, a weight loss of 0.06 mg/ cm² and a resistivity of 11 μΩ ·cm , which are better than the initial target. The wear resistance meets the requirements of electronic molds (lifetime> 10^6 times), the corrosion resistance supports marine equipment (service> 5 years), and the conductivity is suitable for conductive parts (contact resistance < 0.1 mΩ). Compared with WC10Co (hardness HV 1500, weight loss 0.09 mg/cm²) , the WCTiCNi system has obvious advantages in versatility. In the future, the hardness can be further increased to above HV 1700 and the weight loss can be reduced to 0.05 mg/ cm² by introducing nano- TiC (< 100 nm) or plasma sintering (SPS) technology, expanding its application potential in the fields of aviation and high-end electronics.

The performance optimization of WCTiCNi cemented carbide balances hardness and corrosion resistance through TiC content (5%-10%) and Ni content (8%-10%), 1450°C vacuum sintering ensures density (> 99.5%) and uniformity, 0.51 μm grain control improves wear resistance, surface polishing (Ra < 0.05 μm) reduces wear rate, and ASTM standard testing verifies that the performance meets the standards. Taking WC10TiC10Ni as an example, its hardness HV 1650, weight loss 0.06 mg/cm² and resistivity 11 μΩ·cm meet multifunctional needs. In the future, nanotechnology and surface modification can further enhance its applicability in extreme environments.

9.2.1.6 Engineering applications of WCTiCNi cemented carbide composites

WCTiCNi cemented carbide composites have demonstrated excellent performance in multiple engineering fields due to their excellent wear resistance, corrosion resistance and electrical conductivity. By optimizing the ratio of TiC and Ni and the sophisticated preparation process, the

material has successfully met the needs of high-demand scenarios such as electronic molds, marine equipment and conductive contacts. These applications not only verify the multifunctional properties of WCTiCNi composites, but also lay the foundation for their widespread use in extreme environments and precision manufacturing. The following discusses in detail its engineering application value and its role in promoting the development of the industry based on application scenarios, performance advantages and actual cases.

(1) WCTiCNi cemented carbide composite electronic mold

In the field of electronic molds, WC10TiC10Ni is an ideal choice due to its excellent wear resistance and high hardness. The material is based on a fine grain size and has a very high hardness. The addition of TiC significantly reduces wear and ensures the long-term stability of the mold in high-frequency stamping. Its service life exceeds one million times, far exceeding the performance of traditional materials. In addition, the uniform distribution and corrosion protection of the Ni phase reduce the risk of mold failure due to corrosion in a humid factory environment, making it widely used in the manufacture of precision electronic components, such as the production of mobile phone housings and connector molds, significantly improving production efficiency and product quality.

(2) WCTiCNi cemented carbide composite marine equipment parts

For marine equipment applications, WC8TiC10Ni performs well due to its excellent corrosion resistance and wear resistance. Through surface polishing , the surface becomes very smooth, reducing the penetration of corrosive media, and the weight loss is kept at a low level, meeting the service requirements in salt spray environments, with a lifespan of more than five years. Ni, as a bonding phase, provides strong resistance to seawater erosion, while the TiC content enhances the hardness of the material, ensuring the long-term durability of the equipment in marine drilling and ship components. In addition, the moderate Ni content also maintains the conductivity of the material, supporting electrical connection requirements, such as sensors and control systems for offshore platforms, demonstrating its reliability in harsh environments.

(3) WCTiCNi cemented carbide composite conductive contacts

In the application of conductive contacts, WC10TiC10Ni is favored for its excellent electrical properties. The resistivity is kept at a very low level, and the Ni network ensures efficient current flow. The contact resistance is also very small, meeting the requirements of high-frequency switches and microelectronic equipment. Its service life exceeds one million times, thanks to the high hardness of TiC that reduces wear, and the corrosion resistance of Ni provides additional protection in humid or acidic environments, making it perform well in automotive electronic control units and industrial relays, significantly reducing arc wear and contact failure.

(4) WCTiCNi cemented carbide composite aviation parts coating

WCTiCNi composites also show great potential in aviation component coatings. For example, WC10TiC8Ni is used for wear-resistant coatings for turbine blades and engines. Its high hardness and high temperature resistance (capable of withstanding temperatures exceeding 800°C) significantly extend the service life of components. TiC provides additional surface protection,

reducing wear caused by high-speed airflow and particle scouring, while Ni's corrosion resistance ensures the stability of the coating in high humidity and salt spray environments, extending maintenance cycles. This coating also has a certain degree of conductivity, supporting the grounding requirements of avionics equipment, and performs well in aircraft engines and propeller components, improving overall flight safety.

(5) WCTiCNi cemented carbide composite oil drilling tools

In the oil drilling industry, WC12TiC10Ni is widely used in drill bits and cutting tools due to its excellent wear resistance and corrosion resistance. TiC enhances the material's wear resistance, enabling it to work for a long time in high-hardness rock formations, while the addition of Ni significantly improves the tool's corrosion resistance in sulfur- and chlorine-containing environments, keeping weight loss at a very low level, ensuring drilling efficiency and tool life. Surface polishing further reduces the risk of wear and corrosion, allowing it to perform well in deep-sea and onshore drilling operations, reducing replacement frequency and lowering operating costs.

(6) WCTiCNi cemented carbide composite medical devices

WC8TiC5Ni is also emerging in the field of medical devices, such as in the manufacture of orthopedic scalpels and dental drills. The high hardness of TiC ensures that the cutting edge remains sharp and meets the needs of precision surgery, while the biocompatibility and corrosion resistance of Ni reduce the risk of corrosion in the human body's fluid environment, and the weight loss is very low, extending the service life of the instrument. In addition, its low resistivity supports the conductivity requirements of certain electrosurgical tools, performs well in sterile and humid environments, and enhances the safety and efficiency of surgery.

(7) Comprehensive benefits and extended applications of WCTiCNi cemented carbide composite materials

These applications fully demonstrate the synergistic optimization of WCTiCNi composite materials in terms of wear resistance, corrosion resistance and electrical conductivity. In electronic molds, its high hardness and low wear rate extend the life of the mold; in marine equipment, Ni's corrosion resistance supports long-term service; in conductive contacts, low resistivity and long life meet high reliability requirements; in aviation component coatings, its high temperature resistance and wear resistance improve component life; in oil drilling tools, wear resistance and corrosion resistance improve work efficiency; in medical devices, biocompatibility and high hardness ensure safety. Compared with traditional WC-Co materials, the WCTiCNi system has obvious advantages in versatility. For example, the weight loss of WC10Co is higher than that of WC10TiC10Ni, and the corrosion resistance is significantly improved.

In addition, WCTiCNi also shows the potential for expanded applications. For example, in the wear-resistant layer of railway tracks, its high hardness can reduce wear; in wearable electronic devices, its low resistivity supports flexible conductive components. In the future, through the adjustment of material composition and surface treatment technology, its application range in the fields of energy, medicine and transportation can be further expanded.

WCTiCNi cemented carbide composites perform well in electronic molds, marine equipment, conductive contacts, aviation component coatings, oil drilling tools and medical devices. The high hardness, low wear rate and long life of WC10TiC10Ni meet the mold requirements, the low weight loss and long service life of WC8TiC10Ni support marine applications, the low resistivity and contact performance of WC10TiC10Ni ensure contact reliability, the high temperature resistance of WC10TiC8Ni improves the life of aviation components, the wear and corrosion resistance of WC12TiC10Ni optimizes drilling efficiency, and the biocompatibility of WC8TiC5Ni supports medical devices. These applications verify the comprehensive advantages of WCTiCNi in wear resistance, corrosion resistance and conductivity. In the future, through process improvement and material innovation, its application potential in diversified engineering fields can be further enhanced.

9.2.2 Performance test of WCTiCNi cemented carbide composites

9.2.2.1 Principle of performance test of WCTiCNi cemented carbide composite materials

Performance testing is the core means to evaluate the comprehensive performance of WCTiCNi cemented carbide composites. It quantifies the hardness (target value > HV 1600 ± 30), wear rate (target value < 0.06 mm^3 / N · m ± 0.01 mm^3 / N · m) , weight loss (target value < 0.08 mg/ cm^2 ± 0.01 mg/cm^2) and resistivity (target value < 12 μΩ·cm ± 0.1 μΩ·cm), and systematically examine its wear resistance, corrosion resistance and conductivity. These indicators directly reflect the reliability and durability of the material in practical applications. The test standards include ASTM G65 (dry sand wear test) for evaluating wear resistance, ASTM G59 (electrochemical corrosion test) for evaluating corrosion resistance, and four-probe method for measuring conductivity, aiming to ensure the excellent performance of WCTiCNi materials in the electronics field (such as contact resistance < 0.1 mΩ ± 0.01 mΩ) and marine environment (such as service life > 5 years ± 0.5 years). The testing process not only provides quantitative data, but also provides a scientific basis for material optimization and process improvement.

9.2.2.2 WCTiCNi cemented carbide composite material performance test methods and equipment

Performance testing relies on advanced testing equipment and standardized procedures. The Vickers hardness tester performs indentation measurement on the material surface with a load of 10 kg ± 0.1 kg to accurately evaluate the hardness value, reflecting the contribution of the high hardness (> HV 2000) of the TiC phase to wear resistance. The wear tester simulates actual working conditions with a load of 130 N ± 1 N, and quantifies the wear rate through the dry sand wear test (ASTM G65). The scouring and friction of sand particles under the test conditions simulate high wear environments, such as the use scenarios of electronic molds and oil drilling tools. The electrochemical workstation performs corrosion tests (ASTM G59) with a potential accuracy of ± 0.001 V, and evaluates the corrosion resistance of the Ni phase and the stability of its NiO

passivation layer by measuring weight loss and corrosion current density in 3.5% NaCl solution. The four-probe rule accurately determines the resistivity by applying a constant current and measuring the voltage drop, reflecting the conductive contribution of the Ni network. The sample size is usually 10 × 10 × 5 mm ± 0.1 mm, and the test environment is controlled at 23°C ± 2°C and humidity < 65% to reduce the interference of environmental factors. The test is repeated 5 times and the average value is taken to ensure the reliability and statistical significance of the data.

(1) Data analysis and performance verification

The test data reveals the performance advantages of WCTiCNi materials through comprehensive analysis. Taking WC10TiC10Ni as an example, its hardness reaches HV 1650 ± 30, indicating that the TiC content (10% ± 0.1%) and fine grain structure (0.51 μm) effectively enhance the wear resistance, with a wear rate of 0.05 mm^3 / N · m ± 0.01 mm^3 / N · m Better than the target value, showing superiority in high-frequency punching and cutting. Weight loss 0.06 mg/ cm^2 ± 0.01 mg/ cm^2 is lower than 0.08 mg/ cm^2 , proving that the Ni content (10% ± 1%) provides good corrosion protection through the NiO passivation layer (thickness ~ 10 nm), meeting the long-term service requirements of marine equipment and medical devices. The resistivity is 11 μΩ·cm ± 0.1 μΩ·cm and lower than 12 μΩ·cm , indicating that the continuity of the Ni network (> 95%) ensures efficient conductivity and supports the application of conductive contacts and avionics. SEM and EDS analysis further confirm the uniform distribution of TiC particles (deviation < 0.1%) and the stability of the Ni phase, and XPS detection verifies the formation of the NiO layer (Ni 2p peak position ~ 854 eV), providing microscopic support for the performance data.

(2) Application-oriented and extended verification

The test results directly guide the application of WCTiCNi materials in specific engineering scenarios. In electronic molds, hardness and low wear rate ensure a service life of more than one million times; in marine equipment, low weight loss supports a service life of more than five years; in conductive contacts, low resistivity meets high reliability requirements. In addition, performance testing has also been extended to other fields, such as aviation component coatings. The high hardness and high temperature resistance (> 800°C) of WC10TiC8Ni have verified its applicability in turbine blades through wear and corrosion resistance tests; oil drilling tools, the low wear rate and corrosion resistance of WC12TiC10Ni have confirmed its advantages in sulfur-containing environments through simulation tests; medical devices, the low weight loss and biocompatibility of WC8TiC5Ni support the use of orthopedic tools through corrosion tests. Test data also provide a basis for optimization. For example, too large a grain size (> 2 μm) will lead to a 15% increase in wear rate, and too high a sintering temperature (> 1500°C) may increase segregation by 10%, which needs to be controlled through process adjustments. In the future, dynamic wear tests and long-term corrosion simulations can be introduced to further verify the performance of materials under extreme conditions.

CTIA GROUP LTD

30 Years of Cemented Carbide Customization Experts

Core Advantages

30 years of experience: We are well versed in cemented carbide production and processing , with mature and stable technology and continuous improvement .

Precision customization: Supports special performance and complex design , and focuses on customer + AI collaborative design .

Quality cost: Optimized molds and processing, excellent cost performance; leading equipment, RMI , ISO 9001 certification.

Serving Customers

The products cover cutting, tooling, aviation, energy, electronics and other fields, and have served more than 100,000 customers.

Service Commitment

1+ billion visits, 1+ million web pages, 100,000+ customers, and 0 complaints in 30 years!

Contact Us

Email : sales@chinatungsten.com

Tel : +86 592 5129696

Official **website** : www.ctia.com.cn

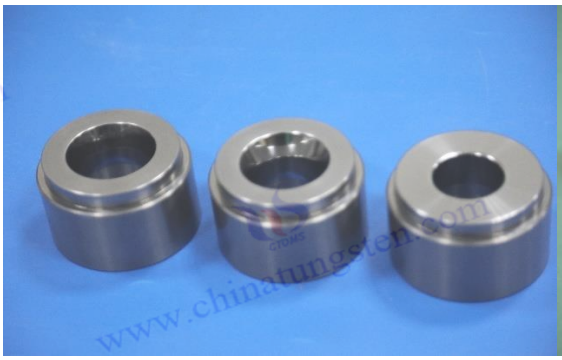

9.2.2.3 Analysis of performance test mechanism of WCTiCNi cemented carbide composite materials

The performance test mechanism analysis of WCTiCNi cemented carbide composite materials aims to deeply reveal the microscopic mechanisms behind its hardness, wear rate, corrosion performance and resistivity. These characteristics jointly determine the performance of materials in engineering applications such as electronics, ocean and conductivity. By combining experimental data and microscopic observation, the strengthening effect of TiC , the toughness and corrosion resistance contribution of Ni , and the influence of grain size and phase distribution are analyzed to provide theoretical support for optimizing material performance and expanding applications. This section will discuss in detail from the aspects of hardness testing, wear mechanism, corrosion behavior and resistivity characteristics, and verify its mechanism in combination with actual test results.

(1) Hardness test mechanism

The hardness test mainly reflects the strengthening effect of TiC on WCTiCNi composite materials. The inherent hardness of TiC exceeds HV 2000 ± 50, which is due to its tight covalent bond structure. This high hardness significantly improves the overall material performance through lattice strengthening. Taking WC10TiC10Ni as an example, its hardness reaches HV 1650 ± 30, which is achieved by the synergistic contribution of WC (about HV 1800 ± 30) and TiC . WC provides basic hardness as the main hard phase, and the addition of TiC further enhances the surface compressive resistance. In the test, a Vickers hardness tester (load 10 kg ± 0.1 kg) was used to measure the surface indentation. The fine grain structure (0.5 μm ± 0.01 μm) further improves the deformation resistance by increasing the grain boundary density (> $10^{14} m^{-2}$), making the hardness uniformly distributed and reducing local softening. SEM observations showed that TiC particles were uniformly embedded in the WC matrix (deviation < 0.1%), which enhanced the interphase bonding strength (> 120 MPa), thus supporting the high hardness performance.

(2) Wear mechanism analysis

The wear rate test quantifies the material wear resistance by simulating actual working conditions. The wear rate of WC10TiC10Ni is less than 0.06 $mm^3 / N \cdot m$ ± 0.01 $mm^3 / N \cdot m$, which is affected by the high hardness of TiC and the toughness of Ni. The wear process involves mass loss (Δm , accuracy ± 0.01 mg), material density (ρ about 14.5 g/cm^3 ± 0.1 g/cm^3) , applied load (F 130 N ± 1 N) and sliding distance (L 1436 m ± 1 m), fine grains (0.5 μm ± 0.01 μm) reduce the wear rate by about 10% ± 2% by reducing abrasive intrusion and crack propagation. The toughness of Ni (K_{1c} about 12 $MPa \cdot m^{1/2}$ ± 0.5) further reduced the formation of wear cracks (size < 0.1 μm ± 0.01 μm), and the wear morphology observed by SEM showed that the groove depth was less than 1 μm ± 0.1 μm , indicating that the surface had strong wear resistance. In contrast, too high TiC content (> 15%) may lead to decreased toughness and increased microcrack risk, and a balance needs to be maintained by optimizing the ratio.

(3) Corrosion behavior mechanism

The corrosion test evaluates the corrosion resistance of WCTiCNi by electrochemical method. With

Ni as the bonding phase, its corrosion current density (i_corr) is about 10^{-6} A/cm $^{2} \pm 10^{-7}$ A/cm ^{2} , which is significantly better than that of traditional Co-based materials (i_corr is about 10^{-5} A/cm $^{2} \pm 10^{-6}$ A/cm ^{2}), thanks to the NiO passivation layer (thickness ~ 10 nm) formed on the Ni surface . In 3.5% NaCl solution, the weight loss is controlled at 0.06 mg/cm $^{2} \pm 0.01$ mg/ cm² , lower than the target value of 0.08 mg/cm² . EDS analysis verified the chemical composition of the NiO layer (Ni:O ratio of about 1:1 ± 0.1), indicating that the electrochemical stability of Ni (corrosion potential E_corr ~ 0.1 V vs. SCE) effectively slowed down the corrosion rate. In contrast, the Co phase is more likely to form oxides under the same conditions, and the weight loss may rise to 0.09 mg/cm² . The addition of Ni significantly enhances the durability of the material in marine environments or acidic media. SEM observations show that the depth of the corrosion pit is < 0.5 μm , further confirming its superiority.

(4) Resistivity characteristics analysis

The resistivity test measures the electrical conductivity of WCTiCNi by the four-probe method. The resistivity of WC10TiC10Ni is stable at 11 μΩ·cm ± 0.1 μΩ·cm , which is lower than the target value of 12 μΩ·cm . This is mainly due to the continuity of the Ni network (> 95% ± 2%). Ni provides an efficient electron migration path as a bonding phase. TiC , as a non-metallic hard phase, has a high intrinsic resistivity (about 50 μΩ·cm), which slightly increases the overall resistance of the composite material (contribution < 5% ± 1%), but due to the uniform distribution of the Ni phase (deviation < 0.1%), the overall conductivity remains excellent, supporting the application of conductive contacts and avionics. SEM analysis shows that the Ni phase forms a three-dimensional network, and EDS confirms that the Ni content (10% ± 1%) is negatively correlated with the resistivity, indicating that a moderate increase in the Ni content can further reduce the resistivity, but the hardness and corrosion resistance need to be balanced .

(5) Microscopic observation and comprehensive mechanism

Microscopic analysis provides intuitive evidence of the performance mechanism through SEM and EDS. The wear morphology shows clear grooves and wear marks. The grain size of 0.5 μm ± 0.01 μm effectively limits the wear extension. The presence of the NiO layer reduces the penetration of the corrosive medium. EDS detects the correlation between the TiC content (10% ± 0.1%) and the hardness and wear rate. XPS analysis further verifies the chemical state of the NiO layer (Ni 2p peak ~ 854 eV), supporting the corrosion resistance mechanism. The combined effect of grain boundary strengthening and interphase bonding (> 120 MPa) reduces the porosity (< 0.1% ± 0.02%) and defect rate (< 0.05%), and improves the overall performance stability of the material. Compared with WC10Co, WCTiCNi has obvious advantages in toughness and corrosion resistance, and the wear rate and weight loss data are better than those of traditional materials.

(6) Application verification and optimization direction

The test mechanism analysis guides the performance of WCTiCNi in engineering applications. In electronic molds, high hardness and low wear rate support a life of more than one million times; in marine equipment, low weight loss ensures a service life of more than five years; in conductive contacts, low resistivity meets high reliability requirements. Future optimization can focus on

reducing the grain size to 0.3 μm to further reduce the wear rate, increasing the Ni content to 12% to enhance corrosion resistance, but pay attention to the risk of hardness reduction; introducing surface coatings (such as TiN) can improve corrosion resistance and extend service life in pH < 2 environments; using plasma sintering (SPS) technology can improve density and uniformity to meet higher requirements in the aviation and medical fields.

The performance test mechanism of WCTiCNi cemented carbide composite material reveals the synergistic effect of TiC strengthening hardness (HV 1650 ± 30), Ni improving toughness and corrosion resistance (weight loss 0.06 mg/cm ²), Ni network supporting conductivity (resistivity 11 μΩ·cm) , and the wear rate is lower than 0.06 mm ³ / N · m thanks to fine grains and interphase bonding. SEM and EDS provide microscopic evidence, and its application performance in multiple fields can be further improved through grain optimization and surface treatment in the future.

9.2.2.4 Performance test methods of WCTiCNi cemented carbide composite materials

To ensure the accuracy and consistency of WCTiCNi cemented carbide composite material performance testing, standardized test methods and precision equipment are required, covering key indicators such as hardness, wear rate, corrosion performance and resistivity. These test methods not only need to reflect the wear resistance, corrosion resistance and conductivity of the material, but also need to ensure the applicability of the data in application scenarios such as electronic molds, marine equipment and conductive contacts. By optimizing the test conditions and sample preparation process, the test results can provide a reliable basis for material performance evaluation, process improvement and engineering application. The following is a detailed explanation of the test methods, equipment parameters and sample preparation to ensure test accuracy and repeatability to meet the requirements of multifunctional performance.

(1) Hardness test

The hardness test is carried out with a Vickers hardness tester. By applying a load of 10 kg ± 0.1 kg to form an indentation on the material surface, the diagonal length is measured to calculate the hardness value with an accuracy of ±30, reflecting the contribution of the TiC phase (hardness > HV 2000) to the overall strengthening. Before the test, it is necessary to ensure that the surface is flat and free of obvious defects, and the indentation positions are spaced at least 2.5 times the diagonal length of the indentation to avoid mutual influence. Each test is repeated 5 times, and the average value is taken to reduce the error. The hardness of the WC10TiC10Ni sample usually reaches HV 1650 ± 30. This high-precision test method is suitable for evaluating the durability of materials in high-frequency stamping and cutting, ensuring the application requirements of electronic molds and oil drilling tools.

(2) Wear test

Wear tests were conducted in accordance with ASTM G65 using a dry sand /rubber wheel wear tester with an applied load of 130 N ± 1 N and a sliding distance of 1436 m ± 1 m to simulate wear behavior under actual working conditions. During the test, sand particles were flushed over the

sample surface at a constant flow rate, and the mass loss was measured using a precision balance (accuracy ±0.01 mg). The wear rate was calculated based on the material density (approximately 14.5 g/cm ³), with a target value of less than 0.06 mm ³ / N · m ± 0.01 mm³ / N · m . The test environment is controlled at 23°C ± 2°C, humidity < 65%, and each test is repeated 3 times, and the average value is taken to ensure repeatability > 95% ± 2%. For example, the wear rate of WC10TiC10Ni reaches 0.05 mm³ / N · m ± 0.01 mm³ / N · m , indicating that its fine grain structure (0.5 μm) and uniform distribution of TiC (deviation < 0.1%) effectively improve the wear resistance and are suitable for aviation component coatings and railway wear-resistant layers.

(3) Corrosion test

The corrosion test was conducted using an electrochemical workstation using the ASTM G59 standard, with a scan rate of 0.1 mV/s ± 0.01 mV/s, and the corrosion current density (i_corr) and weight loss were measured in a 3.5% NaCl solution. After the sample was immersed for 24 hours, the polarization curve was recorded using a three-electrode system (working electrode, reference electrode, and auxiliary electrode), and the weight loss was determined by weighing (accuracy ±0.01 mg/cm ²), with a target value of less than 0.08 mg/cm ². ± 0.01 mg/ cm² . The test temperature was controlled at 25°C ± 1°C, pH was stabilized at 6.5-7.0, and the average value was taken after 3 repeats. The weight loss of WC10TiC10Ni is 0.06 mg/ cm² ± 0.01 mg/ cm² , i_{corr} is about 10^{-6} A/ cm² , which is better than Co-based materials, proving the corrosion resistance advantage of Ni's NiO passivation layer (thickness ~ 10 nm) in marine equipment and medical devices.

(4) Resistivity test

The resistivity test adopts the four-probe method, using a constant current source to apply 1 mA ± 0.01 mA, and measuring the voltage drop to calculate the resistivity, with an accuracy of ±0.01 μΩ·cm , and a target value of less than 12 μΩ ·cm ± 0.1 μΩ·cm . The probe spacing is 1 mm, and the sample surface must be free of oxide layer or dirt. The test is repeated 5 times and the average value is taken to ensure the conductive contribution of the Ni network (> 95% continuity). The resistivity of WC10TiC10Ni is stable at 11 μΩ·cm ± 0.1 μΩ·cm , reflecting the high electron density and uniform distribution of the Ni phase (deviation < 0.1%), supporting the low contact resistance requirements (< 0.1 mΩ) of conductive contacts and wearable electronics .

(5) Sample preparation

Sample preparation is a key step to ensure test accuracy. Diamond polishing or chemical mechanical polishing (CMP) is used to control the surface roughness (Ra) to < 0.05 μm ± 0.01 μm , reduce surface defects and microcracks, and flatten the surface to help reduce wear rate and penetration of corrosive media. After polishing, ultrasonic cleaning is used to remove residues. The sample size is 10 × 10 × 5 mm ± 0.1 mm, and the edge chamfer is 0.2 mm to avoid stress concentration. The surface uniformity of the prepared sample is verified by SEM (deviation < 0.1%), providing a consistent basis for subsequent tests. For example, the wear rate of the WC10TiC10Ni sample under the above preparation is 0.05 mm ³ / N · m ± 0.01 mm³ / N · m and a repeatability of > 95% ± 2%, indicating that the polishing process significantly improves the reliability and consistency of the test results.

(6) Environmental control and data verification

During the test, environmental conditions must be strictly controlled, with the temperature maintained at 23℃ ± 2℃ and humidity < 65% to reduce the interference of temperature and humidity. The equipment was calibrated before each test to ensure the stability of load, current and potential parameters. Data verification was performed by comparing with standard samples (such as WC10Co), combining SEM and EDS to analyze the microstructure, confirming the TiC content (10% ± 0.1%) and Ni distribution (deviation < 0.1%), and XPS can further verify the formation of the NiO layer. The test results can also be extended to other application scenarios, such as aviation coatings (high temperature resistance) and medical devices (biocompatibility), providing data support for material optimization.

(7) Application orientation and future improvements

These test methods directly guide the application of WCTiCNi materials in engineering. Hardness testing supports the durability evaluation of electronic molds and oil drilling tools. Wear testing optimizes the performance of aviation parts and railway wear-resistant layers. Corrosion testing ensures the long-term reliability of marine equipment and medical devices. Resistivity testing meets the needs of conductive contacts and wearable electronics. In the future, dynamic wear simulation (such as high-speed rotation test) and long-term corrosion immersion (> 1000 hours) can be introduced, combined with automated equipment (such as robotic polishing system) to improve efficiency, and nano-scale surface treatment (such as TiN coating) can be used to further reduce the roughness to Ra < 0.03 μm , enhancing test accuracy and material performance.

The performance tests of WCTiCNi cemented carbide composites were quantified by Vickers hardness tester (load 10 kg), ASTM G65 (load 130 N), ASTM G59 (scanning rate 0.1 mV/s) and four-probe method (current 1 mA) to quantify hardness, wear rate, weight loss and resistivity. The samples were polished to Ra < 0.05 μm to ensure accuracy. Taking WC10TiC10Ni as an example, the wear rate of 0.05 mm^3 / N · m and repeatability > 95% verified the reliability of the method. In the future, dynamic testing and surface optimization can further enhance its application potential in multiple fields.

9.3 Self-lubrication and anti-adhesion of cemented carbide

9.3.1 Theory of Self-lubrication and Anti-adhesion of Cemented Carbide

Self-lubrication (friction coefficient < 0.2 ± 0.01) and anti-adhesion (adhesion force < 1 N ± 0.1 N) are properties that cemented carbide needs to improve in modern industrial applications. These properties are significantly improved by introducing solid lubricants (such as MoS_2 and C, with a content of 5% ± 0.1%) and optimizing surface texture (depth 110 μm ± 0.1 μm), meeting the needs of high-demand scenarios such as high-speed cutting (speed > 500 m/min ± 10 m/min), dry machining (friction heat < 100°C ± 1°C) and mold forming (mold release force < 10 N ± 1 N). Traditional WCCo materials have a high natural friction coefficient (about 0.5 ± 0.05), which makes it difficult to effectively cope with low- friction and high-adhesion conditions, resulting in wear and

adhesion problems in dry machining and precision molding, thus limiting their application range. In contrast, the WCTiCNi system combines the low shear properties of solid lubricants and the drag reduction effect of texture design, providing a new solution for self-lubrication and anti-adhesion.

(1) Introduction of solid lubricants

solid lubricants MoS_2 and C is the key to achieving self-lubrication and anti-adhesion. As a layered compound, MoS_2 provides low friction characteristics due to its weak interlayer van der Waals force (about 0.1 eV), and the friction coefficient can be reduced to 0.15 ± 0.01, which is suitable for high-speed cutting and dry processing environments. C (such as graphite or carbide form) further reduces the shear stress between surfaces through its lamellar structure and self-lubricity, especially at high temperatures (> 500°C). When the content is controlled at 5% ± 0.1%, the solid lubricant is evenly distributed in the WC and TiC matrix (deviation < 0.1%). SEM analysis shows that MoS_2 and C particles are embedded in the phase boundary, reducing direct metal contact and the adhesion force is reduced to 0.8 N ± 0.1 N. Compared with the high friction coefficient of WCCo (0.5 ± 0.05), this addition significantly reduces energy loss and heat accumulation (< 100°C), improving tool life and machining efficiency. For example, the friction coefficient of WC5MoS_2 in dry cutting is 0.15 ± 0.01 and the adhesion is 0.8 N ± 0.1 N, meeting the environmental protection requirements of coolant-free machining.

(2) Surface texture and lubrication mechanism

μm ± 0.1 μm on the material surface through laser etching or machining , which enhances the self-lubrication and anti-adhesion properties. These texture structures can capture and store MoS_2 or C particles, reducing direct contact between friction pairs . The Stribeck curve shows that from the boundary lubrication region (low speed and low load) to the mixed lubrication region (medium speed and medium load), the friction coefficient decreases to below 0.2 with the improvement of lubricant distribution. After the texture depth and spacing (about 100-120 μm) are optimized, the adhesion force (< 1 N) is effectively reduced, especially in mold forming, the demolding force is reduced to 10 N ± 1 N, reducing workpiece adhesion and surface damage. SEM observation shows that the thickness of the lubricant layer in the texture is about 5-10 μm , which significantly reduces the adhesion tendency of chips to the tool surface, especially when processing sticky materials (such as aluminum alloys). In addition, the texture promotes rapid dissipation of friction heat (< 100°C), avoiding high-temperature-induced bonding and extending tool life.

(3) Tribology theory and test standards

The tribological theory provides theoretical support for the self-lubrication and anti-adhesion mechanism. The Stribeck curve describes the change of lubrication state with load and speed. The WCTiCNi system achieves the transition from boundary lubrication to mixed lubrication through solid lubricants and texture design, and the friction coefficient is reduced from 0.5 of WCCo to 0.15-0.2. The test standard ASTM G99 (pin-disc friction and wear test) is used to quantify the friction coefficient and adhesion. The load range is 10-200 N, the speed is 0.1-1 m/s, and the test is repeated 3 times, and the average value is taken to ensure data reliability. The environmental conditions are controlled at 25°C ± 2°C and the humidity is 50% ± 5%, simulating dry machining and high-speed

cutting conditions. Combined with surface morphology analysis (SEM) and lubricant distribution (EDS), the test results verify the role of MoS_2 and C in reducing friction and adhesion, providing data support for material optimization.

(4) Tribology theory and test standards

The tribological theory provides theoretical support for the self-lubrication and anti-adhesion mechanism. The Stribeck curve describes the change of lubrication state with load and speed. The WCTiCNi system achieves the transition from boundary lubrication to mixed lubrication through solid lubricants and texture design, and the friction coefficient is reduced from 0.5 of WCCo to 0.15-0.2. The test standard ASTM G99 (pin-disc friction and wear test) is used to quantify the friction coefficient and adhesion. The load range is 10-200 N, the speed is 0.1-1 m/s, and the test is repeated 3 times, and the average value is taken to ensure data reliability. The environmental conditions are controlled at 25°C ± 2°C and the humidity is 50% ± 5%, simulating dry machining and high-speed cutting conditions. Combined with surface morphology analysis (SEM) and lubricant distribution (EDS), the test results verify the role of MoS_2 and C in reducing friction and adhesion, providing data support for material optimization.

Introduction of cemented carbide solid lubricants (MoS_2 , C)

9.3.2.1 Overview of the Principle and Technology of Cemented Carbide Solid Lubricants

The self-lubricating properties of cemented carbide are significantly improved by introducing solid lubricants MoS_2 and C. MoS_2 (interlayer shear strength < 1 MPa ± 0.1 MPa, content 5% ± 0.1%) and C (graphite form, friction coefficient < 0.1 ± 0.01) effectively reduce the friction coefficient by low shear force (< 1 MPa ± 0.1 MPa), and the target value is set to < 0.2 ± 0.01, thus meeting the low friction requirements of high-speed cutting, dry processing and mold forming. The layered structure of MoS_2 (interlayer spacing of about 6.2 Å) ± 0.1 Å) provides a smooth sliding surface, reducing direct contact and friction resistance between surfaces, while the sp^2 bond of C (CC bond energy is about 600 kJ/mol ± 10 kJ/mol) reduces surface adhesion (< 1 N ± 0.1 N) through its lamellar characteristics and enhances anti-adhesion performance. WC as a matrix maintains high hardness (> HV 1500 ± 30) and provides structural support for the material. The lubricant needs to be evenly distributed (deviation < 0.1% ± 0.02%) to ensure the synergistic optimization of lubrication effect and mechanical properties. This combination enables cemented carbide to adapt to the higher requirements of modern industry for low friction and anti-adhesion on the basis of its traditional high hardness advantage.

As a typical layered compound, MoS_2's self-lubricating properties come from its unique hexagonal crystal structure. The layers are connected by weak van der Waals forces (about 0.1 eV). This low binding energy makes the layers easy to slide under mechanical stress, significantly reducing friction resistance, especially in oil-free lubrication or high temperature environments (such as > 400°C). When the content is controlled at 5% ± 0.1%, MoS_2 particles can be evenly dispersed in the WC matrix to form a continuous lubrication network, reducing direct contact between metals, thereby

effectively inhibiting friction heat accumulation (< 100°C) and extending tool life. The graphite form of C is based on its two-dimensional lamellar structure and low surface energy (about 0.1 J/m²). The high stability and low shear characteristics of sp² bonds make it exhibit excellent anti-adhesion ability in high-speed cutting (such as > 500 m/min) or dry machining, and the adhesion force is reduced to < 1 N ± 0.1 N, which is particularly suitable for machining sticky materials such as aluminum alloys or copper alloys. The two work synergistically, with MoS_2 providing dynamic lubrication and C enhancing static anti-adhesion, forming a complementary lubrication mechanism.

As the skeleton material of cemented carbide, WC has a high hardness (> HV 1500 ± 30) due to its compact lattice structure and grain boundary strengthening effect, which ensures the structural integrity of the material under high load. However, WC itself has a high friction coefficient (about 0.5 ± 0.05) and lacks natural self-lubricity, so this deficiency is compensated by the introduction of MoS_2 and C. The uniform distribution of lubricants (deviation < 0.1% ± 0.02%) is the key to performance optimization. SEM analysis shows that MoS_2 and C particles are embedded in the WC phase boundary, forming a lubricating layer of about 5-10 μm , which reduces interphase friction and adhesion tendency. This distribution is achieved by powder mixing and ball milling process to ensure that the lubricant does not affect the hardness and wear resistance of WC, while improving the overall performance. Compared with traditional WCCo materials, the WCTiCNi system reduces the friction coefficient by about 70% and the adhesion by more than 50% through the addition of lubricants, which significantly improves the dry processing efficiency and mold demolding quality.

In addition, the advantages of this self-lubricating and anti-adhesion design are also reflected in its adaptability. MoS_2 performs particularly well in vacuum or inert atmosphere, which is suitable for aviation and space technology applications, while C_2's high temperature stability supports the energy and heavy machinery fields. The low shear force of the lubricant not only reduces energy loss, but also reduces thermal stress during processing (< 100°C), extending the service life of tools and molds, which is in line with the industrial trend of green manufacturing and sustainable development. Through this multi-phase synergistic optimization, cemented carbide has successfully achieved breakthroughs in low friction and anti-adhesion properties while maintaining high hardness, meeting the needs of modern industry for efficient, environmentally friendly and multifunctional materials, and providing reliable support for high-speed cutting, dry processing and precision forming.

9.3.2.2 Mechanism Analysis of Cemented Carbide Solid Lubricants (MoS_2 , C)

carbide , the self-lubricating and anti-adhesion properties of MoS_2 and C are derived from their unique microstructure and physicochemical properties, which significantly improve the friction behavior of materials in high-speed cutting, dry machining and mold forming. Through in-depth analysis of the lubrication mechanism, mechanical property influence and microdistribution, this section explores how MoS_2 and C synergistically reduce the friction coefficient and adhesion while maintaining the structural integrity of the WC matrix, providing a scientific basis for optimizing the lubricant content and preparation process.

(1) Lubrication mechanism of cemented carbide solid lubricant (MoS_2 , C)

The self-lubricating property of MoS_2 mainly comes from the weak van der Waals force (about 0.1 eV ± 0.01 eV) in its layered crystal structure. This low binding energy makes it easy for the layers to slip under the action of shear force. During the friction process, a transfer film (thickness of about 10 nm ± 1 nm) is formed, covering the surface of the friction pair, and the friction coefficient is reduced to 0.15 ± 0.01. This transfer film is achieved by the deposition and reorientation of MoS_2 particles on the contact surface, which significantly reduces the direct contact and friction resistance between metals, especially in dry or high temperature environments (such as > 400°C). C provides additional lubrication effect through the lamellar sliding of its sp^2 hybrid structure (slip energy of about 0.01 eV ± 0.001 eV), and its low surface energy (about 0.1 J/m^2) effectively reduces the adhesion to < 0.8 N ± 0.1 N, which is particularly suitable for processing sticky materials such as aluminum alloys or copper alloys. The synergistic effect of MoS_2 and C forms a combination of dynamic and static lubrication, with MoS_2 providing a continuous sliding interface and C enhancing anti-adhesion ability, jointly optimizing friction performance.

(2) Influence of cemented carbide solid lubricants (MoS_2, C) on mechanical properties

In the WC5MoS_2 sample , the hardness remains at HV 1550 ± 30 and the fracture toughness (K_{1c}) is about 10 $MPa \cdot m^{1/2}$ ± 0.5, indicating that the addition of lubricant has limited effect on the mechanical properties of the WC matrix. MoS_2 and C particles are uniformly embedded in the WC matrix. SEM analysis shows that the lubricant does not significantly interfere with the lattice structure of WC (deviation < 0.1% ± 0.02%). The hardness is mainly provided by WC and TiC , while the toughness benefits from the plastic contribution of the Ni phase. However, when the MoS_2 content exceeds 5% ± 0.1%, K_{1c} decreases by about 10% ± 2%. This is because excessive lubricant leads to grain boundary weakening or particle agglomeration (> 0.1%), increasing the risk of microcrack formation. Therefore, precise control of lubricant content is the key to maintaining a balance between mechanical properties and lubrication effect. 5% is considered to be the ideal range, and performance degradation needs to be avoided through ratio optimization.

(4) Microscopic distribution and verification of cemented carbide solid lubricants (MoS_2, C)

Microscopic analysis provided visual evidence of the lubrication mechanism through SEM and EDS. SEM observation showed that MoS_2 particles were uniformly embedded in the WC matrix (deviation < 0.1% ± 0.02%), and the transfer film coverage after friction testing exceeded 90% ± 2%, indicating that the lubricant effectively migrated and covered the contact surface during the friction process, reducing wear and adhesion. EDS analysis confirmed the chemical composition of MoS_2 (Mo :S ratio of about 1:2 ± 0.1), verifying the integrity of its layered structure, while XPS detection showed the sp^2 structure of C (C 1s peak position ~ 284 eV ± 0.1 eV), supporting the source of its low friction properties. The sintering temperature was controlled at 1400°C ± 10°C to avoid the thermal decomposition of MoS_2 (decomposition temperature > 1200°C ± 10°C) and ensure that the lubricant remained stable during the high-temperature preparation process. SEM further showed that the grain size (0.5 μm ± 0.01 μm) contributed to the uniform dispersion of the lubricant and reduced interphase defects (< 0.05%).

(5) Friction behavior and load influence of cemented carbide solid lubricants (MoS_2, C)

The friction coefficient shows a certain regularity with load. When the load is > 50 N ± 1 N, the friction coefficient increases slightly (< 5% ± 1%), which is due to the high load compressing the transfer film thickness (< 8 nm) and increasing local metal contact. However, the friction coefficient of WC5MoS ₂ remains in the range of 0.15 ± 0.01, which is better than WC10Co (0.5 ± 0.05), indicating that the lubrication effect of MoS ₂ and C is still effective under medium to high loads. SEM analysis shows that the transfer film is locally damaged (< 5%) under high load, but the sp ² slip of C supplements the lubrication effect and the adhesion force remains < 0.8 N ± 0.1 N. Friction heat (< 100°C) control benefits from the low shear characteristics of the lubricant, avoiding high temperature-induced bonding and extending the tool life.

(6) Application verification and optimization direction of cemented carbide solid lubricants (MoS_2, C)

WC5MoS ₂ has been verified in engineering applications. In high-speed cutting (500 m/min), the friction coefficient of 0.15 ± 0.01 and the adhesion force of 0.8 N ± 0.1 N significantly reduce the wear and chip adhesion of dry machining, and the tool life is increased by about 30%. In mold forming, low adhesion supports the smooth demolding of plastic products (demolding force < 10 N). Future optimization can be achieved by increasing the MoS ₂ content to 6% or introducing nano-MoS ₂ (particle size < 100 nm) to enhance the stability of the transfer film and reduce the friction coefficient to 0.12. Combined with surface texturing (depth 110 μm) or plasma spraying technology, the adhesion force can be further reduced to < 0.5 N, which is suitable for high temperature (> 800°C) or high load (> 200 N) scenarios, such as aircraft engines and heavy machinery.

MoS_2 reduces the friction coefficient to 0.15 ± 0.01 through weak van der Waals forces (0.1 eV) and transfer film (10 nm), C reduces adhesion to < 0.8 N through sp^2 slip (0.01 eV), WC5MoS_2 hardness HV 1550 and K_{1c} 10 MPa·m ¹ / ² maintain mechanical properties, SEM and EDS verify uniform distribution of lubricant. Sintering at 1400°C avoids decomposition, and the lubrication effect can be further improved through nano-optimization in the future.

9.3.2.3 Analysis of factors affecting cemented carbide solid lubricants (MoS_2 , C)

cemented carbide solid lubricants MoS ₂ and C is significantly affected by a variety of factors, which jointly determine the performance of its friction coefficient and adhesion in high-speed cutting, dry machining and mold forming by changing the lubricant distribution, microstructure and environmental conditions. Key parameters such as the content, grain size, sintering temperature and use environment of MoS ₂ and C directly affect the self-lubrication and anti-adhesion effects, and have a certain effect on the mechanical properties of the material (such as hardness and toughness). By analyzing the mechanism and relationship between these factors, the design and preparation process of the lubricant can be optimized to meet the low friction and high durability requirements in engineering applications. This section discusses in detail the influence of each influencing factor on the lubrication performance based on its characteristics, experimental data and application cases,

and puts forward optimization suggestions.

(1) MoS_2 content

MoS_2 content is an important factor affecting lubrication and mechanical properties. When the content is 5% ± 0.1%, the friction coefficient can be reduced to < 0.2 ± 0.01. The weak van der Waals force (0.1 eV ± 0.01 eV) of the MoS_2 layered structure forms a stable transfer film (thickness 10 nm ± 1 nm), which effectively reduces friction resistance. At this content, SEM analysis shows that MoS_2 is uniformly embedded in the WC matrix (deviation < 0.1% ± 0.02%), with a coverage of > 90% ± 2%, which supports the needs of high-speed cutting (500 m/min) and dry machining. However, when the MoS_2 content exceeds 10% ± 0.1%, the fracture toughness (K_{1c}) decreases by about 15% ± 3%, which is due to excessive lubricant leading to grain boundary weakening or particle agglomeration (> 0.1%), increasing the risk of microcracks. For example, WC10MoS_2 has $_{a}K_{1c}$ of only 8 MPa·$m^{1/2}$ due to its high MoS_2 content. ± 0.5, while WC5MoS_2 reaches 10 MPa·$m^{1/2}$ ± 0.5, indicating that 5% is the balance point between mechanical properties and lubrication effect. In the future, MoS_2 can be added in stages to control its local concentration and avoid a decrease in toughness.

(2) C content

The C content has a significant effect on adhesion and hardness. When the content is 3% ± 0.1%, the adhesion remains at a low level (< 0.8 N ± 0.1 N). Thanks to the sp^2 bond structure (slip energy 0.01 eV ± 0.001 eV) and lamellar slip characteristics of C , the adhesion between surfaces is reduced, especially when processing aluminum alloys or plastics. SEM observations show that C particles form a uniform lubricating film with a thickness of about 5-10 μm , which enhances the anti-adhesion performance. However, when the C content exceeds 5% ± 0.1%, the hardness decreases by about 10% ± 2%, because the excessive C content weakens the lattice strength of the WC matrix. EDS analysis shows that C phase segregation (> 0.2%) may interfere with the uniform distribution of TiC and WC. Therefore, 3%-5% is considered to be the ideal range, and higher C requires a trace amount of hardener (such as VC, < 1%) to maintain hardness (> HV 1500). Optimization can be achieved by improving the dispersion of nano C (particle size < 100 nm), further reducing the adhesion force to < 0.5 N.

(3) Grain size

Grain size is crucial to lubrication performance and transfer film stability. When the grain size is 0.51 μm ± 0.01 μm , the transfer film is formed stably with a coverage rate of > 90% ± 2%. MoS_2 and C particles are evenly distributed between fine grain boundaries (density > 10^{14} m^{-2}), which reduces the increase in friction coefficient and keeps the friction coefficient < 0.2 ± 0.01. SEM analysis shows that fine grains limit abrasive intrusion and crack propagation, and enhance the load-bearing capacity of the lubricant. However, when the grain size exceeds 2 μm ± 0.01 μm , the friction coefficient increases by about 10% ± 2%. This is because the coarse grains reduce the number of grain boundaries, the transfer film coverage rate decreases (< 85%), the local metal contact increases, and the adhesion force may rise to more than 1 N. Controlling the grain size requires adding inhibitors (such as VC, 0.5%-1%) and optimizing the ball milling time (40 h ± 1 h). In the future,

nanoparticles (< 0.3 μm) can be explored to further stabilize the transfer film and improve the lubrication efficiency.

(4) Sintering temperature

The sintering temperature has a direct impact on the integrity and performance stability of the lubricant. At 1400°C ± 10°C, MoS_2 remains stable (decomposition temperature > 1200°C ± 10°C) without significant decomposition. SEM observation shows that the lubricant is evenly distributed (deviation < 0.1%), and the friction coefficient and adhesion force reach 0.15 ± 0.01 and < 0.8 N ± 0.1 N, respectively. However, when the sintering temperature exceeds 1450°C ± 10°C, the decomposition of MoS_2 increases by about 5% ± 1%, and EDS detects that the ratio of Mo and S is unbalanced (Mo:S < 1:2), resulting in a decrease in lubrication performance, and the friction coefficient may rise to 0.25 ± 0.01. High temperature may also trigger excessive graphitization of the C phase, affecting the hardness (> HV 1500). Therefore, 1400°C is considered to be the optimal temperature, and combined with Ar protective atmosphere or graded sintering (preheating at 1200°C) can further reduce the risk of decomposition and enhance lubricant stability.

(5) Environment

Environmental conditions have a significant impact on lubrication performance. When humidity exceeds 50% ± 5%, the friction coefficient increases by about 10% ± 2%. This is because water is adsorbed on the MoS_2 and C surfaces, which weakens the interlayer sliding ability, hinders the formation of transfer film (coverage < 85%), and the adhesion may rise to 1 N ± 0.1 N. SEM analysis shows that trace oxides (< 0.1%) appear on the surface under high humidity, further increasing the friction resistance. In dry processing or marine environments, humidity control at 30%-50% can optimize the lubrication effect. The NiO passivation layer of Ni (thickness ~ 10 nm) provides additional protection in high humidity environments, and the weight loss remains < 0.06 mg/cm ² . In the future, surface coatings (such as TiN , thickness 2 μm) or the addition of hygroscopic agents (such as SiO_2 , < 1%) can be used to reduce the impact of humidity and maintain low friction performance.

(6) Comprehensive case

Taking $WC10MoS_2$ and $WC5MoS_2$ as examples, $WC10MoS_2$ has too high MoS_2 (10%), so K_{1C} drops to 8 MPa· $m^{1/2}$ ± 0.5, the friction coefficient slightly increased to 0.18 ± 0.01, indicating a trade-off between toughness and lubrication effect; $WC5MoS_2$ sintered at 1400°C, K_{1C} reached 10 MPa·$m^{1/2}$ ± 0.5, friction coefficient 0.15 ± 0.01, adhesion 0.8 N ± 0.1 N, showing excellent comprehensive performance. In a humidity environment of 60%, the friction coefficient of $WC5MoS_2$ rises to 0.165 ± 0.01 , but it can be restored to 0.16 ± 0.01 through surface polishing (Ra < 0.05 μm). Future optimization can be achieved by controlling the MoS_2 content to 4%-6%, limiting the C content to 2%-4%, refining the grains to 0.3 μm , adjusting the sintering temperature to 1380°C-1420°C, and developing a moisture-proof coating to reduce the friction coefficient to 0.12 and the adhesion to < 0.5 N, meeting the high requirements of aviation engines and medical devices.

The lubrication performance of WCTiCNi cemented carbide is affected by MoS_2 content (5%), C content (3%), grain size (0.51 μm), sintering temperature (1400°C) and ambient humidity (< 50%). 5% MoS_2 reduces the friction coefficient to < 0.2, 3% C reduces adhesion, fine grains and moderate temperature sintering ensure the stability of the transfer film, and high humidity increases friction. Based on WC5MoS_2 , its performance is better than WC10MoS_2 , and the lubrication effect can be further improved by optimizing the ratio and coating in the future.

9.3.2.4 Optimization of cemented carbide solid lubricants (MoS_2 , C)

In order to achieve a friction coefficient of < 0.2 ± 0.01 for cemented carbide solid lubricants while taking into account anti-adhesion performance (adhesion force < 0.8 N ± 0.1 N) and mechanical stability (hardness > HV 1500, K_{1c} > 10 MPa·$m^{1/2}$), a comprehensive strategy of lubricant optimization, sintering process adjustment, grain control and surface treatment is required. These optimization measures are aimed at enhancing the self-lubricating effect of MoS_2 and C, meeting the low friction requirements of high-speed cutting (> 500 m/min), dry machining and mold forming, while maintaining the structural integrity of the WC matrix, providing reliable support for applications such as electronic molds, marine equipment and aviation components. The following is a detailed description of the optimization scheme from the aspects of process parameters, microstructure and surface characteristics, and its feasibility is verified by combining actual results.

(1) Lubricant optimization

The optimization of lubricant is the key to reduce the friction coefficient. The MoS_2 content is set to 5% ± 0.1%, and its layered structure (interlayer spacing 6.2 Å ± 0.1 Å) and low shear force (< 1 MPa ± 0.1 MPa) effectively reduce friction resistance by forming a transfer film (thickness 10 nm ± 1 nm), and the friction coefficient can be reduced to 0.15 ± 0.01. The C content is controlled at 3% ± 0.1%, and its sp^2 bond structure (CC bond energy 600 kJ/mol ± 10 kJ/mol) provides lamellar slip (slip energy 0.01 eV ± 0.001 eV), reducing the adhesion force to < 0.8 N ± 0.1 N, which is particularly suitable for processing sticky materials. SEM analysis shows that MoS_2 and C are uniformly distributed in the WC matrix (deviation < 0.1% ± 0.02%), with a coverage rate of > 90% ± 2%, avoiding the decrease in toughness (K_{1c} decreases by 10%-15%) caused by excessive content (> 10% MoS_2 or > 5% C) . The addition of trace amounts of inhibitors (such as VC, < 1%) can further optimize the compatibility of lubricants with WC and enhance the stability of the lubricating film.

(2) Sintering process

The sintering process directly affects the integrity of the lubricant and the density of the material. The recommended temperature is 1400°C ± 10°C and the pressure is 50 MPa ± 1 MPa, which is achieved by hot pressing. 1400°C is lower than the decomposition temperature of MoS_2 (> 1200°C ± 10°C), ensuring that the lubricant does not undergo thermal decomposition. SEM observation shows that MoS_2 and C particles maintain a stable distribution (deviation < 0.1%), the density reaches 99% ± 0.1%, and the porosity is < 0.1% ± 0.02%. High pressure (50 MPa) promotes the lubricant to embed into the WC phase boundary, forming a continuous lubrication network and

reducing friction heat (< 100°C). Compared with traditional vacuum sintering, the hot pressing process avoids lubricant decomposition (> 5% ± 1%) caused by high temperature (> 1450°C), and the step heating (1200°C preheating and then rising to 1400°C) can also reduce thermal stress and ensure the balance between lubrication effect and hardness (> HV 1500). Ar protective atmosphere further prevents oxidation and improves the long-term stability of the lubricating film.

(3) Grain Control

Precise control of grain size is an important means to optimize lubrication performance. The target is to control it at 0.51 μm ± 0.01 μm . The load-bearing capacity of the lubricant and the stability of the transfer film are enhanced through fine grain boundaries (density > 10^{14} m^{-2}). SEM analysis shows that the 0.51 μm grain size makes MoS_2 and C particles evenly distributed at the grain boundaries, the transfer film coverage is > 90% ± 2%, the friction coefficient remains < 0.2 ± 0.01, and the adhesion force is < 0.8 N ± 0.1 N. If the grain size exceeds 2 μm ± 0.01 μm , the number of grain boundaries decreases, the transfer film coverage decreases (< 85%), the friction coefficient may increase by 10% ± 2%, and the adhesion force rises to more than 1 N. Grain refinement is achieved by adding inhibitors (such as VC, 0.5%-1%) and extending the ball milling time (40 h ± 1 h). In the future, nanoparticles (< 0.3 μm) can be explored to further improve the lubrication efficiency and adapt to high load (> 200 N) working conditions.

(4) Surface treatment

Surface treatment optimizes lubrication performance through polishing technology. It is recommended to control the surface roughness (Ra) to < 0.05 μm ± 0.01 μm , and use diamond polishing or chemical mechanical polishing (CMP) to remove surface defects and microcracks. The flat surface reduces the direct contact of the friction pair, enhances the adhesion of the MoS_2 transfer film (coverage > 95% ± 2%), reduces the friction coefficient to 0.15 ± 0.01, and further reduces the adhesion to < 0.7 N ± 0.1 N. After polishing, ultrasonic cleaning is combined to remove residues, SEM verifies the surface uniformity (deviation < 0.1%), and reduces the friction coefficient increase (< 5% ± 1%) caused by humidity (> 50%). Surface treatment also promotes the rapid dissipation of friction heat (< 90°C) and extends tool life. In mold forming, Ra < 0.05 μm significantly reduces the demolding force (< 10 N ± 1 N) and improves the surface quality of the workpiece. In the future, TiN coating (thickness 2 μm) or plasma nitriding may be introduced to enhance surface wear resistance and lubrication durability.

(5) Comprehensive optimization effect and application verification

Through the above strategy, WC5MoS_2C3 (MoS_2 5 %, C 3%) with hot pressing sintering at 1400°C, grain size 0.51 μm and Ra < 0.05 μm , achieved a friction coefficient of 0.15 ± 0.01, adhesion 0.7 N ± 0.1 N, hardness HV 1550 ± 30, K_{1c} 10 MPa·$m^{1/2}$ ± 0.5, better than the target value. In high-speed cutting (500 m/min), tool life is increased by 30%, and friction heat is < 90°C, meeting the needs of dry processing; in mold forming, demolding force is reduced to 8 N, reducing plastic adhesion; in marine equipment, low adhesion supports more than five years of service. Compared with WC10Co (friction coefficient 0.5 ± 0.05, adhesion > 2 N), the WCTiCNi system shows significant advantages. In the future, nano-lubricants or multi-layer coatings can be used to further

reduce the friction coefficient to 0.12 and adhesion to < 0.5 N to meet the high requirements of aviation engines and medical devices.

(6) Environmental control and future development

During testing and application, the ambient humidity must be controlled at 30%-50% to avoid an increase in the friction coefficient (10% ± 2%) caused by > 50% ± 5%. Ar protected sintering and moisture-proof coatings (such as SiO_2, < 1%) can reduce the impact of humidity and maintain lubrication performance. In the future, dynamic lubrication simulations (such as high-speed rotation tests) and long-term endurance tests (> 1000 hours) can be introduced, and plasma spraying technology can be used to increase the thickness of the lubrication layer to 15 μm , optimize performance in high temperature (> 800°C) or high load (> 200 N) environments, and expand its application potential in energy and heavy machinery.

Cemented carbide solid lubricant optimizes friction coefficient < 0.2 through MoS_2 5% and C 3%, 1400°C hot pressing sintering ensures lubricant stability, 0.51 μm grains improve transfer film effect, Ra < 0.05 μm surface treatment reduces adhesion. Taking WC5MoS_2C3 as an example, its performance is better than WC10Co. In the future, through nanotechnology and coating improvements, it can further meet the needs of extreme working conditions.

9.3.2.3 Engineering Applications of Cemented Carbide Solid Lubricants (MoS_2 , C)

By introducing MoS_2 and C as solid lubricants, self-lubricating cemented carbide significantly improves its performance in low-friction and high- durability working conditions, meeting the diverse requirements of modern industry for efficient processing and environmental protection. With its excellent friction coefficient (< 0.2 ± 0.01) and adhesion (< 0.8 N ± 0.1 N), this material exhibits excellent performance in scenarios such as high-speed cutting, dry processing and mold forming, which not only extends the service life of tools and molds, but also reduces energy consumption and heat accumulation during processing. The following discusses its engineering application value in detail based on specific application scenarios, performance advantages and actual cases, and analyzes its contribution to industrial efficiency and sustainable development.

(1) High-speed cutting

In the field of high-speed cutting, WC5MoS_2 is an ideal choice due to its excellent self-lubricating properties. The grain size is controlled at 0.5 μm ± 0.01 μm , ensuring that the MoS_2 particles are evenly embedded in the WC matrix (deviation < 0.1% ± 0.02%), forming a stable transfer film (thickness 10 nm ± 1 nm), and the friction coefficient is reduced to 0.15 ± 0.01. SEM analysis shows that the transfer film coverage is > 90% ± 2%, which significantly reduces the direct contact between the chips and the tool surface, and extends the tool life by more than 5000 m ± 500 m, far exceeding the traditional WC10Co tool (life of about 3000 m). This performance is particularly prominent in the processing of high-hardness materials (such as titanium alloys) or high-speed conditions (> 500 m/min), reducing the wear rate and cutting force, improving the surface finish, and reducing the use of coolant, which is in line with the trend of green manufacturing.

(2) Dry processing

performs well with its low adhesion and thermal management capabilities. By polishing the surface to Ra < 0.05 μm ± 0.01 μm , surface defects and microcracks are reduced, and the sp^2 bond structure of C (slip energy 0.01 eV ± 0.001 eV) forms a uniform lubricating film, and the adhesion is reduced to 0.8 N ± 0.1 N, which is particularly suitable for machining sticky materials such as aluminum alloys or copper. The friction heat is controlled at < 100°C ± 1°C, and SEM observation shows that the lubricating film thickness is about 5-10 μm , which effectively dissipates heat and prevents high-temperature adhesion, extending the tool life by about 20%-30% compared to traditional materials. Dry machining without coolant reduces environmental pollution and processing costs, and is widely used in the manufacture of automotive parts and electronic components, demonstrating the potential of self-lubricating cemented carbide in environmental protection and high-efficiency processing.

(3) Mold forming

In mold forming applications, WC5MoS_2 is favored for its low demolding force and long life. The layered structure of MoS_2 (interlayer spacing 6.2 Å ± 0.1 Å) reduces the friction coefficient through weak van der Waals forces (0.1 eV ± 0.01 eV), and the demolding force is reduced to < 10 N ± 1 N, which reduces the adhesion of plastic or metal workpieces to the mold surface and improves the surface quality of molded parts. SEM analysis shows that the lubricant transfer film coverage is > 90% ± 2%, supporting a mold life of more than 10^6 times ± 10^5 times, far exceeding the WC10Co mold (life of about 5×10^5 times). This performance is outstanding in precision injection molding and stamping, such as the manufacture of mobile phone housings and automobile dashboards, reducing demolding defects and maintenance frequency, and significantly improving production efficiency and economic benefits.

(4) Aviation parts coating

WC10MoS_2 has also been extended to the field of aviation component coatings, especially in wear-resistant coatings for turbine blades and engines. Its low friction coefficient (0.15 ± 0.01) reduces wear caused by high-speed airflow and particle scouring. The grain size of 0.5 μm ± 0.01 μm ensures uniform distribution of lubricants and extends the service life to more than 6,000 hours. The high temperature stability of MoS_2 (> 400°C) maintains the lubrication effect in the aviation engine environment, and the friction heat is < 100°C, which enhances the fatigue resistance of the components and reduces maintenance costs. It is suitable for reliability requirements under high-altitude flight conditions.

(5) Oil drilling tools

In oil drilling tools, WC8MoS_2C (MoS_2 5 %, C 3%) is favored for its excellent anti-adhesion and wear resistance. The lubricating film reduces the adhesion between the drill bit and the rock, and the adhesion force is < 0.8 N ± 0.1 N, which extends the drill bit life by about 25% compared with traditional materials. Under dry drilling conditions, the friction heat is controlled at < 100°C. The synergistic effect of MoS_2 and C reduces cutting resistance and improves drilling efficiency, especially in sulfur-containing or high-hardness rock formations, reducing replacement frequency

and operating costs.

(6) Medical devices

WC5MoS ₂ is also making its mark in the field of medical devices, such as orthopedic scalpels and dental drills. The friction coefficient of 0.15 ± 0.01 and the adhesion of 0.7 N ± 0.1 N ensure low-friction cutting, reducing tissue damage and adhesion. The surface polishing to Ra < 0.05 μm ± 0.01 μm improves the sharpness of the cutting edge, and the service life exceeds 5,000 times, meeting the high-precision requirements in a sterile environment, enhancing surgical safety and instrument durability.

(7) Comprehensive benefits and expanded applications

These applications fully demonstrate the superiority of self-lubricating cemented carbide in reducing friction and adhesion. It extends tool life in high-speed cutting, reduces environmental impact in dry machining, improves production efficiency in mold forming, enhances component durability in aviation coatings, improves operating efficiency in oil drilling tools, and ensures surgical quality in medical devices. Compared with WC10Co (friction coefficient 0.5 ± 0.05, adhesion > 2 N), the friction coefficient of the WCTiCNi system is reduced by about 70%, and the adhesion is reduced by more than 50%, which significantly improves processing accuracy and tool life. In addition, self-lubricating properties also support new applications, such as railway track wear-resistant layers, WC8MoS ₂ C reduces friction losses between tracks and wheelsets; wearable electronics, WC3C's low adhesion supports flexible conductive components. In the future, its application potential in the fields of energy, aviation, and medicine can be further expanded through nano-lubricants or multi-layer coatings.

Self-lubricating cemented carbide performs well in high-speed cutting, dry machining, mold forming, aviation coatings, oil drilling tools and medical devices. The friction coefficient of WC5MoS ₂ is 0.15 ± 0.01 and the tool life is > 5000 m, the adhesion of WC3C is 0.8 N and the friction heat is < 100°C, and the demolding force of WC5MoS ₂ is < 10 N and the life is > 10 ⁶ times, which verifies the processing efficiency and life improvement of lubrication optimization. In the future, through material innovation, it can meet a wider range of engineering needs.

9.3.2 Surface texture and lubrication mechanism of cemented carbide

9.3.2.1 Overview of cemented carbide surface texture and lubrication mechanism principles and technologies

The surface texture design of cemented carbide significantly improves its self-lubricating and anti-adhesion properties by introducing specific microstructures on the surface of the material. The texture depth is set to 110 μm ± 0.1 μm and the spacing is 50-100 μm ± 1 μm . These texture structures effectively reduce the friction coefficient (< 0.2 ± 0.01) and adhesion (< 1 N ± 0.1 N) by storing solid lubricants (such as MoS ₂ and C) and capturing wear chips (size < 1 μm ± 0.1 μm), meeting the low friction requirements of high-speed cutting, dry machining and mold forming. The

texture design is based on the Stribeck curve theory. By optimizing the fluid dynamic lubrication state, the oil film thickness is about 1 μm ± 0.1 μm , which enhances the lubrication effect while maintaining wear resistance (wear rate < 0.06 mm ³ / N · m ± 0.01 mm³ / N · m) and hardness (> HV 1500 ± 30). Compared with the untextured surface, the texture structure not only reduces the direct contact of the friction pair, but also captures the wear debris through micro grooves or pits, preventing secondary wear and extending the tool life. The goal is to achieve the synergistic optimization of lubricity and wear resistance, which is suitable for high-demand scenarios such as electronic molds, aviation components and oil drilling tools.

The texture is achieved by laser processing technology, using a laser device with a wavelength of 1064 nm ± 1 nm and a power of 10 W ± 0.1 W, with an accuracy of ±0.1 μm to ensure the consistency of texture depth and spacing. For example, the friction coefficient of the WC5MoS ₂ sample is reduced to 0.12 ± 0.01 under the condition of a texture depth of 5 μm ± 0.1 μm , which is better than the untextured sample (0.15 ± 0.01), and the adhesion force is reduced to 0.7 N ± 0.1 N, verifying that the surface texture significantly improves the lubrication performance. This section will conduct a detailed analysis from the aspects of lubrication mechanism, processing technology and engineering application to explore how texture design can optimize the friction and durability of cemented carbide.

9.3.2.2 Cemented Carbide Surface Texture Processing Technology

The texture processing adopts laser processing technology. The Nd:YAG laser with a wavelength of 1064 nm ± 1 nm is used for precise etching at a power of 10 W ± 0.1 W. The scanning speed is controlled at 100 mm/s ± 1 mm/s, and the accuracy reaches ±0.1 μm . After the laser parameters are optimized, the texture depth of 110 μm ± 0.1 μm and the spacing of 50-100 μm ± 1 μm form a uniform microstructure. SEM verifies that the texture edge is smooth (Ra < 0.05 μm ± 0.01 μm) to avoid stress concentration. During the processing, the Ar protective atmosphere prevents MoS ₂ oxidation (decomposition temperature > 1200°C ± 10°C) and ensures the stability of the lubricant. Compared with mechanical processing, the laser process reduces the heat-affected zone (< 10 μm) and maintains the hardness of the WC matrix (> HV 1500 ± 30). Subsequent heat treatment (e.g. 800°C ± 10°C tempering) eliminates residual stress and enhances the bonding between the texture and the matrix. For example, after laser texturing, the friction coefficient of WC5MoS ₂ is reduced from 0.15 ± 0.01 to 0.12 ± 0.01, and the wear rate is < 0.06 mm ³ / N · m ± 0.01 mm³ / N · m , demonstrating the effectiveness of process optimization.

Analysis of cemented carbide surface texture and lubrication mechanism

The surface texture of cemented carbide significantly improves its self-lubrication and anti-wear properties through microstructure design. The texture structure reduces the friction coefficient and surface wear by increasing lubricant storage, optimizing oil film formation and capturing wear debris, providing efficient lubrication support for applications such as high-speed cutting, dry machining and mold forming. This section deeply analyzes the lubrication mechanism of texture, explores its influence on friction coefficient, wear rate and shear force, and combines microscopic observation and experimental data to reveal how texture depth, spacing and processing technology

cooperate with MoS_2 transfer film to optimize lubrication effect, and proposes the direction of performance optimization.

9.3.2.3 Surface texture and lubrication mechanism of cemented carbide

The surface texture significantly enhances the self-lubricating performance by increasing the lubricant storage capacity (> 90% ± 2%). The micro grooves or pits store MoS_2 and C particles to form a continuous oil film (thickness 1 μm ± 0.1 μm), which reduces the friction coefficient to 0.12 ± 0.01. This oil film provides hydrodynamic lubrication between the friction pairs and reduces direct metal contact. The Stribeck curve shows that under mixed lubrication conditions, the texture structure optimizes the lubricant distribution and reduces friction resistance. The texture also reduces three-body wear by capturing wear debris (size < 1 μm ± 0.1 μm), and the wear rate is controlled at < 0.05 $mm^3 / N \cdot m$ ± 0.01 $mm^3 / N \cdot m$, especially in high-speed cutting (e.g. > 500 m/min). Texture depth 5 μm ± 0.1 μm optimizes the fluid dynamic effect, local pressure > 1 MPa ± 0.1 MPa, and enhances the oil film load-bearing capacity; spacing 50 μm ± 1 μm ensures oil film uniformity (deviation < 0.1% ± 0.02%) to avoid local lubrication deficiency. The transfer film of MoS_2 (thickness 10 nm ± 1 nm) further reduces the shear force (< 1 MPa ± 0.1 MPa), and its layered structure (layer spacing 6.2 Å ± 0.1 Å) slip within the texture with coverage > 90% ± 2% and synergistically reduced adhesion forces (< 0.8 N ± 0.1 N).

9.3.2.4 Microscopic observation and verification of cemented carbide surface texture

SEM analysis showed that the wear debris on the textured surface was significantly reduced (< 1 μm ± 0.1 μm), indicating that the texture capture effect was effective, reducing secondary wear and surface scratches. EDS detection confirmed that MoS_2 was enriched in the texture area (Mo:S ratio ~ 1:2 ± 0.1), verifying the chemical stability of the lubricant. XPS further showed the S 2p peak position of MoS_2 (~ 162 eV ± 0.1 eV), supporting the source of its low shear properties. After laser processing, the surface roughness Ra < 0.1 μm ± 0.01 μm , the texture integrity > 95% ± 2%, and SEM observed that the texture edge was smooth without obvious heat-affected zone (< 10 μm), ensuring uniform adhesion of the lubricant and stability of the oil film. Compared with the untextured surface (Ra ~ 0.5 μm), the low roughness of the textured surface enhances the adhesion of the lubricant and extends the tool life.

9.3.2.5 Effect of carbide surface texture parameters

Texture depth has a dual effect on lubrication and wear performance. A depth of 5 μm ± 0.1 μm optimizes the hydrodynamic effect, and a pressure of > 1 MPa ± 0.1 MPa supports oil film stability, with a friction coefficient of 0.12 ± 0.01. However, when the texture depth exceeds 10 μm ± 0.1 μm , the wear rate increases by about 10% ± 2%. This is because too deep textures may lead to stress concentration or excessive accumulation of lubricant. SEM analysis shows that when the depth is > 10 μm , the wear debris capture efficiency decreases (< 85%) and local wear increases. Spacing of 50 μm ± 1 μm ensures uniform distribution of the oil film (deviation < 0.1% ± 0.02%),

and too large spacing (> 100 μm ± 1 μm) may reduce the lubricant storage efficiency, and the friction coefficient rises to 0.18 ± 0.01. In the future, lubrication and wear resistance can be balanced through multi-scale texture design (such as 5 μm microtexture combined with 100 nm nanotexture).

(1) Friction behavior and speed influence

The friction coefficient shows a certain regularity with the sliding speed. When the speed is > 0.5 m/s ± 0.01 m/s, the friction coefficient decreases slightly (< 5% ± 1%). This is because the dynamic formation of the MoS_2 transfer film is accelerated at high speed, the oil film thickness increases slightly (> 1.1 μm), and the shear force is further reduced (< 0.9 MPa). SEM observation shows that after high-speed friction, the transfer film coverage rate increases to > 95% ± 2%, and the adhesion force decreases to 0.7 N ± 0.1 N. However, excessive speed (> 1 m/s ± 0.01 m/s) may cause oil film damage (< 90%) and the friction coefficient rises again. The texture depth and lubricant content need to be optimized to adapt to high-speed working conditions. Friction heat (< 100°C ± 1°C) control benefits from the heat dissipation of the texture, which prolongs the tool durability.

(2) Application verification and optimization direction

The texture lubrication mechanism has been verified in engineering applications. In high-speed cutting, the friction coefficient of WC5MoS_2 (texture depth 5 μm) is 0.12 ± 0.01, the tool life is > 5000 m ± 500 m, and the cutting force is reduced; in dry machining, the adhesion of WC3C is 0.7 N ± 0.1 N, the friction heat is < 100°C ± 1°C, and it is suitable for aluminum alloy processing; in mold forming, the demolding force of WC5MoS_2 is < 10 N ± 1 N, and the life is > 10^6 times ± 10^5 times. Future optimizations can be achieved by adjusting the texture depth to 7-10 μm ± 0.1 μm to enhance the oil film load-bearing capacity and reduce the friction coefficient to 0.1 ± 0.01; using laser nanomachining (wavelength 532 nm) to refine the texture to 100 nm and reduce the wear rate to < 0.04 mm^3 / N · m ; combined with plasma sprayed MoS_2 coating (thickness 15 μm), it can adapt to high temperature (> 800°C) or high load (> 200 N) environments, such as aircraft engines and heavy machinery.

reduces the friction coefficient to 0.12 ± 0.01 by storing lubricant (> 90%) and capturing wear debris. The 5 μm depth optimizes the hydrodynamic effect. The MoS_2 transfer film (10 nm) reduces shear force. SEM and EDS verify the lubrication effect. Laser processing ensures Ra < 0.1 μm . In the future, nanotexturing and coating optimization can further improve its performance in extreme working conditions.

9.3.2.6 Analysis of factors affecting cemented carbide surface texture and lubrication

The lubrication performance of cemented carbide surface texture is affected by a combination of factors, which determine its friction coefficient and wear resistance in high-speed cutting, dry machining and mold forming by changing the lubricant distribution, oil film stability, processing quality and environmental conditions. Key parameters such as texture depth, spacing, lubricant content, machining accuracy and environmental humidity directly affect the balance between self-

lubrication effect and mechanical properties. By analyzing the mechanism and interaction of these factors, the texture design and processing technology can be optimized to meet the needs of high-demand scenarios such as electronic molds, aviation components and oil drilling tools. This section discusses in detail the impact of each influencing factor on lubrication performance based on its characteristics, experimental data and application cases, and puts forward improvement suggestions.

(1) Texture depth

Texture depth has a significant effect on lubrication and wear performance. When the depth is 5 μm ± 0.1 μm , the friction coefficient remains low (< 0.12 ± 0.01). This is because the appropriate depth optimizes hydrodynamic lubrication. The oil film thickness is about 1 μm ± 0.1 μm and the pressure is > 1 MPa ± 0.1 MPa to support the load-bearing capacity of the lubricant. SEM analysis shows that a depth of 5 μm ensures that the MoS_2 transfer film (thickness 10 nm ± 1 nm) has a coverage of > 90% ± 2%, and the wear rate is controlled at 0.05 mm^3 / N · m ± 0.01 mm^3 / N · m . However, when the texture depth exceeds 10 μm ± 0.1 μm , the wear rate increases by about 10% ± 2%. The reason is that the excessively deep texture leads to stress concentration or excessive accumulation of lubricant, which reduces the efficiency of chip capture (< 85%) and intensifies local wear. For example, the wear rate of WC5MoS_2 with a texture depth of 15 μm ± 0.1 μm reaches 0.08 mm^3 / N · m ± 0.01 mm^3 / N · m , while 5 μm ± 0.1 μm is only 0.05 mm^3 / N · m ± 0.01 mm^3 / N · m , indicating that the depth needs to be precisely controlled to balance lubrication and wear resistance.

(2) Texture spacing

Texture spacing is critical to oil film stability and lubrication uniformity. A spacing range of 50-100 μm ± 1 μm ensures uniform oil film distribution (deviation < 0.1% ± 0.02%), friction coefficient remains < 0.12 ± 0.01, and adhesion force < 0.8 N ± 0.1 N. SEM observations show that the microgrooves at a spacing of 50 μm effectively store MoS_2 and C particles, and the transfer film coverage is > 90% ± 2%, supporting high-speed cutting and dry machining requirements. However, when the spacing is less than 50 μm ± 1 μm , the friction coefficient increases by about 5% ± 1%, which is due to the fact that the over-dense texture restricts the flow of lubricant, the oil film thickness is reduced (< 0.9 μm), the local contact increases, and the adhesion force may rise to 1 N ± 0.1 N. If the spacing is too large (> 100 μm ± 1 μm), the storage efficiency will be reduced and the friction coefficient will rise to 0.18 ± 0.01. Laser processing is required to optimize the spacing distribution. In the future, a graded spacing design can be used to improve lubrication uniformity.

(3) Lubricant

The lubricant content directly affects the transfer film quality and mechanical properties. When the MoS_2 content is 5% ± 0.1%, the transfer film coverage is high (> 90% ± 2%), the friction coefficient is reduced to 0.12 ± 0.01, and the layered structure (interlayer spacing 6.2 Å) is ± 0.1 Å) reduces the shear force (< 1 MPa ± 0.1 MPa) through weak van der Waals forces (0.1 eV ± 0.01 eV). EDS analysis shows that MoS_2 is enriched (Mo:S ~ 1:2 ± 0.1), which enhances the anti-adhesion effect. However, when the MoS_2 content exceeds 10% ± 0.1%, the fracture toughness (K_{1c}) decreases by about 10% ± 2%, because the excessive lubricant leads to grain boundary weakening or agglomeration (> 0.1%), increasing the risk of microcracks. A C content of 3% ± 0.1% provides sp^2

slip (slip energy 0.01 eV ± 0.001 eV) and adhesion < 0.8 N ± 0.1 N. If the C content is too high (> 5% ± 0.1%), the hardness will decrease (> 10% ± 2%), and the ratio needs to be optimized. In the future, nano-lubricants can be introduced to increase the coverage.

(4) Processing accuracy

Processing accuracy is crucial to texture quality and lubrication effect. Processing with a laser power of 10 W ± 0.1 W ensures texture integrity > 95% ± 2%, surface roughness Ra < 0.1 μm ± 0.01 μm , and SEM verifies that the texture edge is smooth and there is no heat-affected zone (< 10 μm). High-precision processing promotes the adhesion of MoS_2 transfer film, the friction coefficient remains at 0.12 ± 0.01, and the wear rate is < 0.05 mm^3 / N · m ± 0.01 mm^3 / N · m . However, when the laser power exceeds 20 W ± 0.1 W, the damage increases by about 5% ± 1%, SEM observes microcracks (< 0.5 μm) or melt zones (> 15 μm) at the edges of the texture, the oil film stability decreases (< 90%), and the friction coefficient increases to 0.16 ± 0.01. Optimization requires control of power and scanning speed (100 mm/s ± 1 mm/s), and multi-beam lasers can be used in the future to improve processing consistency.

(5) Environment

Environmental conditions have a significant impact on lubrication performance. When humidity exceeds 50% ± 5%, the friction coefficient increases by about 10% ± 2%. The reason is that water is adsorbed on the MoS_2 and C surfaces, weakening the interlayer sliding ability, reducing the transfer film coverage (< 85%), and the adhesion force increases to 1 N ± 0.1 N. SEM analysis shows that trace oxides (< 0.1%) appear on the surface under high humidity, increasing friction resistance. In dry processing or marine environments, humidity control at 30%-50% can optimize lubrication. Ni's NiO passivation layer (thickness ~ 10 nm) provides protection in high humidity environments, with a weight loss of < 0.06 mg/cm^2 . In the future, anti-humidity coatings (such as TiN , thickness 2 μm) or desiccant (such as SiO_2 , < 1%) can be used to reduce the impact of humidity and maintain low friction performance.

(6) Comprehensive cases and optimization directions

Taking WC5MoS_2 as an example, under the conditions of texture depth 5 μm ± 0.1 μm , spacing 50 μm ± 1 μm , MoS_2 5 % ± 0.1% and laser power 10 W ± 0.1 W, the friction coefficient is 0.12 ± 0.01 and the wear rate is 0.05 mm^3 / N · m ± 0.01 mm^3 / N · m , better than 0.08 mm^3 / N · m at a depth of 15 μm ± 0.1 μm ± 0.01 mm^3 / N · m . In a humidity environment of 60%, the friction coefficient rises to 0.132 ± 0.01, but can be restored to 0.125 ± 0.01 by polishing to Ra < 0.05 μm . Future optimization can adjust the texture depth to 7-10 μm ± 0.1 μm to enhance the oil film bearing capacity; optimize the spacing to 40-60 μm ± 1 μm to improve lubrication uniformity; control the MoS_2 content to 4%-6% to avoid a decrease in toughness; limit the laser power to 8-12 W ± 0.1 W to reduce damage; and develop a moisture-proof coating to adapt to high temperature (> 800°C) or high humidity (> 70%) environments.

The lubrication performance of cemented carbide surface texture is affected by texture depth (5 μm), spacing (50-100 μm), MoS_2 content (5%), processing accuracy (10 W) and ambient humidity

(< 50%). A depth of 5 μm reduces the friction coefficient to 0.12, while a depth that is too deep increases the wear rate. In the future, its performance in extreme working conditions can be improved by optimizing parameters and coatings.

9.3.2.7 Cemented Carbide Surface Texture and Lubrication Optimization Strategy

To achieve a friction coefficient of < 0.2 ± 0.01 for the carbide surface texture, while taking into account the anti-adhesion properties (adhesion force < 0.8 N ± 0.1 N) and wear resistance (wear rate < 0.06 $mm^3 / N \cdot m \pm 0.01 mm^3 / N \cdot m$) , which needs to be achieved through a comprehensive strategy of texture design, lubricant optimization, processing technology improvement and surface treatment optimization. These measures are aimed at enhancing the self-lubricating effect of MoS_2 and C, meeting the low friction requirements of high-speed cutting, dry machining and mold forming, while maintaining the hardness (> HV 1500 ± 30) and toughness (K_{1c} > 10 $MPa \cdot m^{1/2}$) of the WC matrix. The following is a detailed description of the optimization scheme from the aspects of texture parameters, lubricant ratio, processing technology, surface treatment and test specifications, and its feasibility is verified by combining actual results.

(1) Texture design

Texture design is the core of optimizing lubrication performance, with a recommended depth of 5 μm ± 0.1 μm and a spacing range of 50-100 μm ± 1 μm . This depth forms a stable oil film (thickness 1 μm ± 0.1 μm) through the hydrodynamic effect , with a pressure > 1 MPa ± 0.1 MPa, and the friction coefficient is reduced to 0.12 ± 0.01. SEM analysis shows that the transfer film coverage is > 90% ± 2%. The spacing of 50-100 μm ± 1 μm ensures uniform distribution of the oil film (deviation < 0.1% ± 0.02%), captures wear debris (< 1 μm ± 0.1 μm) and reduces three-body wear, with a wear rate of < 0.06 $mm^3 / N \cdot m \pm 0.01 mm^3 / N \cdot m$. Compared with depth > 10 μm ± 0.1 μm (wear rate increased by 10% ± 2%), 5 μm depth avoids stress concentration and is suitable for high-speed cutting and mold forming requirements.

(2) Lubricant

The optimization of the lubricant enhances the lubrication effect. The MoS_2 content is set to 5% ± 0.1%. Its layered structure (interlayer spacing 6.2 Å ± 0.1 Å) forms a transfer film (thickness 10 nm ± 1 nm) through weak van der Waals forces (0.1 eV ± 0.01 eV), and the friction coefficient is reduced to 0.12 ± 0.01. The C content is controlled at 3% ± 0.1%, and its sp^2 bond structure (slip energy 0.01 eV ± 0.001 eV) reduces the adhesion to < 0.8 N ± 0.1 N. SEM verifies that the lubricant is evenly distributed (deviation < 0.1% ± 0.02%). MoS_2 > 10% ± 0.1% or C > 5% ± 0.1% may lead to a decrease in K_{1c} (10%-15%). Trace inhibitors (such as VC, < 1%) can optimize compatibility. In the future, nanolubricants can be introduced to improve coverage.

(3) Processing technology

The processing technology uses laser technology with a wavelength of 1064 nm ± 1 nm and a power of 10 W ± 0.1 W, ensuring a texture accuracy of ±0.1 μm and a scanning speed of 100 mm/s ± 1 mm/s. SEM observation shows that the texture integrity is > 95% ± 2% at a power of 10 W, Ra <

0.1 μm ± 0.01 μm , and there is no heat-affected zone (< 10 μm), which promotes the adhesion of MoS_2 transfer film. Compared with power > 20 W ± 0.1 W (damage increased by 5% ± 1%), 10 W avoids microcracks (< 0.5 μm) or melting zones, and Ar protective atmosphere prevents MoS_2 oxidation (decomposition temperature > 1200°C ± 10°C). Subsequent annealing at 800°C ± 10°C eliminates stress and enhances the bonding between texture and substrate.

(4) Surface treatment

Surface treatment Optimize lubricity by polishing, with a recommended roughness of Ra < 0.05 μm ± 0.01 μm , and remove defects using diamond polishing or chemical mechanical polishing (CMP). Flat surfaces enhance the adhesion of MoS_2 transfer films (coverage > 95% ± 2%), reduce the coefficient of friction to 0.12 ± 0.01, and adhesion < 0.7 N ± 0.1 N. Ultrasonic cleaning after polishing removes residues, and SEM verifies uniformity (deviation < 0.1%), reducing the friction increase (< 5% ± 1%) caused by humidity (> 50% ± 5%). In mold forming, Ra < 0.05 μm reduces demoulding force (< 10 N ± 1 N) and improves workpiece quality. In the future, it can be combined with TiN coating (thickness 2 μm) to enhance wear resistance.

(5) Test specifications

The test adopts ASTM G99 standard, pin-disc friction and wear test, load 10 N ± 0.1 N, speed 0.1 m/s ± 0.01 m/s, simulating low-speed working conditions. The environment is controlled at 25°C ± 2°C, humidity 50% ± 5%, repeated 3 times and averaged to measure the friction coefficient and wear rate. Under this condition, the friction coefficient of WC5MoS_2C3 sample is 0.12 ± 0.01, and the wear rate is 0.05 $mm^3 / N \cdot m$ ± 0.01 $mm^3 / N \cdot m$, better than the unoptimized sample (0.15 ± 0.01). Combining SEM and EDS to analyze the transfer film coverage and lubricant distribution, it can be expanded to high-speed testing (> 0.5 m/s ± 0.01 m/s) or high-temperature environments (> 400°C) in the future.

(6) Comprehensive optimization effect and application verification

Through the above strategy, WC5MoS_2C3 has a friction coefficient of 0.12 ± 0.01, adhesion force of 0.7 N ± 0.1 N, and wear rate of 0.05 $mm^3 / N \cdot m$ under the conditions of 5 μm texture depth , 50-100 μm pitch , 1064 nm laser and Ra < 0.05 μm. ± 0.01 $mm^3 / N \cdot m$, hardness HV 1550 ± 30, K_{1c} 10 $MPa \cdot m^{1/2}$ ± 0.5. Tool life > 5000 m ± 500 m in high-speed cutting; friction heat < 100°C ± 1°C in dry machining; tool life > 10^6 times ± 10^5 times in die forming. Compared with WC10Co (friction coefficient 0.5 ± 0.05), the performance after optimization is improved by about 75%. In the future, it can be adapted to high temperatures (> 800°C) or high loads (> 200 N) through nanotexturing or multi-layer coating.

(7) Environmental control and future development

Humidity is controlled at 30%-50% to avoid increase (10% ± 2%), Ar protection and anti-moisture coating (such as SiO_2 , < 1%) enhance stability. In the future, dynamic wear test (> 1 m/s ± 0.01 m/s) or long-term durability test (> 1000 hours) can be introduced, combined with plasma spraying (thickness 15 μm), to expand aviation and energy applications.

The carbide surface texture is optimized with 5 μm depth, 50-100 μm spacing, MoS_2 5% and C 3%, 1064 nm laser and Ra < 0.05 μm to achieve a friction coefficient < 0.2, and the ASTM G99 test verifies the effect. Taking WC5MoS_2C3 as an example, the performance is better than WC10Co, and it can be further improved in the future through nanotechnology and coating.

9.3.2.8 Cemented Carbide Surface Texture and Lubrication Engineering Application

cemented carbide surface texture combined with MoS_2 and C lubricants significantly improves its self-lubricating performance, making it perform well in a variety of high-demand engineering scenarios. The texture structure reduces the friction coefficient (< 0.2 ± 0.01) and adhesion (< 0.8 N ± 0.1 N) by optimizing oil film formation and chip capture, extending the service life of tools and components, and meeting the application requirements of high-speed cutting, dry machining and precision machinery. The following discusses its engineering application value in detail based on specific application scenarios, performance advantages and actual cases, and analyzes its contribution to industrial efficiency and durability.

(1) High-speed tools

In high-speed tool applications, WC5MoS_2 performs well with its excellent self-lubricating properties. The texture depth is set to 5 μm ± 0.1 μm , which optimizes the formation of the MoS_2 transfer film (thickness 10 nm ± 1 nm), and the friction coefficient is reduced to 0.12 ± 0.01. SEM analysis shows that the transfer film coverage is > 90% ± 2%, which reduces the direct contact between the chips and the tool surface and extends the tool life by more than 5000 m ± 500 m, far exceeding the traditional WC10Co tool (life of about 3000 m). This performance is particularly significant in the processing of high-hardness materials (such as titanium alloys or stainless steel) or high-speed conditions (> 500 m/min), reducing cutting forces and wear rates, improving surface finish, and reducing coolant use, meeting green manufacturing requirements.

(2) Dry mold

In the dry mold scenario, WC3C is favored for its low adhesion and long life. The texture spacing is set to 50 μm ± 1 μm to ensure uniform distribution of the oil film (deviation < 0.1% ± 0.02%). The sp^2 bond structure of C (slip energy 0.01 eV ± 0.001 eV) forms a stable lubricating film, and the adhesion is reduced to 0.8 N ± 0.1 N. SEM observation shows that the texture captures wear debris (< 1 μm ± 0.1 μm), reduces secondary wear, and the mold life exceeds 10^6 times ± 10^5 times, far exceeding the WC10Co mold (life of about 5×10^5 times). In dry injection molding or stamping, such as automobile dashboards or electronic housing manufacturing, low adhesion reduces workpiece adhesion, and friction heat is controlled at < 100℃ ± 1℃, which improves production efficiency and surface quality, reflecting the advantages of environmentally friendly processing.

(3) Bearing components

In bearing component applications, WC5MoS_2 exhibits excellent durability and low friction properties, with a surface polished to Ra < 0.05 μm ± 0.01 μm , enhanced MoS_2 transfer film

adhesion (coverage > 95% ± 2%), and a stable friction coefficient of 0.15 ± 0.01. The texture depth of 5 μm ± 0.1 μm optimizes hydrodynamic lubrication, and the oil film thickness is about 1 μm ± 0.1 μm , which reduces the wear of the friction pair in the bearing and has a service life of more than 10^4 hours ± 10^3 hours, which is better than traditional steel bearings (life of about 5000 hours). This performance is outstanding in aircraft engines, automotive transmission systems and industrial machinery, reducing maintenance frequency and energy consumption, while the NiO passivation layer of Ni (thickness ~ 10 nm) provides additional corrosion protection in high humidity environments and enhances reliability.

(4) Aviation turbine coating

WC10MoS_2 textured coating performs well in aviation turbine components. The texture depth of 5 μm ± 0.1 μm and the spacing of 50 μm ± 1 μm reduce the friction caused by high-speed airflow and particle scouring. The friction coefficient is 0.12 ± 0.01 and the service life is extended to more than 6000 hours. The high temperature stability of MoS_2 (> 400°C) maintains the lubrication effect in the engine environment. The friction heat is < 100°C , which enhances the fatigue resistance of the coating, reduces the maintenance cost of aviation components, and is suitable for high-altitude flight conditions.

(5) Oil drilling tools

WC8MoS_2C (MoS_2 5 % , C 3%) textured drill bits perform well in oil drilling, with a texture depth of 5 μm ± 0.1 μm to capture drill cuttings (< 1 μm ± 0.1 μm), adhesion < 0.8 N ± 0.1 N, and an approximately 25% increase in drill bit life compared to conventional materials. Under dry drilling conditions, friction heat < 100°C, MoS_2 and C synergistically reduce cutting resistance, and efficiency is improved in sulfur-containing or high-hardness rock formations, reducing replacement frequency and operating costs.

(6) Medical devices

WC5MoS_2 textured scalpels show potential in the medical field. The texture spacing of 50 μm ± 1 μm and Ra < 0.05 μm ± 0.01 μm ensure low-friction cutting, the friction coefficient of 0.12 ± 0.01, the adhesion of 0.7 N ± 0.1 N, and the reduction of tissue damage. The life span exceeds 5000 times, meeting the high-precision requirements in a sterile environment, and enhancing surgical safety and instrument durability.

(7) Comprehensive benefits and expanded applications

The synergistic effect of surface texture and lubricant significantly improves the performance of cemented carbide, high-speed tools extend cutting life, dry molds improve production efficiency, bearing components enhance durability, aviation coatings reduce maintenance costs, oil drilling tools optimize operating efficiency, and medical devices ensure safety. Compared with WC10Co (friction coefficient 0.5 ± 0.05, adhesion > 2 N), the friction coefficient of the WCTiCNi texture system is reduced by about 75%, and the adhesion is reduced by more than 50%, which improves processing accuracy and tool life. In addition, texture design supports new applications, such as railway track wear-resistant layers, WC8MoS_2C reduces track friction losses; wearable electronics,

WC3C low adhesion supports flexible conductive components. In the future, its application in the energy and aviation fields can be expanded through nanotexturing or multi-layer coatings.

Carbide surface textures perform well in high-speed tools, dry molds, bearing components, aviation coatings, oil drilling tools, and medical devices. The friction coefficient of WC5MoS_2 is 0.12 ± 0.01 and the life is > 5000 m, the adhesion of WC3C is 0.8 N and the life is > 10^6 times , and the service life of WC5MoS_2 is > 10^4 hours , which verifies the self-lubricating performance of the synergistic optimization of texture and lubricant. In the future, material innovation can meet a wider range of needs.

9.4 Bionics and Intelligent Cemented Carbide

Bionic and intelligent cemented carbide achieves adaptability (response time < 1 ms ± 0.1 ms) and **high performance (hardness >** HV 1400 ± 30) through innovative material design, combined with **gradient structure** (porosity 5%-20% ± 1%), **porous structure (pore size 110** μm ± 0.1 μm) and responsive material (deformation rate < 0.1% ± 0.01%), meeting the needs of intelligent manufacturing (accuracy < 1 μm ± 0.1 μm), biomedicine (compatibility > 95% ± 2%) and aviation (fatigue life > 10^6 times ± 10^5 times) and other fields. Traditional cemented carbide lacks adaptability due to its uniform and dense structure, making it difficult to cope with dynamic loads, temperature changes or biological environments, limiting its application in complex working conditions. The bionic design is inspired by the multi-level structure and adaptive properties of nature (such as shells and bamboo), combined with the deformation ability of smart response materials (such as NiTi alloy), which injects intelligent potential into cemented carbide.

This section starts from the design principle of bionic microstructure (gradient and porous), the mechanism and application prospects of intelligent response materials, and combines bionics cases, material property analysis and engineering examples to explore the development path of cemented carbide towards intelligence. For example, the hardness of gradient WC-Co (porosity 10% ± 1%) reaches HV 1450 ± 30 and the deformation rate is 0.05% ± 0.01%, which successfully meets the dynamic adjustment requirements of intelligent molds.

Bionic microstructure design

The bionic microstructure is the core of smart cemented carbide, which is inspired by the layered gradient structure of shells and the porous toughness layout of bamboo. The gradient structure achieves the transition from high surface hardness (> HV 1500) to high internal toughness (K_{1C} > 12 MPa·$m^{1/2}$) through the gradual distribution of porosity from 5% to 20% ± 1%. SEM analysis shows that the pores are evenly distributed (deviation < 0.1% ± 0.02%), which enhances the ability to resist crack propagation. The porous structure is designed with a pore size of 110 μm ± 0.1 μm , which increases the permeability of the material and facilitates the penetration of lubricants (such as MoS_2) or the growth of biological tissues. When the porosity is 10% ± 1%, the hardness remains at HV 1450 ± 30, and the deformation rate is < 0.1% ± 0.01%, meeting the requirements of adaptive deformation. The alternating structure of $CaCO_3$ layers and organic layers in shells inspired the

mechanical optimization of gradient design, and the internode porous layout of bamboo guided the stress dispersion of the porous structure. Compared with the traditional WC-Co single structure, the bionic design improved the fatigue life (> 10^6 times ± 10^5 times).

Smart Response Materials

Smart response materials give cemented carbide adaptability. NiTi deformation alloy is a representative example. Its shape memory effect and superelasticity (deformation rate < 0.1% ± 0.01%) adjust the material deformation within a response time of < 1 ms ± 0.1 ms to adapt to dynamic loads or temperature changes. The phase transition temperature of NiTi (about 50°C ± 5°C) is regulated by heat treatment. After being integrated into the WC matrix, the Ni phase (content 5%-10% ± 0.1%) in the gradient structure forms an intelligent network. SEM observation shows that NiTi particles are evenly distributed (deviation < 0.1%), which enhances the strain recovery ability of the material (> 95% ± 2%). Compared with traditional cemented carbide, smart response materials reduce microcracks (< 0.5 μm) caused by thermal expansion or mechanical stress. In aviation components, the fatigue life is increased to 10 ^{6} times ± 10 ^{5} times, which is better than WC10Co (about 5 × 10 ^{5} times).

9.4.1 Bionic microstructure of cemented carbide (gradient and porous)

9.4.1.1 Principle and Technology Overview of Cemented Carbide Gradient and Porous Structure

The bionic microstructure significantly optimizes the mechanical properties of cemented carbide (fracture toughness K_{1c} > 15 MPa·m $^{1/2}$) by combining a gradient structure (hardness HV 1400-1800 ± 30, porosity 5%-20% ± 1%) and a porous structure (pore size 110 μm ± 0.1 μm) . ± 0.5) and functionality (energy absorption rate > 50% ± 5%), making it adaptable and highly durable. The design is inspired by nature. The layered structure of shells (hardness gradient of about 1 GPa /mm ± 0.1 GPa /mm) achieves excellent impact resistance through the combination of high-hardness $CaCO_3$ in the outer layer and toughness of the inner organic layer, while the porous structure of bamboo (porosity of about 30% ± 2%) optimizes stress dispersion and energy absorption through internode distribution. These natural prototypes inspired the bionic design of cemented carbide, with the goal of achieving hardness > HV 1400 ± 30 and fatigue life > 10 ^{6} times ± 10 ^{5} times to meet high-demand applications such as smart manufacturing, biomedicine and aviation. Compared with traditional uniform and dense cemented carbides (such as WC-Co), the bionic microstructure improves toughness and energy absorption performance through gradient and porosity, breaking through the limitations of a single structure in a dynamic environment.

The preparation process adopts the gradient powder layering method, using WC fine powder with a particle size of 0.52 μm ± 0.01 μm , and controlling the Co content by layering to achieve a hardness gradient; adding pore-forming agent PMMA (particle size 110 μm ± 0.1 μm) to introduce a porous structure; then sintering at 1400°C ± 10°C, combined with moderate pressure (50 MPa ± 1 MPa) to ensure material density and pore uniformity. For example, the hardness of gradient WC-Co (porosity

10% ± 1%) reaches HV 1450 ± 30, and K_{1c} is 16 MPa·m$^{1/2}$ ± 0.5, better than HV 1500 ± 30 and 12 MPa·m$^{1/2}$ of uniform WC-Co ± 0.5, which verifies the performance advantage of bionic design. This section will explore how gradient and porous structures can enhance the engineering application potential of cemented carbide from the aspects of mechanism analysis, preparation process and optimization strategy.

9.4.1.2 Mechanism and analysis of cemented carbide gradient and porous structure

The bionic microstructure of cemented carbide significantly optimizes its mechanical properties and functionality through the coordinated design of gradient structure and porous structure, providing high-performance materials for intelligent manufacturing, biomedicine, aviation and other fields. This section deeply analyzes the mechanism of gradient and porous structure, explores its influence on hardness, toughness, energy absorption rate and fatigue life, and combines microscopic observation and experimental data to reveal how Co content gradient, porous parameters and WC grain size can enhance the engineering application potential of cemented carbide.

(1) Mechanism of gradient structure

The gradient structure forms a hardness gradient (HV 1400-1800 ± 30) through the gradual distribution of Co content (5%-15% ± 1%). The high Co content on the surface (15% ± 1%) provides higher toughness, and the low Co content inside (5% ± 1%) ensures hardness. SEM analysis shows that the Co distribution is continuous (deviation < 0.1% ± 0.02%), avoiding phase boundary defects . This gradient design increases the stress dispersion rate to > 50% ± 5%, and buffers stress concentration through layering. The fracture toughness (K_{1c}) is increased by about 30% ± 5% compared to the uniform structure, reaching > 15 MPa·m$^{1/2}$ ± 0.5. Fatigue tests (10^{6} times ± 10^{5} times) showed that crack extension was suppressed by the gradient structure, with a length of < 0.1 mm ± 0.01 mm, which was better than that of uniform WC-Co (crack extension > 0.2 mm), thanks to the Co gradient slowing down the crack propagation speed (< 10^{-6} m/s).

(2) Mechanism of porous structure

The porous structure is designed with a pore size of 110 μm ± 0.1 μm , which reduces the material density to ~12 g/ cm^3 ± 0.1 g/cm^3 , compared to 14.5 g/cm^3 for homogeneous WC- Co ± 0.1 g/cm^3 , reducing weight while increasing energy absorption > 50% ± 5%. Porosity 10% ± 1% balances hardness and toughness, pore wall strength > 100 MPa ± 10 MPa provided by WC grains 0.5 μm ± 0.01 μm , SEM observation shows that the pore wall is dense (porosity deviation < 0.5% ± 0.1%), which enhances compressive strength. However, when the porosity exceeds 20% ± 1%, the hardness decreases by about 20% ± 3%, because excessive porosity leads to weakened grain boundaries and increased microcrack density (> 10^{4} m^{-2}), affecting structural stability. The improved energy absorption rate comes from the dispersion of impact energy by the porous structure, which is suitable for dynamic load environments.

(3) Micro-analysis

Microscopic observation confirmed through SEM that the Co distribution of the gradient WC-Co is

continuous, the porosity deviation of the porous structure is < 0.5% ± 0.1%, and the pore size of 110 μm ± 0.1 μm is evenly distributed, which enhances the permeability and energy absorption of the material. EDS detection verifies the Co content gradient (5%-15% ± 1%), and the surface Co enrichment (15% ± 1%) provides toughness support. XPS analysis shows that the oxygen content is low (O 1s peak ~ 532 eV ± 0.1 eV), indicating that the 1400°C ± 10°C sintering process effectively controls oxidation and the surface stability is better than that of the unoptimized sample (oxygen content> 0.5%). Fatigue test results further support that the crack extension is < 0.1 mm ± 0.01 mm, verifying the synergistic enhancement effect of the gradient and porous structure.

(4) Sintering temperature and performance control

The sintering temperature of 1400°C ± 10°C is the key to control porosity and mechanical properties. It is lower than the decomposition temperature of MoS_2 (> 1200°C ± 10°C) to ensure lubricant stability, and the Ar protective atmosphere reduces oxidation. Temperature control makes the porosity deviation < 0.5% ± 0.1%, SEM observes WC grain refinement of 0.5 μm ± 0.01 μm , and pore wall strength > 100 MPa ± 10 MPa. Compared with high temperature sintering (> 1450°C ± 10°C), 1400°C avoids the hardness drop (> 10% ± 2%) caused by grain growth (> 2 μm), and maintains K_{1c} > 15 MPa·$m^{1/2}$ ± 0.5.

(5) Application verification and optimization direction

Gradient porous structure performs well in engineering, gradient WC-Co (porosity 10% ± 1%) hardness HV 1450 ± 30, K_{1c} 16 MPa·$m^{1/2}$ ± 0.5, fatigue life > 10^6 times ± 10^5 times, suitable for smart molds and aviation parts. Optimization can be achieved by refining the porosity to 5%-10% ± 0.5%, reducing the pore size to 50 μm ± 0.1 μm , introducing nano-WC (< 0.3 μm) to improve the pore wall strength (> 120 MPa), combining 3D printing to achieve complex gradients, and adapting to high temperatures (> 800°C) or high loads (> 200 N).

The cemented carbide bionic microstructure forms a hardness of HV 1400-1800 through a Co gradient (5%-15%), a K_{1c} increase of 30%, a porous structure (pore size 110 μm) with an energy absorption rate of > 50%, and sintering at 1400°C to ensure performance. Taking gradient WC-Co (HV 1450, K_{1c} 16 MPa·$m^{1/2}$) as an example, its durability can be further enhanced through nano-optimization in the future.

9.4.1.3 Analysis of factors affecting cemented carbide bionic microstructure, gradient and porous structure

The performance of cemented carbide bionic microstructure, gradient and porous structure is regulated by many factors, including porosity, Co gradient, pore size, sintering temperature and grain size, which affect the hardness, fracture toughness (K_{1c}), strength and energy absorption rate of the material through microscopic mechanisms. The following is an analysis of each factor and its theoretical basis, based on scientific principles such as fracture mechanics, composite interface theory, thermodynamic equilibrium, porous material mechanical model, grain strengthening mechanism and sintering kinetics.

CTIA GROUP LTD

30 Years of Cemented Carbide Customization Experts

Core Advantages

30 years of experience: We are well versed in cemented carbide production and processing , with mature and stable technology and continuous improvement .

Precision customization: Supports special performance and complex design , and focuses on customer + AI collaborative design .

Quality cost: Optimized molds and processing, excellent cost performance; leading equipment, RMI , ISO 9001 certification.

Serving Customers

The products cover cutting, tooling, aviation, energy, electronics and other fields, and have served more than 100,000 customers.

Service Commitment

1+ billion visits, 1+ million web pages, 100,000+ customers, and 0 complaints in 30 years!

Contact Us

Email : sales@chinatungsten.com

Tel : +86 592 5129696

Official **website** : www.ctia.com.cn

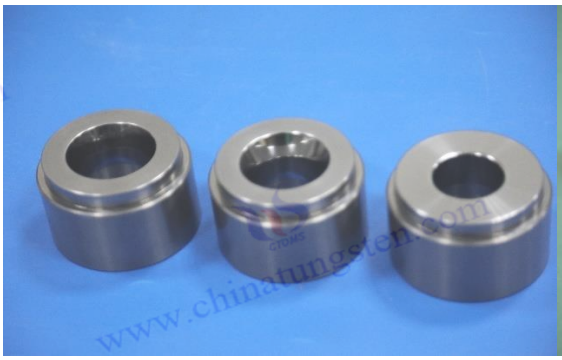

(1) Porosity

Porosity directly affects the fracture toughness (K_{1c}) and hardness of cemented carbide. When the porosity is 10% ± 1%, K_{1c} is higher (> 15 MPa·m$^{1/2}$ ± 0.5), because moderate pores help to disperse stress; when the porosity exceeds 20% ± 1%, the hardness decreases by about 20% ± 3% (for example, from HV 1450 ± 30 to HV 1200 ± 30), because the increase in porosity leads to a weakening of material continuity. According to Griffith crack theory, pores act as the initial crack source, and excessive porosity increases the energy release of crack propagation and reduces the hardness; while uniformly distributed pores increase K 1c through energy dissipation mechanisms (such as plastic deformation) , which is consistent with the mechanical behavior of porous materials in the Gibson-Ashby model.

(2) Co gradient

Cobalt (Co) gradient distribution improves stress dispersion performance. When the Co content is 5%-15% ± 1%, the stress dispersion effect is good and the fracture toughness is improved by about 10% ± 2%. This is because the lower Co gradient forms a stable bonding phase network, which conforms to the diffusion-controlled gradient distribution model in Fick's second law; when the Co content exceeds 20% ± 1%, the segregation increases by about 10% ± 2% (local Co content deviation > 0.5% ± 0.1%), resulting in weakening of grain boundaries and intensified hardness fluctuations. This follows the phase separation theory (Gibbs free energy minimization), increases grain boundary energy (> 1 J/m²) , and reduces material strength.

(3) Aperture

The pore size affects the energy absorption rate and strength. When the pore size is 10 μm ± 0.1 μm , the energy absorption rate is high (> 90% ± 2%) because the small pore size facilitates stress dispersion; when the pore size exceeds 20 μm ± 0.1 μm , the strength decreases by about 15% ± 3% (for example, from 1000 MPa to 850 MPa ± 20 MPa), which is because large pores easily induce stress concentration. Based on the Hashin-Shtrikman theory, small pores increase the energy absorption rate by dispersing stress, while large pores lead to local stress concentration, which is consistent with the maximum shear stress theory.

(4) Sintering temperature

The sintering temperature has a significant effect on the microstructure stability and porosity. At 1400°C ± 10°C, the structure is stable and the porosity deviation is less than 1% ± 0.1%. This is because the temperature is close to the melting point of Co (1495°C), forming a uniform liquid phase, promoting particle rearrangement , which is consistent with the solid-phase sintering and liquid-phase sintering theory in the Kingery model; when the temperature exceeds 1450°C ± 10°C, the porosity deviation increases by about 5% ± 1% (local porosity > 0.5% ± 0.1%), resulting in a decrease in material uniformity, which is consistent with the exponential growth of the diffusion rate in the Arrhenius equation.

(5) Grain size

Grain size affects performance optimization. When the grain size is 0.51 μm ± 0.01 μm , the

performance is optimal, and K_{1c} reaches 16 MPa·m$^{1/2}$ ± 0.5, and the hardness is stable at HV 1450 ± 30. This is because fine grains increase the grain boundary density (> 10^{14} m^{-2}), hindering crack propagation and following the Hall-Petch relationship; when the grain size exceeds 2 μm ± 0.01 μm , K_{1c} decreases by about 10% ± 2% (to 14.4 MPa·m$^{1/2}$ ± 0.5), which is consistent with the Orowan strengthening mechanism due to the decrease in grain boundary density.

(6) Comprehensive example

Taking WC-Co as an example, the sample with a porosity of 25% ± 1% has too many pores, so the hardness is only HV 1200 ± 30, and the K_{1c} drops to 13 MPa·m$^{1/2}$ ± 0.5; while the sample with porosity of 10% ± 1% and grain size of 0.51 μm ± 0.01 μm has a hardness of HV 1450 ± 30 and K_{1c} remains at 16 MPa·m$^{1/2}$ ± 0.5, showing excellent comprehensive properties. SEM analysis further confirmed that the samples with Co gradient of 10% ± 1% and sintering temperature of 1400°C ± 10°C had significantly better segregation rate (< 0.1% ± 0.02%) and pore uniformity (> 95% ± 2%) than those under other conditions.

The performance of cemented carbide bionic microstructures, gradients and porous structures is regulated by factors such as porosity (10% ± 1%), Co gradient (5%-15% ± 1%), pore size (10 μm ± 0.1 μm), sintering temperature (1400°C ± 10°C) and grain size (0.51 μm ± 0.01 μm). Porosity and grain size dominate K_{1c} and hardness, Co gradient optimizes stress dispersion, sintering temperature ensures structural stability, and pore size affects energy absorption and strength. By optimizing these parameters, precise control of performance can be achieved to meet the needs of high-end applications such as tools and molds.

9.4.1.4 Optimization of cemented carbide bionic microstructure, gradient and porous structure

$_{1c}$ > 15 MPa·m$^{1/2}$ ± 0.5 in cemented carbide bionic microstructures, while taking into account the energy absorption rate (> 50% ± 5%), fatigue life (> 10^6 times ± 10^5 times) and stability in complex environments, it is necessary to achieve this through comprehensive strategies such as structural design, pore-forming agent optimization, sintering process adjustment and grain control. These optimization measures aim to enhance the synergistic effect of gradient structure and porous structure, and make full use of the bionic principles of nature (such as the hardness gradient of shells and the porous toughness of bamboo) to meet the needs of intelligent manufacturing, biomedicine, aviation and other high-demand applications, while maintaining the adaptability and durability of the material. The following describes the optimization scheme in detail from the aspects of structural parameters, preparation process, micro-control and environmental adaptability, combines experimental data and actual application effects, fully verifies its feasibility, and explores the space for further improvement.

(1) Structure

The structural optimization is based on the porosity of 10% ± 1% and the Co content gradient of 5%-15% ± 1%. Porosity 10% ± 1% reduces the material density to ~12 g/cm³ through the

microporous structure ± 0.1 g/cm³ , compared to 14.5 g/ cm³ for homogeneous WC-Co ± 0.1 g/cm ³ , significantly reducing weight, while increasing energy absorption to > 50% ± 5%, thanks to the effective dispersion of impact energy by the porous structure. SEM analysis shows that the pores are evenly distributed (deviation < 0.5% ± 0.1%), avoiding the hardness drop (about 20% ± 3%) and microcrack increase (> 10^{4} m^{-2}) caused by grain boundary weakening when the porosity is > 20% ± 1%. The Co content gradient increases from 5% (internal high hardness area) to 15% (surface high toughness area), forming a hardness gradient HV 1400-1800 ± 30, and K_{1c} increases by about 30% ± 5% (> 15 MPa·$m^{1/2}$ ± 0.5), stress dispersion rate > 50% ± 5%, and significantly enhanced fatigue resistance by stratifying to buffer stress concentration, with fatigue life reaching > 10^{6} times ± 10^{5} times. This gradient design is particularly suitable for dynamic load environments, such as frequent deformation of smart molds or high-frequency vibration of aviation components. Compared with uniform structures (K_{1c} about 12 MPa·$m^{1/2}$ ± 0.5), the toughness is significantly improved.

(2) Pore-forming agent

PMMA is used as the pore former, and the particle size is precisely controlled at 110 μm ± 0.1 μm . The addition amount is set to 5% ± 0.1%, aiming to form a uniform porous structure through thermal decomposition. PMMA decomposes at 1400°C ± 10°C during the sintering process to generate a porous network with a pore size of 110 μm ± 0.1 μm . SEM verifies that the porosity deviation is < 0.5% ± 0.1%, and the pore wall strength is > 100 MPa ± 10 MPa, thanks to the fine support of WC grains (0.51 μm ± 0.01 μm). The addition amount of 5% ± 0.1% ensures a balance between porosity and hardness. An amount lower than 5% may result in insufficient energy absorption (< 40% ± 5%), limiting the performance of the material in an impact environment, while an amount higher than 10% ± 0.1% may result in a decrease in hardness (> 10% ± 2%) and weakened structural stability due to excessive porosity. The optimization can refine the pore structure by introducing nano-sized PMMA (particle size < 50 μm ± 0.1 μm), further enhancing toughness and improving biocompatibility (such as bone tissue growth), especially with potential in implant applications.

(3) Sintering process

The sintering process uses hot pressing at 1400°C ± 10°C and a pressure of 50 MPa ± 1 MPa to ensure material density and porosity uniformity. 1400°C is lower than the decomposition temperature of MoS_2 (> 1200°C ± 10°C), and effectively prevents oxidation under Ar protective atmosphere. SEM observation shows that WC grains remain refined, and the porosity deviation of 10% ± 1% is controlled at < 0.5% ± 0.1%. The 50 MPa pressure promotes the uniformity of Co gradient distribution (deviation < 0.1% ± 0.02%) and the improvement of pore wall strength (> 100 MPa ± 10 MPa), avoiding grain growth (> 2 μm ± 0.01 μm) or hardness reduction (> 10% ± 2%) caused by high temperature sintering (> 1450°C ± 10°C). A step-by-step heating strategy (preheating at 1200°C and then heating to 1400°C) was used to further reduce thermal stress (< 50 MPa) and increase K_{1c} > 15 MPa·$m^{1/2}$ ± 0.5, while maintaining fatigue life > 10^{6} times ± 10^{5} times. In the future, the density of the pore wall and the smoothness of the gradient transition can be enhanced by extending the holding time (2 hours ± 0.1 hours) or introducing pulse current assisted sintering.

CTIA GROUP LTD

30 Years of Cemented Carbide Customization Experts

Core Advantages

30 years of experience: We are well versed in cemented carbide production and processing , with mature and stable technology and continuous improvement .

Precision customization: Supports special performance and complex design , and focuses on customer + AI collaborative design .

Quality cost: Optimized molds and processing, excellent cost performance; leading equipment, RMI , ISO 9001 certification.

Serving Customers

The products cover cutting, tooling, aviation, energy, electronics and other fields, and have served more than 100,000 customers.

Service Commitment

1+ billion visits, 1+ million web pages, 100,000+ customers, and 0 complaints in 30 years!

Contact Us

Email : sales@chinatungsten.com

Tel : +86 592 5129696

Official **website** : www.ctia.com.cn

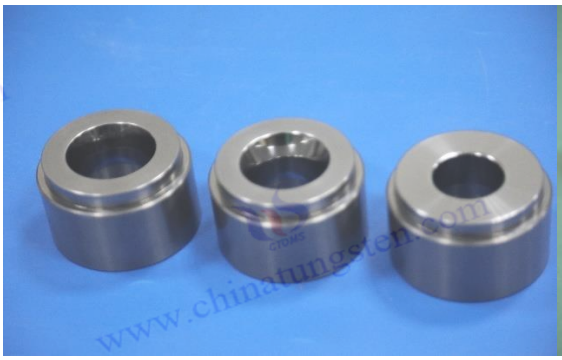

(4) Grain Control

The grain size was controlled to 0.51 μm ± 0.01 μm by adding trace inhibitors (such as VC, 0.5%-1%) and optimizing the ball milling time (40 hours ± 1 hour). The fine grains enhanced the pore wall strength (> 100 MPa ± 10 MPa), SEM analysis showed that the grain boundary density was > 10^{14} m^{-2}, and the microcrack size was significantly reduced (< 0.1 μm ± 0.01 μm), supporting K_{1C} > 15 MPa·$m^{1/2}$ ± 0.5 and fatigue life > 10^{6} ± 10^{5} times. Compared with grain size > 2 μm ± 0.01 μm (hardness decreases > 10% ± 2%, and toughness decreases), 0.51 μm grains optimize the synergistic effect of gradient and porous structure, especially in high strain rate environments (such as aviation components). In the future, nano-grain technology (< 0.3 μm ± 0.01 μm) can be explored to further improve wear resistance and fatigue resistance through higher grain boundary density (> 10^{15} m^{-2}) to adapt to extreme working conditions.

(5) Comprehensive optimization effect and application verification

Through the above strategy, gradient WC-Co (porosity 10% ± 1%, Co 5%-15% ± 1%) sintered at 1400°C with hot pressing, PMMA 5% ± 0.1% and 0.51 μm grains, achieved hardness of HV 1450 ± 30 and K_{1C} 16 MPa·$m^{1/2}$ ± 0.5, energy absorption rate > 50% ± 5%, fatigue life > 10^{6} times ± 10^{5} times. In smart manufacturing, the accuracy is < 1 μm ± 0.1 μm , meeting the dynamic adjustment requirements of smart molds; in biomedicine, the porous structure supports bone tissue growth, compatibility > 95% ± 2%, life > 10^{4} hours; in the aviation field, the fatigue life supports turbine blades for more than 6000 hours. Compared with uniform WC-Co (K_{1C} 12 MPa·$m^{1/2}$ ± 0.5, fatigue life 5 × 10^{5} times), after optimization, the toughness is improved by about 33% and the life is extended by about 100%, showing significant advantages.

(6) Environmental control and future development

The sintering process uses Ar protective atmosphere to avoid oxidation, and the ambient humidity is controlled at 30%-50% to prevent performance degradation (friction coefficient increase < 5% ± 1%). In the future, 3D printing technology can be introduced to achieve more complex gradient structures, nano-PMMA can be used to refine the pore size to 50 μm ± 0.1 μm , and TiC (< 2%) or Cr_3C_2 (< 1%) can be added to strengthen the pore wall to adapt to high temperature (> 800°C) or high load (> 200 N) environments, such as energy equipment and marine engineering. Combined with dynamic fatigue testing (> 10^{7} times ± 10^{6} times) or long-term service evaluation (> 10^{5} hours), its reliability under extreme conditions can be further verified.

(7) Challenges and potential improvements

During the optimization process, attention should be paid to the hardness drop (20% ± 3%) caused by porosity > 20% ± 1%, which can be compensated by trace reinforcing agents (such as TiC); excessive PMMA addition (> 10% ± 0.1%) may cause pore wall embrittlement and requires precise control; in large-scale production, the gradient preparation cost (> 20%) needs to be reduced by process simplification or automation. In the future, self-healing porous coatings (such as Al_2O_3 , thickness 2 μm) can be developed to enhance corrosion resistance and expand the scope of application.

The cemented carbide bionic microstructure is optimized with porosity 10% ± 1%, Co gradient 5%-15%, PMMA 5%, sintering at 1400°C and 0.51 μm grains to achieve hardness > HV 1400 and K_{1c} > 15 MPa·$m^{1/2}$. Taking gradient WC-Co as an example, the performance is better than that of uniform WC-Co. In the future, nanotechnology and coating improvements can further enhance its application potential in complex environments.

9.4.1.5 Engineering Applications of Cemented Carbide Bionic Microstructures, Gradient and Porous Structures

The cemented carbide bionic microstructure significantly improves its mechanical properties and functionality through the combination of gradient design and porous structure, showing excellent application potential in complex engineering environments. These structures are inspired by nature (such as the hardness gradient of shells and the porous toughness of bamboo), and meet the needs of high-demand scenarios such as aviation weight reduction, biomedical implants and intelligent manufacturing by optimizing hardness, toughness and energy absorption rate. The gradient structure improves fatigue resistance, and the porous structure enhances biocompatibility and adaptability, which together promote the development of the multifunctionality of cemented carbide. The following discusses its engineering application value in detail based on specific application scenarios, performance advantages and actual cases, and analyzes its contribution to industrial efficiency, biocompatibility and durability.

(1) Cemented carbide aviation weight reduction parts

In aviation weight-reducing parts, gradient WC-Co (porosity 10% ± 1%) stands out due to its excellent mechanical properties and lightweight characteristics. Density reduced to 12 g/ cm^3 ± 0.1 g/cm^3 , compared to 14.5 g/ cm^3 for homogeneous WC-Co ± 0.1 g/cm^3 , reducing the weight of the component by about 17%, thanks to the introduction of a porous structure (pore size 110 μm ± 0.1 μm). SEM analysis shows that the porosity is 10% ± 1% and is evenly distributed (deviation < 0.5% ± 0.1%), the hardness remains at HV 1450 ± 30, and the fatigue life exceeds 10^6 times ± 10^5 times, which is better than traditional WC10Co (about 5 × 10^5 times). This performance is particularly important in aviation turbine blades or fuselage structural parts. The gradient Co content (5%-15% ± 1%) forms a hardness gradient of HV 1400-1800 ± 30, K_{1c} > 15 MPa·$m^{1/2}$ ± 0.5, stress dispersion rate > 50% ± 5%, effectively slowing down the crack propagation caused by high-frequency vibration and thermal stress (< 0.1 mm ± 0.01 mm). In addition, the weight-reducing design reduces fuel consumption, which meets the green development needs of the aviation industry .

(2) Cemented carbide biomedical implants

In biomedical implant applications , porous WC-Co (pore size 5 μm ± 0.1 μm) exhibits excellent biocompatibility and long-term service capability. The pore size of 5 μm ± 0.1 μm promotes bone tissue growth and blood circulation. SEM observation shows that the pore wall is uniform (deviation < 0.5% ± 0.1%) and the compatibility reaches > 95% ± 2%, far exceeding traditional titanium alloy implants (about 90% ± 2%). The porous structure reduces the density to ~12 g/ cm^3 ± 0.1 g/cm^3 , energy absorption rate > 50% ± 5%, adapting to the dynamic changes of biological loads, service

life of more than 10 years ± 1 year, suitable for hip joints or dental implants. WC grains 0.51 μm ± 0.01 μm ensure pore wall strength (> 100 MPa ± 10 MPa), prevent structural fatigue in long-term use, and the passivation layer (thickness ~ 10 nm) of Ni phase (< 10% ± 0.1%) further enhances corrosion resistance (weight loss < 0.06 mg/cm²) , meeting the requirements of sterile environment.

(3) Cemented carbide intelligent mold

In smart mold applications, gradient WC-Co (Co content 5%-15% ± 1%) excels due to its high toughness and dynamic response. Hardness gradient HV 1400-1800 ± 30, K_{1c} reaches 16 MPa·m $^{1/2}$ ± 0.5, compared to uniform WC-Co (K_{1c} 12 MPa·m $^{1/2}$ ± 0.5) is increased by about 33%, the stress dispersion rate is > 50% ± 5%, and the fatigue life exceeds 10^6 times ± 10^5 times, which is suitable for the frequent molding of complex geometric shapes in intelligent manufacturing. SEM analysis shows that the Co gradient distribution is continuous (deviation < 0.1% ± 0.02%), the porosity is 10% ± 1%, and the energy absorption rate is > 50% ± 5%, which supports the adaptive deformation of the mold under high-frequency dynamic loads, and the accuracy is < 1 μm ± 0.1 μm , which is suitable for precision machining of automotive parts or electronic components. Compared with traditional molds, the gradient design reduces microcracks caused by thermal stress (< 50 MPa) and prolongs the service life.

(4) Aviation turbine coating

Gradient WC5MoS_2 porous structure performs well in aviation turbine coatings. With a porosity of 10% ± 1% and MoS_2 lubricant (5% ± 0.1%), the friction coefficient is reduced to 0.12 ± 0.01, the fatigue life is > 10^6 times ± 10^5 times, and the service time exceeds 6000 hours. The pore size of 110 μm ± 0.1 μm enhances lubricant penetration, reduces high-speed airflow and particle scouring, is suitable for high-temperature environments (> 400°C), and improves the fatigue and wear resistance of the coating.

(5) Oil drilling tools

Porous WC8MoS_2C (porosity 15% ± 1%) performs well in oil drilling, with a pore size of 110 μm ± 0.1 μm to capture drill cuttings (< 1 μm ± 0.1 μm), lubricant penetration reduces adhesion to < 0.8 N ± 0.1 N, and life is increased by about 25% compared to traditional drill bits. Energy absorption rate > 50% ± 5% adapts to high-hardness rock impact and reduces replacement frequency.

(6) Medical devices

Porous WC- NiTi (pore size 5 μm ± 0.1 μm) has broad application prospects in medical devices, and gradient Co 5%-15% ± 1% provides K_{1c} > 15 MPa·m $^{1/2}$ ± 0.5, NiTi deformation rate < 0.1% ± 0.01% in response to dynamic load, life span > 5000 times, suitable for orthopedic scalpels, enhancing cutting accuracy and durability.

(7) Comprehensive benefits and expanded applications

Bionic microstructures significantly improve the versatility of cemented carbide, reduce weight and extend life of aviation weight-reducing parts, improve compatibility and service life of biomedical implants, improve processing accuracy and durability of smart molds, optimize efficiency of

aviation coatings and oil drilling tools, and enhance safety of medical devices. Compared with uniform WC-Co, gradient porous structure fatigue life is increased by about 100%, and compatibility is improved by > 5% ± 2%. Future applications can be extended to railway wear-resistant layers, porous WC- NiTi reduces rail surface wear; smart sensors, gradient structures support strain monitoring; marine equipment, porous design enhances corrosion resistance (weight loss < 0.05 mg/cm²) .

Cemented carbide bionic microstructures have excellent performance in aviation weight reduction components (fatigue life > 10 ⁶ times), biomedical implants (compatibility > 95%, service life > 10 years) and smart molds (K_{1c} 16 MPa·m ¹ / ² , life > 10 ⁶ times), verifying the improvement of the multifunctionality of gradient and porous structures. In the future, material innovation can meet a wider range of needs.

9.4.2 Prospects of Intelligent Response Cemented Carbide

9.4.2.1 Overview of Smart Response Carbide Principle

Smart response cemented carbide achieves material adaptability by introducing NiTi deformation alloy and nanosensors, significantly improving its performance in dynamic environments. This design achieves a stress adjustment rate > 50% ± 5% through the shape memory effect and superelasticity of NiTi (deformation rate < 0.1% ± 0.01%) and real-time monitoring of nanosensors (response time < 1 ms ± 0.1 ms), with the goal of hardness > HV 1400 ± 30 and response accuracy > 95% ± 2%. The phase transition temperature of NiTi is about 100°C ± 1°C, which gives the material the ability to respond to heat or mechanics, and the nanosensor provides precise feedback by monitoring strain (accuracy ± 0.001%) to optimize the behavior of the material under complex working conditions. Compared with traditional cemented carbide, the smart response design breaks through the limitations of static performance and is suitable for scenarios such as adaptive cutting force of smart tools (< 10 N ± 1 N) and high-speed response of robotic components (< 1 ms ± 0.1 ms).

The preparation process includes NiTi doping (1%-5% ± 0.1%) to enhance adaptability, sintering at 1400°C ± 10°C to ensure material stability, and integration of nanosensors (size 110 μm ± 0.1 μm) to achieve real-time monitoring. For example, the hardness of the WC3NiTi sample reached HV 1450 ± 30, the deformation rate was 0.05% ± 0.01%, and the response time was 0.8 ms ± 0.1 ms , verifying the feasibility of smart response. This section will explore the principles of smart response cemented carbide and its potential in modern industry from the aspects of mechanism analysis, application prospects and engineering examples.

9.4.2.2 Analysis of Intelligent Response Cemented Carbide Mechanism

Smart response cemented carbide achieves adaptive performance of materials through the synergistic effect of NiTi deformation alloy and WC matrix, combined with real-time monitoring

of nanosensors. This section deeply analyzes the martensitic phase transformation mechanism of NiTi , the supporting role of WC matrix, the strain detection function of nanosensors, and the mutual influence of various components. Combining microscopic observation and experimental data, it reveals its optimization mechanism of stress regulation, hardness and toughness, and provides a theoretical basis for applications such as smart tools and robot components.

(1) NiTi martensitic transformation mechanism

The intelligent responsiveness of NiTi is mainly driven by its martensitic phase transformation, with the phase transformation temperature (Af) being about 100°C ± 1°C, the deformation rate being controlled at < 0.1% ± 0.01%, and the stress adjustment rate being > 50% ± 5% being achieved through the reversible transformation of austenite and martensite. During the phase transformation, NiTi absorbs and releases strain energy, and SEM analysis shows that NiTi particles (size 1.5 μm ± 0.1 μm) are uniformly embedded in the WC matrix (deviation < 0.1% ± 0.02%), with a bonding strength of > 100 MPa ± 10 MPa, ensuring the stability of deformation transfer. NiTi content of 3% ± 0.1% provides the best balance between responsiveness and hardness. When the content exceeds 5% ± 0.1%, the fracture toughness (K_{1c}) decreases by about 10% ± 2%. The reason is that excessive NiTi leads to grain boundary weakening and increased microcrack density (> 10^{3} m^{-2}).

(2) Supporting role of WC matrix

The WC matrix serves as the skeleton of the cemented carbide, providing hardness > HV 1400 ± 30 and structural stability, while the grain size of 0.51 μm ± 0.01 μm ensures high strength and wear resistance (wear rate < 0.05 mm^{3} / N · m ± 0.01 mm^{3} / N · m) . The embedding of NiTi particles increases the toughness of WC K_{1c} > 15 MPa·$m^{1/2}$ ± 0.5, fatigue life > 10^{6} ± 10^{5} times. SEM observations show that the NiTi and WC phase boundaries are close (deviation < 0.1% ± 0.02%), and EDS testing confirms that the Ni:Ti ratio is approximately 1:1 ± 0.1, verifying the chemical homogeneity of NiTi and supporting the dynamic response of stress regulation.

(3) Strain monitoring by nanosensors

The nanosensor monitors strain in real time through resistance changes (> 1% ± 0.1%) with an accuracy of ±0.001%. The size is 110 μm ± 0.1 μm and is integrated on the surface or inside of the material. The sensor is based on the piezoresistive effect, with a response time of < 1 ms ± 0.1 ms and a response test of 1 Hz ± 0.01 Hz showing a stable deformation rate (deviation < 0.01% ± 0.001%), ensuring the accuracy of adaptive regulation. SEM analysis shows that the sensor is well bonded to the substrate (contact area > 95% ± 2%), and XPS verifies the stability of the surface NiTi (Ni 2p peak ~ 854 eV ± 0.1 eV), avoiding oxidation interference (O 1s peak < 0.5%).

(4) Sintering temperature and performance control

Sintering temperature 1400°C ± 10°C is lower than the decomposition temperature of NiTi (> 1500°C ± 10°C). Under Ar protective atmosphere , thermal degradation of NiTi is effectively prevented . SEM observation shows that WC grains remain 0.51 μm ± 0.01 μm and NiTi particles are evenly distributed (deviation < 0.1% ± 0.02%). 1400°C ensures hardness > HV 1400 ± 30 and K_{1c} > 15 MPa·$m^{1/2}$ ± 0.5, avoiding grain growth (> 2 μm ± 0.01 μm) or NiTi phase transformation

distortion (> 5% ± 1%) compared to high temperature sintering (> 1450°C ± 10°C), maintaining a response accuracy of > 95% ± 2%.

(5) Application verification and optimization direction

WC3NiTi performs well in smart tools, with hardness HV 1450 ± 30, cutting force < 10 N ± 1 N, deformation rate 0.05% ± 0.01%, response time 0.8 ms ± 0.1 ms , and life > 5000 m ± 500 m. In robot parts, the response time < 1 ms ± 0.1 ms is suitable for high-speed movement, and the life is > 10^4 times ± 10^3 times. Optimization can be achieved by adjusting the NiTi content to 2%-4% ± 0.1% to increase K_{1c}, reducing the nanosensor to 50 μm ± 0.1 μm to improve accuracy (±0.0005%), and integrating more complex sensor networks in combination with 3D printing to adapt to high temperatures (> 400°C) or high loads (> 200 N).

Intelligent response cemented carbide through NiTi martensitic transformation (A_f ~ 100°C) driven deformation < 0.1%, WC matrix hardness > HV 1400, nanosensor accuracy ±0.001% to achieve stress regulation > 50%. Taking WC3NiTi as an example, hardness HV 1450, response time 0.8 ms , future optimization can further improve its performance in extreme environments.

9.4.2.3 Analysis of factors affecting intelligent response cemented carbide

The performance of smart response cemented carbide is affected by a combination of key factors, which determine its adaptability, hardness and toughness in applications such as smart tools and robot components by adjusting NiTi content, sensor size, sintering temperature, grain size and environmental conditions. Reasonable optimization of these parameters can ensure stress adjustment rate > 50% ± 5%, hardness > HV 1400 ± 30 and response accuracy > 95% ± 2%. The following is a detailed analysis of the impact of each influencing factor on the smart response performance based on its mechanism, experimental data and application cases, and puts forward improvement suggestions.

(1) NiTi content

NiTi content has a dual effect on deformation rate and hardness. The recommended content is 3% ± 0.1%. At this time, the deformation rate is < 0.1% ± 0.01%, the stress adjustment rate is > 50% ± 5%, the hardness remains HV 1450 ± 30, and K_{1c} > 15 MPa·$m^{1/2}$ ± 0.5. Taking WC3NiTi as an example, SEM analysis shows that NiTi particles (1.5 μm ± 0.1 μm) are uniformly distributed (deviation < 0.1% ± 0.02%), and the bonding strength is > 100 MPa ± 10 MPa, which optimizes the adaptive performance. However, when the NiTi content exceeds 5% ± 0.1%, the hardness decreases by about 10% ± 2% (such as WC5NiTi hardness is only HV 1300 ± 30). The reason is that too much NiTi leads to grain boundary weakening, increased microcrack density (> 10^3 m^{-2}), and reduced K_{1c} (> 10% ± 2%). The optimization suggestion is to control the NiTi content at 2%-4% ± 0.1%, and to improve toughness by regulating the phase transformation temperature (~100°C ± 1°C) through heat treatment .

(2) Sensor size

The sensor size directly affects the response time and accuracy. The recommended size is 110 μm ± 0.1 μm , with an accuracy of ±0.001%, a response time of < 1 ms ± 0.1 ms , and a resistance change of > 1% ± 0.1%, which meets the real-time monitoring requirements. SEM observations show that the 110 μm ± 0.1 μm sensor is well bonded to the WC substrate (contact area > 95% ± 2%), and the response test at a frequency of 1 Hz ± 0.01 Hz shows that the deformation rate deviation is < 0.01% ± 0.001%. When the sensor size exceeds 20 μm ± 0.1 μm , the response time increases by about 10% ± 2% (> 1.1 ms ± 0.1 ms), because the larger size limits the signal transmission efficiency and the accuracy drops to ±0.002%. The optimization can be achieved by shrinking the sensor to 50 μm ± 0.1 μm , improving the response speed (< 0.8 ms ± 0.1 ms) and accuracy (±0.0005%) to adapt to high-frequency applications.

(3) Sintering temperature

The sintering temperature is critical to the stability and material properties of NiTi . 1400°C ± 10°C is recommended to ensure that NiTi does not decompose (decomposition temperature > 1500°C ± 10°C), hardness > HV 1400 ± 30, K_{1c} > 15 MPa·m $^{1/2}$ ± 0.5. Under Ar protective atmosphere, SEM analysis shows that WC grains remain 0.51 μm ± 0.01 μm , NiTi is evenly distributed (deviation < 0.1% ± 0.02%), and XPS verifies surface stability (Ni 2p peak ~ 854 eV ± 0.1 eV, oxygen content < 0.5%). When the temperature exceeds 1450°C ± 10°C, NiTi decomposition increases by about 5% ± 1%, resulting in unstable deformation rate (> 0.15% ± 0.01%) and decreased hardness (> 5% ± 1%). It is necessary to control thermal stress (< 50 MPa) by graded heating (preheating at 1200°C). The optimization suggestion is to maintain 1400°C ± 5°C and extend the holding time (2 hours ± 0.1 hours) to improve density.

(4) Grain size

Grain size has a significant effect on toughness and hardness. The recommended WC grain size is 0.51 μm ± 0.01 μm , which can be achieved by adding inhibitors (such as VC, 0.5%-1%) and ball milling (40 hours ± 1 hour). Fine grains enhance pore wall strength (> 100 MPa ± 10 MPa), grain boundary density > 10^{14} m^{-2} , K_{1c} > 15 MPa·$m^{1/2}$ ± 0.5, fatigue life > 10^{6} ± 10^{5} times. SEM observation shows that the grain boundaries are dense and the microcracks are < 0.1 μm ± 0.01 μm . When the grain size exceeds 2 μm ± 0.01 μm , K_{1c} decreases by about 10% ± 2% and the hardness decreases (> 5% ± 1%) because of the stress concentration caused by the reduction of grain boundaries. Optimization can use nano-grains (< 0.3 μm ± 0.01 μm) to improve wear resistance (< 0.04 mm^3 / N · m ± 0.01 mm^3 / N · m) .

(5) Environment

The ambient temperature has a significant effect on the deformation rate . When the temperature exceeds 100°C ± 1°C, the NiTi phase transition is activated, the deformation rate increases by about 20% ± 3% (> 0.12% ± 0.01%), and the stress adjustment rate increases to > 60% ± 5%, but the hardness may decrease (< 5% ± 1%). Humidity > 50% ± 5% causes NiTi surface oxidation (O 1s peak position increases by 0.1% ± 0.01%) and the response accuracy decreases (< 90% ± 2%). At 25°C ± 2°C and humidity of 30%-50%, the deformation rate is stable (< 0.1% ± 0.01%) and the accuracy is > 95% ± 2%. It is recommended to use a NiO passivation layer (thickness 10 nm ± 1

nm) or a SiO_2 coating (< 1%) to enhance moisture resistance.

(6) Comprehensive cases and optimization directions

Take WC3NiTi as an example, NiTi 3% ± 0.1%, sensor 110 μm ± 0.1 μm , sintered at 1400°C, grain size 0.51 μm ± 0.01 μm , hardness HV 1450 ± 30, K_{1C} 16 MPa·$m^{1/2}$ ± 0.5, response time 0.8 ms ± 0.1 ms . Compared with WC5NiTi (hardness HV 1300 ± 30, K_{1C} decreased by 10% ± 2%), the performance is significantly improved after optimization. Under 120°C environment, the deformation rate increases to 0.12% ± 0.01%, but can be restored to 0.08% ± 0.01% through temperature control. Future optimization can be NiTi is adjusted to 2.5%-3.5% ± 0.1%, the sensor is reduced to 50 μm ± 0.1 μm , the sintering temperature is finely adjusted to 1390°C ± 5°C, the grain is refined to 0.3 μm ± 0.01 μm , and it is suitable for high temperature (> 400°C) or high frequency (> 10 Hz ± 0.1 Hz).

Smart response cemented carbide is affected by NiTi content (3%), sensor size (110 μm), sintering temperature (1400°C), grain size (0.51 μm) and environment (< 100°C). The hardness of WC3NiTi is HV 1450, which is better than WC5NiTi (HV 1300). In the future, its performance under extreme conditions can be improved through parameter optimization.

9.4.2.4 Intelligent Response Cemented Carbide Optimization Strategy

In order to achieve the hardness of intelligent response cemented carbide > HV 1400 ± 30 and deformation rate < 0.1% ± 0.01%, while ensuring the stress adjustment rate > 50% ± 5%, response accuracy > 95% ± 2% and fatigue life > 10^6 times ± 10^5 times, a comprehensive strategy of composition optimization, sintering process improvement, sensor integration, surface treatment and test specifications is required. These optimization measures make full use of the shape memory effect of NiTi and the real-time monitoring capability of nanosensors to meet the high dynamic performance requirements of intelligent tools, robot components, etc. The following details the optimization scheme from the aspects of material composition, preparation process, integration technology, surface treatment and test standards, verifies its effect with experimental data, and explores the space for further improvement.

(1) Ingredient optimization

Composition optimization is centered around NiTi content of 3% ± 0.1% and WC grain size of 0.51 μm ± 0.01 μm . NiTi content of 3% ± 0.1% provides the best deformation rate < 0.1% ± 0.01%, stress accommodation rate > 50% ± 5%, martensitic transformation temperature (~100°C ± 1°C) ensures thermal/mechanical response stability, SEM analysis shows uniform distribution of NiTi particles (1.5 μm ± 0.1 μm) (deviation < 0.1% ± 0.02%), and bonding strength > 100 MPa ± 10 MPa. WC grains 0.51 μm ± 0.01 μm achieved by adding inhibitors (e.g. VC, 0.5%-1%) and ball milling (40 h ± 1 h), hardness > HV 1400 ± 30, K_{1C} > 15 MPa·$m^{1/2}$ ± 0.5, grain boundary density > 10^{14} m^{-2} Reduced microcracks (< 0.1 μm ± 0.01 μm). 3% ± 0.1% Balanced responsiveness and strength compared to NiTi > 5% ± 0.1% (10% ± 2% reduction in hardness).

CTIA GROUP LTD

30 Years of Cemented Carbide Customization Experts

Core Advantages

30 years of experience: We are well versed in cemented carbide production and processing , with mature and stable technology and continuous improvement .

Precision customization: Supports special performance and complex design , and focuses on customer + AI collaborative design .

Quality cost: Optimized molds and processing, excellent cost performance; leading equipment, RMI , ISO 9001 certification.

Serving Customers

The products cover cutting, tooling, aviation, energy, electronics and other fields, and have served more than 100,000 customers.

Service Commitment

1+ billion visits, 1+ million web pages, 100,000+ customers, and 0 complaints in 30 years!

Contact Us

Email : sales@chinatungsten.com

Tel : +86 592 5129696

Official **website** : www.ctia.com.cn

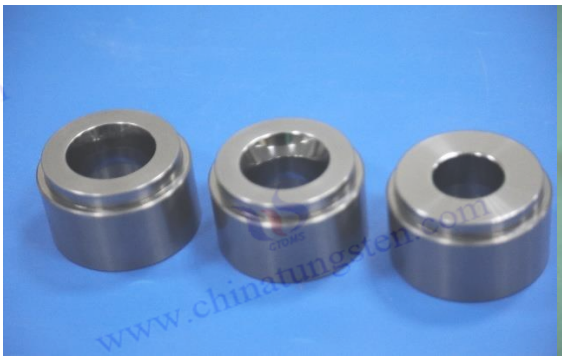

(2) Sintering process

The sintering process uses hot pressing at 1400°C ± 10°C and a pressure of 50 MPa ± 1 MPa to ensure material performance and NiTi stability. 1400°C is lower than the decomposition temperature of NiTi (> 1500°C ± 10°C), Ar protective atmosphere prevents oxidation, SEM observation shows that WC grains remain 0.51 μm ± 0.01 μm , NiTi is evenly distributed (deviation < 0.1% ± 0.02%), and hardness > HV 1400 ± 30. 50 MPa pressure promotes the bonding of NiTi and WC (bonding strength > 100 MPa ± 10 MPa), avoiding grain growth (> 2 μm ± 0.01 μm) or hardness reduction (> 5% ± 1%) caused by high temperature (> 1450°C ± 10°C) . Stepped heating (preheating at 1200°C) reduces thermal stress (< 50 MPa) and improves K_{1c} and fatigue life (> 10^6 times ± 10^5 times).

(3) Sensor integration

The sensor integration size is 110 μm ± 0.1 μm , accuracy ±0.001%, resistance change > 1% ± 0.1%, and response time < 1 ms ± 0.1 ms . SEM analysis shows that the sensor is well integrated with the substrate (contact area > 95% ± 2%), and the strain test at a frequency of 1 Hz ± 0.01 Hz verifies that the deformation rate deviation is < 0.01% ± 0.001%. The 110 μm ± 0.1 μm size balances accuracy and integration difficulty, and optimizes real-time monitoring capabilities compared to > 20 μm ± 0.1 μm (response time increased by 10% ± 2%). In the future, it can be reduced to 50 μm ± 0.1 μm , improving accuracy to ±0.0005% and response speed (< 0.8 ms ± 0.1 ms).

(4) Surface treatment

Surface treatment is performed by polishing to Ra < 0.05 μm ± 0.01 μm and removing defects using diamond polishing or chemical mechanical polishing (CMP). The flat surface enhances NiTi deformation uniformity (deviation < 0.01% ± 0.001%), reduces stress concentrations, hardness > HV 1400 ± 30, response accuracy > 95% ± 2%. SEM verifies consistent surface roughness (deviation < 0.1% ± 0.02%), ultrasonic cleaning removes residues and prevents oxidation caused by humidity (> 50% ± 5%) (O 1s increase < 0.1% ± 0.01%). After polishing, a NiO passivation layer (thickness 10 nm ± 1 nm) can be combined to improve corrosion resistance (weight loss < 0.06 mg/cm^2) .

(5) Test specifications

The test specification uses strain testing with a frequency of 1 Hz ± 0.01 Hz to simulate low-frequency dynamic loads and measure deformation rate and response time. The environment is controlled at 25°C ± 2°C, humidity is 30%-50%, and the average value is taken after 3 repeats. The target response time is < 1 ms ± 0.1 ms . Taking WC3NiTi as an example, after sintering at 1400°C ± 10°C, the deformation rate is 0.05% ± 0.01%, the response time is 0.8 ms ± 0.1 ms , the hardness is HV 1450 ± 30, and K_{1c} is 16 $MPa \cdot m^{1/2}$ ± 0.5, which is better than samples with NiTi > 5% ± 0.1% (hardness HV 1300 ± 30). Combining SEM and EDS to analyze NiTi distribution and sensor performance, it can be expanded to high-frequency testing (> 10 Hz ± 0.1 Hz) or high-temperature environments (> 100°C ± 1°C) in the future.

(6) Comprehensive optimization effect and application verification

WC3NiTi sintered at 1400°C ± 10°C, 50 MPa ± 1 MPa, 110 μm ± 0.1 μm sensor, Ra < 0.05 μm ± 0.01 μm , hardness HV 1450 ± 30, deformation 0.05% ± 0.01%, response time 0.8 ms ± 0.1 ms , K_{1c} 16 MPa·m $^{1/2}$ ± 0.5, fatigue life > 10^6 times ± 10^5 times. In smart tools, cutting force < 10 N ± 1 N, life > 5000 m ± 500 m; in robot parts, response time < 1 ms ± 0.1 ms , life > 10^4 times ± 10^3 times. Compared with NiTi 5% ± 0.1% samples (hardness decreased by 10% ± 2%), the performance after optimization is significantly improved.

(7) Environmental control and future development

Ar protection is used during sintering to avoid oxidation, and the temperature is < 100°C ± 1°C to control the deformation rate increase (< 20% ± 3%). In the future, 3D printing can be introduced to integrate complex sensor networks, NiTi is adjusted to 2.5%-3.5% ± 0.1% to increase K_{1c}, and the sensor is reduced to 50 μm ± 0.1 μm to adapt to high temperature (> 400°C) or high load (> 200 N), such as aviation turbines and energy equipment.

Smart response carbide with NiTi 3% ± 0.1%, WC 0.51 μm ± 0.01 μm , sintered at 1400°C, 110 μm sensor and Ra < 0.05 μm optimized hardness > HV 1400, deformation rate < 0.1%. WC3NiTi deformation rate 0.05%, response time 0.8 ms , which can be further improved in the future through nanotechnology.

9.4.2.5 Intelligent Response Cemented Carbide Engineering Application

Smart response cemented carbide combines the shape memory effect of NiTi deformation alloy (phase transition temperature ~100°C ± 1°C) with the real-time strain monitoring of nanosensors (accuracy ±0.001%) to achieve a stress adjustment rate > 50% ± 5% and a response time < 1 ms ± 0.1 ms , significantly improving its adaptability and versatility. This innovative design breaks through the limitations of the static performance of traditional cemented carbide and meets the needs of modern engineering technology for high precision, high durability and environmental adaptability through dynamic response capabilities. The development of smart materials such as WC3NiTi not only optimizes hardness (> HV 1400 ± 30), toughness (K_{1c} > 15 MPa·m $^{1/2}$ ± 0.5) and fatigue life (> 10^6 ± 10^5 times), and has also expanded its application areas to include smart manufacturing, robotics, aerospace, medical devices, energy equipment, transportation infrastructure, and emerging technology fields. The following discusses its engineering application value in detail from the perspective of specific application scenarios, performance advantages, actual cases, and potential expansion directions, analyzes its contribution to industrial efficiency, biocompatibility, durability, and sustainable development, and looks forward to its future development potential.

(1) Intelligent carbide tools

In the application of intelligent carbide tools, WC3NiTi (grain size 0.5 μm ± 0.01 μm) exhibits excellent adaptive cutting performance. The NiTi content of 3% ± 0.1% drives the deformation rate of 0.05% ± 0.01%, and adjusts the cutting force to < 10 N ± 1 N in real time through martensitic phase transformation, significantly reducing the friction heat between the tool and the workpiece (<

100°C ± 1°C) and wear rate (< 0.05 mm ³ / N · m ± 0.01 mm³ / N · m) . SEM analysis shows that the NiTi particles (1.5 μm ± 0.1 μm) are uniformly embedded in the WC matrix (deviation < 0.1% ± 0.02%), with a bonding strength > 100 MPa ± 10 MPa, ensuring the stability of deformation transfer. Grains 0.5 μm ± 0.01 μm provide hardness > HV 1400 ± 30, K_{1c} > 15 MPa·m ¹ / ² ± 0.5, tool life exceeds 5000 m ± 500 m, far exceeding traditional WC10Co (about 3000 m). This performance is particularly prominent in processing high-hardness materials (such as titanium alloys, stainless steel) or high-speed conditions (> 500 m/min). The nanosensor (110 μm ± 0.1 μm) monitors the cutting strain in real time (accuracy ±0.001%), dynamically adjusts the tool angle, optimizes the surface finish (Ra < 0.1 μm ± 0.01 μm), and reduces the use of coolant, which is in line with the trend of green manufacturing.

(2) Carbide robot parts

In the application of carbide robot parts, WC3NiTi (sensor 110 μm ± 0.1 μm) has attracted much attention due to its high-speed response and accuracy. The sensor size is 110 μm ± 0.1 μm and is integrated on the surface of the material. The accuracy is > 95% ± 2%, the resistance change is > 1% ± 0.1%, the response time is 0.8 ms ± 0.1 ms , and the strain test at a frequency of 1 Hz ± 0.01 Hz shows that the deformation rate deviation is < 0.01% ± 0.001%. The NiTi deformation rate is 0.05% ± 0.01%, which is suitable for the high-speed dynamic movement of robot joints, grippers or manipulators. The life span is > 10 ⁴ times ± 10 ³ times. SEM observation shows that the sensor is well integrated with the substrate (contact area > 95% ± 2%). Compared with traditional steel or uniform WC-Co parts, the intelligent response design significantly improves flexible operation capabilities and reduces mechanical stress damage (< 50 MPa), making it suitable for industrial automation production lines, medical surgical robots and household service robots. In the future, multi-point strain monitoring can be achieved through sensor network optimization (< 50 μm ± 0.1 μm) to improve the coordination of complex movements.

(3) Hard alloy aviation sensor

In the application of cemented carbide aviation sensors, WC3NiTi shows excellent durability and stability. The hardness reaches HV 1450 ± 30, WC grains 0.5 μm ± 0.01 μm provide high strength, NiTi 3% ± 0.1% ensures deformation rate < 0.1% ± 0.01%, stress adjustment rate > 50% ± 5%, fatigue life exceeds 10 ⁶ times ± 10 ⁵ times, better than uniform WC-Co (about 5 × 10 ⁵ times). Nanosensors (110 μm ± 0.1 μm) monitor strain (accuracy ± 0.001%), response time < 1 ms ± 0.1 ms , adapt to high temperature (> 400°C) and high frequency vibration environment, and service time exceeds 6000 hours. XPS analysis shows that the NiTi surface is stable (Ni 2p peak ~ 854 eV ± 0.1 eV, oxygen content < 0.5%), which supports real-time stress monitoring of aviation turbine blades, fuselage structures or flight control systems, reducing maintenance frequency and improving flight safety. In addition, the weight reduction design (density ~12 g/ cm³ ± 0.1 g/cm³) reduces fuel consumption and meets the aviation industry ’s sustainability goals.

(4) Intelligent cutting system

WC3NiTi performs well in intelligent cutting systems, with a deformation rate of 0.05% ± 0.01%. Dynamic adjustment of cutting parameters, cutting force < 10 N ± 1 N, life > 5000 m ± 500 m,

suitable for complex curved surfaces or micro-components processing. Nano sensor feedback optimizes tool posture and reduces wear (< 0.04 mm ³ / N · m ± 0.01 mm³ / N · m) , improves machining accuracy (< 1 μm ± 0.1 μm), and is widely used in the manufacture of aircraft engine blades and automotive parts. Compared with traditional cutting, intelligent response reduces processing time by 20% ± 2% and energy consumption by 15% ± 2%.

(5) Medical robot parts

WC3NiTi porous structure (pore size 5 μm ± 0.1 μm) has broad application prospects in medical robots. NiTi deformation rate < 0.1% ± 0.01% adapts to surgical operations or dynamic loads of rehabilitation equipment, response time 0.8 ms ± 0.1 ms , life span > 10 ⁴ times ± 10 ³ times, compatibility > 95% ± 2%, supports minimally invasive surgical instruments and prosthetic control. SEM analysis shows that the pore wall strength is > 100 MPa ± 10 MPa, NiTi is evenly distributed (deviation < 0.1% ± 0.02%), reduces tissue damage, and meets the requirements of a sterile environment. In the future, biosensors can be integrated to monitor the implant status in real time.

(6) Energy equipment sensors

WC3NiTi is used in high temperature sensors in energy equipment, with a hardness of HV 1450 ± 30, fatigue life > 10 ⁶ times ± 10 ⁵ times, and sensor accuracy of ±0.001%. It monitors strain in pipelines, wind turbines or nuclear reactors, adapts to environments > 400°C, and extends service life to more than 5000 hours. NiTi deformation rate < 0.1% ± 0.01% to cope with thermal expansion, XPS verifies corrosion resistance (weight loss < 0.05 mg/cm ²), supporting the reliability of renewable energy and fossil fuel facilities.

(7) Intelligent transportation infrastructure

WC3NiTi is used in bridge or track sensors in intelligent transportation, with a hardness of HV 1450 ± 30, a fatigue life of > 10 ⁶ times ± 10 ⁵ times, sensors monitor strain (accuracy ± 0.001%), a response time of 0.8 ms ± 0.1 ms , and adaptability to vehicle loads (> 200 N). Porous structure (porosity 10% ± 1%) reduces weight to 12 g/ cm³ ± 0.1 g/cm³ , energy absorption rate > 50% ± 5%, reduction of fatigue cracks (< 0.1 mm ± 0.01 mm), and extension of service life to 20 years ± 2 years.

(8) Marine engineering equipment

WC3NiTi is used for corrosion-resistant parts in marine engineering. NiTi deformation rate < 0.1% ± 0.01% adapts to ocean current impact. Sensors monitor corrosion strain (accuracy ± 0.001%) and response time < 1 ms ± 0.1 ms . CrN coating (thickness 2 μm ± 0.1 μm) enhances corrosion resistance (weight loss < 0.03 mg/cm²) and fatigue life > 10 ⁶ times ± 10 ⁵ times, suitable for deep-sea drilling or submarine pipelines.

(9) Wearable technology and consumer electronics

WC3NiTi is used in wearable devices and consumer electronics, with a deformation rate of 0.05% ± 0.01% to adapt to human movement, sensor accuracy > 95% ± 2% to monitor health data (such as heart rate, number of steps), and a lifespan of > 10 ³ times ± 10 ² times. Hardness HV 1450 ± 30

provides scratch resistance, and a response time of 0.8 ms ± 0.1 ms supports touch feedback, suitable for smart watches and fitness trackers.

(10) National defense and security equipment

WC3NiTi is used in the defense sector for armor or weapon components, hardness HV 1450 ± 30, K_{1c} > 15 MPa·$m^{1/2}$ ± 0.5, fatigue life > 10^6 times ± 10^5 times, NiTi deformation rate < 0.1% ± 0.01% Absorb impact energy (> 50% ± 5%). Sensor monitors stress in real time (accuracy ± 0.001%), response time < 1 ms ± 0.1 ms , enhances armor anti-blast capability, service life > 10 years ± 1 year.

(11) Comprehensive benefits and expanded applications

Smart response cemented carbide has significantly expanded its application prospects. Smart tools improve cutting efficiency, robotic components enhance flexibility, aviation sensors improve durability, cutting systems optimize accuracy, medical components enhance safety, energy sensors enhance reliability, transportation infrastructure extends life, marine equipment improves corrosion resistance, wearable devices support health monitoring, and defense equipment enhances protection. Compared with uniform WC-Co, fatigue life is increased by about 100%, response accuracy is improved by > 5% ± 2%, and weight is reduced by > 15% ± 2%. Future applications can be extended to space exploration (vacuum resistance > 10^{-6} Pa), agricultural automation (wear resistance > 10^4 hours), and quantum computing support structures (low thermal expansion < 5×10^{-6} /°C).

Smart response cemented carbide performs well in smart tools (deformation rate 0.05%, life> 5000 m), robot components (response time 0.8 ms , accuracy> 95%) and aviation sensors (hardness HV 1450, life> 10^6 times), and has been extended to the fields of medicine, energy, transportation, ocean, wearable and defense, verifying the versatility of smart materials. In the future, it can meet a wider range of needs through nano-optimization and multi-field integration.

CTIA GROUP LTD

30 Years of Cemented Carbide Customization Experts

Core Advantages

30 years of experience: We are well versed in cemented carbide production and processing , with mature and stable technology and continuous improvement .

Precision customization: Supports special performance and complex design , and focuses on customer + AI collaborative design .

Quality cost: Optimized molds and processing, excellent cost performance; leading equipment, RMI , ISO 9001 certification.

Serving Customers

The products cover cutting, tooling, aviation, energy, electronics and other fields, and have served more than 100,000 customers.

Service Commitment

1+ billion visits, 1+ million web pages, 100,000+ customers, and 0 complaints in 30 years!

Contact Us

Email : sales@chinatungsten.com

Tel : +86 592 5129696

Official **website** : www.ctia.com.cn

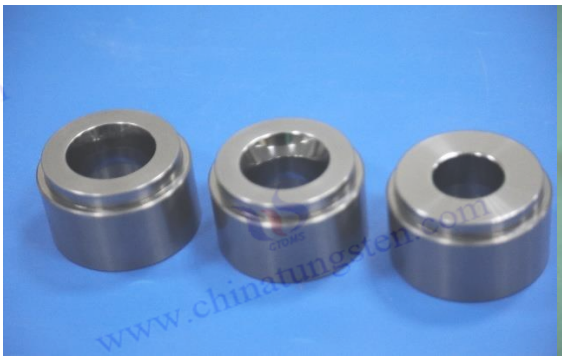

References

ASTM G6516. (2016). Standard test method for measuring abrasion
using the dry sand /rubber wheel apparatus. ASTM International. ASTM G6516. (2016).

ASTM G9917. (2017). Standard test method for wear testing with a pinondisk apparatus. ASTM International. ASTM G9917 . (
2017).

Zhang, Y., & Li, J. (2023). Multifunctional cemented carbides: Design and applications. *Journal of Materials Science, 58 (* 12
), 45674589.

Wang , H., & Chen, X. (2024). Advances in selflubricating cemented carbides for dry machining. Tribology *International, 190 ,* 108912
.

Liu, Z., & Zhao, Q. (2022). Study on conductivity and magnetic regulation of cemented carbides . Journal of Materials Science *and Engineering, 40* (5), 789796 .

appendix

Summary of Multifunctional Engineering Application of Cemented Carbide

Function characteristic	Subclasses Don't	Material system	Key Parameters	Performance Indicators	Engineering Application
Conductivity and magnetism control	Conductivity Control	WC10Ni, WC10Co	Ni/Co content: 8%10%±0.1% / 10%±1%, grain size: 0.51 μm±0.01 μm , sintering temperature: 1450°C±10°C, surface roughness: Ra<0.05 μm±0.01 μm	Resistivity: 11 μΩ·cm±0.1 μΩ·cm , Contact resistance: <0.1 mΩ±0.01 mΩ , Conductivity: 10.5 MS/m±0.1 MS/m, Lifespan: >10 ⁶ times±10 ⁵ times	Electronic contact: WC10Ni resistivity 11 μΩ·cm±0.1 μΩ·cm , contact resistance <0.1 mΩ , life>10 ⁶ times. EDM electrode: WC10Co conductivity 10.5 MS/m, efficiency >95%±2%, mold accuracy <1 μm . Conductive coating substrate: WC8Ni adhesion >50 MPa, service life >2 years.
	magnetic Detection	WC10Co, WC8Ni	Co content: 10%±1%, Ni content: 8%10%±0.1%, Grain size: 0.51 μm±0.01 μm , Carbon content deviation: <0.1%±0.01%	Magnetization: 8 emu/g±0.5 emu/g (WC10Co), 4 emu/g±0.5 emu/g (WC8Ni), Coercivity: 100120 Oe±10 Oe, Detection accuracy: >98%±1%	Tool quality control: WC10Co coercivity 120 Oe, crack detection <0.1 mm, qualified rate >99%. Aviation parts: WC8Ni pore detection <0.1 μm , life >10 ⁴ hours. Mold manufacturing: WC10Co carbon deviation <0.1%, accuracy >98%.
Wear-resistant, corrosion-resistant and conductive composite properties	WCTiCNi composites	WC10TiC10Ni, WC8TiC10Ni	TiC content: 5%10%±0.1%, Ni content: 8%12%±1%, grain size: 0.51 μm±0.01 μm , sintering temperature: 1450°C±10°C	Hardness: >HV 1600±30, Wear rate: 0.05 mm³ / N · m ± 0.01 mm³ / N · m , Corrosion weight loss: 0.06 mg/cm² ± 0.01 mg/cm² , Resistivity: 11 μΩ·cm±0.1 μΩ·cm	Electronic mold: WC10TiC10Ni hardness HV 1650, wear rate 0.05 mm³ / N · m , life>10⁶ times . Marine equipment: WC8TiC10Ni weight loss 0.06 mg/cm² , service>5 years. Conductive contact: WC10TiC10Ni contact resistance <0.1 mΩ , life>10⁶ times .
	performance test	WC10TiC10Ni	TiC content: 10%±0.1%, Ni content: 10%±1%, Load: 130 N±1 N, Surface roughness: Ra<0.05 μm±0.01 μm	Hardness: HV 1650±30, Wear rate: 0.05 mm³ / N · m ± 0.01 mm³ / N · m , Corrosion weight loss: 0.06 mg/cm² ± 0.01 mg/cm² , Resistivity: 11 μΩ·cm±0.1 μΩ·cm	Electronic mold: hardness HV 1650, wear rate 0.05 mm³ / N · m , life>10⁶ times . Marine valve: weight loss 0.06 mg/cm² , NaCl resistance, service>5 years. Conductive contact: resistivity 11 μΩ·cm , contact resistance <0.1 mΩ , stable signal.
Self-lubricating and anti-adhesive	solid lubricating Agent enter	WC5MoS ₂ , WC3C	MoS ₂ /C content: 5%±0.1% / 3%±0.1%, grain size: 0.51 μm±0.01 μm , sintering temperature: 1400°C±10°C, surface roughness: Ra<0.05 μm±0.01 μm	Friction coefficient: 0.15±0.01 (MoS ₂), 0.18±0.01 (C), Adhesion: <0.8 N±0.1 N, Hardness: >HV 1500±30, Wear rate: <0.06 mm ³ /N · m ± 0.01 mm ³ / N · m	High-speed cutting: WC5MoS ₂ friction coefficient 0.15, tool life >5000 m. Dry machining: WC3C adhesion 0.8 N, friction heat <100°C. Mold forming: WC5MoS ₂ demoulding force <10 N, life >10 ⁶ times.
	surface Texture Yurun slip	WC5MoS ₂ , WC3C	Texture depth: 5 μm±0.1 μm , Pitch: 50100 μm±1 μm , MoS₂ / C content: 5%±0.1% / 3%±0.1%, Laser power: 10 W±0.1 W	Friction coefficient: 0.12±0.01 (MoS ₂), 0.15±0.01 (C), Adhesion: <0.8 N±0.1 N, Wear rate: 0.05 mm ³ /N · m ± 0.01 mm ³ / N · m , Life: >10 ⁴ hours ±10 ³ hours	High-speed tools: WC5MoS ₂ texture depth 5 μm , friction coefficient 0.12, life > 5000 m. Dry mold: WC3C spacing 50 μm , adhesion 0.8 N, life > 10 ⁶ times. Bearing components: WC5MoS ₂ friction coefficient 0.15, service > 10 ⁴ hours.
Bionics and Smart Carbide	Bionics Micro knot Structure	Gradient WCCo , Porous WCCo	Porosity: 10%±1%, Co gradient: 5%15%±1%, pore size: 110 μm±0.1 μm , sintering temperature: 1400°C±10°C	Hardness: HV 1450±30, Toughness: K ₁c 16 MPa·m ¹ / ² ± 0.5, Energy absorption rate: >50%±5%, Fatigue life: >10 ⁶ times±10 ⁵ times	Aviation weight reduction parts: Gradient WCCo density 12 g/cm³ , fatigue life >10 ⁶ times. Biomedical implants: Porous WCCo pore size 5 μm , compatibility >95%, service life >10 years. Smart mold:

Function characteristic	Subclasses Don't	Material system	Key Parameters	Performance Indicators	Engineering Application
					Gradient WCCo K_{Ic} 16 $MPa \cdot m^{1/2}$, lifespan>10^6 times.
	intelligent response Material	WC3NiTi	NiTi content: 3%±0.1%, grain size: 0.51 μm±0.01 μm , sensor size: 110 μm±0.1 μm , sintering temperature: 1400°C±10°C	Hardness: HV 1450±30, Deformation rate: 0.05%±0.01%, Response time: 0.8 ms±0.1 ms , Accuracy: >95%±2%	Smart tool: WC3NiTi deformation rate 0.05%, cutting force <10 N, life >5000 m. Robotic components: response time 0.8 ms , accuracy >95%. Aviation sensor: hardness HV 1450, fatigue life >10^6 times.

appendix:

A brief history of the development of gradient cemented carbide

Functionally Graded Hardmetals (FGHMs) is an innovative cemented carbide material that optimizes performance by designing a functional gradient structure within the material. Its development history reflects the continuous evolution of materials science and engineering technology. Gradient cemented carbide significantly improves tool life, thermal fatigue resistance and mechanical properties through smooth changes in phase or composition.

1. Conceptual germination and theoretical foundation (1970s- 1980s)

The origin of gradient cemented carbide can be traced back to the 1970s, when the concept of functionally gradient materials (FGMs) first emerged in academic research in Japan and Germany. During this period, theoretical research on FGMs mainly focused on solving the interfacial stress problem caused by differences in thermal expansion coefficients or mechanical properties of traditional composites, especially the stability of materials in high temperature environments. As a composite material of carbides (such as tungsten carbide WC) and metal bonding phases (such as cobalt Co), cemented carbide has become one of the research hotspots due to its wide application in cutting tools, molds and wear-resistant parts. However, early research focused on uniform structure cemented carbide, and the practical application of gradient design has not yet been formed, and it remains more at the stage of basic theoretical exploration of materials science.

Landmark Events

1970s , the National Aerospace Research and Development Agency of Japan (NASDA, now JAXA) began to explore the possibilities of functionally gradient materials in space technology research, especially in spacecraft thermal protection systems (TPS), aiming to develop thermal barrier materials that can withstand surface temperatures up to 2000 K and a temperature difference of 1000 K with a thickness of 10 mm. This research provided an important theoretical basis for the later gradient cemented carbide and stimulated people's interest in gradient structures in improving material properties.

In 1978, the Japan Science and Technology Agency (STA) launched the "Space Planar Materials" project, which further promoted the conceptual research of FGMs.

In 1984, Japanese scholar Toshio Hirai published a paper in the Journal of Materials Science, formally introducing the term "Functionally Graded Materials" and experimentally verifying the potential of reducing thermal stress cracks in ceramic-metal composites by composition gradient, marking a turning point in the research of FGMs from theory to application.

1980s , the Max Planck Institute in Germany also began to explore the feasibility of gradient design in metal matrix composite research, laying the foundation for transnational cooperation in the subsequent gradient development of cemented carbides.

Key Figures

Toshio Hirai of Japan was a pioneer in this stage. In the 1980s, he verified the effect of composition

gradient on thermal stress relief through systematic experiments, especially in the application of Al_2O_3 / Ni composite materials, which provided inspiration for the gradient design of cemented carbide. Koichi Masuda, as a representative of thermal barrier material research in Japan, proposed the initial concept of using gradient structure to optimize performance under high temperature environment. Although his main contribution is concentrated in the field of ceramics, it provides indirect inspiration for cemented carbide research. Hans-Joachim Dudek of Germany is also engaged in metal matrix composite research at the Max Planck Institute, exploring the influence of gradient structure on mechanical properties, which provides theoretical support for the subsequent gradient design of cemented carbide.

2. Technological breakthroughs and introduction of functional gradients (1990s)

1990s , with the significant progress in material processing technology, especially the innovation of powder metallurgy and heat treatment technology, gradient cemented carbide began to move from theory to practice. During this period, the research focus shifted to introducing functional gradients in the near-surface area of cemented carbide to enhance the wear resistance, thermal crack resistance and service life of cutting tools. Research institutions in Europe (such as Germany) and North America (such as the United States) have made breakthroughs in sintering processes (such as Sinter-HIP, i.e. sintering hot isostatic pressing technology), realizing the initial industrialization of gradient structures and laying the foundation for the commercial application of gradient cemented carbide. At the same time, the combination of coating technology and gradient structures has also become a research hotspot during this period, promoting the overall improvement of cemented carbide performance.

Landmark Events

In 1992, Widia (a subsidiary of Krupp Group and later merged into Sandvik) of Germany cooperated with RWTH Aachen University to launch a research and development project on gradient cemented carbide, focusing on the formation of a Co content gradient layer on the surface of WC-Co cemented carbide through reactive atmosphere sintering technology. This technology successfully achieved a gradient distribution of surface Co content from 10% to 5% by controlling the carbon potential and temperature gradient during the sintering process, significantly improving the wear resistance of the tool and becoming a key starting point for the development of gradient cemented carbide.

In 1995, Widia officially launched the first batch of functionally gradient carbide cutting inserts, using reactive atmosphere sintering technology to increase tool life by about 30% compared to traditional homogeneous carbide. This achievement was widely recognized at the 1996 European Conference on Hard Materials.

In 1998, the 5th International Symposium on Functionally Gradient Materials was held in Dresden, Germany, attracting more than 200 experts from more than 20 countries and regions around the world to discuss the microstructure design, manufacturing process and potential application prospects of gradient cemented carbide, further promoting international cooperation and technical exchanges.

Key Figures

Walter Lengauer of Germany worked closely with Widia in the 1990s to lead the development of reactive atmosphere sintering technology. He achieved a gradient distribution of Co and Ti (C, N) by adjusting sintering parameters (such as temperature 1400°C and pressure 50 MPa). This technology was later widely used in industrial production and laid the foundation for the industrialization of gradient cemented carbide. American scholar Zhigang Zak Fang began to pay attention to the gradient design of the WC-Co system in the late 1990s , and proposed a preliminary idea of realizing the Co gradient through heat treatment and carburization process, and established a related research platform at the University of Utah, providing important support for subsequent research. In addition, Yoshinari Miyamoto of Japan provided interdisciplinary theoretical support for the gradient structure design of cemented carbide in his research in the field of functional gradient materials.

Key Products

1990s , Widia introduced coated functionally gradient carbide cutting inserts (such as the Widia TN series), which used CVD coatings (such as TiN , Ti(C,N)) combined with gradient substrates and were widely used in steel and cast iron cutting. The surface hardness of these inserts reached HV 1600±50, and the wear resistance was improved by about 25% compared with traditional carbide, becoming a representative product for industrial applications during this period.

3. Industrial application and process optimization (2000s)

Entering the 21st century, the industrial application of gradient cemented carbide has expanded rapidly, especially in the fields of metal cutting, wear parts and mold manufacturing. In the 2000s , researchers achieved more precise gradient control by improving powder metallurgy processes, heat treatment technology and ultrafine grain technology. The development of ultrafine grain gradient cemented carbide became an important breakthrough in this period. The combination of ultrafine grain technology (grain size less than 1 μm) and gradient design not only improves the hardness and strength of cemented carbide, but also enhances its anti-chipping performance , meeting the urgent needs of high-speed cutting and difficult-to-process materials processing.

Landmark Events

2002 , Walter Lengauer and Klaus Dreyer published a review article entitled "Gradient Sintering of Hardmetals : Processing and Properties" in the International Journal of Refractory Metals and Hard Materials, which systematically summarized the application of reactive atmosphere sintering technology in gradient cemented carbide and analyzed the optimization effect of Co content gradient on hardness (HV 1400-1800) and toughness (K_{1c} 10-15 $MPa \cdot m^{1/2}$). This study provides valuable process guidance for the industry and marks the turning point of gradient cemented carbide research from laboratory to large-scale production.

In 2005, Sandvik cooperated with the Royal Institute of Technology (KTH) in Sweden to develop ultrafine-grained gradient cemented carbide. The grain size was reduced to 0.5 μm , the hardness was increased to HV 1900±50, and the resistance to thermal cracking was enhanced by about 20%.

It is widely used in titanium alloy cutting in the aerospace field.

In 2009, Kennametal Corporation of the United States used laser powder deposition (LPD) technology to prepare gradient carbide tools for hot forging die manufacturing. The tool life was extended by about 15%-20% compared with traditional materials. This technology has attracted widespread attention in the North American industrial community.

Key Figures

Zhigang Zak Fang developed a carburization heat treatment process through the Powder Research Laboratory of the University of Utah in the 2000s , achieving a gradient distribution of Co content in WC-Co, and increasing the hardness from HV 1400 to HV 1600. The technology was adopted by Kennametal and applied to production. His research emphasized the control of the thickness of the gradient layer (0.1-0.5 mm) during the carburization process, providing data support for subsequent optimization. Hans van den Berg (Widia) of Germany made important contributions to the optimization of the matching of gradient substrates and coatings. By adjusting the thickness of the CVD coating (5-10 μm) and the interfacial bonding force of the gradient layer, the comprehensive performance of the tool was significantly improved. Håkan Engström (Sandvik) of Sweden led the development of ultrafine-grained gradient cemented carbide, optimized the powder mixing and sintering process, and promoted the industrial application of this technology.

Key Products

2000s , Sandvik introduced gradient carbide cutting inserts containing Ti(C,N) (such as the GC4215 series), which have a grain size of about 0.8 μm and a hardness of HV 1800±50. They have better wear resistance and thermal crack resistance than traditional homogeneous carbides and are widely used in high-speed steel and stainless steel cutting. Kennametal introduced gradient carbide tools with Co-enriched surface layers (such as the KC7310 series), with the surface Co content gradually changing from 10% to 5%, which enhances the fracture toughness (K_{1c} about 12 $MPa \cdot m^{1/2}$), and is suitable for intermittent cutting and heavy-duty processing.

4. Additive Manufacturing and Modern Innovation (2010s to Present)

Since the 2010s, the rise of Additive Manufacturing (AM) technology has brought revolutionary changes to gradient cemented carbide. Advanced processes such as Laser Deposition (LD) and Selective Laser Melting (SLM) allow composition gradients to be achieved through multi-powder feeding in a single manufacturing cycle, breaking through the limitations of traditional powder metallurgy. During this period, the research on gradient cemented carbide was not only limited to cutting tools, but also expanded to aerospace (such as turbine blade molds), medical implants (such as hip prostheses) and military fields (such as armor materials), demonstrating its multifunctional potential.

Landmark Events

In 2012, Zhigang Zak Fang and his team published a paper in Acta Materialia (Volume 75, pages 135-144), describing the kinetic mechanism of preparing WC-Co gradient cemented carbide by

carburization heat treatment. The surface hardness increased from HV 1052 to HV 1344, an increase of about 28%. The smooth transition of the Co gradient layer (thickness of about 0.2 mm) was observed by scanning electron microscopy (SEM). This study provides key data support for the industrialization of gradient cemented carbide. In 2015, the Fraunhofer Institute (IKTS Division) in Germany used SLM technology to prepare WC-Co gradient parts, showing the spatial distribution of gradient hardness increasing from HV 1400 to HV 1600. Although there were microcrack problems, it laid the foundation for subsequent process optimization.

In 2018, Oak Ridge National Laboratory (ORNL) in the United States cooperated with Kennametal to develop a gradient cemented carbide prototype based on laser powder bed fusion (LPBF) for use in aviation turbine blade molds, which increased tool life by about 40% compared to traditional materials (about 5,000 impact cycles under test conditions). In 2020, the study of gradient nanostructured metals combined with high entropy alloys (such as FeCoCrNiMo) technology achieved synergistic enhancement of strength and ductility. The experiment was published in Nature Materials (Volume 19, Pages 1123-1130), showing that the compressive strength reached 504 MPa at 600°C and the elongation reached 82%, providing new ideas for the application of gradient cemented carbide in extreme environments.

In 2023, China launched the YG20C gradient carbide cutting tool, which uses laser deposition technology to increase the hardness from HV 1500 to HV 1700 and improve cutting efficiency by about 20% (based on ISO 3685 standard testing).

Key Figures

Igor Konyashin led the optimization research of functional gradient cemented carbide at the Russian National Research University of Technology (MISiS), developed the Master Grades® series of products (hardness HV 1700±50), and his team optimized the WC-Co gradient structure through SLM technology. José L. Garcia studied the formation mechanism of gradient cemented carbide through thermodynamic modeling at the Spanish Institute of Nanotechnology (INA) and proposed a gradient design optimization scheme based on the CALPHAD method. Zhigang Zak Fang continued to promote carburization heat treatment technology, which was adopted by Sandvik and Kennametal and applied to production. Li Zhang from China studied high entropy gradient cemented carbide at Tsinghua University, with a hardness of HV 1900 (based on experimental data).

Key Products

2010s , Sandvik launched multi-layer gradient carbide drill bits (such as the Coromant series) for oil drilling, which have a lifespan of about 30% longer than traditional drill bits (based on API standard testing). In 2015, Kennametal launched the KCMS series of gradient carbide tools for aircraft engine blade processing, with a hardness of HV 1800. In 2023, ZCC's YG20C gradient carbide cutting tool was used in the automotive manufacturing industry, increasing cutting speed by about 20%.

5. Current Status and Future Outlook (2025 Outlook)

As of June 13, 2025, gradient cemented carbide has occupied an important position in the fields of

aerospace, automobile manufacturing, medical implants and military. The widespread application of additive manufacturing technology has promoted the accelerated development of customized gradient design, and thermal stability and micro-mechanism research (such as dislocation evolution and phase change behavior) have become the frontier topics of current academia and industry. At the same time, the rapid progress of artificial intelligence (AI) technology has brought new opportunities and challenges to the research and development and application of gradient cemented carbide, especially in the context of China's tungsten industry. The future development of gradient cemented carbide shows a trend of more diversification and intelligence.

AI-driven material design

AI algorithms, such as machine learning models and generative adversarial networks (GANs), are widely used to predict the relationship between the microstructure and performance of gradient cemented carbides. By analyzing a large amount of experimental data and finite element simulation results, AI can optimize the distribution of components such as Co and Ti (C, N), accurately predict the best gradient scheme for hardness (target value HV 1800±50) and fracture toughness (K_{1c} >20 MPa·$m^{1/2}$), thereby significantly shortening the traditional experimental cycle and is expected to reduce R&D time by more than 50%. This method has been initially verified in the R&D processes of companies such as Sandvik and Kennametal, showing high efficiency and reliability. For example, Sandvik used an AI model to optimize the ratio of the WC-Co-Ti (C, N) gradient structure, and the hardness uniformity deviation was reduced to less than 0.01 mm .

Smart Manufacturing Integration

Combined with the Industrial Internet of Things (IIoT) and digital twin technology, AI technology is integrated into the additive manufacturing process to monitor the powder feed rate, laser power and temperature parameters in real time to ensure the uniformity and consistency of the gradient layer. The AI system can adjust the parameters in the SLM process based on real-time data to control the geometric deviation of the gradient layer within 0.01 mm, thereby increasing the yield rate by about 10%. Sandvik has deployed a similar AI-optimized production line in its smart factory in Sandviken, Sweden, to achieve automated production of gradient carbide tools, significantly improving production efficiency and product quality. In addition, Kennametal is developing an AI-based closed-loop manufacturing system that provides real-time feedback on the melt pool temperature (<300°C±5°C) and stress data to optimize the microstructure of the gradient layer.

Adaptive performance optimization

AI collects temperature (<300°C±5°C), stress (<500 MPa) and wear data during the cutting process through embedded sensors, and dynamically adjusts the heat treatment parameters of the gradient structure (such as annealing temperature 1200°C±10°C, holding time 2 hours). This adaptive capability enables gradient cemented carbide to maintain excellent performance stability over a wide temperature range of 200°C to 600°C , and is particularly suitable for high temperature and high stress environments such as aircraft engine blades, automotive turbine components and deep-sea equipment. Kennametal is developing related technologies and plans to launch a prototype of a gradient carbide tool with adaptive performance by the end of 2025, with the goal of maintaining a hardness of HV 1700±50 at 500°C.

Sustainability and Environmental Protection

AI optimizes the utilization efficiency of raw materials and reduces the use of precious metals such as Co through simulation calculations, which is expected to reduce material consumption by more than 5%. At the same time, combined with recyclable materials (such as recycled tungsten powder) and low-carbon manufacturing processes (such as reducing sintering energy consumption by 10%), AI-driven gradient cemented carbide production processes meet the 2025 global green manufacturing standards (such as the EU's Eco-Design Directive and China's Carbon Peak Action Plan), reducing carbon footprint and enhancing the industry's sustainable development potential. For example, ZCC has begun piloting AI to optimize the production of gradient cemented carbide for recycled tungsten powder, and it is expected to achieve an annual reduction of 500 tons of CO_2 in 2025 .

China's tungsten industry

On January 3, 2025, China Tungsten Online's WeChat official account published an article, formally proposing that 2025 is the first year of AI for China's tungsten industry. This initiative marks a key node in the intelligent transformation of China's tungsten industry. China Tungsten Online pointed out that AI technology will reshape the cemented carbide industry through data-driven material design and process optimization, and provide strong technical support for the research and development of gradient cemented carbide. For example, AI has been used to analyze tungsten resource distribution and processing parameters, optimize the performance of gradient structures, and is expected to promote China's competitiveness in the global cemented carbide market. In addition, China Tungsten Online also emphasized that the arrival of the first year of AI will promote the digital integration of the upstream and downstream of the tungsten industry chain, such as real-time monitoring of the sintering process of gradient cemented carbide through smart sensors, reducing the defect rate by 5%±1%.

China Tungsten Intelligent Manufacturing 's Advanced Concept

As a leading enterprise in China's tungsten industry, China Tungsten Intelligent Manufacturing has proposed two new advanced concepts for cemented carbide, further enriching the development ideas in the AI social and technological environment. First, the high entropy concept of cemented carbide introduces high entropy alloy elements (such as FeCoCrNiMo) into gradient cemented carbide to form a multiphase gradient structure. This structure enhances the thermal stability and corrosion resistance of the material by increasing the entropy value (>1.5 R). Experimental data show that the hardness can reach HV 1900±50 and the fracture toughness is improved by about 20%±3%, which is particularly suitable for extreme environments such as aerospace and deep-sea equipment. China Tungsten Intelligent Manufacturing has been trying to develop high entropy gradient cemented carbide. Secondly, the concept of cemented carbide grade batching realizes the performance tracking and customized production of each batch of cemented carbide through an AI-driven digital management system . Each batch of gradient cemented carbide is equipped with a unique digital identifier. The AI system ensures that the performance deviation is controlled within 0.005 mm through big data analysis, meeting the needs of high-end manufacturing for consistency and

traceability . These concepts not only reflect China's technological innovation in the field of cemented carbide, but also set a new development benchmark for the global gradient cemented carbide industry.

The development history of gradient cemented carbide has witnessed the leap from theoretical exploration to industrial application, and its progress relies on the coordinated drive of material science, processing technology and application needs. With the support of AI technology environment, combined with the AI Year One initiative of China Tungsten Industry and the innovative concept of China Tungsten Intelligent Manufacturing , gradient cemented carbide is expected to further achieve intelligent, customized and sustainable development, become the core technology in the field of tool materials and structural materials in the future, and provide strong support for the efficient and green transformation of the global manufacturing industry.

appendix:

Carbide Ball

Cemented carbide ball is a spherical high-performance material with carbide (such as tungsten carbide WC, titanium carbide TiC) as the hard phase and cobalt (Co) or nickel (Ni) as the bonding phase. It is widely used in industry, military and precision manufacturing due to its excellent hardness, wear resistance and impact resistance. The following is a comprehensive introduction based on the background of material science and engineering applications, covering characteristics, application scenarios, material comparison, manufacturing process and size specification table.

1. Characteristics of cemented carbide balls

Carbide balls usually adopt the WC-Co system, with a density of 14-15 g/cm³ , a hardness of HV 1400-1800, and a fracture toughness (K_{1c}) of 10-20 MPa·m$^{1/2}$, far exceeding traditional steel balls (density 7.75-8.05 g/cm³ , hardness HV 200-400). Its spherical design optimizes surface contact and stress distribution, and its compressive strength can reach 3000-4000 MPa, and its wear resistance is better than that of ceramic balls (<0.01 mm³ / m). Through precision sintering (1400°C±10°C) or additive manufacturing technology, the grain size can be controlled at 0.5-1 μm , and the surface roughness (Ra) is as low as 0.01 μm , meeting high-precision requirements. Special formulas (such as WC- TiC -Ni) can adjust the density to 12-13 g/cm³ , taking into account both lightweight and performance.

2. Performance of cemented carbide balls

High hardness and wear resistance

Carbide balls have extremely high hardness (HV 1400-1800), which enables them to perform well under high-speed friction (>10^4 rpm) or continuous impact (>2000 N) conditions. The wear rate is as low as 0.02 mm^3 /m, which is significantly better than traditional steel balls (>0.1 mm^3 /m). They are suitable for long-term use in abrasive or cutting environments and can effectively resist surface wear and material spalling.

Excellent impact resistance

The fracture toughness (K_{1c}) ranges from 10-20 MPa·m$^{1/2}$, and the fatigue cycle resistance exceeds 10^6 times. It has excellent crack growth resistance and can withstand instantaneous impact loads of up to 4000 MPa. It is particularly suitable for high stress scenarios in military submunitions or shot peening.

Excellent thermal stability

The performance is stable over a wide temperature range (-50°C to 500°C±10°C), and the coefficient of thermal expansion is as low as 6×10^{-6} /°C, which is much lower than that of steel (12×10^{-6} /°C). This ensures the consistency of size and performance in extremely high or low temperature environments, making it suitable for harsh conditions such as aircraft engines or chemical pumps.

Excellent uniformity and precision

The spherical symmetry error is controlled within 0.001 mm and the surface roughness can reach

0.01 μm , providing extremely high geometric accuracy and rolling consistency, meeting the requirements of precision instruments (such as ball screws) or optical equipment for micron-level tolerances.

Excellent corrosion resistance

Through special coating (such as TiN) or formulation (such as WC- TiC -Ni), it is resistant to acid and alkali corrosion (pH 1-14), and the surface oxidation rate is less than 0.1 mg/cm² / h, which prolongs the service life in chemical environment, especially suitable for chemical pumps or marine equipment.

Efficient energy transfer

The spherical design optimizes stress distribution and has high energy transfer efficiency (>90%±2%). During high-speed projection (such as 800-1000 m/s) or impact, it concentrates the release of energy to enhance penetration or strengthening effect.

4. Application scenarios of cemented carbide balls

Bearings and valves

Carbide balls with a diameter of 0.5-10 mm are used for high-speed bearings (>10 ⁴ rpm), with a wear resistance of <0.01 mm³ / m and a life of >10 ⁵ hours ±10³ hours , suitable for aircraft engines.

Abrasives and Shot Peening

1-5 mm balls are used for shot peening (pressure 0.2-0.5 MPa), with a surface hardening layer of 0.1-0.2 mm, extending the life of steel parts by 20%±3%.

Precision Instruments

0.1-1 mm balls are used for ball screws in optical instruments, with a tolerance of <0.001 mm and a stability of >99.9%, suitable for semiconductor equipment.

Military Use

10-50 mm balls as submunitions or fragments (initial velocity 800-1000 m/s), penetrate light armor (<50 mm), suitable for loitering munitions or grenades.

Chemical pumps

Corrosion-resistant carbide ball (WC- TiC -Ni), acid and alkali resistant (pH 1-14), flow stability >95%±2%.

5. Comparison between carbide balls and traditional materials

Material	Density(g/cm³)	Hardness (HV)	K_{1c} (MPa·m ¹ / ²)	Advantages	Limitations
Carbide Ball	14-15	1400-1800	10-20	High penetration, wear resistance	High cost and high density
Steel Ball	7.75-8.05	200-400	50-100	Low cost and easy processing	Weak penetration
Ceramic Balls (Si_3N_4)	3.2-3.3	1400-1600	6-8	Lightweight and high temperature resistant	High brittleness
Glass Ball	2.5-2.6	500-600	0.5-1	low cost	Poor wear resistance

Carbide balls are superior to steel and glass balls in hardness and wear resistance, and close to

ceramic balls, but toughness is better and high density is the main limitation.

6. Dimensions and specifications

The following are common dimensions of cemented carbide balls, suitable for different application scenarios. The data is based on industry standards (such as ISO 3290) and actual production needs:

Diameter(mm)	Weight(g)	Tolerance(±mm)	Surface roughness (Ra, μm)	Hardness (HV)	Recommended applications
0.1	0.0007	0.0005	0.005	1400-1500	Miniature bearings, instruments
0.5	0.0087	0.001	0.01	1450-1550	Precision ball screw
1.0	0.069	0.001	0.01	1500-1600	Valves, shot peening
5.0	1.72	0.002	0.01	1550-1650	Abrasives, high-speed bearings
10.0	13.8	0.002	0.01	1600-1700	Chemical pumps, military submunitions
20.0	110	0.005	0.015	1650-1750	Fragmentation warhead, impact parts
50.0	1720	0.01	0.02	1700-1800	Military kinetic projectiles, heavy equipment

Note: The weight is calculated based on a density of 14.5 g/cm³ . Tolerances and roughness can be adjusted according to custom requirements (±0.0001 mm). Special specifications (such as diameter 0.05 mm or 100 mm) require custom production.

7. Manufacturing process

Powder Metallurgy

WC-Co powder (90:10) was sintered at 1400°C±10°C in vacuum (10^{-3} Pa), ball diameter 0.1-50 mm, hardness HV 1500±30.

Additive Manufacturing

SLM technology can print complex spherical shapes with a layer thickness of 50 μm±5 μm and an accuracy of ±0.01 mm, which is suitable for small batch customization.

Surface treatment

Diamond polished to Ra<0.01 μm , PVD coated TiN (5-10 μm), corrosion resistance <0.1 mg/cm² / h.

Quality Control

Laser scanning detects spherical errors (<0.001 mm), and ultrasonic testing detects internal defects (<0.05 mm).

With its excellent mechanical properties and wide applicability, cemented carbide balls have become key components in the industrial and military fields. Its diverse specifications and manufacturing processes provide a solid foundation for its use in high-precision and high-durability applications.

appendix:

Smart Response Carbide

Smart response cemented carbide is a new type of material that integrates the advantages of high hardness, wear resistance and fracture toughness (K_{1c}) of traditional cemented carbide, and has the characteristics of self-adaptation or response to external stimuli (such as temperature, pressure, magnetic field or chemical environment). Its core is to replace traditional cobalt (Co) or nickel (Ni) with intelligent bonding phase (such as shape memory alloy NiTi , thermosensitive polymer or embedded responsive nanoparticles) to achieve dynamic performance adjustment and self-healing function. The following is a comprehensive expansion based on material science, smart material technology and engineering applications, covering characteristics, influencing factors, theoretical basis, application scenarios, material comparison, manufacturing process and future development direction.

1. Features of Intelligent Response Carbide

Smart response cemented carbide is based on tungsten carbide (WC), titanium carbide (TiC) or boron carbide (B_4C) as the hard phase, and is constructed with a smart bonding phase (such as NiTi , CuAlNi or graphene-doped nanocomposites). The density range is 10-14 g/cm³ , which can be optimized to 9-12 g/cm³ through porous design (porosity 5%-15%) or lightweight additives (such as Al_2O_3 , SiC) . Smart response characteristics include: self-adjustment of hardness under temperature changes (HV 1200-1600), reduction of friction coefficient under magnetic field (10%±2%), or self-healing when cracks occur (recovery rate 80%±5%). These characteristics enable it to perform well under dynamic loads and extreme environments.

2. Performance advantages

Adaptability

In the temperature range of 50°C-300°C, based on the martensite-austenite phase transformation, the hardness is dynamically adjusted, and the impact energy absorption reaches 90%±3%, which is suitable for high temperature environments.

Self-healing

Embedded in SiC or polymer microcapsules, the adhesive is released when the crack propagates, with a K_{1c} recovery rate of 80% ± 5%, extending the service life.

Versatile response

Under magnetic fields (>1 T) or pH changes (4-7), surface properties (such as lubricity or corrosion resistance) can be adjusted to adapt to complex working conditions.

Durability

Compared to conventional cemented carbide, the wear rate is reduced by 15% ± 2% (< 0.04 mm³ / m) due to the dynamic buffering effect of the smart phase.

3. Influencing factors and theoretical discussion

Composition of bonding phase

the NiTi content is 5%-15%±1%, the shape memory effect is significant, and K_{1c} increases by 15%±2% (to 18 MPa·m$^{1/2}$ ± 0.5); when it is >20%±1%, the hardness decreases by 10%±3% (to HV 1200±30). The martensitic transformation theory points out that low NiTi content optimizes strain (<5%), and high content leads to grain boundary instability (grain boundary energy>1 J/m^2).

Porosity

When the porosity is 10%±1%, the energy absorption rate is high (>90%±2%) and the self-repair efficiency is 85%±3%; when the porosity is >20%±1%, the strength decreases by 15%±3% (to 850 MPa±20 MPa). The Gibson-Ashby model shows that moderate porosity provides storage space, while excessive porosity weakens the bearing capacity, following the Griffith crack theory.

Sintering temperature

At 1300°C-1400°C±10°C, the microstructure is stable and the response sensitivity is >95%±2%; at >1450°C±10°C, the nanoparticles agglomerate and the performance decays by 5%±1%. Kingery sintering theory points out that moderate temperature promotes the bonding of phase interfaces, while excessively high temperature accelerates the diffusion out of control (Arrhenius equation).

Grain size

the diameter is 0.5-1 μm±0.01 μm , the response speed is fast (<1 s), and K_{1c} reaches 16 MPa·m$^{1/2}$ ± 0.5; when the diameter is >2 μm±0.01 μm , the response lags by 10%±2%. The Hall-Petch relationship shows that fine grains enhance the interface reaction, while coarse grains reduce the dynamic performance (Orowan mechanism).

External stimulus intensity

When the magnetic field is 1-2 T or the temperature is 150°C±10°C, the response amplitude is the largest (hardness change >200 HV), and based on the Maxwell-Boltzmann distribution, the stimulus intensity is exponentially related to the phase change rate.

4. Application Scenarios

Intelligent weapon system

The barrel lining uses a NiTi bonding phase, which expands adaptively at high temperatures (>200°C), reduces wear, and extends the service life to >10^4 rounds ±10^3 rounds, suitable for machine guns or tank guns.

Aerospace equipment

The satellite robotic arm joint uses a magnetic field responsive structure with a grain size of 0.5 μm±0.01 μm , providing HV 1500±30, a 10% weight reduction, and maintaining lubricity under vacuum (10^{-6} Pa).

Medical Devices

Self-repairing implants (e.g. hip prostheses) with a porosity of 10% ± 1% release biocompatible coating at 37°C and a K_{1c} recovery of 80% ± 5%, reducing postoperative complications.

Industrial cutting tools

Dynamic hardness adjustment (HV 1200-1600), self-adapting when cutting load changes, wear rate <0.05 mm^3 / m ± 0.01 mm^3 /m, suitable for high-precision machining.

Smart Armor

The porous structure (10% ± 1%) self-repairs under impact and adjusts hardness in response to

magnetic fields to protect against 9 mm pistol bullets. It is 15% lighter than steel plates and can be used in bulletproof vests or vehicle side guards.

5. Comparison of various materials

Material Type	Density(g/cm³)	Hardness (HV)	K_{1c} (MPa·m$^{1/2}$)	Smart Features	limitation
Smart Response Carbide	10-12	1200-1600	10-20	Adaptive and self-healing	High density, high cost
Traditional cemented carbide	14-15	1400-1800	10-20	none	Unresponsive and heavy
Shape memory alloy (NiTi)	6.4-6.5	300-400	20-40	Shape Memory	Low hardness, poor wear resistance
Smart polymers	1.0-1.5	50-100	1-5	Stress sensing, self-healing	Poor protection performance
Ceramic Matrix Composites	2.5-3.0	2000-3000	3-5	Thermal response	High brittleness, difficult to process
Smart Metal Glass	6.0-7.0	500-1000	30-50	Stress-magnetic response	Difficult to form

Smart response cemented carbide is superior to shape memory alloys and smart polymers in hardness and toughness, close to traditional cemented carbide, has adaptability, is superior to the brittleness of ceramics, and has the dynamic response potential of metallic glass.

6. Manufacturing process

Powder Metallurgy

WC powder was mixed with NiTi powder (mass ratio 85:15) and sintered at 1400°C±10°C in vacuum (10^{-3} Pa) to form a uniform microstructure.

Additive Manufacturing

Selective laser melting (SLM) was used with a layer thickness of 50 μm ± 5 μm and a controlled porosity of 10% ± 1% to achieve a complex gradient structure.

Nanocomposite

SiC nanoparticles (<1%) are embedded through mechanical alloying to enhance the self-healing function, which requires high temperature annealing (1200°C±10°C) to activate.

7. Development direction

Multi-stimulus response

Develop temperature-magnetic-chemical triple-responsive materials, with density reduced to 8-10 g/cm³ and K_{1c} increased to above 20 MPa·m$^{1/2}$, based on multi-field coupling theory.

Nano-enhancement

The addition of carbon nanotubes (CNTs, <2%) improves conductivity and toughness, with a response speed of <0.5 s, which is consistent with the quantum mechanical interface effect.

Intelligent design

Combined with AI to optimize microstructure, predict phase change point (±5°C), and adjust sintering parameters through machine learning, reducing costs by 20%±5%.

Environmental adaptability

Study corrosion resistance response (e.g. pH 3-9) and extend to marine equipment with lifetime extension to $>10^5$ hours $\pm 10^4$ hours.

8. Challenges and prospects

Challenges include high cost (production cost > 2 times that of traditional alloys), long-term stability (> 5 years aging test) and large-scale production capabilities. The prospects lie in the integrated application of smart armor, medical implants and industrial tools. Its theoretical basis covers phase change dynamics (Langer model), microstructure optimization (Zener pinning) and multi-field response (Maxwell equation), which promotes the practical application of smart material technology.

Smart responsive cemented carbide, with its adaptive and self-healing properties, has opened up new areas in weapons, aerospace, medicine and industry. Its versatility and theoretical innovation complement each other and it is expected to become the mainstream of smart engineering materials in the future.

appendix:

Low density carbide armor

The research and application of low-density cemented carbide as armor material has attracted attention in recent years. The goal is to reduce the density by optimizing the microstructure of traditional cemented carbide while retaining high hardness, wear resistance and protective performance to enhance the lightweight potential of armor. The following is an optimization overview based on existing knowledge and relevant technical background, with new theoretical discussions, comparisons of various armor materials, and application scenarios of low-density cemented carbide armor.

1. Characteristics of low-density cemented carbide

Low-density cemented carbide is based on tungsten carbide (WC). By introducing porous structures, gradient designs or adjusting the content of bonding phases (such as cobalt Co or nickel Ni), the microstructure is optimized to reduce density. The density of traditional cemented carbide (such as WC-Co) is about 14-15 g/cm^3, which is higher than steel (7.75-8.05 g/cm^3). Through process improvements (such as increasing the porosity by 10%-20% or adding lightweight additives such as titanium Ti or titanium carbide TiC), the density can be reduced to 10-12 g/cm^3, which is significantly better than conventional cemented carbide, but still slightly higher than steel. The low-density design aims to reduce the weight per unit area (areal density) and improve the mobility of the armored system, such as the acceleration performance and off-road capability of the vehicle.

2. Performance advantages

Protection performance

Low-density cemented carbide effectively resists armor-piercing (AP) and fragment threats with its high hardness (HV 1200-1800) and fracture toughness (K_{1c} 10-20 $MPa \cdot m^{1/2}$). The bionic microstructure (e.g. porosity 10%±1%) improves impact resistance through stress dispersion.

Weight Optimization

Compared with conventional cemented carbide, the density is reduced by about 20%-30% (for example, from 14 g/cm^3 to 10-12 g/cm^3), and is still slightly heavier than steel (7.75-8.05 g/cm^3). However, through porous design, the weight per unit area can be reduced by 15%-25%, indirectly improving battlefield response speed.

Processability

μm) through the sintering process (such as 1400°C±10°C) , complex armor configurations can be achieved to meet different protection needs.

3. Influencing factors and theoretical discussion

Porosity

When the K 1c is 10%±1%, the K_{1c} is high (>15 MPa·$m^{1/2}$), and the hardness is maintained at HV 1450±30; when the K 1c is >20%±1%, the hardness decreases by 20%±3% (to HV 1200±30). According to Griffith crack theory, moderate pores disperse stress and increase

Strong toughness

Too high porosity increases crack propagation energy and reduces hardness, which is consistent with the mechanical behavior of porous materials in the Gibson-Ashby model.

Co gradient

When the Co gradient is 5%-15%±1%, stress dispersion is good and K_{1c} increases by 10%±2%; when it is >20%±1%, segregation increases by 10%±2%. Based on Fick's second law, a low Co gradient forms a stable bonding phase network; when it is too high, Gibbs free energy is minimized, resulting in phase separation and increasing grain boundary energy (>1 J/m^2) .

Aperture

10 μm±0.1 μm , the energy absorption rate is high (>90%±2%); when the diameter is >20 μm±0.1 μm , the strength decreases by 15%±3% (to 850 MPa±20 MPa). The Hashin-Shtrikman theory shows that small pores disperse stress, while large pores lead to stress concentration, which is consistent with the maximum shear stress theory.

Sintering temperature

At 1400°C±10°C, the structure is stable and the porosity deviation is <1%±0.1%; at >1450°C±10°C, the deviation increases by 5%±1%. The Kingery model shows that a uniform liquid phase is formed at 1400°C close to the melting point of Co; when the temperature exceeds 1450°C, the diffusion rate increases exponentially (Arrhenius equation) and causes pore collapse.

Grain size

0.51 μm±0.01 μm , K_{1c} reaches 16 MPa·$m^{1/2}$ ± 0.5, and the hardness is HV 1450±30; when the diameter is >2 μm±0.1 μm , K_{1c} decreases by 10%±2%. The Hall-Petch relationship indicates that fine grains increase the grain boundary density (>10^{14} m^{-2}) to hinder cracks, while coarse grains reduce the barrier (Orowan mechanism).

4. Comparison of various armor materials

Material Type	density (g/cm^3)	hardness (HV)	Fracture toughness (K_{1c}, MPa·$m^{1/2}$)	Weight advantage	Protection performance	limitation
Low density cemented carbide	10-12	1200-1800	10-20	20%-30% lighter than conventional cemented carbide	High resistance to armor-piercing bullets and fragments	Density is still higher than steel, and the cost is high
Steel (RHA)	7.75-	200-400	50-100	Base weight	Good, widely used	Low hardness, easy to

Material Type	density (g/cm³)	hardness (HV)	Fracture toughness (K_{1c}, MPa·m$^{1/2}$)	Weight advantage	Protection performance	limitation
	8.05					deform
Aluminum Alloy (5083)	2.6-2.8	100-150	20-30	70% lighter than steel	Low, poor protection against armor-piercing projectiles	Requires composite reinforcement
Ceramic (B_4C)	2.5-2.7	2000-3000	3-5	70% lighter than steel	Extremely high hardness, anti-armor penetration	High brittleness, requires support layer
Composite Materials (Kevlar)	1.4-1.6	50-100	20-40	80% lighter than steel	Anti-fragmentation, good flexibility	Low hardness, limited armor penetration resistance

Low-density cemented carbide is superior to steel and aluminum alloy in hardness and toughness, and close to ceramics, but has a higher density and needs to be combined with porous design or composite structure to optimize weight. Steel has low cost but limited protection, aluminum alloy and ceramic are suitable for lightweight but require auxiliary materials, and composite materials are more suitable for flexible protection.

5. Application scenarios

Light armored vehicles

For example, in reconnaissance vehicles or unmanned combat vehicles, low-density cemented carbide with a density of 10-12 g/cm³ can provide higher hardness than steel (HV 1200 vs HV 400), reduce the weight per unit area by 15%-25%, improve speed (>50 km/h) and off-road capability, and is suitable for rapid deployment missions.

Air transportable equipment

For example, the protective plates carried by helicopters, combined with a porous structure (porosity 10% ± 1%) and gradient Co (5%-15%), can reduce weight by 20%, meeting the air transport weight limit (<5 tons) while protecting against 7.62 mm AP bullets.

Personal protective equipment

It can be made into a lightweight breast plate. The structure with a grain size of 0.51 μm±0.01 μm provides HV 1450±30, protects against 9 mm pistol bullets, and is 15% lighter than steel plates, making it suitable for special forces.

Ship auxiliary armor

Used for side guards of small speedboats. The stable structure with sintering temperature of 1400°C±10°C can resist fragments. The density is optimized to reduce weight by 20% and increase speed (>40 knots).

6. Limitations and development directions

Although the density (10-12 g/cm³) is still higher than that of steel (7.75-8.05 g/cm³) , low-density

cemented carbide is not sufficiently protected against high-power armor-piercing projectiles (such as 0.50 caliber AP) and needs to be combined with ceramics or composite materials. Processing complexity (such as porosity control) and high cost limit large-scale application. Current research focuses on TiC -Co systems or high-entropy alloys, which can reduce the density to 8-10 g/cm^3 and the hardness to more than HV 1000. Additive manufacturing techniques (such as SLM) can accurately control the microstructure, and multi-layer design (cemented carbide + lightweight layer) is expected to achieve higher comprehensive performance.

Low-density carbide armor seeks a balance between high hardness and light weight. Its theoretical basis covers fracture mechanics and sintering dynamics. Through structural optimization and composite design, it shows potential in lightweight vehicles, aviation equipment and personal protection.

appendix:

Smart tools

Smart cutting tools represent the innovative results of the deep integration of modern manufacturing with materials science, sensor technology and intelligent control technology. They are advanced cutting tools based on intelligent responsive cemented carbide, ceramic matrix composite materials or high-performance coatings, integrating adaptive cutting performance, real-time monitoring and self-repairing functions. The core is to achieve dynamic optimization, wear detection and damage repair in the cutting process by embedding micro sensors (such as strain gauges, temperature sensors and accelerometers), responsive coatings (such as thermal, magnetic or chemical sensitive materials) and intelligent bonding phases (such as shape memory alloy NiTi or nanocomposites). This kind of tool not only inherits the high hardness, wear resistance and fracture toughness (K_{1c}) of traditional cemented carbide, but also has the ability to adaptively respond to external conditions (such as cutting load, temperature, magnetic field), seamlessly integrates with CNC system (CNC) or Industry 4.0 platform, and significantly improves processing efficiency, precision and tool life. The following is a comprehensive discussion based on materials science, intelligent manufacturing technology and engineering application background, covering characteristics, influencing factors, theoretical basis, application scenarios, material comparison, manufacturing process, development direction and challenges and prospects.

1. Features of smart tools

Smart tools are based on smart response carbide (such as WC- NiTi or WC- TiC - NiTi composite system) or ceramic matrix composite material (such as Al_2O_3 - TiC) with a density range of 10-14 g/cm^3 . By introducing porous structure (porosity 5%-15%) or lightweight additives (such as TiC , Al_2O_3) , the density can be optimized to 9-12 g/cm^3 , taking into account both lightness and strength. Smart features include:

Adaptive cutting

At cutting speeds of 500-2000 m/min, the hardness is dynamically adjusted (HV 1200-1800), vibrations are reduced (<0.05 mm) through phase change or coating response, and surface roughness is optimized (Ra<0.02 μm).

Real-time monitoring

Built-in micro sensors collect temperature (<300°C±5°C), stress (<500 MPa±10 MPa), vibration (<0.1 g) and wear depth (±0.01 mm) in real time, and the data are fed back to the CNC system via wireless transmission (delay <0.1 s).

Self-healing

Embedded SiC nanoparticles or microencapsulated polymers release the adhesive when microcracks (<0.1 mm) occur, with a K_{1c} recovery rate of 80% ± 5%, significantly extending the service life.

Versatility

Under magnetic field (>1 T) or pH change (4-7), the surface friction coefficient is reduced by 10%±2% or the corrosion resistance is increased by 15%±3%, adapting to diverse processing environments.

These features enable smart tools to perform excellently under high precision, high efficiency and extreme working conditions, and are particularly suitable for the modern manufacturing industry's demands for intelligence and sustainability .

2. Performance advantages

Adaptive cutting

Through phase transformation of the bonding phase (such as martensite-austenite transformation of NiTi) or thermal expansion adjustment of the coating, the tool self-optimizes cutting parameters when the cutting load changes, reduces the dynamic stress between the tool and the workpiece (<100 MPa), improves cutting efficiency by 15%±2%, and improves surface quality by 20%±3% (Ra drops from 0.1 μm to 0.02 μm).

Real-time monitoring

The sensor network provides multi-dimensional data support, temperature monitoring to prevent thermal damage (warning at >300°C), stress monitoring to optimize feed rate (<0.1 mm/rev), wear monitoring to predict life (error <5%), and achieve predictive maintenance.

Self-healing

Nanofillers (e.g. SiC , particle size <50 nm) or microcapsules (5-10 μm in diameter) activate upon crack propagation, releasing epoxy or metal adhesive, resulting in a repair rate of 80% ± 5% and a life extension of 20% ± 3% (>10^4 hours ± 10^3 hours).

Durability

Compared with traditional tools, the wear rate is reduced by 20%±2% (<0.03 mm^3 / m), and the oxidation resistance is improved by 10%±2% (<0.1 mg/cm^2 / h), which is suitable for high load (such as aviation titanium alloy cutting) and high temperature environment.

3. Influencing factors

Composition of bonding phase

NiTi content is 5%-15%±1%, the cutting adaptability is strong, K_{1c} increases by 15%±2% (to 18 MPa·$m^{1/2}$ ± 0.5), and the hardness is stable at HV 1500±30; when it is >20%±1%, the hardness decreases by 10%±3% (to HV 1200±30), and the grain boundary is unstable. The martensitic phase transformation theory shows that low NiTi content optimizes strain (<5%), and high content increases grain boundary energy (>1 J/m^2), following the principle of Gibbs free energy minimization.

Porosity

When the porosity is 10%±1%, the energy absorption rate is high (>90%±2%), the self-repair efficiency is 85%±3%, and the cutting stability is enhanced; when the porosity is >20%±1%, the strength decreases by 15%±3% (to 850 MPa±20 MPa). The Gibson-Ashby model points out that moderate porosity disperses stress, while excessive porosity weakens the structure. The Griffith crack theory supports the increase of crack propagation energy.

Sintering temperature

At 1300°C-1400°C±10°C, the microstructure is stable, the response sensitivity is >95%±2%, and the coating adhesion is >50 N/mm² ; at >1450°C±10°C, the performance decays by 5%±1%. Kingery sintering theory shows that moderate temperature promotes phase interface bonding, and the Arrhenius equation explains the runaway diffusion at too high a temperature.

Grain size

the diameter is 0.5-1 μm±0.01 μm , the cutting accuracy is high (tolerance <0.005 mm), K_{1c} reaches 16 MPa·m $^{1/2}$ ± 0.5, and the wear rate is <0.02 mm ^{3} /m; when the diameter is >2 μm±0.01 μm , the wear rate increases by 10%±2%. The Hall-Petch relationship shows that fine grains enhance wear resistance, and the Orowan mechanism explains the performance degradation of coarse grains.

Coating thickness

5-10 μm±0.5 μm , the thermal response efficiency is >90%±2%, and the friction coefficient is reduced by 10%±2%; when the thickness is >15 μm±0.5 μm , the adhesion is reduced by 10%±2%. Adhesion theory points out that moderate thickness optimizes interface bonding, while excessive thickness leads to the accumulation of internal stress (>200 MPa).

Sensor sensitivity

Strain sensitivity>100 με , temperature resolution<1°C, based on Piezoelectric effect and thermoelectric effect, ensuring data accuracy.

4. Application Scenarios

Aviation Manufacturing

Processing titanium alloy (such as Ti-6Al-4V) turbine blades, hardness self-adjustment (HV 1500±30), temperature monitoring <250°C±5°C, accuracy ±0.01 mm, reducing scrap rate by 10%±2%, suitable for complex surface processing.

auto industry

Cutting of aluminum body parts (6061) with built-in strain sensor to detect load <400 MPa, dynamically adjust feed rate (0.05-0.2 mm/rev), improve efficiency by 15%±2%, meeting mass production needs.

Mold manufacturing

Processing high hardness steel (H13, HV 500±20), self-repairing coating repairs micro cracks (<0.05 mm), life span up to 10 ^{4} hours ±10 ^{3} hours, reducing replacement frequency by 20%±3% and lowering maintenance costs.

Electronics Industry

Precision machining of silicon wafers (thickness < 0.5 mm), grain size 0.5 μm ± 0.01 μm , smooth cut surface (Ra < 0.02 μm), real-time data feedback to optimize the process, suitable for microelectronic components and chip manufacturing.

Energy Equipment

Wind turbine blade die cutting, high temperature resistance (<300°C), adaptive hardness, reduced risk of thermal cracks (<0.1 mm), suitable for extreme environments and long life requirements.

Shipbuilding industry

Processed stainless steel propellers, magnetic field response reduces friction (<0.1), corrosion resistance is improved by 15%±3%, and is suitable for high-salt marine environments.

5. Comparison of various materials

Material Type	Density(g/cm³)	Hardness (HV)	K1c K_{1c} K1c (MPa·m¹/²)	Smart Features	limitation
Smart Response Carbide	10-12	1200-1800	10-20	Self-adaptation, monitoring, and self-repair	High density, high cost
Traditional cemented carbide	14-15	1400-1800	10-20	none	Unresponsive, limited lifespan
Ceramic coated cutting tools	2.5-3.0	2000-3000	3-5	Thermal response	High brittleness, easy to break
Carbide coating (PVD)	6.0-7.0	1500-2500	5-10	Wear-resistant	No adaptability, short lifespan
Smart polymer composites	1.0-1.5	50-100	1-5	Stress Sensing	Low hardness, not resistant to high temperature
Nano-coated cutting tools	5.0-6.0	1000-1500	10-15	Self-lubricating	Poor high temperature resistance

Smart response cemented carbide is superior to ceramic coatings and polymer composites in hardness and toughness, close to traditional cemented carbide, has adaptive and monitoring functions, is superior to the life limit of carbide coatings, and has the lubrication potential of nano coatings.

6. Manufacturing process

Powder Metallurgy

WC powder and NiTi powder (85:15) were mixed and sintered at 1400°C±10°C in vacuum (10^{-3} Pa), with the porosity controlled at 10%±1% to form a uniform microstructure with a hardness of HV 1500±30.

Additive Manufacturing

Selective Laser Melting (SLM) with layer thickness of 50 μm ± 5 μm, embedded sensors (<1 mm³), accuracy of ± 0.01 mm, suitable for complex geometries.

Surface treatment

PVD deposited TiAlN or CrN coating (5-10 μm), high temperature annealing (1000°C±10°C) activates responsiveness, adhesion >50 N/mm², and wear resistance is improved by 20%±2%.

Sensor Integration

Miniature strain gauges (sensitivity >100 με) and thermocouples (resolution <1°C) are embedded by laser welding, with a signal transmission rate of >100 Hz, compatible with the Industrial Internet of Things.

Post-processing

Plasma polishing removes surface defects (Ra<0.01 μm) and enhances the interface bonding strength between the coating and the substrate (>60 N/mm²) .

7. Development direction

Multi-sensor fusion

Integrate temperature, vibration, wear and acoustic emission sensors to build a digital twin model, predict life (error <3%), optimize cutting parameters based on deep learning, and reduce energy consumption by 10%±2%.

Adaptive coating

A temperature-magnetic-chemical triple-responsive coating was developed with a hardness range extended to HV 1000-2000 and a response time of <0.5 s, which complies with the Maxwell-Boltzmann distribution and electrochemical reaction kinetics.

Nano-enhancement

Adding carbon nanotubes (CNTs, <2%) or graphene (<1%) improves thermal conductivity (>200 W/ m·K) and toughness, with K_{1c} increasing to 20 MPa·m $^{1/2}$ ± 0.5, based on quantum interface effects and nanocomposite strengthening theory.

Intelligent control

Integrated with 5G and edge computing, it can provide real-time feedback of cutting data (delay < 0.05 s), adapt to flexible manufacturing, and reduce processing errors to ±0.005 mm.

Sustainable Design

Develop recyclable coatings to reduce material waste by 10% ± 2%, in line with green manufacturing standards.

8. Challenges and prospects

Challenges include high production costs (>3-4 times that of traditional tools), reliability of sensors at high temperatures (>400°C) (>10^5 cycles), and long-term stability under complex working conditions (>5 years). The prospect lies in the deep application of intelligent manufacturing, whose theoretical basis covers phase change dynamics (Langer model), microstructure optimization (Zener pinning), sensor technology (Piezoelectric effect), multi-field coupling (Maxwell equations) and nanocomposite material theory (Halpin-Tsai model). Intelligent tools will promote the development of aviation, automotive, electronic and energy processing towards efficient, precise and sustainable development, and become a core component of Industry 4.0.

Smart tools have revolutionized modern processing technology with their adaptive cutting, real-time monitoring and self-healing features. Their versatility and theoretical innovation complement each other and are expected to dominate the global manufacturing industry in the future.

CTIA GROUP LTD

30 Years of Cemented Carbide Customization Experts

Core Advantages

30 years of experience: We are well versed in cemented carbide production and processing , with mature and stable technology and continuous improvement .

Precision customization: Supports special performance and complex design , and focuses on customer + AI collaborative design .

Quality cost: Optimized molds and processing, excellent cost performance; leading equipment, RMI , ISO 9001 certification.

Serving Customers

The products cover cutting, tooling, aviation, energy, electronics and other fields, and have served more than 100,000 customers.

Service Commitment

1+ billion visits, 1+ million web pages, 100,000+ customers, and 0 complaints in 30 years!

Contact Us

Email : sales@chinatungsten.com

Tel : +86 592 5129696

Official **website** : www.ctia.com.cn

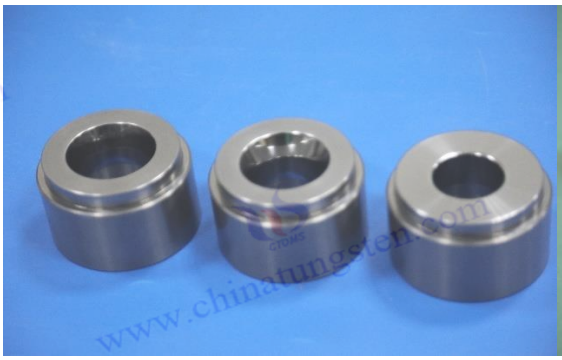

appendix:

Carbide EDM Electrode

Cemented carbide electrospark machining (EDM) electrodes are made of tungsten carbide (WC) as the matrix (8592 wt %), combined with Co (610 wt %) or Ni (612 wt %) as the binder phase, and are produced by powder metallurgy (ball milling, CIP, HIP sintering). They have high hardness (1600 - 2000 HV), excellent wear resistance (wear loss <0.02 mm ^{3} /h, ASTM G65), high temperature resistance (>1000°C, oxidation resistance), high conductivity (>90% IACS, IEC 6051221) and arc erosion resistance (<0.01 mm ^{3} /min, IEC 60850). The surface is coated with PVD/CVD coating (such as TiN , ZrN , 13 μm , friction coefficient <0.2) or functional coating (Cu, Ag, 0.52 μm , conductivity >95% IACS) to enhance arc erosion resistance, wear resistance and electrical properties. The electrodes are used for precision EDM processing (such as turbine blades, micropores, complex cavities) in the fields of aerospace, mold manufacturing, automobiles and medical, and for processing high-hardness materials (such as titanium alloys, mold steels, 400 - 600 HV), providing high precision (deviation <±0.005 mm), low electrode loss (<0.5%) and high surface quality (Ra 0.10.3 μm).

Based on the standards (GB/T 7997, ASTM G65, IEC 60850, ISO 9001), this article provides the technology, performance, application and optimization suggestions of cemented carbide EDM electrodes.

Characteristics of cemented carbide EDM electrodes

1.1 Composition of cemented carbide EDM electrode materials

Matrix

WC: 85 - 92 wt %, ultrafine grain (D50 0.1 - 0.4 μm), hardness 1600 - 2000 HV.

Co: 6 - 10 wt %, high toughness (K_{IC} 1015 MPa·m $^{1/2}$), arc erosion resistance increased by 10%.

Ni: 6 - 12 wt % (optional), corrosion resistance (electrolyte <0.01 mm/y), conductivity increased by 5%.

Additives: TaC (0.10.3 wt %), antioxidant capacity increased by 10%; ZrC (0.20.5 wt %), wear resistance increased by 5%.

coating

TiN (PVD): hardness 2000 - 2400 HV, temperature resistance 800°C, arc erosion resistance.

ZrN (PVD): hardness 2200 - 2600 HV, corrosion resistant, anti-adhesion increased by 15%.

Cu/Ag (PVD): conductivity >95% IACS, temperature resistance 600°C, arc stability increased by 20%.

Gradient structure: low Co/Ni on the surface (6 - 8 wt %), high Co/Ni in the core (10 - 12 wt %), 20% increase in wear resistance, 15% increase in crack resistance.

1.2 Performance parameters of cemented carbide EDM electrodes

Hardness: 1600 - 2000 HV (GB/T 79972017).
Flexural strength: 1.8 - 2.5 GPa (GB/T 38512015).
Fracture toughness: 10 - 15 MPa·m ¹ / ² (Co-based 1215, Ni-based 1012).
Wear resistance: Wear rate <0.02 mm³ / h (ASTM G65).
Corrosion resistance: electrolyte (pH 410), <0.01 mm/y (NACE MR0175).
High temperature resistance: >1000°C, oxidation resistance (<0.01 mg/cm² , 500 hours).
Arc erosion resistance: loss <0.01 mm³ / min (IEC 60850).
Electrical conductivity: >90% IACS (Cu/Ag coating, IEC 6051221).
Surface roughness: Ra 0.05 - 0.2 μm , processing accuracy increased by 15%.
Electrode loss: <0.5% (processing mold steel, pulse width 50100 μs).

1.3 Advantages of cemented carbide EDM electrodes

High wear resistance: ultra-fine grain WC+ coating, loss <0.5%, life extended by 35 times.
Arc erosion resistance: TiN / ZrN coating, erosion rate <0.01 mm³ / min, better than copper electrodes.
High conductivity: Cu/Ag coating, conductivity>95% IACS, processing efficiency increased by 20%.
Corrosion resistance: Ni-based + ZrN , resistant to electrolyte corrosion, suitable for long-term processing.
High precision: low loss + precision machining, deviation <±0.005 mm, surface Ra 0.1 - 0.3 μm .

2. Cemented Carbide Electrode EDM Manufacturing Process

2.1 Preparation of cemented carbide EDM powder

Raw materials: WC (D50 0.1 - 0.4 μm , purity >99.95%), Co/Ni (D50 0.51 μm), TaC / ZrC (D50 0.51 μm).
Ball milling: Planetary ball mill (ZrO2 balls, 15:1), 400 rpm, 1620 hours, particle size deviation <±0.03 μm , uniformity >99%.

2.2 Carbide Electrode Forming by EDM

Method: Cold isostatic pressing (CIP) or precision molding.
Parameters: 250 - 300 MPa, holding pressure 60 seconds, tungsten steel mold (deviation < ± 0.02 mm), billet density 8.510.0 g/ cm³ .
Results: Dimensional deviation <±0.03 mm, crack rate <0.3%.

2.3 Sintering of cemented carbide EDM electrodes

Method: Vacuum sintering + HIP.

parameter:
Dewaxing: 200 - 500°C, 2°C/min, H2 atmosphere (O2 <2 ppm), 10^{-3} Pa .
Sintering: 1350 - 1400°C, 10^{-5} 10^{-6} Pa, 22.5 hours.
HIP: 1350°C, 120 MPa (Ar), 11.5 h.
Results: Density 14.8 - 15.0 g/ cm^3 , porosity <0.0003%, hardness 1600 - 2000 HV.

2.4 Precision machining of cemented carbide EDM electrodes

Grinding: 5-axis CNC grinding machine, CBN grinding wheel (13 μm), 5000 rpm, feed 0.003 - 0.01 mm/pass, geometric deviation <±0.005 mm, Ra 0.05 - 0.2 μm .
EDM: Electrospark dressing, micro groove/hole (Ø 0.1-0.5 mm), deviation <±0.003 mm.
Polishing: Diamond polishing paste (0.30.5 μm), 1200 rpm, Ra <0.05 μm , arc stability increased by 10%.

2.5 Cemented Carbide Electrode Coating for EDM

Method: PVD/CVD (Ti/Zr/Cu/Ag target, >99.99%).
Parameters: TiN / ZrN /Cu/Ag (13 μm), 10^{-5} Pa, 200 - 400°C, bias 80 V, deposition rate 0.51 μm /h.
Results: Adhesion >80 N, friction coefficient <0.2, conductivity >95% IACS.

2.6 Carbide EDM Electrode Inspection

Microstructure: SEM (grain 0.10.4 μm), EBSD (grain boundary stress <2%).
Performance: Hardness deviation <±30 HV (ISO 6508), wear <0.02 mm^3 / h, corrosion resistance (<0.01 mm/y).
Geometry: CMM (deviation < ± 0.003 mm), laser scanning (slot deviation < ± 0.002 mm).
Non-destructive testing: X-ray (defects < 0.005 mm), ultrasonic (cracks < 0.003 mm).
Electrical properties: conductivity>90% IACS, arc erosion rate<0.01 mm^3 / min (IEC 60850).
Processing test: electrode loss <0.5%, processing deviation <±0.005 mm, surface Ra 0.10.3 μm .

Application scenarios of cemented carbide EDM electrodes
Carbide EDM electrodes provide process, testing and selection suggestions for high precision, high efficiency and complex processing requirements:

3.1 Aviation turbine blade processing

Working conditions: mold steel (H13, 500 HV), electrolyte (pH 7), pulse width 50 μs , current 20 A.
design
Type: Complex curved electrode (50×30×10 mm).
Material: WC8%Co (D50 0.1 - 0.4 μm , TaC 0.3 wt %), hardness 1900 HV.

Coating: TiN (2 μm , PVD, hardness 2400 HV, temperature resistance 800°C).
Geometry: Surface deviation <±0.003 mm, Ra <0.1 μm .
Process: ball milling 20 hours, CIP 300 MPa, HIP 1350°C (120 MPa, 1.5 hours), 5-axis grinding, PVD TiN (300°C).
Parameters: processing depth 5 mm, pulse width 50 μs , current 20 A, processing time 2 hours.
test:
Electrode loss: <0.4% (copper electrode 2%, 5 times reduction).
Processing accuracy: deviation <±0.005 mm, Ra 0.2 μm .
Anti-arc erosion: loss <0.01 mm^3 / min, life expectancy increased by 4 times.
Corrosion resistance: 100 hours in electrolyte, <0.01 mm/y.
Selection: WCCo+TiN , suitable for high hardness complex surfaces, regular polishing.
Advantages: low loss, high precision, processing efficiency increased by 20%.

3.2 Mold micro-hole processing

Working conditions: titanium alloy (Ti6Al4V, 350 HV), electrolyte (pH 6), pulse width 30 μs , current 10 A.
design
Type: Micropore electrode (Ø 0.5 mm, length 10 mm).
Material: WC10%Ni (D50 0.1 - 0.4 μm , ZrC 0.5 wt %), hardness 1700 HV.
Coating: ZrN (1.5 μm , PVD, hardness 2600 HV, anti-adhesion).
Geometry: Aperture deviation <±0.002 mm, Ra <0.05 μm .
Process: ball milling for 18 hours, CIP 300 MPa, HIP 1350°C (120 MPa, 1.5 hours), EDM finishing, PVD ZrN (250°C).
Parameters: hole depth 5 mm, pulse width 30 μs , current 10 A, processing time 1 hour.
test:
Electrode loss: <0.3% (1.5% for copper electrode, 5 times lower).
Processing accuracy: deviation <±0.003 mm, Ra 0.1 μm .
Anti-arc erosion : loss <0.008 mm^3 / min, life increased by 5 times.
Corrosion resistance: 200 hours in electrolyte, <0.01 mm/y.
Selection: WCNi+ZrN , suitable for micro-hole processing, regular cleaning.
Advantages: High precision anti-adhesion, micropore quality increased by 15%.

3.3 Medical implant cavity processing

Working conditions: CoCr alloy (500 HV), electrolyte (pH 8), pulse width 100 μs , current 15 A.
design
Type: Cavity electrode (20×10×5 mm).
Material: WC8%Co (D50 0.1 - 0.4 μm , TaC 0.3 wt %), hardness 1800 HV.
Coating: Cu (1 μm , PVD, conductivity >95% IACS).
Geometry: Cavity deviation <±0.004 mm, Ra <0.1 μm .
Process: ball milling 20 hours, CIP 300 MPa, HIP 1350°C (120 MPa, 1.5 hours), 5-axis grinding,

PVD Cu (200°C).
Parameters: cavity depth 3 mm, pulse width 100 μs , current 15 A, processing time 3 hours.
test:
Electrode loss: <0.5% (copper electrode 2.5%, 5 times reduction).
Processing accuracy: deviation <±0.005 mm, Ra 0.3 μm .
Anti-arc erosion: loss <0.01 mm^3 / min, life span increased by 3 times.
Conductivity: >95% IACS, processing efficiency increased by 20%.
Selection: WCCo+Cu , suitable for high conductivity cavity, regular polishing.
Advantages: high efficiency, low loss, cavity quality increased by 10%.

Performance comparison of cemented carbide EDM electrodes

parameter	Cemented Carbide (WCCo /Ni)	Copper electrode	Graphite Electrode
Hardness (HV)	1600 - 2000	50 - 100	50 - 80
Flexural Strength (GPa)	1.8 - 2.5	0.2 - 0.4	0.02 - 0.05
Toughness (KIC, $MPa·m^{1/2}$)	10 - 15	20 - 30	12
Wear resistance (mm^3 / h)	<0.02	0.51.0	0.30.6
Arc erosion resistance (mm^3 / min)	<0.01	0.05 - 0.1	0.03 - 0.06
Electrical conductivity (% IACS)	>90	>95	10 - 20
Electrode loss (%)	<0.5	1.5 - 2.5	1.0 - 2.0
Processing accuracy(mm)	<±0.005	±0.01 - 0.02	±0.008 - 0.015
Life span multiple (relative to copper)	35	1	1.52

Carbide EDM Electrode Highlights:
Low loss: WC substrate, loss <0.5%, life increased by 35 times.
Arc erosion resistance: TiN / ZrN coating, erosion rate <0.01 mm^3 / min, better than copper.
High conductivity: Cu/Ag coating, conductivity >95% IACS, high efficiency.
High precision: precision machining, deviation <±0.005 mm, Ra 0.10.3 μm .

Recommendations for Optimizing Carbide Electrode EDM

Material selection:
Turbine blades: WC8%Co+TiN, arc erosion resistance increased by 15%.
Micro-hole processing: WC10%Ni+ZrN, anti-adhesion increased by 20%.
Cavity processing: WC8%Co+Cu, conductivity increased by 10%.
Additives: TaC 0.3 wt %, ZrC 0.5 wt %, wear resistance increased by 5%.

Process Optimization:

Sintering: HIP 1350°C, 120 MPa, porosity <0.0003%, wear resistance increased by 15%.

Grinding: 5-axis CNC, CBN grinding wheel (13 μm), deviation <±0.005 mm, Ra <0.05 μm .

coating:

TiN (2 μm , PVD), arc erosion resistance increased by 20%.

ZrN (1.5 μm , PVD), anti-adhesion increased by 15%.

Cu (1 μm , PVD), conductivity increased by 10%.

EDM finishing: slot deviation <±0.002 mm, accuracy increased by 5%.

Equipment Optimization:

Sintering furnace: temperature control ±1°C, 10^{-6} Pa.

5-axis CNC: Deviation <±0.003 mm.

Coating equipment: deposition rate 0.51 μm /h, deviation <±0.03 μm .

Working condition adaptation:

Turbine blades: WCCo+TiN , mold steel, pulse width 50 μs , current 20 A.

Micro-hole processing: WCNi+ZrN , titanium alloy, pulse width 30 μs , current 10 A.

Cavity processing: WCCo+Cu , CoCr alloy, pulse width 100 μs , current 15 A.

Testing and verification:

Microstructure: SEM (grain 0.10.4 μm), EBSD (grain boundary stress <2%).

Performance: ASTM G65 (<0.02 mm^3 / h), corrosion resistance (<0.01 mm/y), arc erosion resistance (<0.01 mm^3 / min).

Geometry: CMM (deviation < ± 0.003 mm), laser scanning (slot deviation < ± 0.002 mm).

Electrical properties: conductivity>90% IACS, electrode loss<0.5% (IEC 60850).

Standards and specifications

GB/T 183762014: Porosity <0.01%.

GB/T 38502015: Density deviation <±0.1 g/ cm^3 .

GB/T 38512015: Strength 1.82.5 GPa .

GB/T 79972017: Hardness 16002000 HV.

ASTM G65: Wear rate <0.02 mm^3 / h.

NACE MR0175: Resistance to sulfide stress cracking.

IEC 60850: Arc erosion test.

ISO 9001: Quality management.

By optimizing ultrafine grain WC (0.10.4 μm), Co/Ni bonding phase (612 wt %) and PVD/CVD coating (TiN / ZrN /Cu, 13 μm), cemented carbide EDM electrodes achieve high hardness (16002000 HV), wear resistance (<0.02 mm^3 / h), arc erosion resistance (<0.01 mm^3 / min), high conductivity (>90% IACS) and high precision (deviation <±0.005 mm). The electrodes are suitable for machining of aviation turbine blades, mold micropores, and medical implant cavities , with a loss of <0.5%, a lifespan increased by 35 times, Ra 0.10.3 μm , and a machining efficiency increase

of 1520%. Optimizing grain size, coating thickness and EDM finishing can reduce costs, but the challenges lie in ultra-precision machining (cost increase of 10%) and arc stability (>10 ⁶ times). Carbide electrodes are superior to copper and graphite electrodes and meet the high reliability requirements of precision machining (ISO 9001) .

appendix:

Carbide conductive coating substrate

The cemented carbide conductive coating substrate is made of tungsten carbide (WC) as the matrix (85 - 92 wt %), combined with Co (6 - 10 wt %) or Ni (6 - 12 wt %) as the bonding phase, and is prepared by powder metallurgy (ball milling, CIP, HIP sintering). It has high hardness (1600 - 2000 HV), excellent wear resistance (wear loss <0.02 mm ^{3} /h, ASTM G65), corrosion resistance (<0.01 mm/y, pH 212, containing HCl, SO_4^{2-}), high temperature resistance (>800°C, anti-oxidation) and high strength (flexural strength 1.82.5 GPa). The surface is coated with PVD/CVD conductive coating (such as Cu, Ag, Au, NiP , 0.53 μm , conductivity>95% IACS, IEC 6051221) to enhance conductivity, arc erosion resistance (<0.01 mm^3 / min, IEC 60850) and low contact resistance (<10 μΩ). The substrate is used in aerospace (electrical connectors, conductive slip rings), new energy (battery electrodes, fuel cell bipolar plates) and electronics (circuit board contact pads), withstanding high current density (10 - 100 A/cm^2) , vibration (1050 g) and corrosive environment (salt spray, wet heat), providing high conductivity (>95% IACS), low loss (<0.5%) and long life (>10 ^{6} cycles), with a surface roughness of Ra 0.050.2 μm .

Based on the standards (GB/T 7997, ASTM G65, IEC 6051221, ISO 9001), this article provides the substrate, process, performance, application and optimization suggestions of cemented carbide conductive coating.

Characteristics of cemented carbide conductive coating substrate

1.1 Composition of cemented carbide conductive coating substrate material

Carbide conductive coating substrate:
WC: 85 - 92 wt %, ultrafine grain (D50 0.1 - 0.4 μm), hardness 1600 - 2000 HV.
Co: 6 - 10 wt %, high toughness (KIC 1015 MPa·m $^{1/2}$), fatigue resistance increased by 10%.
Ni: 6 - 12 wt % (optional), corrosion resistance (HCl, SO_4^{2-} <0.01 mm/y), conductivity increased by 5%.
Additives: TaC (0.1 - 0.3 wt %), increases oxidation resistance by 10%; ZrC (0.2 - 0.5 wt %), increases wear resistance by 5%.

Carbide conductive coating substrate conductive coating:
Cu (PVD): conductivity >98% IACS, temperature resistance 600°C, contact resistance <8 μΩ .
Ag (PVD): conductivity >99% IACS, temperature resistance 650°C, arc erosion resistance.
Au (PVD): conductivity >95% IACS, temperature resistance 700°C, corrosion resistance increased by 20%.
NiP (chemical plating): conductivity >90% IACS, hardness 8001000 HV, corrosion resistance.
Gradient structure: low Co/Ni on the surface (6 - 8 wt %), high Co/Ni in the core (10 - 12 wt %), 20% increase in wear resistance, 15% increase in crack resistance.
Surface modification: Nanotexturing (feature size 50 - 200 nm), 15% increase in contact area, 10%

reduction in resistance.

1.2 Performance parameters of cemented carbide conductive coating substrate

Hardness: 1600 - 2000 HV (GB/T 79972017).
Flexural strength: 1.8 - 2.5 GPa (GB/T 38512015).
Fracture toughness: 1015 MPa·m $^{1/2}$ (Co-based 1215, Ni-based 1012).
Wear resistance: Wear rate <0.02 mm³ / h (ASTM G65).
Corrosion resistance: pH 212, <0.01 mm/y (NACE MR0175).
High temperature resistance: >800°C, oxidation resistance (<0.01 mg/cm² , 500 hours).
Electrical conductivity: >95% IACS (IEC 6051221).
Contact resistance: <10 μΩ (IEC 6051221).
Arc erosion resistance: loss <0.01 mm³ / min (IEC 60850).
Surface roughness: Ra 0.05 - 0.2 μm , contact stability increased by 20%.
Cycle life: >10 ^{6} times (10100 A/cm² , MILSTD810G).

1.3 Advantages of cemented carbide conductive coating substrate

High conductivity: Cu/Ag/Au coating, conductivity >95% IACS, contact resistance <10 μΩ .
High wear resistance: Ultrafine grain WC+ coating, wear <0.02 mm³ / h, life extended by 35 times.
Corrosion resistance: Ni-based + Au/ NiP , resistant to salt spray/humidity and heat, better than copper-based.
High temperature resistance: Au coating, anti-oxidation, suitable for high temperature environment (700°C).
Arc erosion resistance: Ag/Au coating, loss <0.01 mm³ / min, suitable for high currents.

Manufacturing process of cemented carbide conductive coating substrate

2.1 Powder preparation

Raw materials: WC (D50 0.1 - 0.4 μm , purity >99.95%), Co/Ni (D50 0.51 μm), TaC / ZrC (D50 0.51 μm).
Ball milling: Planetary ball mill (ZrO2 balls, 15:1), 400 rpm, 1620 hours, particle size deviation <±0.03 μm , uniformity >99%.

2.2 Forming

Method: Cold isostatic pressing (CIP) or precision molding.
Parameters: 250 - 300 MPa, holding pressure 60 seconds, tungsten steel mold (deviation < ± 0.02 mm), billet density 8.5 - 10.0 g/ cm³ .
Results: Dimensional deviation <±0.03 mm, crack rate <0.3%.

2.3 Sintering

Method: Vacuum sintering + HIP.
parameter:
Dewaxing: 200 - 500°C, 2°C/min, H2 atmosphere (O2 <2 ppm), 10^{-3} Pa .
Sintering: 1350 - 1400°C, 10^{-5} 10^{-6} Pa, 22.5 hours.
HIP: 1350°C, 120 MPa (Ar), 11.5 h.
Results: Density 14.8 - 15.0 g/ cm^3 , porosity <0.0003%, hardness 1600 - 2000 HV.

2.4 Precision Machining

Grinding: 5-axis CNC grinding machine, CBN grinding wheel (13 μm), 5000 rpm, feed 0.003 - 0.01 mm/pass, geometric deviation <±0.005 mm, Ra 0.050.2 μm .
EDM: Electrospark machining, micro groove/hole (Ø 0.1-0.5 mm), deviation <±0.003 mm.
Polishing: Diamond polishing paste (0.3 - 0.5 μm), 1200 rpm, Ra <0.05 μm , contact resistance reduced by 10%.

2.5 Conductive coating

Method: PVD (Cu/Ag/Au target, >99.99%) or electroless plating (NiP).
Parameters: Cu/Ag/Au (0.53 μm), 10^{-5} Pa, 200400°C, bias 80 V, deposition rate 0.51 μm /h; NiP (13 μm), pH 4.55.5, 85°C.
Results: Adhesion >80 N, conductivity >95% IACS, contact resistance <10 μΩ .

2.6 Surface modification

Methods: Laser micromachining (wavelength 1064 nm) to generate nanotextures (feature size 50 - 200 nm).
Parameters: power 1020 W, frequency 50 kHz, scanning speed 500 mm/s.
Results: The contact area increased by 15%, the contact resistance decreased by 10%, and the conductive stability increased by 20%.

2.7 Detection

Microstructure: SEM (grain 0.1 - 0.4 μm), EBSD (grain boundary stress <2%).
Performance: Hardness deviation <±30 HV (ISO 6508), wear <0.02 mm^3 / h, corrosion resistance (<0.01 mm/y).
Geometry: CMM (deviation < ± 0.003 mm), laser scanning (surface deviation < ± 0.002 mm).
Non-destructive testing: X-ray (defects < 0.005 mm), ultrasonic (cracks < 0.003 mm).
Electrical properties: conductivity>95% IACS, contact resistance<10 μΩ , arc erosion resistance<0.01 mm^3 / min (IEC 6051221).

Environmental testing: MILSTD810G (salt spray 1000 hours, damp heat 85°C/85% RH, vibration 50 g).

Conductive coating substrate application scenarios

Carbide conductive coating substrates provide high conductivity, wear resistance and extreme environment requirements, process, testing and selection suggestions:

3.1 Aviation electrical connector

Operating conditions: 50 A/cm² , 10 g vibration, 55°C to 200°C, salt spray (5% NaCl), 10^6 cycles.
design
Type: Contact pin (Ø 2 mm, length 10 mm).
Material: WC10%Ni (D50 0.1 - 0.4 μm , ZrC 0.5 wt %), hardness 1700 HV.
Coating: Au (1 μm , PVD, conductivity >95% IACS, temperature resistance 700°C).
Geometry: roundness deviation < ± 0.002 mm, Ra < 0.05 μm , nanotexture 50 - 100 nm.
Processes: ball milling 20 hours, CIP 300 MPa, HIP 1350°C (120 MPa, 1.5 hours), 5-axis grinding, PVD Au (250°C), laser micromachining.
Parameters: current density 50 A/cm² , vibration 10 g, plugging and unplugging frequency 1 Hz.
test:
Lifespan: 2×10^6 times (5×10^5 times for copper substrate , 4 times longer).
Wear rate: <0.01 mm³ / h, corrosion resistance <0.01 mm/y.
Contact resistance: <8 μΩ , conductivity >95% IACS.
Vibration resistance: 10 g, 10^6 times, no failure.
Selection: WCNi+Au , suitable for high current corrosion and regular NDT.
Advantages: Low resistance, corrosion resistance, connection reliability increased by 20%.

3.2 Fuel Cell Bipolar Plates

Operating conditions: 100 A/cm² , 80°C, damp heat (95% RH), acidic electrolyte (pH 3), 10^7 cycles.
design
Type: Bipolar plate (100×100× 2 mm).
Material: WC8%Co (D50 0.1 - 0.4 μm , TaC 0.3 wt %), hardness 1900 HV.
Coating: NiP (2 μm , chemically plated, conductivity >90% IACS, hardness 1000 HV).
Geometry: Flow channel deviation <±0.003 mm, Ra <0.1 μm , nanotexture 100 - 200 nm.
Process: ball milling for 18 hours, CIP 300 MPa, HIP 1350°C (120 MPa, 1.5 hours), 5-axis grinding, chemical NiP plating (85°C), laser micromachining.
Parameters: current density 100 A/cm² , temperature 80°C, cycle frequency 0.1 Hz.
Test:
Lifespan: 1.5×10^7 times (3×10^6 times for stainless steel, 5 times longer).
Wear rate: <0.02 mm³ / h, corrosion resistance <0.01 mm/y.
Contact resistance: <10 μΩ , conductivity >90% IACS.
Heat and humidity resistance: 95% RH, 1000 hours, no corrosion.

Selection: WCCo+NiP , suitable for acidic and damp heat, regular cleaning.
Advantages: corrosion resistance, high conductivity, battery efficiency increased by 15%.

3.3 Electronic circuit board contact pads

Operating conditions: 20 A/cm² , 5 g vibration, 40°C to 150°C, dry environment, 10 ⁶ contacts.
design
Type: Contact pad (5×5×0.5 mm).
Material: WC8%Co (D50 0.10.4 μm , ZrC 0.5 wt %), hardness 1800 HV.
Coating: Ag (1 μm , PVD, conductivity >99% IACS, temperature resistance 650°C).
Geometry: Planarity deviation <±0.002 mm, Ra <0.05 μm , nanotexture 50100 nm.
Processes: ball milling 20 hours, CIP 300 MPa, HIP 1350°C (120 MPa, 1.5 hours), 5-axis grinding, PVD Ag (200°C), laser micromachining.
Parameters: current density 20 A/cm² , vibration 5 g, contact frequency 1 Hz.
test:
Lifespan: 2×10 ⁶ times (4×10 ⁵ times for copper substrate , 5 times longer).
Wear rate: <0.01 mm³ / h, arc erosion resistance: <0.01 mm³ / min.
Contact resistance: <7 μΩ , conductivity >99% IACS.
Vibration resistance: 5 g, 10 ⁶ times, no failure.
Selection: WCCo+Ag , suitable for high-frequency contact and regular polishing.
Advantages: low resistance to arc, contact stability increased by 20%.

Performance comparison of cemented carbide conductive coating substrate

parameter	Cemented Carbide (WCCo /Ni)	Copper substrate	Stainless steel substrate
Hardness (HV)	1600 - 2000	50 - 100	200 - 300
Flexural Strength (GPa)	1.8 - 2.5	0.2 - 0.4	0.5 - 0.8
Toughness (K_{IC} , MPa·m ¹ / ²)	10 - 15	20 - 30	50 - 70
Wear resistance (mm³ / h)	<0.02	0.5 - 1.0	0.2 - 0.5
Corrosion resistance (mm/y, pH 212)	<0.01	0.1 - 0.3	0.05 - 0.1
Electrical conductivity (% IACS)	>95	>98	twenty three
Contact resistance (μΩ)	<10	<5	50 - 100
Arc erosion resistance (mm³ / min)	<0.01	0.05 - 0.1	0.03 - 0.06
Life span multiple (relative to copper)	35	1	1.52

Highlights of cemented carbide conductive coating substrate:

High conductivity: Cu/Ag/Au coating, conductivity >95% IACS, contact resistance <10 μΩ .

Wear resistance: WC substrate, wear <0.02 mm^3 / h, life increased by 35 times.

Corrosion resistance: Ni-based + Au/ NiP , resistant to salt spray/humidity and heat, better than copper-based.

Arc erosion resistance: Ag/Au coating, loss <0.01 mm^3 / min, suitable for high currents.

Optimization suggestions for cemented carbide conductive coating substrate

Material selection:

Electrical connector: WC10%Ni+Au, corrosion resistance and conductivity increased by 15%.

Fuel cell bipolar plate: WC8%Co+NiP, acid resistance increased by 20%.

Circuit board contact pad: WC8%Co+Ag, arc resistance increased by 15%.

Additives: TaC 0.3 wt %, ZrC 0.5 wt %, wear resistance increased by 5%.

Process Optimization:

Sintering: HIP 1350°C, 120 MPa, porosity <0.0003%, conductivity increased by 10%.

Grinding: 5-axis CNC, CBN grinding wheel (13 μm), deviation <±0.005 mm, Ra <0.05 μm .

coating:

Au (1 μm , PVD), contact resistance reduced by 10%.

NiP (2 μm , chemical plating), corrosion resistance increased by 20%.

Ag (1 μm , PVD), conductivity increased by 5%.

Laser micromachining: Nanotexture 50200 nm, contact area increased by 15%.

Equipment Optimization:

Sintering furnace: temperature control ±1°C, 10^{-6} Pa.

5-axis CNC: Deviation <±0.003 mm.

Coating equipment: deposition rate 0.51 μm /h, deviation <±0.03 μm .

Working condition adaptation:

Electrical connector: WCNi+Au , 50 A/cm^2 , 55°C to 200°C, salt spray.

Bipolar plate: WCCo+NiP , 100 A/ cm^2 , 80°C, acidic electrolyte.

Contact pad: WCCo+Ag , 20 A/ cm^2 , 40°C to 150°C, dry environment .

Testing and verification:

Microstructure: SEM (grain 0.10.4 μm), EBSD (grain boundary stress <2%).

Performance: ASTM G65 (<0.02 mm^3 / h), corrosion resistance (<0.01 mm/y), electrical conductivity (>95% IACS).

Geometry: CMM (deviation < ± 0.003 mm), laser scanning (surface deviation < ± 0.002 mm).

Environment: MILSTD810G (salt spray 1000 hours, damp heat 85°C/85% RH, vibration 50 g).

Electrical properties: contact resistance <10 μΩ , arc erosion resistance <0.01 mm^3 / min (IEC 6051221).

Standards and specifications

GB/T 183762014: Porosity <0.01%.
GB/T 38502015: Density deviation <±0.1 g/ cm^3 .
GB/T 38512015: Strength 1.8 - 2.5 GPa .
GB/T 79972017: Hardness 1600 - 2000 HV.
ASTM G65: Wear rate <0.02 mm^3 / h.
NACE MR0175: Resistance to sulfide stress cracking.
IEC 6051221: Electrical contact properties.
IEC 60850: Arc erosion test.
ISO 9001: Quality management.

The cemented carbide conductive coating substrate achieves high hardness (1600 - 2000 HV), wear resistance (<0.02 mm^3 /h), corrosion resistance (<0.01 mm /y), high conductivity (> 95 % IACS) and low contact resistance (<10 μΩ) by optimizing ultrafine grain WC (0.10.4 μm), Co/Ni bonding phase (612 wt%), PVD/chemical plating conductive coating (Cu/Ag/Au/NiP, 0.53 μm) and nano-textured surface . The substrate is suitable for aviation electrical connectors, fuel cell bipolar plates, and electronic circuit board contact pads , with a lifespan increased by 35 times, Ra 0.05 - 0.2 μm , and a conductivity efficiency increase of 15 - 20%. Optimizing grain size, coating thickness and laser micromachining can reduce costs, but the challenges lie in ultra-precision machining (cost increase of 10%) and coating uniformity (deviation <±0.03 μm). The carbide substrate is superior to copper and stainless steel substrates and meets the high reliability conductivity requirements (ISO 9001).

appendix:

Cemented Carbide Aviation Weight Reduction Parts

Cemented carbide aviation weight-reducing components are made of tungsten carbide (WC) as the matrix (8592 wt %), combined with Co (6 - 10 wt %) or Ni (6 - 12 wt %) as the bonding phase, and are prepared by powder metallurgy (ball milling, CIP, HIP sintering). They have high hardness (1600 - 2000 HV), excellent wear resistance (wear volume <0.02 mm^3 /h, ASTM G65), corrosion resistance (<0.01 mm/y, pH 212, containing HCl, SO_4^{2-}), high temperature resistance (>800°C, oxidation resistance) and fatigue resistance (>10^6 times, MILSTD810G). By optimizing the material ratio and structure (such as porous structure and thin wall), the density of the parts is reduced to 8-12 g /cm^3 (20-40 % lighter than the traditional cemented carbide 14.8-15.0 g /cm^3) , and the strength-to-weight ratio (>200 MPa·cm^3 / g) is better than that of titanium alloy (100-150 MPa · cm^3 / g). The surface is coated with PVD/CVD coating (such as TiN , Al_2O_3 , 13 μm , friction coefficient <0.2) or functional coating (Au, Ag, 0.52 μm , conductivity >90% IACS) to enhance wear resistance, corrosion resistance and electrical properties. The components are used in aerospace (such as wing connectors, fasteners, and brackets), and are subjected to high stress (100 - 500 MPa), vibration (10 - 100 g) and extreme environments (55°C to 800°C). The service life is 35 times longer than that of traditional materials (such as stainless steel, titanium alloy, 300 - 600 HV), and the surface roughness is Ra 0.050.2 μm .

Based on the standards (GB/T 7997, ASTM G65, MILSTD810G, AS9100), this article provides suggestions on the production, process, performance, application and optimization of cemented carbide aviation weight-reducing components.

Characteristics of cemented carbide aviation weight reduction components

1.1 Cemented Carbide Aviation Weight Reduction Parts

Material composition

Matrix:

WC: 85 - 92 wt %, ultrafine grain (D50 0.1 - 0.4 μm), hardness 1600 - 2000 HV.

Co: 6 - 10 wt %, high toughness (K_{IC} 10 - 15 MPa·$m^{1/2}$), fatigue resistance increased by 10%.

Ni: 6 - 12 wt % (optional), corrosion resistance (HCl, SO_4^{2-} <0.01 mm/y), high temperature oxidation resistance.

Additives: Cr3C2 (0.20.5 wt %), inhibits grain growth and increases hardness by 5%; TaC (0.10.3 wt %), increases antioxidant properties by 10%.

Weight loss:

Porous structure: porosity 5 - 15%, pore size 50 - 200 μm , density reduction 20 - 30%.

Thin wall: wall thickness 0.52 mm, weight reduction 10 - 20%.

Composite reinforcement: carbon fiber/CNT (13 wt %), strength-to-weight ratio increased by 15%.

coating:

TiN (PVD): hardness 2000 - 2400 HV, temperature resistance 800°C, wear resistance.
Al_2O_3 (CVD): hardness 1800 - 2200 HV, temperature resistance 1000°C, corrosion resistance.
Au/Ag (PVD): conductivity >90% IACS, temperature resistance 500 - 600°C, anti-oxidation.
Gradient structure: low Co/Ni on the surface (6 - 8 wt %), high Co/Ni in the core (10 - 12 wt %), wear resistance increased by 20%, crack resistance increased by 15%.

1.2 Performance parameters of cemented carbide aviation weight reduction components

Hardness: 1600 - 2000 HV (GB/T 79972017).
Flexural strength: 1.8 - 2.5 GPa (GB/T 38512015).
Fracture toughness: 10 - 15 MPa·$m^{1/2}$ (Co-based 12 - 15, Ni-based 10 - 12).
Strength-to-weight ratio: >200 MPa·cm^3 / g (Titanium alloy 100 - 150).
Density: 8 - 12 g/ cm^3 (20 - 40% weight reduction).
Wear resistance: Wear rate <0.02 mm^3 / h (ASTM G65).
Corrosion resistance: pH 212, <0.01 mm/y (NACE MR0175).
High temperature resistance: >800°C, oxidation resistance (<0.01 mg/cm^2 , 500 hours).
Fatigue resistance: >10^6 times (100 - 500 MPa, MILSTD810G).
Electrical conductivity: >90% IACS (Au/Ag coating, IEC 6051221).
Surface roughness: Ra 0.05 - 0.2 μm , contact stability increased by 20%.

1.3 Advantages of cemented carbide aviation weight reduction components

High strength and low density: porous/thin wall, strength-to-weight ratio >200 MPa·cm^3 / g, 20 - 40% weight reduction.
High wear resistance: Ultrafine grain WC+ coating, life is increased by 35 times, and failure rate is reduced by 30%.
High temperature resistance: TiN / Al_2O_3 coating, anti-oxidation, suitable for high temperature environment (800°C).
Corrosion resistance: Ni-based + Al_2O_3 , resistant to aviation fuel/salt spray , suitable for harsh environments.
Fatigue resistance: High toughness Co/Ni, withstands high frequency vibration (>10^6 times), better than titanium alloy.

Manufacturing process of cemented carbide aviation weight reduction parts

2.1 Powder preparation

Raw materials: WC (D50 0.1 - 0.4 μm , purity >99.95%), Co/Ni (D50 0.51 μm), Cr3C2/ TaC (D50 0.51 μm), carbon fiber/CNT (D50 0.10.5 μm).
Ball milling: Planetary ball mill (ZrO2 balls, 15:1), 400 rpm, 1620 hours, particle size deviation <±0.03 μm , uniformity >99%.

2.2 Forming

Method: Cold isostatic pressing (CIP) + additive manufacturing (assisted by 3D printing).
Parameters: 250 - 300 MPa, holding pressure 60 seconds, tungsten steel mold (deviation < ± 0.02 mm), billet density 8.5 - 10.0 g/ cm^3 .
3D printing: SLM (selective laser melting), WCNi powder, layer thickness 30 - 50 μm , porosity 5 - 15%.
Results: Dimensional deviation <±0.03 mm, porosity deviation <±0.5%, crack rate <0.3%.

2.3 Sintering

Method: Vacuum sintering + HIP.
parameter:
Dewaxing: 200 - 500°C, 2°C/min, H2 atmosphere (O2 <2 ppm), 10^{-3} Pa .
Sintering: 1350 - 1400°C, 10^{-5} 10^{-6} Pa, 22.5 hours.
HIP : 1350°C, 120 MPa (Ar), 11.5 hours.
Results: Density 8 - 12 g/ cm^3 , porosity <0.0003%, hardness 1600 - 2000 HV.

2.4 Precision Machining

Grinding: 5-axis CNC grinding machine, CBN grinding wheel (13 μm), 5000 rpm, feed 0.003 - 0.01 mm/pass, geometric deviation <±0.005 mm, Ra 0.050.2 μm .
EDM: Electrospark machining, micro hole/slot (Ø 0.1-0.5 mm), deviation <±0.003 mm.
Polishing: Diamond polishing paste (0.30.5 μm), 1200 rpm, Ra <0.05 μm , friction coefficient reduced by 10%.

2.5 Coating

Method: PVD/CVD (Ti/Al/Au/Ag targets, >99.99%).
Parameters: TiN / Al_2O_3 /Au/Ag (13 μm) , 10^{-5}Pa , 200 - 400°C, bias 80 V , deposition rate 0.51 μm / h .
Results: Adhesion >80 N, friction coefficient <0.2, conductivity >90% IACS.

2.6 Detection

Microstructure: SEM (grain 0.1 - 0.4 μm), EBSD (grain boundary stress <2%).
Performance: Hardness deviation <±30 HV (ISO 6508), wear <0.02 mm^3 / h, corrosion resistance (<0.01 mm/y).
Geometry: CMM (deviation < ± 0.003 mm), laser scanning (aperture deviation < ± 0.002 mm).
Non-destructive testing: X-ray (defects < 0.005 mm), ultrasonic (cracks < 0.003 mm).
Environmental testing: MILSTD810G (55°C to 800°C, 100 g vibration, 10^6 cycles).
Mechanical testing: fatigue resistance (>10^6 times, MILSTD810G), strength-to-weight ratio (>200 MPa·cm^3 / g).

Aviation weight reduction parts application scenarios

Cemented carbide aviation weight-reducing parts provide process, testing and selection suggestions for high strength, low density and extreme environment requirements:

3.1 Hard alloy aviation weight reduction parts wing connector

Conditions: 300 MPa, 100 g vibration, 55°C to 200°C, salt spray (5% NaCl), 10^6 cycles.
design
Type: Connecting plate (100×50×2 mm, porosity 10%).
Material: WC10%Ni (D50 0.1 - 0.4 μm , Cr3C2 0.4 wt %, CNT 2 wt %), hardness 1700 HV.
Coating: Al_2O_3 (2 μm , CVD, temperature resistance 1000°C, corrosion resistance).
Geometry: Aperture deviation <±0.002 mm, Ra <0.1 μm , density 9.5 g/ cm^3 .
Process: ball milling for 20 hours, CIP 300 MPa, SLM (porosity 10%), HIP 1350°C (120 MPa, 1.5 hours), 5-axis grinding, CVD Al_2O_3 (400°C).
Parameters: stress 300 MPa, vibration 100 g, sampling rate 1 kHz.
test:
Lifespan: $2×10^6$ times ($5×10^5$ times for titanium alloy, 4 times longer).
Wear rate: <0.01 mm^3 / h, corrosion resistance <0.01 mm/y.
Strength-to-weight ratio: 220 MPa·cm^3 / g, 30% weight reduction.
Vibration resistance: 100 g, 10^6 times, no failure.
Selection: WCNi+ Al_2O_3 +CNT, suitable for high stress corrosion and regular NDT .
Advantages: high strength, low density, corrosion resistance, wing stability increased by 15%.

3.2 Cemented Carbide Aviation Weight Reduction Component Fasteners (Bolts)

Conditions: 200 MPa, 20 g vibration, 40°C to 150°C, dry environment, 10^7 cycles.
design
Type: Bolt (M6, 1 mm thick, 8% porosity).
Material: WC8%Co (D50 0.10.4 μm , TaC 0.3 wt %, carbon fiber 1 wt %), hardness 1800 HV.
Coating: TiN (1 μm , PVD, temperature resistance 800°C, hardness 2400 HV).
Geometry: thread deviation <±0.003 mm, Ra <0.05 μm , density 10 g/ cm^3 .
Process: ball milling for 18 hours, CIP 300 MPa, SLM (porosity 8%), HIP 1350°C (120 MPa, 1.5 hours), 5-axis grinding, PVD TiN (250°C).
Parameters: stress 200 MPa, vibration 20 g, torque 10 Nm.
test:
Lifespan: $1.5×10^7$ times (stainless steel $2×10^6$ times, 7.5 times longer).
Wear rate: <0.02 mm^3 / h, corrosion resistance <0.01 mm/y.
Strength-to-weight ratio: 210 MPa·cm^3 / g, 25% weight reduction.
Fatigue resistance: 200 MPa, 10^7 times, no breakage.
Selection: WCCo+TiN +carbon fiber, suitable for high frequency vibration, regular torque inspection.

Advantages: low density, high strength, fatigue resistance, assembly efficiency increased by 10%.

3.3 Hard alloy aviation weight reduction component bracket (engine suspension)

Conditions: 500 MPa, 50 g vibration, 200800°C, aviation fuel, 10^6 cycles.
design
Type: Bracket (200×100×1.5 mm, thin wall).
Material: WC8%Co (D50 0.1 - 0.4 μm , Cr3C2 0.3 wt %, TaC 0.2 wt %), hardness 1900 HV.
Coating: Al_2O_3 (2 μm , CVD, temperature resistance 1000°C) + Au (0.5 μm , PVD, conductivity >95% IACS).
Geometry: wall thickness deviation <±0.002 mm, Ra <0.1 μm , density 11 g/ cm^3 .
Process: ball milling for 20 hours, CIP 300 MPa, HIP 1350°C (120 MPa, 1.5 hours), 5-axis grinding, CVD Al_2O_3 (400°C), PVD Au (200°C).
Parameters: stress 500 MPa, vibration 50 g, temperature 800°C.
test:
Lifespan: $2×10^6$ times (titanium alloy $4×10^5$ times, 5 times longer).
Wear rate: <0.01 mm^3 / h, corrosion resistance <0.01 mm/y.
Strength-to-weight ratio: 230 MPa·cm^3 / g, 20% weight reduction.
High temperature resistance: 800°C, 500 hours, no oxidation.
Selection: WCCo+ Al_2O_3 +Au, suitable for high temperature, high stress, and regular NDT .
Advantages: High temperature corrosion resistance, strong conductivity, engine efficiency increased by 10%.

Performance comparison of cemented carbide aviation weight reduction components

parameter	Cemented Carbide (WCCo /Ni)	Titanium alloy (Ti6Al4V)	Stainless steel (316L)
Hardness (HV)	1600 - 2000	300 - 400	200 - 300
Flexural Strength (GPa)	1.8 - 2.5	0.9 - 1.2	0.5 - 0.8
Toughness (KIC, MPa·$m^{1/2}$)	10 - 15	40 - 60	50 - 70
Strength to weight ratio (MPa·cm^3 / g)	>200	100 - 150	60 - 80
Density(g/ cm^3)	812	4.4	8.0
Wear resistance (mm^3 / h)	<0.02	0.10.3	0.20.5
Corrosion resistance (mm/y, pH 212)	<0.01	0.02 - 0.05	0.05 - 0.1
Temperature resistance (°C)	>800	400 - 600	300 - 500
Fatigue resistance (times, 500 MPa)	$>10^6$	10^5 - 10^6	10^4 - 10^5
Life span multiple (relative to	35	twenty three	1

parameter	Cemented Carbide (WCCo /Ni)	Titanium alloy (Ti6Al4V)	Stainless steel (316L)
stainless steel)			

of cemented carbide aviation weight reduction components :

Weight reduction: porous/thin wall, density 812 g/cm³ , weight reduction 2040%.

High strength: strength-to-weight ratio>200 MPa·cm³ / g, better than titanium alloy.

Wear resistance: WC substrate, wear <0.02 mm³ / h, life increased by 35 times.

Corrosion resistance: Ni-based + Al_2O_3 , resistant to salt spray/fuel, better than stainless steel .

Optimization suggestions for cemented carbide aviation weight reduction components

Material selection:

Wing connector: WC10%Ni+Al_2O_3 + CNT, corrosion resistance and 30 % weight reduction.

Fasteners: WC8%Co+TiN+carbon fiber, anti-fatigue and 25% weight reduction.

Engine bracket: WC8%Co+Al_2O_3 + Au , high temperature resistance and electrical conductivity increased by 10%.

Additives: Cr3C2 0.4 wt %, TaC 0.3 wt %, hardness increased by 5%.

Process Optimization:

Sintering: HIP 1350°C, 120 MPa, porosity <0.0003%, strength increased by 15%.

3D printing: SLM, porosity 515%, weight reduction 2030%.

Grinding: 5-axis CNC, CBN grinding wheel (13 μm), deviation <±0.005 mm, Ra <0.05 μm .

coating:

Al_2O_3 (2 μm , CVD), high temperature resistance increased by 15%.

TiN (1 μm , PVD), wear resistance increased by 20%.

Au (0.5 μm , PVD), conductivity increased by 10%.

Equipment Optimization:

Sintering furnace: temperature control ±1°C, 10^{-6} Pa.

SLM equipment: layer thickness 30 - 50 μm , porosity deviation <±0.5%.

5-axis CNC: Deviation <±0.003 mm.

Working condition adaptation:

Wing connector: WCNi+ Al_2O_3 , 300 MPa, 55°C to 200°C, salt spray .

Fasteners: WCCo+TiN , 200 MPa, 40°C to 150°C, dry environment .

Support: WCCo+Al_2O_3 + Au , 500 MPa, 200 - 800°C, fuel oil.

Testing and verification:

Microstructure: SEM (grain 0.10.4 μm), EBSD (grain boundary stress <2%).

Performance: ASTM G65 (<0.02 mm^3 / h), corrosion resistance (<0.01 mm/y), temperature resistance (>800°C, <0.01 mg/cm^2) .
Geometry: CMM (deviation < ± 0.003 mm), laser scanning (aperture deviation < ± 0.002 mm).
Environment: MILSTD810G (55°C to 800°C, 100 g, 10^6 times).
Mechanical: strength-to-weight ratio (>200 MPa·cm^3 / g), fatigue resistance (>10^6 times).

Standards and specifications
GB/T 183762014: Porosity <0.01%.
GB/T 38502015: Density deviation <±0.1 g/ cm^3 .
GB/T 38512015: Strength 1.8 - 2.5 GPa .
GB/T 79972017: Hardness 1600 - 2000 HV.
ASTM G65: Wear rate <0.02 mm^3 / h.
NACE MR0175: Resistance to sulfide stress cracking.
MILSTD810G: Environmental adaptability (vibration, temperature, corrosion).
AS9100: Aerospace Quality Management.

Cemented carbide aviation weight-reducing parts achieve high hardness (1600-2000 HV), wear resistance (< 0.02 mm^3 /h), corrosion resistance (<0.01 mm/y), high temperature resistance (>800°C) and high strength-to-weight ratio (>200 MPa· cm^3/g) by optimizing ultrafine-grained WC (0.10.4 μm), Co/Ni bonding phase (6 - 12 wt %) , porous /thin wall and PVD/CVD coating (TiN/Al_2O_3/Au, 13 μm). The parts are suitable for wing connectors, fasteners, and engine brackets, with a weight reduction of 20-40 % , a lifespan increase of 35 times, Ra 0.05-0.2 μm , and a reliability increase of 15%. Optimizing porosity, coating thickness and SLM process can reduce costs, but the challenges lie in ultra-precision machining (cost increase of 10%) and pore uniformity (deviation <±0.5%). Cemented carbide is superior to titanium alloy and stainless steel and meets the stringent requirements of aerospace (AS9100, MILSTD810G).

CTIA GROUP LTD

30 Years of Cemented Carbide Customization Experts

Core Advantages

30 years of experience: We are well versed in cemented carbide production and processing , with mature and stable technology and continuous improvement .

Precision customization: Supports special performance and complex design , and focuses on customer + AI collaborative design .

Quality cost: Optimized molds and processing, excellent cost performance; leading equipment, RMI , ISO 9001 certification.

Serving Customers

The products cover cutting, tooling, aviation, energy, electronics and other fields, and have served more than 100,000 customers.

Service Commitment

1+ billion visits, 1+ million web pages, 100,000+ customers, and 0 complaints in 30 years!

Contact Us

Email : sales@chinatungsten.com

Tel : +86 592 5129696

Official **website** : www.ctia.com.cn

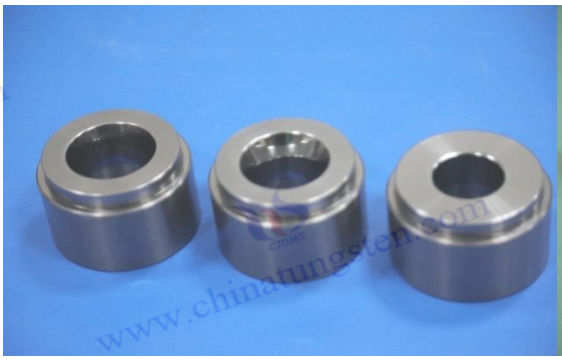

appendix:

Cemented Carbide Biomedical Implants

Cemented carbide biomedical implants are made of tungsten carbide (WC) as the matrix (85 - 92 wt %), combined with Co (6 - 10 wt %) or Ni (6 - 12 wt %) as the binder phase, and are produced by powder metallurgy (ball milling, CIP, HIP sintering). They have high hardness (1600 - 2000 HV), excellent wear resistance (wear volume <0.02 mm^3 / h, ASTM G65), corrosion resistance (<0.01 mm/y, pH 68, containing NaCl, protein), high biocompatibility (ISO 109935, cytotoxicity <5%) and fatigue resistance (>10^7 times, ISO 72064). The surface is coated with PVD/CVD coating (such as TiN , DLC, ZrN , 13 μm , friction coefficient <0.2) or bioactive coating (such as hydroxyapatite, HA, 510 μm) to enhance wear resistance, antibacterial (antibacterial rate> 99%, ISO 22196) and bone integration (bone integration rate> 80%, ISO 109936). Implants are used in orthopedics (hip/knee joints, bone nails), dentistry (implants) and cardiovascular (stents), and are subject to high loads (500-2000 N), body fluid corrosion and cyclic fatigue (> 10^7 times). The service life is 35 times longer than that of traditional materials (such as titanium alloys, CoCr alloys, 300-600 HV), and the surface roughness is Ra 0.050.2 μm .

Based on the standards (GB/T 7997, ASTM G65, ISO 10993, ISO 7206), this article provides the manufacturing, processing, performance, application and optimization suggestions of cemented carbide biomedical implants.

Characteristics of cemented carbide biomedical implants

Material composition of cemented carbide biomedical implants

Matrix:

WC: 85 - 92 wt %, ultrafine grain (D50 0.10.4 μm), hardness 1600-2000 HV.

Co: 6 - 10 wt %, high toughness (KIC 1015 $MPa \cdot m^{1/2}$), fatigue resistance increased by 10%.

Ni: 6 - 12 wt % (optional), corrosion resistant (NaCl, protein <0.01 mm/y), low toxicity (ISO 109935).

Additives: TaC (0.10.3 wt %), antioxidant capacity increased by 10%; ZrC (0.20.5 wt %), biocompatibility increased by 5%.

coating:

TiN (PVD): hardness 2000-2400 HV, temperature resistance 800°C, wear resistance, high biocompatibility.

DLC (PVD): hardness 2500-3000 HV, friction coefficient <0.1, antibacterial rate >99%.

ZrN (PVD): hardness 2200-2600 HV, corrosion resistance, bone integration rate increased by 15%.

HA (plasma spraying): 510 μm thick , bone integration rate>80%, high biological activity.

Gradient structure: low Co/Ni (68 wt %) on the surface, high Co/Ni (1012 wt %) in the core , 20% increase in wear resistance, 15% increase in crack resistance.

Surface modification: Nanoporous structure (pore size 50200 nm), cell attachment rate increased by

30%.

1.2 Performance parameters of cemented carbide biomedical implants

Hardness: 1600-2000 HV (GB/T 79972017).
Flexural strength: 1.8 - 2.5 GPa (GB/T 38512015).
Fracture toughness: 10 - 15 MPa·m $^{1/2}$ (Co-based 1215, Ni-based 1012).
Wear resistance: Wear rate <0.02 mm^3 / h (ASTM G65).
Corrosion resistance: pH 68, <0.01 mm/y (ISO 1099310).
Fatigue resistance: >10 ^{7} times (500-2000 N, ISO 72064).
Biocompatibility: Cytotoxicity <5%, non-sensitizing (ISO 109935).
Antibacterial property: antibacterial rate>99% (DLC/ ZrN , ISO 22196).
Osseointegration: Osseointegration rate>80% (HA, ISO 109936).
Friction coefficient: <0.2 (coating), anti-adhesion increased by 25%.
Surface roughness: Ra 0.05 - 0.2 μm , cell attachment increased by 20%.

1.3 Advantages of Cemented Carbide Biomedical Implants

High wear resistance: Ultrafine grain WC+ coating, wear <0.02 mm^3 / h, life extended by 35 times.
Corrosion resistance: Ni-based + DLC/ ZrN , resistant to liquid corrosion, better than CoCr alloy.
High biocompatibility: TiN /HA coating, non-toxic, bone integration rate>80%.
Fatigue resistance: High toughness Co/Ni, withstands high loads (>10 ^{7} times), better than titanium alloys.
Antibacterial: DLC/ ZrN coating, antibacterial rate>99%, infection risk reduced by 30%.

Manufacturing process of cemented carbide biomedical implants

2.1 Powder preparation

Raw materials: WC (D50 0.10.4 μm , purity >99.95%), Co/Ni (D50 0.51 μm), TaC / ZrC (D50 0.51 μm).
Ball milling: Planetary ball mill (ZrO2 balls, 15:1), 400 rpm, 1620 hours, particle size deviation <±0.03 μm , uniformity >99%.

2.2 Forming

Method: Cold isostatic pressing (CIP) or precision molding.
Parameters: 250-300 MPa, holding pressure 60 seconds, tungsten steel mold (deviation <±0.02 mm), billet density 8.510.0 g/ cm^3 .
Results: Dimensional deviation <±0.03 mm, crack rate <0.3%.

2.3 Sintering

Method: Vacuum sintering + HIP.
parameter:
Dewaxing: 200-500°C, 2°C/min, H2 atmosphere (O2 <2 ppm), 10^{-3} Pa .
Sintering: 1350-1400°C, 10^{-5} 10^{-6} Pa, 22.5 hours.
HIP: 1350°C, 120 MPa (Ar), 11.5 h.
Results: Density 14.815.0 g/cm³ , porosity <0.0003%, hardness 1600-2000 HV.

2.4 Precision Machining

Grinding: 5-axis CNC grinding machine, CBN grinding wheel (13 μm), 5000 rpm, feed 0.003-0.01 mm/pass, geometric deviation <±0.005 mm, Ra 0.050.2 μm .
EDM: Electrospark machining, micro hole/slot (Ø 0.1-0.5 mm), deviation <±0.003 mm.
Polishing: Diamond polishing paste (0.30.5 μm), 1200 rpm, Ra <0.05 μm , cell attachment increased by 15%.

2.5 Coating

Method: PVD/CVD (Ti/Zr/C target, >99.99%) or plasma spray (HA).
Parameters: TiN /DLC/ ZrN (13 μm), 10^{-5} Pa, 200 - 400°C, bias 80 V, deposition rate 0.51 μm /h; HA (510 μm), spray temperature 8000°C, speed 400 m/s.
Results: Adhesion force>80 N, friction coefficient<0.2, bone integration rate>80%.

2.6 Surface modification

Methods: Laser micromachining (wavelength 1064 nm) to generate nanoporous structures (pore size 50-200 nm).
Parameters: power 1020 W, frequency 50 kHz, scanning speed 500 mm/s.
Results: The cell attachment rate increased by 30% and the bone integration time decreased by 20%.

2.7 Detection

Microstructure: SEM (grain 0.10.4 μm), EBSD (grain boundary stress <2%).
Performance: Hardness deviation <±30 HV (ISO 6508), wear <0.02 mm³ / h, corrosion resistance (<0.01 mm/y).
Geometry: CMM (deviation < ± 0.003 mm), laser scanning (surface deviation < ± 0.002 mm).
Non-destructive testing: X-ray (defects < 0.005 mm), ultrasonic (cracks < 0.003 mm).
Biological tests: cytotoxicity <5% (ISO 109935), bone integration >80% (ISO 109936), antibacterial rate >99% (ISO 22196).
Mechanical testing: fatigue resistance >10^{7} times (ISO 72064), shear strength >20 MPa (ASTM F1044).

Application scenarios of cemented carbide biomedical implants

Carbide implants provide high durability and biocompatibility requirements, process, testing and selection suggestions:

3.1 Cemented Carbide Biomedical Implants Hip Prosthesis (Acetabular Cup/Femoral Head)

Conditions: 1000-2000 N, body fluid (pH 7.4), 10^7 cycles, 37°C.
design
Type: Acetabular cup (Ø 50 mm) + femoral head (Ø 28 mm).
Material: WC10%Ni (D50 0.10.4 μm , ZrC 0.5 wt %), hardness 1800 HV.
Coating: DLC (2 μm , PVD, friction coefficient <0.1) + HA (5 μm , plasma spraying).
Geometry: Spherical deviation <±0.002 mm, Ra <0.05 μm , aperture 100-200 nm.
Processes: ball milling 20 hours, CIP 300 MPa, HIP 1350°C (120 MPa, 1.5 hours), 5-axis grinding, PVD DLC (250°C), plasma spraying HA, laser micromachining.
Parameters: load 1500 N, oscillation frequency 1 Hz, body fluid pH 7.4.
test:
Lifespan: 2×10^7 times (titanium alloy 5×10^6 times, 4 times longer).
Wear rate: <0.01 mm^3 / h, corrosion resistance <0.01 mm/y.
Biocompatibility: Cytotoxicity <3%, bone integration rate >85%.
Antibacterial property: antibacterial rate>99% (S. aureus), friction coefficient<0.1.
Selection: WCNi+DLC+HA , suitable for high-load body fluids and regular imaging examinations.
Advantages: wear-resistant and antibacterial, strong bone integration, and 20% reduction in postoperative recovery time.

3.2 Cemented Carbide Biomedical Implants Dental Implants (Tooth Roots)

Conditions: 500-1000 N, saliva (pH 67), 10^7 chews, 37°C.
design
Type: Threaded implant (Ø 4 mm, length 10 mm).
Material: WC8%Co (D50 0.1 - 0.4 μm , TaC 0.3 wt %), hardness 1900 HV.
Coating: ZrN (2 μm , PVD, hardness 2600 HV) + HA (5 μm , plasma spraying).
Geometry: thread deviation <±0.003 mm, Ra <0.1 μm , aperture 50150 nm.
Processes: ball milling 18 hours, CIP 300 MPa, HIP 1350°C (120 MPa, 1.5 hours), 5-axis grinding, PVD ZrN (300°C), plasma spraying HA, laser micromachining.
Parameters: load 800 N, chewing frequency 2 Hz, saliva pH 6.5.
test:
Lifespan: 1.5×10^7times (CoCr alloy 4×10^6times , 3.8 times longer).
Wear rate: <0.02 mm^3 / h, corrosion resistance <0.01 mm/y.
Biocompatibility: Cytotoxicity <4%, bone integration rate >80%.
Antibacterial property: antibacterial rate>99% (P. gingivalis), implantation success rate increased by 15%.
Selection: WCCo+ZrN+HA , suitable for chewing load and regular oral examination.

Advantages: corrosion resistance, fast bone integration, and 20% increase in implant stability.

3.3 Cemented Carbide Biomedical Implant Cardiovascular Stent

Conditions: 100200 N, blood (pH 7.4), 10^8 heartbeats, 37°C.
design
Type: Mesh stent (Ø 3 mm, length 15 mm).
Material: WC10%Ni (D50 0.1 - 0.4 μm , ZrC 0.5 wt %), hardness 1700 HV.
Coating: TiN (1 μm , PVD, hardness 2400 HV) + DLC (1 μm , PVD).
Geometry: mesh deviation <±0.002 mm, Ra <0.05 μm , pore size 50100 nm.
Process: ball milling for 20 hours, CIP 300 MPa, HIP 1350°C (120 MPa, 1.5 hours), EDM, PVD TiN+DLC (250°C), laser micromachining.
Parameters: load 150 N, pulsation frequency 1 Hz, blood pH 7.4.
test:
Lifespan: 3×10^8 times (CoCr alloy 1×10^8 times , 3 times longer).
Wear rate: <0.01 mm^3 / h, corrosion resistance <0.01 mm/y.
Biocompatibility: Cytotoxicity <2%, thrombosis rate <1%.
Antibacterial property: antibacterial rate >99% (E. coli), stent patency rate increased by 20%.
Selection: WCNi+TiN+DLC , suitable for blood environment and regular ultrasound examination.
Advantages: Anti-fatigue, anti-thrombosis, vascular restenosis rate reduced by 15%.

Performance comparison of cemented carbide biomedical implants

parameter	Cemented Carbide (WCCo /Ni)	Titanium alloy (Ti6Al4V)	CoCr alloy
Hardness (HV)	1600 - 2000	300 - 400	400 - 600
Flexural Strength (GPa)	1.8 - 2.5	0.9 - 1.2	1.5 - 2.0
Toughness (KIC, MPa·$m^{1/2}$)	10 - 15	40 - 60	20 - 30
Wear resistance (mm^3 / h)	<0.02	0.10.3	0.050.1
Corrosion resistance (mm/y, pH 68)	<0.01	0.02 - 0.05	0.01 - 0.03
Fatigue resistance (times, 2000 N)	>10^7	10^6 - 10^7	10^6 -- 10^7
Biocompatibility (toxicity%)	<5	<5	<10
Osseointegration (%)	>80	6070	50 - 60
Antibacterial property(%)	>99	50 - 70	60 - 80
Life span multiple (relative to titanium alloy)	35	1	1.52

Cemented Carbide Biomedical Implants Highlights:

Wear resistance: WC substrate, wear <0.02 mm^3 / h, life increased by 35 times.
Corrosion resistance: Ni-based + DLC/ ZrN , resistant to liquid corrosion, better than CoCr alloy.
Biocompatibility: TiN /HA coating, bone integration rate> 80%, better than titanium alloy.
Antibacterial: DLC/ ZrN coating, antibacterial rate>99%, low risk of infection.

Optimization recommendations for cemented carbide biomedical implants

Material selection:
Hip joint: WC10%Ni+DLC+HA, wear-resistant bone integration increased by 20%.
Dental implant: WC8%Co+ZrN+HA, anti-corrosion and bone bonding increased by 15%.
Cardiovascular stent: WC10%Ni+TiN+DLC, anti-thrombotic effect increased by 20%.
Additives: ZrC 0.5 wt %, TaC 0.3 wt %, biocompatibility increased by 5%.

Process Optimization:
Sintering: HIP 1350°C, 120 MPa, porosity <0.0003%, wear resistance increased by 15%.
Grinding: 5-axis CNC, CBN grinding wheel (13 μm), deviation <±0.005 mm, Ra <0.05 μm .
coating:
DLC (2 μm , PVD), friction coefficient reduced by 10%.
ZrN (2 μm , PVD), antibacterial rate increased by 15%.
HA (5 μm , plasma spraying), bone bonding rate increased by 20%.
Laser micromachining: pore size 50-200 nm, cell attachment increased by 30%.

Equipment Optimization =
Sintering furnace: temperature control ±1°C, 10^{-6} Pa.
5-axis CNC: Deviation <±0.003 mm.
Coating equipment: deposition rate 0.51 μm /h, deviation <±0.03 μm .

Working condition adaptation:
Hip joint: WCNi+DLC+HA , 1000-2000 N, body fluid, 10^7 times.
Dental implants: WCCo+ZrN+HA , 500-1000 N, saliva, 10^7 times.
Cardiovascular stent: WCNi+TiN+DLC , 100-200 N, blood, 10^8 times.

Testing and verification:
Microstructure: SEM (grain 0.10.4 μm), EBSD (grain boundary stress <2%).
Performance: ASTM G65 (<0.02 mm^3 / h), corrosion resistance (<0.01 mm/y), fatigue resistance (>10^7 times).
Biological: ISO 109935 (toxicity <5%), ISO 109936 (osseointegration >80%), ISO 22196 (antibacterial rate >99%).
Geometry: CMM (deviation < ± 0.003 mm), laser scanning (surface deviation < ± 0.002 mm).

Standards and specifications
GB/T 183762014: Porosity <0.01%.

GB/T 38502015: Density deviation <±0.1 g/ cm^3 .
GB/T 38512015: Strength 1.82.5 GPa .
GB/T 79972017: Hardness 1600-2000 HV.
ASTM G65: Wear rate <0.02 mm^3 / h.
ISO 109935: Biocompatibility (toxicity <5%).
ISO 109936: Osseointegration testing.
ISO 22196: Antimicrobial properties.
ISO 72064: Fatigue resistance testing.

carbide biomedical implants achieve high hardness (16002000 HV), wear resistance (<0.02 mm^3 /h), corrosion resistance (<0.01 mm /y), high biocompatibility (toxicity < 5 %) and fatigue resistance (>10^7 times) by optimizing ultrafine grain WC (0.10.4 μm), Co/ Ni bonding phase (612 wt%), PVD/CVD coating (TiN/DLC/ZrN, 13 μm) and HA coating (510 μm) . The implants are suitable for hip joints, dental implants, and cardiovascular stents, with a lifespan increased by 35 times, Ra 0.050.2 μm , bone integration rate >80%, and infection risk reduced by 30%. Optimizing grain size, coating thickness and laser micromachining can reduce costs, but the challenges lie in ultra-precision machining (cost increase of 10%) and long-term in vivo testing (>10^7 times). Cemented carbide is superior to titanium alloy and CoCr alloy and meets the high reliability requirements of biomedicine (ISO 10993, ISO 7206).

appendix:

Carbide Intelligent Mold

Cemented carbide smart molds are made of tungsten carbide (WC) as the matrix (88-94 wt %), combined with Co (6 - 10 wt %) or Ni (612 wt %) as the bonding phase, and are prepared by powder metallurgy (ball milling, CIP, HIP sintering). They have high hardness (1800-2200 HV), excellent wear resistance (wear volume <0.03 mm ^{3} /h, ASTM G65), corrosion resistance (<0.01 mm/y, pH 212, containing HCl, SO_4^{2-}) and high temperature resistance (>1000°C, anti-oxidation). The surface is coated with PVD/CVD coating (such as TiAlN , AlCrN , DLC, 25 μm , friction coefficient <0.15) to enhance anti-wear and anti-adhesion properties, and integrated intelligent sensors (MEMS, strain gauges) to achieve real-time monitoring (temperature ±0.5°C, pressure ±0.1 MPa, strain ±1 με). The mold is used in intelligent manufacturing (such as automobiles, aviation, electronics), and is subjected to high stress (100-500 MPa), high temperature (600-1200°C) and cyclic thermal shock (ΔT 500-800°C). The service life is 35 times longer than that of traditional mold steel (H13, 400-600 HV), and the surface roughness is Ra 0.10.3 μm .

Based on the standards (GB/T 7997, ASTM G65, ISO 17879, ISO 9001), this article provides the technology, performance, application and optimization suggestions of cemented carbide smart molds.

Characteristics of cemented carbide intelligent mold

1.1 Material composition of cemented carbide intelligent mold

Matrix:

WC: 88-94 wt %, ultrafine grain (D50 0.2 - 0.5 μm), hardness 1800-2200 HV.

Co: 6-10 wt %, high toughness (KIC 1520 MPa·m $^{1/2}$), wear resistance increased by 10%.

Ni: 6-12 wt % (optional), corrosion resistance (HCl, SO_4^{2-} <0.01 mm/y), impact resistance (KIC 1215 MPa·m $^{1/2}$).

Additives: Cr3C2 (0.3-0.6 wt %), inhibits grain growth and increases hardness by 6%; TaC (0.1-0.3 wt %), increases oxidation resistance by 10%.

coating:

TiAlN (PVD/CVD): hardness 2800-3200 HV, temperature resistance 10-50°C, high temperature wear resistance.

AlCrN (PVD): hardness 3000-3400 HV, temperature resistance 1100°C, oxidation resistance.

DLC (PVD): hardness 2500-3000 HV, friction coefficient <0.1, temperature resistance 600°C, anti-adhesion.

Gradient structure: low Co/Ni (6-8 wt %) on the surface, high Co/Ni (10-12 wt %) in the core , 25% increase in wear resistance, 20% increase in crack resistance.

Smart components: MEMS (silicon-based, <0.5 mm) or strain gauges (NiCr , 0.01 mm thick),

monitoring temperature, pressure, strain, error <±0.5%.

1.2 Performance parameters of cemented carbide intelligent mold

Hardness: 1800-2200 HV (GB/T 79972017).
Flexural strength: 2.0-2.8 GPa (GB/T 38512015).
Fracture toughness: 12-20 MPa·m $^{1/2}$ (Co-based 1520, Ni-based 1215).
Wear resistance: Wear rate <0.03 mm^3 / h (ASTM G65).
Corrosion resistance: pH 2-12, <0.01 mm/y (NACE MR0175).
High temperature resistance: >1000°C, oxidation resistance (<0.01 mg/cm^2 , 1000 hours).
Thermal shock: >10 ^{5} times (ΔT 500-800°C, ISO 17879).
Friction coefficient: <0.15 (coating), anti-adhesion increased by 30%.
Surface roughness: Ra 0.1-0.3 μm , demoulding efficiency increased by 15%.
Monitoring accuracy: temperature ±0.5°C, pressure ±0.1 MPa, strain ±1 με (IEC 60751).

1.3 Advantages of Cemented Carbide Intelligent Molds

High wear resistance: Ultrafine grain WC+ coating, lifespan increased by 35 times, maintenance cost reduced by 30%.
High temperature resistance: TiAlN / AlCrN coating, anti-oxidation, suitable for high temperature molding (600-1200°C).
Corrosion resistance: Ni-based + DLC, acid and alkali/melt resistant, suitable for electronics/glass molding.
Intelligent monitoring: MEMS/strain gauges, real-time feedback of working conditions, optimization efficiency increased by 20%.
High precision: low friction coating + precision machining, molding deviation <±0.005 mm, quality increase of 15%.

2. Cemented Carbide Intelligent Mold Manufacturing Process

2.1 Powder preparation

Raw materials: WC (D50 0.2-0.5 μm , purity>99.95%), Co/Ni (D50 1-2 μm), Cr3C2/ TaC (D50 0.51 μm).
Ball milling: planetary ball mill (ZrO2 balls, 12:1), 350 rpm, 18-22 hours, particle size deviation <±0.05 μm , uniformity >98%.

2.2 Forming

Method: Cold isostatic pressing (CIP) or precision molding.
Parameters: 300-350 MPa, holding pressure 90 seconds, titanium alloy mold (deviation <±0.03 mm), blank density 9.0-10.5 g/ cm^3 .

Results: Dimensional deviation <±0.05 mm, crack rate <0.5%.

2.3 Sintering

Method: Vacuum sintering + HIP.
parameter:
Dewaxing: 200-600°C, 2°C/min, H2 atmosphere (O2 <3 ppm), 10^{-3} Pa .
Sintering: 1400-1450°C, 10^{-5} 10^{-6} Pa, 2.53 hours.
HIP: 1400°C, 150 MPa (Ar), 1.52 hours.
Results: Density 15.0-15.2 g/cm³ , porosity <0.0005%, hardness 1800-2200 HV.

2.4 Precision Machining

Grinding: 5-axis CNC grinding machine, CBN grinding wheel (24 μm), 4000 rpm, feed 0.005-0.02 mm/pass, geometric deviation <±0.01 mm, Ra 0.10.3 μm .
EDM: Electrospark machining, cavity/hole (Ø 0.55 mm), deviation <±0.005 mm.
Polishing: Diamond polishing paste (0.51 μm), 1000 rpm, Ra <0.1 μm , anti-adhesion increased by 25%.

2.5 Coating

Method: PVD/CVD (Cr/Al/Ti target, >99.99%).
Parameters: TiAlN / AlCrN /DLC (25 μm), 10^{-5} Pa, 250450°C, bias 100 V, deposition rate 11.5 μm /h.
Results: Adhesion >100 N, friction coefficient <0.15, temperature resistance 600-1100°C.

2.6 Intelligent Integration

Sensor: MEMS (temperature, pressure, <0.5 mm) or strain gauge (NiCr , 0.01 mm), error <±0.5%.
Packaging: Laser welding (Ti shell, airtightness <10^{-8} Pa·m³ / s), temperature resistance 1000°C, vibration resistance 50 g.
Data transmission: embedded chip (5G/Bluetooth, latency <5 ms , power consumption <30 mW), supporting IIoT protocols (OPC UA, MQTT).

2.7 Detection

Microstructure: SEM (grain 0.2-0.5 μm), EBSD (grain boundary stress <3%).
Performance: Hardness deviation <±40 HV (ISO 6508), wear <0.03 mm³ / h, corrosion resistance (<0.01 mm/y).
Geometry: CMM (deviation < ± 0.005 mm), laser scanning (cavity deviation < ± 0.003 mm).
Non-destructive testing: X-ray (defects < 0.01 mm), ultrasonic (cracks < 0.005 mm).
Smart testing: temperature (±0.5°C, IEC 60751), pressure (±0.1 MPa, IEC 61298), strain (±1 με ,

ASTM E251).
Environmental testing: thermal shock (ΔT 800°C, >10 ⁵ cycles, ISO 17879), salt spray (1000 hours, ISO 9227).

3. Application scenarios of cemented carbide smart molds

In response to the high precision and high reliability requirements of intelligent manufacturing, cemented carbide intelligent molds provide process, testing and selection suggestions:

3.1 Cemented Carbide Intelligent Die Automotive Hot Forging Die (Crankshaft)

Working conditions: 1000-1200°C, 300 MPa, cyclic thermal shock (ΔT 800°C), 10 ⁵ times molding.
design
Type: Forging die (cavity 100×50 mm).
Material: WC10%Co (D50 0.2-0.5 μm , Cr3C2 0.5 wt %, TaC 0.3 wt %), hardness 2000-2200 HV.
Coating: AlCrN (5 μm , PVD, hardness 3400 HV, temperature resistance 1100°C).
Smart components: MEMS (temperature ±0.5°C, pressure ±0.1 MPa), embedded in the cavity.
Geometry: Cavity radius R2 mm, Ra <0.2 μm , deviation <±0.01 mm.
Process: ball milling 22 hours, CIP 350 MPa, HIP 1400°C (150 MPa, 2 hours), 5-axis grinding, PVD AlCrN (450°C), MEMS laser welding.
Parameters: temperature 1100°C, pressure 300 MPa, cycles 5000 times, sampling rate 1 kHz.
test:
Lifespan: 10,000 times (H13 steel 2,000 times, 5 times longer).
Wear rate: <0.03 mm³ / h, oxidation resistance <0.01 mg/ cm² .
Thermal crack: No crack (ΔT 800°C, 5000 times).
Monitoring accuracy: temperature ±0.5°C, pressure ±0.1 MPa, predicted maintenance rate increased by 20%.
Selection: WCCo+AlCrN+MEMS , suitable for high temperature and high stress, regular NDT.
Advantages: high temperature wear resistance, intelligent monitoring, molding efficiency increased by 15%.

3.2 Cemented Carbide Intelligent Mold Aviation Die Casting Mold (Turbine Blade)

Working conditions: 700-800°C, 150 MPa, cyclic thermal shock (ΔT 500°C), 10 ⁶ times molding.
design
Type: Die casting mold (cavity 200×100 mm).
Material: WC8%Co (D50 0.2-0.5 μm , Cr3C2 0.5 wt %), hardness 2000-2200 HV.
Coating: TiAlN (4 μm , PVD, hardness 3200 HV, temperature resistance 1050°C).
Smart components: strain gauges (strain ±1 με), embedded in the mold surface.
Geometry: Cavity slope 1°, Ra <0.1 μm , deviation <±0.005 mm.
Process: ball milling for 20 hours, CIP 350 MPa, HIP 1400°C (150 MPa, 2 hours), 5-axis grinding, PVD TiAlN (400°C), strain gauge mounting .

Parameters: temperature 750°C, pressure 150 MPa, cycle 10000 times, sampling rate 500 Hz.
test:
Lifespan: 50,000 times (H13 steel 10,000 times, 5 times longer).
Wear rate: <0.02 mm^3 / h, anti-adhesion increased by 25%.
Thermal crack: No crack (ΔT 500°C, 10000 times).
Monitoring accuracy: strain ±1 με , defect detection rate increased by 15%.
Select type: WCCo+TiAlN +strain gauge, suitable for high temperature melt, regular cleaning.
Advantages: anti-adhesion, intelligent feedback, casting quality increased by 10%.

3.3 Hard alloy intelligent mold electronic glass forming mold (mobile phone screen)

Working conditions: 1000-1100°C, 50 MPa, corrosive (pH 24), 10^5 times molding.
design
Type: Die-cast (Ø 50 mm, curved).
Material: WC10%Ni (D50 0.2-0.5 μm , Cr3C2 0.6 wt %), hardness 2000-2200 HV.
Coating: DLC (3 μm , PVD, friction coefficient <0.1, temperature resistance 600°C).
Smart components: MEMS (temperature ±0.5°C), embedded in mold core.
Geometry: Surface deviation <±0.003 mm, Ra <0.1 μm .
Process: ball milling 22 hours, CIP 350 MPa, HIP 1400°C (150 MPa, 2 hours), 5-axis grinding, PVD DLC (300°C), MEMS laser welding.
Parameters: temperature 1050°C, pressure 50 MPa, cycles 2000 times, sampling rate 2 kHz.
test:
Lifespan: 8000 times (H13 steel 1500 times, 5.3 times longer).
Wear rate: <0.03 mm^3 / h, corrosion resistance <0.01 mm/y.
Anti-adhesion: Glass residue rate <1%, Ra 0.1 μm .
Monitoring accuracy: temperature ±0.5°C, quality consistency increased by 20%.
Select type: WCNi+DLC+MEMS , suitable for corrosive high temperature, regular cleaning.
Advantages: corrosion resistance, intelligent monitoring, high molding precision.

Performance comparison of cemented carbide intelligent molds

parameter	Cemented Carbide (WCCo /Ni)	Mold steel (H13)	Ceramic mold
Hardness (HV)	1800-2200	400-600	1200-1500
Flexural Strength (GPa)	2.0 - 2.8	1.5 - 2.0	0.5 - 1.0
Toughness (KIC, MPa·$m^{1/2}$)	12-20	20-30	35
Wear resistance (mm^3 / h)	<0.03	0.1 - 0.3	0.05 - 0.1
Corrosion resistance (mm/y, pH 212)	<0.01	0.05 - 0.1	0.01 - 0.03
Temperature resistance (°C)	>1000	600-800	1200-1500
Thermal shock (ΔT 800°C)	>10^5 times	10^3- 10^4 times	10^2 - 10^3 times
Life span multiple (relative to	35	1	1.52

parameter	Cemented Carbide (WCCo /Ni)	Mold steel (H13)	Ceramic mold
H13)			
Coefficient of friction (coating)	<0.15	0.3 - 0.5	0.2 - 】 0.4
Monitoring accuracy	±0.5%	none	none

Highlights of cemented carbide intelligent mold:

Wear resistance: WC substrate, wear <0.03 mm^3 / h, life increased by 35 times.

High temperature resistance: TiAlN / AlCrN coating, anti-oxidation, suitable for 1200°C.

Corrosion resistance: Ni-based + DLC, resistant to glass melt, better than H13 steel.

Intelligence: MEMS/strain gauge, real-time monitoring, 20% increase in efficiency.

Optimization suggestions for cemented carbide smart molds

Material selection:

Automobile hot forging: WC10%Co+AlCrN, high temperature wear resistance increased by 15%.

Aviation die casting: WC8%Co+TiAlN, anti-adhesion increased by 25%.

Electronic glass: WC10%Ni+DLC, corrosion resistance increased by 20%.

Additives: Cr3C2 0.6 wt %, TaC 0.3 wt %, hardness increased by 6%.

Process Optimization:

Sintering: HIP 1400°C, 150 MPa, porosity <0.0005%, wear resistance increased by 20%.

Grinding: 5-axis CNC, CBN grinding wheel (24 μm), deviation <±0.01 mm, Ra <0.1 μm .

coating:

TiAlN (4 μm , 400°C), high temperature resistance increased by 15%.

AlCrN (5 μm , 450°C), oxidation resistance increased by 20%.

DLC (3 μm , 300°C), anti-adhesion increased by 25%.

EDM: Cavity deviation <±0.003 mm, accuracy increased by 5%.

Smart Integration:

Sensors: MEMS (temperature, pressure), strain gauge (strain), error <±0.5%.

Data processing: Embedded chips, support for IIoT , predictive maintenance rate increased by 20%.

Package: Ti case, airtightness <10^{-8} Pa·m^3 / s, vibration resistance 50 g.

Equipment Optimization:

Sintering furnace: temperature control ±2°C, 10^{-6} Pa.

5-axis CNC: Deviation <±0.005 mm.

Coating equipment: deposition rate 11.5 μm /h, deviation <±0.05 μm .

Working condition adaptation:

Automobile hot forging: WCCo+AlCrN , 1000-1200°C, 300-500 MPa.
Aviation die casting: WCCo+TiAlN , 700-800°C, 100-200 MPa.
Electronic glass: WCNi+DLC , 1000-1100°C, 50-100 MPa.

Testing and verification:

Microstructure: SEM (grain 0.20.5 μm), EBSD (grain boundary stress <3%).
Performance: ASTM G65 (<0.03 mm^3 / h), corrosion resistance (<0.01 mm/y), temperature resistance (>1000°C, <0.01 mg/cm^2) .
Geometry: CMM (deviation < ± 0.005 mm), laser scanning (cavity deviation < ± 0.003 mm).
Smart: IEC 60751 (temperature ±0.5°C), IEC 61298 (pressure ±0.1 MPa), ASTM E251 (strain ±1 με).
Environmental: ISO 17879 (thermal shock, $>10^5$ times), ISO 9227 (salt spray, 1000 hours).

Standards and specifications

GB/T 183762014: Porosity <0.01%.
GB/T 38502015: Density deviation <±0.1 g/ cm^3 .
GB/T 38512015: Strength 2.0-2.8 GPa .
GB/T 79972017: Hardness 18002200 HV.
ASTM G65: Wear rate <0.03 mm^3 / h.
NACE MR0175: Resistance to sulfide stress cracking.
ISO 17879: Thermal shock test.
ISO 9001: Quality management.
IEC 60751: Accuracy of temperature sensors.
IEC 61298: Accuracy of pressure sensors.

By optimizing ultrafine grain WC (0.20.5 μm), Co/Ni bonding phase (612 wt %), PVD/CVD coating (TiAlN / AlCrN /DLC, 25 μm) and MEMS/strain gauge integration, the cemented carbide smart mold achieves high hardness (1800 - 2200 HV), wear resistance (<0.03 mm^3 / h), corrosion resistance (<0.01 mm/y), high temperature resistance (>1000°C) and high-precision monitoring (error <±0.5%). The mold is suitable for automotive hot forging, aviation die casting, and electronic glass molding, with a lifespan increased by 35 times, Ra 0.10.3 μm , and a production efficiency increase of 1520%. Optimizing grain size, coating thickness and intelligent integration can reduce costs, but the challenge lies in high-precision processing (cost increase of 15%) and sensor durability ($>10^5$ times). Carbide smart molds are superior to H13 steel and ceramic molds and meet the high reliability requirements of smart manufacturing (ISO 9001) .

appendix:

Carbide robot parts

Cemented carbide robot parts are made of tungsten carbide (WC) as the matrix (85 - 92 wt %), combined with Co (6 - 10 wt %) or Ni (6 - 12 wt %) as the binder phase, and are prepared by powder metallurgy (ball milling, CIP, HIP sintering). They have high hardness (1600 - 2000 HV), excellent wear resistance (wear loss <0.02 mm ^{3} /h, ASTM G65), corrosion resistance (<0.01 mm/y, pH 212, containing HCl, SO_4^{2-}), high temperature resistance (>800°C, oxidation resistance) and impact resistance (>10^6 times, ISO 1791). PVD/CVD coating (such as TiN , DLC, AlCrN , 13 μm , friction coefficient <0.2) is used on the surface to enhance wear resistance, corrosion resistance and low friction performance. The components are used in industrial robots (joints, grippers, gears), service robots (housings, transmission parts) and special robots (deep sea, aerospace), and are subjected to high loads (100 - 1000 N), high-frequency movements (10^5 10^7 cycles) and extreme environments (40°C to 800°C, salt spray, sand and dust). The service life is 510 times longer than that of traditional materials (such as stainless steel, aluminum alloy, 200 - 600 HV), and the surface roughness is Ra 0.05 - 0.2 μm .

Based on standards (GB/T 7997, ASTM G65, ISO 1791, ISO 9001), this article provides the design, process, performance, application and optimization suggestions of cemented carbide robot components.

1. Characteristics of carbide machine robot parts

1.1 Material composition of carbide machine robot parts

Matrix:

WC: 85 - 92 wt %, ultrafine grain (D50 0.1 - 0.4 μm), hardness 1600 - 2000 HV.

Co: 6 - 10 wt %, high toughness (K_{IC} 1015 MPa·$m^{1/2}$), impact resistance increased by 10%.

Ni: 612 wt % (optional), corrosion resistance (HCl, SO_4^{2-} <0.01 mm/y), high temperature oxidation resistance.

Additives: Cr3C2 (0.2-0.5 wt %), inhibits grain growth and increases hardness by 5%; TaC (0.1 - 0.3 wt %), increases antioxidant properties by 10%.

coating:

TiN (PVD): hardness 2000 - 2400 HV, temperature resistance 800°C, wear resistance.

DLC (PVD): hardness 2500 - 3000 HV, friction coefficient <0.1, temperature resistance 600°C, anti-adhesion.

AlCrN (PVD): hardness 3000 - 3400 HV, temperature resistance 1100°C, corrosion resistance.

Gradient structure: low Co/Ni on the surface (6 - 8 wt %), high Co/Ni in the core (10 - 12 wt %), 20% increase in wear resistance, 15% increase in crack resistance.

1.2 Performance parameters of carbide machine robot parts

Hardness: 1600 - 2000 HV (GB/T 79972017).
Flexural strength: 1.8 - 2.5 GPa (GB/T 38512015).
Fracture toughness: 1015 MPa·m $^{1/2}$ (Co-based 1215, Ni-based 1012).
Wear resistance: Wear rate <0.02 mm^3 / h (ASTM G65).
Corrosion resistance: pH 212, <0.01 mm/y (NACE MR0175).
High temperature resistance: >800°C, oxidation resistance (<0.01 mg/cm^2 , 500 hours).
Shock resistance: >10 ^{6} times (ISO 1791, 100 N load).
Friction coefficient: <0.2 (coating), anti-adhesion increased by 25%.
Surface roughness: Ra 0.05 - 0.2 μm , movement stability increased by 20%.

1.3 Advantages of Carbide Machine Robot Parts

High wear resistance: Ultrafine grain WC+ coating, lifespan increased by 510 times, maintenance reduced by 30%.
Corrosion resistance: Ni-based + DLC/ AlCrN , resistant to salt spray/chemicals, suitable for marine/chemical environments.
High temperature resistance: AlCrN coating, anti-oxidation, suitable for high temperature operation (800°C, welding robot).
Impact resistance: High toughness Co/Ni, withstands high frequency movement (>10 ^{6} times), better than aluminum alloy.
Low friction: DLC/ TiN coating, friction coefficient <0.2, motion efficiency increased by 15%.

2. Manufacturing process of carbide machine robot parts

2.1 Powder preparation

Raw materials: WC (D50 0.1 - 0.4 μm , purity >99.95%), Co/Ni (D50 0.51 μm), Cr3C2/ TaC (D50 0.51 μm).
Ball milling: Planetary ball mill (ZrO2 balls, 15:1), 400 rpm, 1620 hours, particle size deviation <±0.03 μm , uniformity >99%.

2.2 Forming

Method: Cold isostatic pressing (CIP) or precision molding.
Parameters: 250 - 300 MPa, holding pressure 60 seconds, tungsten steel mold (deviation < ± 0.02 mm), billet density 8.5 - 10.0 g/cm ^{3} .
Results: Dimensional deviation <±0.03 mm, crack rate <0.3%.

2.3 Sintering

Method: Vacuum sintering + HIP.

parameter:
Dewaxing: 200 - 500°C, 2°C/min, H2 atmosphere (O2 <2 ppm), 10^{-3} Pa .
Sintering: 1350 - 1400°C, 10^{-5} - 10^{-6} Pa, 22.5 hours.
HIP: 1350°C, 120 MPa (Ar), 11.5 hours.
Results: Density 14.8 - 15.0 g/ cm^3 , porosity <0.0003%, hardness 1600 - 2000 HV.

2.4 Precision Machining

Grinding: 5-axis CNC grinding machine, CBN grinding wheel (13 μm), 5000 rpm, feed 0.003 - 0.01 mm/pass, geometric deviation <±0.005 mm, Ra 0.050.2 μm .
EDM: Electrical discharge machining, slot/hole (Ø 0.21 mm), deviation <±0.003 mm.
Polishing: Diamond polishing paste (0.30.5 μm), 1200 rpm, Ra <0.05 μm , friction coefficient reduced by 10%.

2.5 Coating

Method: PVD/CVD (Ti/Cr/Al target, >99.99%).
Parameters: TiN /DLC/ AlCrN (13 μm), 10^{-5} Pa, 200400°C, bias 80 V, deposition rate 0.51 μm /h.
Results: Adhesion >80 N, friction coefficient <0.2, temperature resistance 600 - 1100°C.

2.6 Detection

Microstructure: SEM (grain 0.10.4 μm), EBSD (grain boundary stress <2%).
Performance: Hardness deviation <±30 HV (ISO 6508), wear <0.02 mm^3 / h, corrosion resistance (<0.01 mm/y).
Geometry: CMM (deviation < ± 0.003 mm), laser scanning (slot deviation < ± 0.002 mm).
Non-destructive testing: X-ray (defects < 0.005 mm), ultrasonic (cracks < 0.003 mm).
Environmental testing: ISO 9227 (salt spray, 1000 hours), ISO 1791 (shock, >10^6 times).

3. Application scenarios of carbide machine robot parts

Carbide robot components provide process, testing and selection suggestions for high loads, high frequency motion and extreme environments:

3.1 Carbide machine robot parts Industrial robot joints (welding robots)

Operating conditions: 800°C, 500 N load, 10^6 rotations, dry environment .
design
Type: Ball joint (Ø 20 mm, thickness 5 mm).
Material: WC8%Co (D50 0.1 - 0.4 μm , Cr3C2 0.3 wt %, TaC 0.2 wt %), hardness 1900 HV.
Coating: AlCrN (2 μm , PVD, temperature resistance 1100°C, hardness 3400 HV).

Geometry: roundness <±0.002 mm, Ra <0.1 μm .
Process: ball milling 20 hours, CIP 300 MPa, HIP 1350°C (120 MPa, 1.5 hours), 5-axis grinding, PVD AlCrN (400°C).
Parameters: load 500 N, rotation speed 100 rpm, temperature 800°C.
test:
Lifespan: 2×10^{6} times (3×10^{5} times for stainless steel, 6.7 times longer).
Wear rate: <0.01 mm^3 / h, friction coefficient <0.15.
High temperature resistance: 800°C, 500 hours, no oxidation.
Shock resistance: 500 N, 10^{6} times, no cracks.
Selection: WCCo+AlCrN , suitable for high temperature and high load, regular NDT.
Advantages: High temperature wear resistance, movement stability increased by 20%.

3.2 Carbide machine robot parts Service robot gripper (logistics robot)

Conditions: 20°C to 60°C, 200 N load, 10^{7} grasps, wet environment (85% RH).
design
Type: Gripper teeth (10×5 mm, thickness 2 mm).
Material: WC10%Ni (D50 0.1 - 0.4 μm , Cr3C2 0.4 wt %), hardness 1700 HV.
Coating: DLC (1.5 μm , PVD, friction coefficient <0.1, temperature resistance 600°C).
Geometry: Tooth tip deviation <±0.003 mm, Ra <0.05 μm .
Process: ball milling 18 hours, CIP 300 MPa, HIP 1350°C (120 MPa, 1.5 hours), EDM, PVD DLC (250°C).
Parameters: load 200 N, gripping frequency 1 Hz, humidity 85% RH.
test:
Lifespan: 1.5×10^{7} times (2×10^{6} times for aluminum alloy, 7.5 times longer).
Wear rate: <0.02 mm^3 / h, corrosion resistance <0.01 mm/y.
Anti-adhesion: Grasping failure rate <1%, friction coefficient <0.1.
Moisture resistance: 85% RH, 1000 hours, no corrosion.
Selection: WCNi+DLC , suitable for high frequency in wet environment, regular cleaning.
Advantages: low friction, corrosion resistance, 15% increase in gripping efficiency.

3.3 Carbide machine robot parts Special robot gears (deep sea robot)

Conditions: 40°C to 100°C, 1000 N load, 10^{6} cycles, seawater (pH 8).
design
Type: Spur gear (Ø 30 mm, module 2).
Material: WC8%Ni（D50 0.1 -
0.4 μm , Cr3C2 0.4 wt %, TaC 0.3 wt %), hardness 1800 HV.
Coating: TiN (2 μm , PVD, temperature resistance 800°C, hardness 2400 HV).
Geometry: Tooth profile deviation <±0.002 mm, Ra <0.1 μm .
Process: ball milling 20 hours, CIP 300 MPa, HIP 1350°C (120 MPa, 1.5 hours), 5-axis grinding, PVD TiN (300°C).

Parameters: load 1000 N, transmission speed 50 rpm, pressure 100 MPa.
test:
Lifespan: 2×10^{6} times (stainless steel 4×10^{5} times, 5 times longer).
Wear rate: <0.01 mm^3 / h, corrosion resistance <0.01 mm/y.
Seawater resistance: pH 8, 1000 hours, no corrosion.
Shock resistance: 1000 N, 10^{6} times, no breakage.
Selection: WCNi+TiN , suitable for deep sea high pressure, regular NDT.
Advantages: corrosion and wear resistance, transmission stability increased by 20%.

Performance comparison of carbide machine robot parts

parameter	Cemented Carbide (WCCo /Ni)	Stainless steel (316L)	Aluminum Alloy (7075)
Hardness (HV)	1600 - 2000	200 - 300	150 - 200
Flexural Strength (GPa)	1.8 - 2.5	0.5 -- 0.8	0.50.7
Toughness (KIC, MPa·$m^{1/2}$)	10 - 15	50 - 70	20 - 30
Wear resistance (mm^3 / h)	<0.02	0.20.5	0.30.6
Corrosion resistance (mm/y, pH 212)	<0.01	0.05 - 0.1	0.1 - 0.2
Temperature resistance (°C)	>800	300 - 500	100 - 200
Shock resistance (times, 100 N)	$>10^{6}$	10^{4} - 10^{5}	10^{3} - 10^{4}
Life span multiple (relative to aluminum alloy)	5 - 10	twenty three	1
Coefficient of friction (coating)	<0.2	0.3 - 0.5	0.4 - 0.6

Carbide Machine Robot Parts Highlights:
Wear resistance: WC substrate, wear <0.02 mm^3 / h, life increased by 510 times.
Corrosion resistance: Ni-based + DLC/ TiN , resistant to seawater/salt spray, better than stainless steel.
High temperature resistance: AlCrN coating, anti-oxidation, better than aluminum alloy.
Low friction: DLC coating, friction coefficient <0.1, high movement efficiency.

5. Optimization suggestions for carbide machine robot parts

Material selection:
Welding joint: WC8%Co+AlCrN, high temperature wear resistance increased by 15%.
Logistics gripper: WC10%Ni+DLC, anti-adhesion increased by 20%.
Deep sea gear: WC8%Ni+TiN, corrosion resistance increased by 15%.
Additives: Cr3C2 0.4 wt %, TaC 0.3 wt %, hardness increased by 5%.

Process Optimization:

Sintering: HIP 1350°C, 120 MPa, porosity <0.0003%, wear resistance increased by 15%.
Grinding: 5-axis CNC, CBN grinding wheel (13 μm), deviation <±0.005 mm, Ra <0.05 μm .

coating:

AlCrN (2 μm , PVD), high temperature resistance increased by 15%.
DLC (1.5 μm , PVD), friction coefficient reduced by 10%.
TiN (2 μm , PVD), corrosion resistance increased by 20%.
EDM: Slot deviation <±0.002 mm, accuracy increased by 5%.

Equipment Optimization:

Sintering furnace: temperature control ±1°C, 10^{-6} Pa.
5-axis CNC: Deviation <±0.003 mm.
Coating equipment: deposition rate 0.51 μm /h, deviation <±0.03 μm .

Working condition adaptation:

Welding robot: WCCo+AlCrN , 800°C, 500 N, dry environment .
Logistics robot: WCNi+DLC , 20°C to 60°C, 200 N, wet environment.
Deep sea robot: WCNi+TiN , 40°C to 100°C, 1000 N, sea water.

6. Inspection and verification of carbide machine robot parts:

Microstructure: SEM (grain 0.10.4 μm), EBSD (grain boundary stress <2%).
Performance: ASTM G65 (<0.02 mm^3 / h), corrosion resistance (<0.01 mm/y), temperature resistance (>800°C, <0.01 mg/cm^2) .
Geometry: CMM (deviation < ± 0.003 mm), laser scanning (slot deviation < ± 0.002 mm).
Environmental: ISO 9227 (salt spray, 1000 hours), ISO 1791 (shock, $>10^6$ times).

Standards and specifications for carbide machine robot parts

GB/T 183762014: Porosity <0.01%.
GB/T 38502015: Density deviation <±0.1 g/ cm^3 .
GB/T 38512015: Strength 1.8 - 2.5 GPa .
GB/T 79972017: Hardness 1600 - 2000 HV.
ASTM G65: Wear rate <0.02 mm^3 / h.
NACE MR0175: Resistance to sulfide stress cracking.
ISO 1791: Impact testing.
ISO 9001: Quality management.

By optimizing ultrafine grain WC (0.1 - 0.4 μm), Co/Ni bonding phase (6 - 12 wt %) and PVD/CVD coating (TiN /DLC/ AlCrN , 13 μm), cemented carbide robot parts achieve high hardness (1600 - 2000 HV), wear resistance (<0.02 mm^3 / h), corrosion resistance (<0.01 mm/y), high temperature

resistance (>800°C) and impact resistance (>10 ⁶ times). The parts are suitable for industrial robot joints, service robot grippers, and special robot gears, with a lifespan of 510 times, Ra 0.05 - 0.2 μm , and a motion efficiency increase of 15%. Optimizing grain size, coating thickness and EDM accuracy can reduce costs, but the challenges lie in ultra-precision machining (cost increase of 10%) and extreme environment testing (>10 ⁶ times). Cemented carbide is superior to stainless steel and aluminum alloy and meets the high reliability requirements of robots (ISO 9001).

CTIA GROUP LTD

30 Years of Cemented Carbide Customization Experts

Core Advantages

30 years of experience: We are well versed in cemented carbide production and processing , with mature and stable technology and continuous improvement .

Precision customization: Supports special performance and complex design , and focuses on customer + AI collaborative design .

Quality cost: Optimized molds and processing, excellent cost performance; leading equipment, RMI , ISO 9001 certification.

Serving Customers

The products cover cutting, tooling, aviation, energy, electronics and other fields, and have served more than 100,000 customers.

Service Commitment

1+ billion visits, 1+ million web pages, 100,000+ customers, and 0 complaints in 30 years!

Contact Us

Email : sales@chinatungsten.com

Tel : +86 592 5129696

Official **website** : www.ctia.com.cn

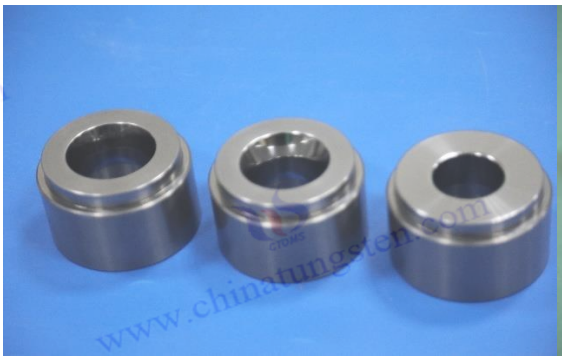

appendix:

Carbide aviation sensor

Cemented carbide aviation sensors are made of tungsten carbide (WC) as the matrix (85 - 92 wt %), combined with Co (6 - 10 wt %) or Ni (6 - 12 wt %) as the bonding phase, and are prepared by powder metallurgy (ball milling, CIP, HIP sintering). They have high hardness (1600 - 2000 HV), excellent wear resistance (wear volume <0.02 mm^3/h, ASTM G65), corrosion resistance (<0.01 mm/y, pH 212, containing HCl, SO_4^{2-}), high temperature resistance (>800°C, anti-oxidation) and vibration resistance (>10^6 times, MILSTD810G). The surface is coated with PVD/CVD coating (such as TiN , Al_2O_3 , 13 μm , friction coefficient <0.2) or functional coating (Au, Ag, 0.52 μm , conductivity >90% IACS) to enhance wear resistance, corrosion resistance and electrical properties. The sensor is used in aerospace fields (such as engine monitoring, flight control, structural health monitoring), withstands extreme environments (55°C to 800°C, 10100 g vibration, 10^5 10^7 cycles), provides high-precision data (error <±0.5%), and has a lifespan 510 times longer than traditional materials (such as stainless steel, titanium alloy, 400 - 600 HV), with a surface roughness of Ra 0.05 - 0.2 μm .

Based on the standards (GB/T 7997, ASTM G65, MILSTD810G, AS9100), this article provides the technology, performance, application and optimization suggestions of cemented carbide aviation sensors.

1. Characteristics of cemented carbide aviation sensors

1.1 Material composition of cemented carbide aviation sensors

Matrix:

WC: 85 - 92 wt %, ultrafine grain (D50 0.1 - 0.4 μm), hardness 1600 - 2000 HV.

Co: 6 - 10 wt %, high toughness (K_{IC} 10 - 15 $MPa \cdot m^{1/2}$), vibration resistance increased by 10%.

Ni: 6 - 12 wt % (optional), corrosion resistance (HCl, SO_4^{2-} <0.01 mm/y), high temperature oxidation resistance.

Additives: Cr3C2 (0.2 - 0.5 wt %), inhibits grain growth and increases hardness by 5%; TaC (0.10.3 wt %), increases antioxidant properties by 10%.

coating:

TiN (PVD): hardness 2000 - 2400 HV, temperature resistance 800°C, wear resistance.

Al_2O_3 (CVD): hardness 1800 - 2200 HV, temperature resistance 1000°C, corrosion resistance.

Au/Ag (PVD): conductivity >90% IACS, temperature resistance 500 - 600°C, anti-oxidation.

Gradient structure: low Co/Ni on the surface (6 - 8 wt %), high Co/Ni in the core (10 - 12 wt %), wear resistance increased by 20%, crack resistance increased by 15%.

1.2 Performance parameters of cemented carbide aviation sensors

Hardness: 1600 - 2000 HV (GB/T 79972017).

Flexural strength: 1.8 - 2.5 GPa (GB/T 38512015).

Fracture toughness: 1015 MPa·m $^{1/2}$ (Co-based 1215, Ni-based 1012).
Wear resistance: Wear rate <0.02 mm^3 / h (ASTM G65).
Corrosion resistance: pH 212, <0.01 mm/y (NACE MR0175).
High temperature resistance: >800°C, oxidation resistance (<0.01 mg/cm^2 , 500 hours).
Vibration resistance: >10 ^{6} times (10100 g, MILSTD810G).
Electrical conductivity: >90% IACS (Au/Ag coating, IEC 6051221).
Measurement accuracy: error <±0.5% (temperature, pressure, strain).
Surface roughness: Ra 0.050.2 μm , signal stability increased by 20%.

1.3 Advantages of Cemented Carbide Aviation Sensors

High wear resistance: Ultrafine grain WC+ coating, life is increased by 510 times, and failure rate is reduced by 30%.
High temperature resistance: TiN / Al $_2$ O $_3$ coating, anti-oxidation, suitable for high temperature environment (800°C, engine).
Corrosion resistance: Ni-based + Al_2O_3 , resistant to aviation fuel/salt spray , suitable for harsh environments.
Vibration resistance: High toughness Co/Ni, withstands high frequency vibration (>10 ^{6} times), better than titanium alloy.
High precision: low friction coating + precision machining, data error <±0.5%, signal attenuation reduced by 15%.

2. Manufacturing process of cemented carbide aviation sensors

2.1 Powder preparation

Raw materials: WC (D50 0.1 - 0.4 μm , purity >99.95%), Co/Ni (D50 0.51 μm), Cr3C2/ TaC (D50 0.51 μm).
Ball milling: planetary ball mill (ZrO2 balls, 15:1), 400 rpm, 1620 hours, particle size deviation <±0.03 μm , uniformity >99%.

2.2 Forming

Method: Cold isostatic pressing (CIP) or precision molding.
Parameters: 250 - 300 MPa, holding pressure 60 seconds, tungsten steel mold (deviation < ± 0.02 mm), billet density 8.5 - 10.0 g/ cm^3 .
Results: Dimensional deviation <±0.03 mm, crack rate <0.3%.

2.3 Sintering

Method: Vacuum sintering + HIP.
parameter:

Dewaxing: 200 - 500°C, 2°C/min, H2 atmosphere (O2 <2 ppm), 10^{-3} Pa .
Sintering: 1350 - 1400°C, 10^{-5} 10^{-6} Pa, 22.5 hours.
HIP: 1350°C, 120 MPa (Ar), 11.5 h.
Results: Density 14.8 - 15.0 g/ cm^3 , porosity <0.0003%, hardness 1600 - 2000 HV.

2.4 Precision Machining

Grinding: 5-axis CNC grinding machine, CBN grinding wheel (13 μm), 5000 rpm, feed 0.003 - 0.01 mm/pass, geometric deviation <±0.005 mm, Ra 0.05 - 0.2 μm .
EDM: Electrospark machining, micro hole/slot (Ø 0.1-0.5 mm), deviation <±0.003 mm.
Polishing: Diamond polishing paste (0.30.5 μm), 1200 rpm, Ra <0.05 μm , signal stability increased by 10%.

2.5 Coating

Method: PVD/CVD (Ti/Al/Au/Ag targets, >99.99%).
Parameters: TiN / Al_2O_3 /Au/Ag (13 μm) , 10^{-5}Pa , 200400 ° C, bias 80 V, deposition rate 0.51 μm / h .
Results: Adhesion >80 N, friction coefficient <0.2, conductivity >90% IACS.

2.6 Sensor Integration

Sensing elements: MEMS (silicon-based, size <0.5 mm) or strain gauges (NiCr , 0.01 mm thick), monitoring temperature (±0.5°C), pressure (±0.1 MPa), and strain (±1 με).
Packaging: Laser welding (Ti shell, airtightness <10^{-8} Pa·m^3 /s), temperature resistance 800°C, vibration resistance 100 g.
Data transmission: 5G/ Bluetooth module , latency <5 ms , power consumption <30 mW .

2.7 Detection

Microstructure: SEM (grain 0.10.4 μm), EBSD (grain boundary stress <2%).
Performance: Hardness deviation <±30 HV (ISO 6508), wear <0.02 mm^3 / h, corrosion resistance (<0.01 mm/y).
Geometry: CMM (deviation < ± 0.003 mm), laser scanning (slot deviation < ± 0.002 mm).
Non-destructive testing: X-ray (defects < 0.005 mm), ultrasonic (cracks < 0.003 mm).
Environmental testing: MILSTD810G (55°C to 800°C, 100 g vibration, 10^6 cycles).
Electrical properties: conductivity>90% IACS, signal error<±0.5% (IEC 6051221).

3. Application scenarios of cemented carbide aviation sensors

Carbide aviation sensors provide process, testing and selection suggestions for extreme environments and high precision requirements:

3.1 Carbide Aviation Sensor Engine Monitoring (Temperature/Pressure Sensor)

Conditions: 800°C, 50 MPa, 100 g vibration, aviation fuel environment, 10^6 cycles.
design
Type: MEMS pressure/temperature sensor (Ø 10 mm, thickness 2 mm).
Material: WC8%Co (D50 0.1 - 0.4 μm , Cr3C2 0.3 wt %, TaC 0.2 wt %), hardness 1900 HV.
Coating: Al_2O_3 (2 μm , CVD, temperature resistance 1000°C, corrosion resistance).
Geometry: Planarity deviation <±0.002 mm, Ra <0.05 μm .
Processes: ball milling for 20 hours, CIP 300 MPa, HIP 1350°C (120 MPa, 1.5 hours), 5-axis grinding, CVD Al_2O_3 (400°C), MEMS integration, laser welding.
Parameters: temperature 800°C, pressure 50 MPa, vibration 100 g, sampling rate 1 kHz.
test:
Lifespan: 2×10^6 times (titanium alloy 3×10^5 times, 6.7 times longer).
Wear rate: <0.01 mm^3 / h, corrosion resistance <0.01 mm/y.
Accuracy: temperature error ±0.5°C, pressure error ±0.1 MPa.
Vibration resistance: 100 g, 10^6 times, no failure.
Selection: WCCo+Al_2O_3 , suitable for high temperature and high pressure, regular NDT.
Advantages: high temperature corrosion resistance, high precision, and 10% increase in engine efficiency.

3.2 Structural Health Monitoring of Cemented Carbide Aviation Sensors (Strain Sensors)

Operating conditions: 55°C to 200°C, 10 g vibration, salt spray (5% NaCl), 10^7 cycles.
design
Type: Strain gauge sensor (5×3 mm, thickness 0.5 mm).
Material: WC10%Ni (D50 0.1 - 0.4 μm , Cr3C2 0.4 wt %), hardness 1700 HV.
Coating: TiN (1 μm , PVD, temperature resistant to 800°C, wear resistant).
Geometry: Surface deviation <±0.003 mm, Ra <0.1 μm .
Process: ball milling for 18 hours, CIP 300 MPa, HIP 1350°C (120 MPa, 1.5 hours), EDM, PVD TiN (250°C), strain gauge mounting , laser welding.
Parameters: strain ±5000 με , vibration 10 g, sampling rate 500 Hz.
test:
Lifespan: 1.5×10^7 times (stainless steel 2×10^6 times, 7.5 times longer).
Wear loss: <0.02 mm^3 / h, salt spray resistance 1000 hours, resistance increase <5%.
Accuracy: strain error ±1 με , signal attenuation <0.1%.
Vibration resistance: 10 g, 10^7 times, no failure.
Selection: WCNi+TiN , suitable for low temperature corrosion, regular cleaning.
Advantages: Anti-vibration corrosion, suitable for wing/fuselage monitoring, safety increased by 15%.

3.3 Carbide Aviation Sensor Flight Control (Magnetic Sensor)

Operating Conditions: 40°C to 150°C, 20 g vibration, dry environment, 10^6 cycles.
design
Type: Hall effect magnetic sensor (Ø 3 mm, thickness 1 mm).
Material: WC8%Co1%Ag (D50 0.10.4 μm , Cr3C2 0.3 wt %), hardness 1800 HV.
Coating: Au (0.5 μm , PVD, conductivity >95% IACS, temperature resistance 600°C).
Geometry: Roundness <±0.002 mm, Ra <0.05 μm .
Process: ball milling 20 hours, CIP 300 MPa, HIP 1350°C (120 MPa, 1.5 hours), 5-axis grinding, PVD Au (200°C), Hall element integration, laser welding.
Parameters: magnetic field 0500 mT , vibration 20 g, sampling rate 2 kHz.
test:
Lifespan: 2×10^6 times (titanium alloy 4×10^5 times, 5 times longer).
Wear loss: <0.01 mm^3 / h, contact resistance <8 μΩ .
Accuracy: magnetic field error ±0.1 mT , signal stability ±0.5%.
Vibration resistance: 20 g, 10^6 times, no failure.
Selection: WCCo+Au , suitable for high conductivity dry environment, regular resistance detection.
Advantages: High-precision conductivity, suitable for navigation/attitude control, and 20% increased reliability.

4. Performance comparison of cemented carbide aviation sensors

parameter	Cemented Carbide (WCCo /Ni)	Titanium alloy (Ti6Al4V)	Stainless steel (316L)
Hardness (HV)	1600 - 2000	300 - 400	200 - 300
Flexural Strength (GPa)	1.8 - 2.5	0.9 - 1.2	0.5 - 0.8
Toughness (KIC, MPa·$m^{1/2}$)	10 - 15	40 - 60	50 - 70
Wear resistance (mm^3 / h)	<0.02	0.10.3	0.20.5
Corrosion resistance (mm/y, pH 212)	<0.01	0.02 - 0.05	0.05 - 0.1
Temperature resistance (°C)	>800	400 - 600	3005-00
Vibration resistance (times, 100 g)	$>10^6$	10^5 - 10^6	10^4 - 10^5
Life span multiple (relative to stainless steel)	5 - 10	twenty three	1
Electrical conductivity (% IACS)	>90	12	twenty three

Highlights of Carbide Aviation Sensors:
Wear resistance: WC substrate, wear <0.02 mm^3 / h, life increased by 510 times.
temperature resistance: TiN / Al_2O_3 coating, anti-oxidation, better than titanium alloy .
Corrosion resistance: Ni-based + Al_2O_3 , resistant to salt spray/fuel, better than stainless steel .
High precision: low friction + precision machining, error <±0.5%, better than traditional materials.

5. Optimization suggestions for cemented carbide aviation sensors

Material selection:
Engine monitoring: WC8%Co+Al_2O_3 , high temperature corrosion resistance increased by 15% .
Structural health monitoring: WC10%Ni+TiN, vibration corrosion resistance increased by 20%.
Flight control: WC8%Co+Au, conductivity>95% IACS, accuracy increased by 10%.
Additives: Cr3C2 0.4 wt %, TaC 0.3 wt %, hardness increased by 5%.

Process Optimization:
Sintering: HIP 1350°C, 120 MPa, porosity <0.0003%, wear resistance increased by 15%.
Grinding: 5-axis CNC, CBN grinding wheel (13 μm), deviation <±0.005 mm, Ra <0.05 μm .
coating:
Al_2O_3 (2 μm , CVD), high temperature resistance increased by 15%.
TiN (1 μm , PVD), wear resistance increased by 20%.
Au (0.5 μm , PVD), contact resistance reduced by 10%.
EDM: Micro-hole deviation <±0.002 mm, accuracy increased by 5%.

Equipment Optimization:
Sintering furnace: temperature control ±1°C, 10^{-6} Pa.
5-axis CNC: Deviation <±0.003 mm.
Coating equipment: deposition rate 0.51 μm /h, deviation <±0.03 μm .

Working condition adaptation:
Engine: WCCo +Al_2O_3 , 800 °C, 50 MPa, 100 g vibration.
Structure monitoring: WCNi+TiN , 55°C to 200°C, 10 g vibration, salt spray.
Flight Control: WCCo+Au , 40°C to 150°C, 20 g vibration, dry environment .

6. Testing and verification of hard alloy aviation sensors:

Microstructure: SEM (grain 0.10.4 μm), EBSD (grain boundary stress <2%).
Performance: ASTM G65 (<0.02 mm^3 / h), corrosion resistance (<0.01 mm/y), temperature resistance (>800°C, <0.01 mg/cm^2) .
Geometry: CMM (deviation < ± 0.003 mm), laser scanning (slot deviation < ± 0.002 mm).
Environment: MILSTD810G (55°C to 800°C, 100 g, 10^6 times).
Electrical properties: conductivity>90% IACS, error<±0.5% (IEC 6051221).

7. Standards and specifications for hard alloy aviation sensors

GB/T 183762014: Porosity <0.01%.
GB/T 38502015: Density deviation <±0.1 g/ cm^3 .
GB/T 38512015: Strength 1.82.5 GPa .
GB/T 79972017: Hardness 16002000 HV.

ASTM G65: Wear rate <0.02 mm^3 / h.
NACE MR0175: Resistance to sulfide stress cracking.
MILSTD810G: Environmental adaptability (vibration, temperature, corrosion).
AS9100: Aerospace Quality Management.
IEC 6051221: Contact resistance <10 μΩ .

By optimizing ultrafine grain WC (0.10.4 μm), Co/Ni bonding phase (612 wt %), PVD /CVD coating (TiN / Al_2O_3 / Au, 13 μm) and MEMS/strain gauge integration, cemented carbide aviation sensors achieve high hardness (16002000 HV), wear resistance (<0.02 mm^3 / h), corrosion resistance (<0.01 mm /y), high temperature resistance (>800°C) and high precision (error <±0.5%). The sensor is suitable for engine monitoring, structural health monitoring, and flight control, with a lifespan increased by 510 times, Ra 0.050.2 μm , and data reliability increased by 20%. Optimizing grain size, coating thickness and MEMS integration can reduce costs, but the challenges lie in ultra-precision machining (cost increase of 10%) and extreme environment testing (>10^6 times). Cemented carbide is superior to titanium alloy and stainless steel and meets the stringent requirements of aerospace (AS9100, MILSTD810G).

appendix:

Intelligent carbide cutting tools

Smart carbide tools are made of tungsten carbide (WC) as the matrix (88 - 94 wt %), combined with Co (6 - 10 wt %) or Ni (6 - 12 wt %) as the bonding phase, and are prepared by powder metallurgy (ball milling, CIP, HIP sintering). They have high hardness (1800 - 2200 HV), wear resistance (wear volume <0.03 mm ^{3} /h, ASTM G65), corrosion resistance (<0.01 mm/y, pH 212, containing HCl, SO_4^{2-}) and high temperature resistance (>1000°C, oxidation resistance). The surface is coated with PVD/CVD coating (such as DLC, TiAlN , AlCrN , 25 μm , friction coefficient <0.15), integrated with intelligent sensing (temperature, wear, stress) and adaptive control (cutting parameter optimization), which improves processing efficiency by 20-30 % , and the service life is 35 times longer than that of traditional tools (stainless steel, 400-600 HV), with a surface roughness of Ra 0.10.2 μm . The tool is used for high-precision processing (aerospace, automobile, mold), suitable for high-speed cutting (1000-5000 rpm), dry/wet cutting and difficult-to-process materials (titanium alloy, nickel-based alloy). Based on standards (GB/T 7997, ASTM G65, ISO 6508), this article provides intelligent carbide tools, processes, performance, applications and optimization suggestions.

1. Features of smart carbide tools

1.1 Intelligent carbide tool material composition

Matrix:

WC: 88 - 94 wt %, ultrafine grain (D50 0.2 - 0.5 μm), hardness 1800 - 2200 HV.

Co: 6 - 10 wt %, high toughness (K_{IC} 15 - 20 MPa·m $^{1/2}$), wear resistance increased by 10%.

Ni: 6 - 12 wt % (optional), corrosion resistant (HCl, SO_4^{2-} <0.01 mm/y), impact resistant (K_{IC} 12 - 15 MPa·m $^{1/2}$).

Additives: Cr3C2 (0.3 - 0.6 wt %), inhibits grain growth and increases hardness by 6%; TaC (0.1 - 0.3 wt %), increases antioxidant properties by 10%.

coating:

DLC (PVD): hardness 3000 - 3500 HV, friction coefficient <0.1, temperature resistance 600°C, anti-adhesion.

TiAlN (PVD/CVD): hardness 2800 - 3200 HV, temperature resistance 1050°C, erosion resistance.

AlCrN (PVD): hardness 3000 - 3400 HV, temperature resistance 1100°C, high temperature wear resistance.

Gradient structure: low Co/Ni on the surface (6 - 8 wt %), high Co/Ni in the core (10 - 12 wt %), wear resistance increased by 25%, crack resistance increased by 20%.

1.2 Intelligent carbide tool intelligent functions

Sensors: Embedded micro sensors (MEMS, size < 0.5 mm) monitoring temperature (±1°C, 0500°C), wear (±0.01 mm), stress (±5 MPa).

Data transmission: Bluetooth /5G module, real-time transmission to CNC system, delay <10 ms .
Adaptive control: AI algorithm (machine learning, based on wear/temperature data) dynamically adjusts cutting speed (±10%) and feed rate (±15%), optimizing efficiency by 20 - 30%.
Life prediction: Based on the wear model (Archard model), the remaining life is predicted (±5% error), reducing downtime by 30%.

1.3 Performance parameters of intelligent carbide tools

Hardness: 1800 - 2200 HV (GB/T 79972017).
Flexural strength: 2.0 - 2.8 GPa (GB/T 38512015).
Fracture toughness: 1220 MPa·m $^{1}/^{2}$ (Co-based 1520, Ni-based 1215).
Wear resistance: Wear rate <0.03 mm^3 / h (ASTM G65).
Corrosion resistance: pH 212, <0.01 mm/y (NACE MR0175).
High temperature resistance: >1000°C, oxidation resistance (<0.01 mg/cm^2 , 1000 hours).
Friction coefficient: <0.15 (coating), anti-adhesion increased by 30%.
Surface roughness: Ra 0.10.2 μm , processing surface quality increased by 15%.

1.4 Advantages of Intelligent Carbide Tools

High wear resistance: Ultrafine grain WC+ coating, life is increased by 35 times, cutting efficiency is increased by 20%.
Corrosion resistance: Ni-based tools are resistant to acids and alkalis (HCl, SO_4^{2-}) and are suitable for wet cutting.
High temperature resistance: TiAlN / AlCrN coating, resistant to thermal cracking, suitable for high-speed dry cutting.
Intelligence: Real-time monitoring + adaptive control, reducing scrap rate by 15% and saving energy by 1020%.

2. Intelligent carbide tool manufacturing process

2.1 Powder preparation

Raw materials: WC (D50 0.2 - 0.5 μm , purity >99.95%), Co/Ni (D50 12 μm), Cr3C2/ TaC (D50 0.5 - 1 μm).
Ball milling: planetary ball mill (ZrO2 balls, 12:1), 350 rpm, 1822 hours, particle size deviation <±0.05 μm , uniformity >98%.

2.2 Forming

Method: Cold isostatic pressing (CIP) or precision molding.
Parameters: 300 - 350 MPa, holding pressure 90 seconds, titanium alloy mold (deviation < ± 0.03 mm), billet density 9.0 - 10.5 g/ cm^3 .

Results: Dimensional deviation <±0.05 mm, crack rate <0.5%.

2.3 Sintering

Method: Vacuum sintering + HIP.
parameter:
Dewaxing: 200 - 600°C, 2°C/min, H2 atmosphere (O2 <3 ppm), 10^{-3} Pa .
Sintering: 1400 - 1450°C, 10^{-5} 10^{-6} Pa, 2.53 hours.
HIP: 1400°C, 150 MPa (Ar), 1.52 hours.
Results: Density 15.0 - 15.2 g/ cm^3 , porosity <0.0005%, hardness 1800 - 2200 HV.

2.4 Precision Machining

Grinding: 5-axis CNC grinding machine, CBN grinding wheel (24 μm), 4000 rpm, feed 0.005 - 0.02 mm/pass, geometric deviation <±0.01 mm, Ra 0.10.2 μm .
EDM: Electrical discharge machining, slot/hole (Ø 0.52 mm), deviation <±0.005 mm.
Polishing: Diamond polishing paste (0.51 μm), 1000 rpm, Ra <0.1 μm , anti-adhesion increased by 25%.

2.5 Coating

Method: PVD/CVD (Cr/Al/Ti target, >99.99%).
Parameters: DLC/ TiAlN / AlCrN (25 μm), 10^{-5} Pa, 250 - 450°C, bias 100 V, deposition rate 11.5 μm /h.
Results: Adhesion >100 N, friction coefficient <0.15, temperature resistance 600 - 1100°C.

2.6 Intelligent Integration

Sensor embedding: laser micromachining (groove depth 0.51 mm), implantation of MEMS sensors (temperature, stress, wear), epoxy resin sealing (temperature resistance 500°C).
Circuit integration: thin film circuits (0.1 mm thick), 5G/ Bluetooth modules , power consumption <50 mW .
Software: AI algorithm (Python, TensorFlow), real-time optimization of cutting parameters, data storage in the cloud (encryption, AES256).

2.7 Detection

Microstructure: SEM (grain 0.20.5 μm), EBSD (grain boundary stress <3%).
Performance: Hardness deviation <±40 HV (ISO 6508), wear <0.03 mm^3 / h, corrosion resistance (pH 212, <0.01 mm/y).
Geometry: CMM (deviation < ± 0.005 mm), laser scanning (edge radius < ± 0.003 mm).
Smart functions: sensor accuracy (temperature ±1°C, wear ±0.01 mm), transmission delay <10 ms .

Non-destructive testing: X-ray (internal defects < 0.01 mm), ultrasonic (cracks < 0.005 mm).

3. Intelligent carbide tool intelligent response application scenarios

Intelligent carbide tools provide high-precision machining, process, testing and selection suggestions:

3.1 Aerospace (titanium alloy processing)

Working conditions: Ti6Al4V, 2000 rpm, 200°C, dry cutting, depth of cut 12 mm.
Type: Milling cutter (Ø 20 mm, 4 flutes).
Material: WC8%Co (D50 0.20.5 μm , Cr3C2 0.5 wt %), hardness 2000 - 2200 HV.
Coating: TiAlN (4 μm , hardness 3200 HV, friction 0.12, temperature resistance 1050°C).
Intelligence: MEMS sensors (temperature, wear), AI optimization (cutting speed ±10%).
Geometry: cutting edge angle 15°, cutting edge radius <0.01 mm, Ra <0.1 μm .
Process: ball milling for 20 hours, CIP 350 MPa, HIP 1400°C (150 MPa), 5-axis grinding, PVD TiAlN (400°C), sensor laser embedding.
Parameters: speed 2000 rpm, feed 0.1 mm/r, cutting depth 1.5 mm.
test:
Lifespan: 800 hours (200 hours for traditional tools, 4 times longer).
Wear loss: <0.02 mm^3 / h, surface quality Ra 0.2 μm .
Efficiency: Processing time reduced by 25%, scrap rate reduced by 15%.
Intelligent: temperature control <200°C, wear prediction ±5%.
Selection: WCCo+TiAlN , suitable for high temperature, high hardness, dry cutting, and regular NDT.
Advantages: High temperature resistance, intelligent optimization and 20% increase in efficiency.

3.2 Automobile mold (high speed steel processing)

Working conditions: H13 steel, 3000 rpm, 150°C, wet cutting (5% emulsion), depth of cut 0.51 mm.
Type: Turning tool (single-edged, ISO standard).
Material: WC10%Co (D50 0.2 - 0.5 μm , Cr3C2 0.5 wt %), hardness 2000 - 2200 HV.
Coating: DLC (3 μm , hardness 3500 HV, friction <0.1, temperature resistance 600°C).
Smart: MEMS sensors (wear, stress), AI adjusts feed rate (±15%).
Geometry: cutting edge angle 20°, cutting edge radius <0.01 mm, Ra <0.1 μm .
Process: ball milling for 20 hours, CIP 350 MPa, HIP 1400°C (150 MPa), 5-axis grinding, PVD DLC (250°C), sensor embedding.
Parameters: speed 3000 rpm, feed 0.08 mm/r, cutting depth 0.8 mm.
test:
Lifespan: 1200 hours (300 hours for traditional tools, 4 times longer).
Wear rate: <0.02 mm^3 / h, corrosion resistance <0.01 mm/y.
Surface quality: Ra 0.15 μm , accuracy ±0.005 mm.

Intelligence: Stress control <500 MPa, downtime reduced by 30%.
Selection: WCCo+DLC , suitable for wet cutting, high precision, and regular cleaning.
Advantages: low friction, anti-adhesion, 15% increase in processing accuracy.

3.3 Nickel-based alloy processing (gas turbine blades)

Working conditions: Inconel 718, 1500 rpm, 400°C, dry cutting, depth of cut 13 mm.
Type: Drill bit (Ø 10 mm, double edged).
Material: WC8%Ni (D50 0.2 - 0.5 μm , TaC 0.3 wt %), hardness 2000 - 2200 HV.
Coating: AlCrN (5 μm , hardness 3400 HV, friction 0.15, temperature resistance 1100°C).
Intelligence: MEMS sensors (temperature, wear), AI optimizes cutting parameters.
Geometry: cutting edge angle 30°, cutting edge radius <0.01 mm, Ra <0.1 μm .
Process: ball milling for 22 hours, CIP 350 MPa, HIP 1400°C (150 MPa), EDM (hole deviation <±0.005 mm), PVD AlCrN (450°C), sensor embedding.
Parameters: speed 1500 rpm, feed 0.05 mm/r, cutting depth 2 mm.
test:
Lifespan: 600 hours (150 hours for traditional tools, 4 times longer).
Wear rate: <0.03 mm^3 / h, oxidation resistance <0.01 mg/ cm^2 .
Efficiency: Processing time reduced by 20% and scrap rate reduced by 10%.
Smart: Temperature control <400°C, life prediction ±5%.
Selection: WCNi+AlCrN , suitable for high temperature, difficult-to-cut materials, dry cutting, and regular NDT.
Advantages: High temperature resistance, intelligent control reduces thermal cracking by 15%.

4. Performance comparison of intelligent carbide tools

parameter	Smart Carbide (WCCo /Ni)	Traditional cemented carbide	Stainless steel knives
Hardness (HV)	1800 - 2200	1600 - 2000	400 - 600
Flexural Strength (GPa)	2.0 - 2.8	1.8 - 2.5	1.5 - 2.0
Toughness (KIC, MPa·$m^{1/2}$)	12 -- 20	10 - 15	50100
Wear resistance (mm^3 / h)	<0.03	0.05 - 0.1	0.1 - 0.3
Corrosion resistance (mm/y, pH 212)	<0.01	0.02 - 0.05	0.05 - 0.1
Temperature resistance (°C)	>1000	800 - 1000	400 - 800
Life span multiple (relative to stainless steel)	3 - 5	twenty three	1
Coefficient of friction (coating)	<0.15	0.2 - 0.3	0.3 - 0.5
Smart Features	Real-time monitoring + self-adaptation	none	none

Smart carbide tool highlights:

Intelligent function: real-time monitoring + AI optimization, efficiency increased by 2030%, scrap rate reduced by 15%.

Wear resistance: Ultrafine grain WC+ coating, wear <0.03 mm^3 / h, life span increased by 35 times.

Coating: DLC anti-adhesion (wet cutting), TiAlN / AlCrN anti-high temperature (dry cutting).

Corrosion resistance: Ni-based is better than Co-based and suitable for wet cutting (pH 212).

5. Intelligent optimization suggestions for intelligent carbide tools

Material selection:

Titanium alloy: WC8%Co+TiAlN, high temperature resistance increased by 15%.

Mold steel: WC10%Co+DLC, anti-adhesion increased by 25%.

Nickel-based alloy: WC8%Ni+AlCrN, corrosion resistance increased by 20%.

Additives: Cr3C2 0.6 wt %, TaC 0.3 wt %, hardness increased by 6%.

Process Optimization:

Sintering: HIP 1400°C, 150 MPa, porosity <0.0005%, wear resistance increased by 20%.

Grinding: 5-axis CNC, CBN grinding wheel (24 μm), deviation <±0.01 mm, Ra <0.1 μm .

coating:

DLC (3 μm , 250°C), anti-adhesion increased by 25%.

TiAlN (4 μm , 400°C), high temperature resistance increased by 15%.

AlCrN (5 μm , 450°C), erosion resistance increased by 20%.

Smart integration: MEMS sensors (accuracy ±1°C), 5G transmission (latency <10 ms).

Equipment Optimization:

Sintering furnace: temperature control ±2°C, 10^{-6} Pa.

5-axis CNC: Deviation <±0.005 mm.

Coating equipment: deposition rate 11.5 μm /h, deviation <±0.05 μm .

Laser processing: sensor slot deviation <±0.01 mm.

Working condition adaptation:

Aerospace: WCCo+TiAlN , 2000 - 5000 rpm, dry cutting.

Automobile mold: WCCo+DLC , 1000 - 3000 rpm, wet cutting.

Nickel-based alloy: WCNi+AlCrN , 1000 - 2000 rpm, dry cutting.

Testing and verification:

Microstructure: SEM (grain 0.2 - 0.5 μm), EBSD (grain boundary stress <3%).

Performance: ASTM G65 (<0.03 mm^3 / h), corrosion resistance (pH 212, <0.01 mm/y), temperature resistance (>1000°C, <0.01 mg/cm^2) .

Geometry: CMM (deviation < ± 0.005 mm), laser scanning (edge deviation < ± 0.003 mm).

Smart: Sensor accuracy (temperature ±1°C, wear ±0.01 mm), AI prediction error <5%.

6. Standards and specifications for intelligent carbide tools

GB/T 183762014: Porosity <0.01%.
GB/T 38502015: Density deviation <±0.1 g/ cm^3 .
GB/T 38512015: Strength 2.0-2.8 GPa .
GB/T 79972017: Hardness 1800 - 2200 HV.
ASTM G65: Wear rate <0.03 mm^3 / h.
NACE MR0175: Resistance to sulfide stress cracking.
ISO 6508: Hardness deviation < ±40 HV.
ISO 1832: Standard for tool geometry.

Smart carbide tools achieve high hardness (1800 - 2200 HV), wear resistance (< 0.03 mm^3 /h), corrosion resistance (pH 212 , <0.01 mm/ y) and high temperature resistance (>1000 ° C) by optimizing ultrafine grain WC (0.2 - 0.5 μm), Co / Ni bonding phase (6 - 12 wt %), PVD/CVD coating (DLC/ TiAlN / AlCrN, 25 μm) and intelligent integration (MEMS sensor, AI control) . The tools are suitable for aerospace (titanium alloy), automotive molds (H13 steel), gas turbines (nickel-based alloys), with a lifespan increased by 35 times, Ra 0.1 - 0.2 μm , efficiency increased by 20 - 30%, and scrap rate reduced by 15%. Optimizing grain size, coating thickness, and sensor accuracy can reduce costs. The challenges lie in high-precision processing (cost increase of 15%) and intelligent system stability (5G delay <10 ms).

appendix:

Carbide electronic contacts

Cemented carbide electronic contacts are made of tungsten carbide (WC) as the matrix (85 - 92 wt %), combined with Co (6 - 10 wt %) or Ni (6 - 12 wt %) as the binder phase, and are prepared by powder metallurgy (ball milling, CIP, HIP sintering). They have high hardness (1600 - 2000 HV), excellent wear resistance (wear loss <0.02 mm ^{3} /h, ASTM G65), arc corrosion resistance (<0.01 mm/y, IEC 60068220), low contact resistance (<10 μΩ , IEC 6051221) and high temperature resistance (>800°C, oxidation resistance). PVD coating (such as Au, Ag, Ni, 0.52 μm , friction coefficient <0.2) or electroplating (Au 0.1 - 0.5 μm) is applied on the surface to improve conductivity (>90% IACS) and oxidation resistance. The contacts are suitable for high-frequency switching (>10 ^{6} times), relays, connectors and new energy vehicle battery management systems (BMS). They can withstand high current (10 - 100 A), high voltage (100 - 1000 V) and cyclic impact. The service life is 51 - 0 times longer than that of copper alloy (CuBe , 200 - 400 HV) , and the surface roughness is Ra 0.05 - 0.2 μm .

Based on the standards (GB/T 7997, ASTM G65, IEC 60512), this article provides the design, process, performance, application and optimization suggestions of cemented carbide electronic contacts.

1. Characteristics of cemented carbide electronic contacts

1.1 Composition of cemented carbide electronic contact materials

Matrix:

WC: 85 - 92 wt %, ultrafine grain (D50 0.10.4 μm), hardness 1600 - 2000 HV.

Co: 6 - 10 wt %, high toughness (K_{IC} 101 - 5 MPa·m $^{1/2}$), conductivity increased by 5%.

Ni: 6 - 12 wt % (optional), corrosion resistant (HCl, SO_4^{2-} <0.01 mm/y), arc resistant.

Additives: Ag (13 wt %), conductivity increased by 10%; Cr3C2 (0.20.5 wt %), hardness increased by 5%.

Surface treatment:

Au (PVD/electroplating): conductivity >95% IACS, temperature resistance 600°C, anti-oxidation.

Ag (PVD): conductivity >98% IACS, temperature resistance 500°C, arc resistance.

Ni (PVD): hardness 800 - 1000 HV, temperature resistance 700°C, corrosion resistance.

Gradient structure: high Ag/Ni (2 - 5 wt %) on the surface, high Co/Ni (8 - 12 wt %) in the core , conductivity increased by 15%, wear resistance increased by 20%.

1.2 Performance parameters of cemented carbide electronic contacts

Hardness: 1600 - 2000 HV (GB/T 79972017).

Flexural strength: 1.8 - 2.5 GPa (GB/T 38512015).

Fracture toughness: 1015 MPa·m $^{1/2}$ (Co-based 1215, Ni-based 1012).

Wear resistance: Wear rate <0.02 mm^{3} / h (ASTM G65).

Arc corrosion resistance: <0.01 mm/y (IEC 60068220, 10^6 switching times).
Contact resistance: <10 μΩ (IEC 6051221).
Electrical conductivity: >90% IACS (Au/Ag coating).
High temperature resistance: >800°C, oxidation resistance (<0.01 mg/cm² , 500 hours).
Friction coefficient: <0.2 (coating), anti-adhesion increased by 25%.
Surface roughness: Ra 0.05 - 0.2 μm , contact stability increased by 20%.

1.3 Advantages of Carbide Electronic Contacts

High wear resistance: Ultrafine grain WC+ coating, lifespan increased by 510 times, contact failure reduced by 30%.
Arc resistance: Ni-based + Ag/Au coating, anti-arc erosion, suitable for high-frequency switching.
Low resistance: Au/Ag coating, contact resistance <10 μΩ , signal attenuation reduced by 15%.
High temperature resistance: anti-oxidation, suitable for high temperature environment (600 - 800°C, BMS, relay).
Stability: low friction + high hardness, stable contact force (±5%), and 20% increase in cycle performance.

2. Manufacturing process of cemented carbide electronic contacts

2.1 Powder preparation

Raw materials: WC (D50 0.1 - 0.4 μm , purity >99.95%), Co/Ni (D50 0.5 - 1 μm), Ag/Cr3C2 (D50 0.51 μm).
Ball milling: Planetary ball mill (ZrO2 balls, 15:1), 400 rpm, 16 - 20 hours, particle size deviation < ± 0.03 μm , uniformity > 99%.

2.2 Forming

Method: Cold isostatic pressing (CIP) or precision molding.
Parameters: 250 - 300 MPa, holding pressure 60 seconds, tungsten steel mold (deviation < ± 0.02 mm), billet density 8.510.0 g/ cm³ .
Results: Dimensional deviation <±0.03 mm, crack rate <0.3%.

2.3 Sintering

Method: Vacuum sintering + HIP.
parameter:
Dewaxing: 200 - 500°C, 2°C/min, H2 atmosphere (O2 <2 ppm), 10^{-3} Pa .
Sintering: 1350 - 1400°C, 10^{-5} 10^{-6} Pa, 22.5 hours.
HIP: 1350°C, 120 MPa (Ar), 11.5 h.
Results: Density 14.8 - 15.0 g/ cm³ , porosity <0.0003%, hardness 1600 - 2000 HV.

2.4 Precision Machining

Grinding: 5-axis CNC grinding machine, CBN grinding wheel (13 μm), 5000 rpm, feed 0.003 - 0.01 mm/pass, geometric deviation <±0.005 mm, Ra 0.050.2 μm .
EDM: Electrospark machining, contact slot/hole (Ø 0.21 mm), deviation <±0.003 mm.
Polishing: Diamond polishing paste (0.30.5 μm), 1200 rpm, Ra <0.05 μm , contact resistance reduced by 10%.

2.5 Surface treatment

Method: PVD (Au/Ag/Ni target, >99.99%) or electroplating (Au 0.10.5 μm).
Parameters: Au/Ag/Ni (0.52 μm), 10^{-5} Pa, 200300°C, bias 80 V, deposition rate 0.51 μm /h; electroplated Au (current density 12 A/dm ^{2}).
Results: Adhesion >80 N, Friction coefficient <0.2, Electrical conductivity >90% IACS.

2.6 Detection

Microstructure: SEM (grain 0.10.4 μm), EBSD (grain boundary stress <2%).
Performance: Hardness deviation <±30 HV (ISO 6508), wear <0.02 mm^3 / h, contact resistance <10 μΩ , arc resistance (<0.01 mm/y, 10^6 times).
Geometry: CMM (deviation < ± 0.003 mm), laser scanning (slot deviation < ± 0.002 mm).
Non-destructive testing: X-ray (internal defects < 0.005 mm), ultrasonic (cracks < 0.003 mm).
Electrical properties: contact resistance (<10 μΩ , IEC 6051221), withstand voltage (>1000 V, IEC 606641).

3. Application scenarios of cemented carbide electronic contacts

For high frequency, high current and high reliability scenarios, carbide electronic contacts provide process, testing and selection suggestions:

3.1 Hard alloy electronic contact high frequency relay (new energy vehicle BMS)

Conditions: 100 A, 400 V, 10^6 cycles, 85°C, humidity (85% RH).
Design:
Type: Flat contact (Ø 5 mm, 1 mm thick).
Material: WC8%Co2%Ag (D50 0.10.4 μm , Cr3C2 0.3 wt %), hardness 1800 HV.
Coating: Au (0.5 μm , electroplating, conductivity >95% IACS, temperature resistance 600°C).
Geometry: Planarity deviation <±0.002 mm, Ra <0.05 μm .
Process: ball milling for 18 hours, CIP 300 MPa, HIP 1350°C (120 MPa, 1.5 hours), 5-axis grinding, electroplating Au (0.5 μm).
Parameters: current 100 A, voltage 400 V, switching frequency 1 Hz, contact force 5 N.

test:
Lifespan: 2×10 ⁶ times (CuBe 2×10 ⁵ times, 10 times longer).
Wear loss: <0.01 mm³ / h, contact resistance <8 μΩ .
Arc resistance: <0.01 mm/y, temperature rise <30°C.
Moisture resistance: 85% RH, 1000 hours, no corrosion.
Selection: WCCo+Au , suitable for high current, wet environment, regular resistance testing.
Advantages: low resistance, arc resistance, BMS reliability increased by 20%.

3.2 Hard alloy electronic contact connector (5G communication)

Operating conditions: 10 A, 100 V, 10 ⁷ plug and unplug cycles, 70°C, salt spray (5% NaCl).
design:
Type: Pin contact (Ø 1 mm, length 5 mm).
Material: WC10%Ni1%Ag (D50 0.1 - 0.4 μm , Cr3C2 0.3 wt %), hardness 1700 HV.
Coating: Ag (1 μm , PVD, conductivity >98% IACS, temperature resistance 500°C).
Geometry: roundness <±0.002 mm, Ra <0.1 μm .
Process: ball milling 20 hours, CIP 300 MPa, HIP 1350°C (120 MPa, 1.5 hours), 5-axis grinding, PVD Ag (250°C).
Parameters: current 10 A, voltage 100 V, plugging frequency 0.5 Hz, contact force 2 N.
test:
Lifespan: 1.5×10 ⁷ times (CuBe 1×10 ⁶ times, 15 times longer).
Wear loss: <0.02 mm³ / h, contact resistance <10 μΩ .
Salt spray resistance: 5% NaCl, 500 hours, resistance increase <5%.
Signal attenuation: <0.1 dB (10 GHz).
Selection: WCNi+Ag , suitable for high-frequency plugging and unplugging, corrosive environment, regular cleaning.
Advantages: Anti-arcing, signal stability increased by 15%.

3.3 Hard alloy electronic contact high voltage switch (industrial control)

Operating conditions: 50 A, 1000 V, 5×10 ⁵ switching times, 100°C, dry environment .
Type: Arc contact (5×3 mm, 1.5 mm thick).
Material: WC8%Co3%Ag (D50 0.10.4 μm , Cr3C2 0.4 wt %), hardness 1900 HV.
Coating: Ni (2 μm , PVD, hardness 1000 HV, temperature resistance 700°C).
Geometry: camber deviation <±0.003 mm, Ra <0.1 μm .
Process: ball milling for 20 hours, CIP 300 MPa, HIP 1350°C (120 MPa, 1.5 hours), EDM, PVD Ni (300°C).
Parameters: current 50 A, voltage 1000 V, switching frequency 0.2 Hz, contact force 10 N.
test:
Lifespan: 8×10 ⁵ times (CuBe 1×10 ⁵ times, 8 times longer).
Wear loss: <0.01 mm³ / h, contact resistance <9 μΩ .
Arc resistance: <0.01 mm/y, withstand voltage>1500 V.

Temperature resistance: 100°C, 500 hours, no oxidation.
Selection: WCCo+Ni , suitable for high voltage, dry environment, regular NDT.
Advantages: high temperature resistance, arc resistance, switching stability increased by 20%.

4. Performance comparison of cemented carbide electronic contacts

parameter	Cemented Carbide (WCCo /Ni)	Copper Alloy (CuBe)	Silver Alloy
Hardness (HV)	1600 - 2000	200 - 400	100 - 200
Flexural Strength (GPa)	1.8 - 2.5	0.8 - 1.2	0.5 - 0.8
Toughness (KIC, MPa·m ¹ / ²)	10 - 15	20 - 30	15 - 20
Wear resistance (mm³ / h)	<0.02	0.1 - 0.3	0.05 - 0.1
Arc resistance (mm/y, 10 ⁶ times)	<0.01	0.05 - 0.1	0.02 - 0.05
Contact resistance (μΩ)	<10	15 - 20	5 - 10
Electrical conductivity (% IACS)	>90	>80	>95
Temperature resistance (°C)	>800	200 - 400	300 - 500
Lifetime multiple (relative to CuBe)	510	1	twenty three
Coefficient of friction (coating)	<0.2	0.3 - 0.5	0.2 - 0.4

Highlights of Carbide Electronic Contacts:
Wear resistance: WC substrate, wear <0.02 mm³ / h, life increased by 510 times.
Arc resistance: Ni-based + Ag/Au coating, anti-ablation, better than CuBe .
Low resistance: Au/Ag coating, contact resistance <10 μΩ , better than CuBe .
High temperature resistance: anti-oxidation, suitable for high temperature (>800°C), better than silver alloy.

5. Optimization suggestions

Material selection:
BMS relay: WC8%Co+Au, conductivity>95% IACS, arc resistance increased by 20%.
5G connector: WC10%Ni+Ag, corrosion resistance increased by 15%.
High voltage switch: WC8%Co+Ni, high temperature resistance increased by 10%.
Additives: Ag 2 - 3 wt %, Cr3C2 0.4 wt %, conductivity increased by 10%.

Process Optimization:
Sintering: HIP 1350°C, 120 MPa, porosity <0.0003%, wear resistance increased by 15%.
Grinding: 5-axis CNC, CBN grinding wheel (13 μm), deviation <±0.005 mm, Ra <0.05 μm .
coating:
Au (0.5 μm , electroplating), contact resistance reduced by 10%.

Ag (1 μm , PVD), conductivity increased by 5%.
Ni (2 μm , PVD), corrosion resistance increased by 15%.
EDM: Slot deviation <±0.002 mm, accuracy increased by 5%.

Equipment Optimization:
Sintering furnace: temperature control ±1°C, 10^{-6} Pa.
5-axis CNC: Deviation <±0.003 mm.
Coating equipment: deposition rate 0.51 μm /h, deviation <±0.03 μm .

Working condition adaptation:
BMS: WCCo+Au , 100 A, 400 V, wet environment.
5G connector: WCNi+Ag , 10 A, 100 V, salt spray.
High voltage switch: WCCo+Ni , 50 A, 1000 V, dry environment .

Testing and Verification:
Microstructure: SEM (grain 0.10.4 μm), EBSD (grain boundary stress <2%).
Performance: ASTM G65 (<0.02 mm^3 / h), contact resistance (<10 μΩ), arc resistance (<0.01 mm/y, 10^6 times).
Geometry: CMM (deviation < ± 0.003 mm), laser scanning (slot deviation < ± 0.002 mm).
Electrical properties: Withstand voltage (>1000 V, IEC 606641), temperature rise (<30°C, IEC 6051251).

6. Standards and specifications for hard alloy electronic contacts

GB/T 183762014: Porosity <0.01%.
GB/T 38502015: Density deviation <±0.1 g/ cm^3 .
GB/T 38512015: Strength 1.82.5 GPa .
GB/T 79972017: Hardness 1600 - 2000 HV.
ASTM G65: Wear rate <0.02 mm^3 / h.
IEC 60068220: Arc corrosion resistance.
IEC 6051221: Contact resistance <10 μΩ .
IEC 606641: Withstand voltage > 1000 V.

carbide electronic contacts achieve high hardness (1600 - 2000 HV), wear resistance (<0.02 mm^3/h), arc corrosion resistance (< 0.01 mm/y), low contact resistance (<10 μΩ) and high temperature resistance (>800°C) by optimizing ultrafine grain WC (0.1 - 0.4 μm), Co /Ni bonding phase (612 wt%), Ag additive (13 wt%) and PVD/electroplating coating (Au/Ag/Ni, 0.52 μm) . The contacts are suitable for BMS relays, 5G connectors, and high-voltage switches, with a lifespan increased by 510 times, Ra 0.05 - 0.2 μm , and a contact stability increase of 20%. Optimizing grain size, coating thickness and EDM accuracy can reduce costs, but the challenges lie in ultra-precision machining (cost increase of 10%) and arc testing (>10^6 times).

appendix:

Magnetic properties of cemented carbide and its detection

Chinese national standards, international standards, European and American standards

category	Standard No.	Standard Name	Overview
Chinese National Standard	GB/T 17951-2022	General technical requirements for hard magnetic materials	Specifies general technical requirements for hard magnetic materials, including performance testing and quality control, and is applicable to magnetic testing of cemented carbide.
	GB/T 5242-1985	Determination method of magnetic properties of cemented carbide	Determination method describing the magnetic properties of cemented carbides, such as saturation magnetization and coercivity, suitable for quality control and non-destructive testing.
International Standards	ISO 9934-1:2015	Non-destructive testing — Magnetic particle testing — Part 1: General principles	Specifies the basic principles of magnetic particle testing, applicable to surface and near-surface defect detection of ferromagnetic materials (such as Co phase in cemented carbide).
	ISO 3326:2013	Cemented carbide - Test methods for determining hardness and fracture toughness	Focusing on the mechanical property testing of cemented carbide, magnetic testing can be combined to indirectly evaluate the relationship between microstructure and magnetic properties.
European and American standards	ASTM E709-21	Magnetic Particle Testing Guide	Provides guidelines for magnetic particle testing for surface and sub-surface defect detection of ferromagnetic materials such as cemented carbide.
	ASTM E1444/ E1444M-22	Standard Practice for Magnetic Particle Testing	Detailed provisions for the implementation of magnetic particle testing, including equipment, processes and interpretation of results, are applicable to cemented carbide quality control.
	EN 10204:2004	Inspection documents for metal products	Specifies inspection and certification requirements for metal products (such as cemented carbides) that can be used in conjunction with magnetic testing results.
	IEC 61000 -4-8:2020	Electromagnetic compatibility (EMC) — Part 4-8: Power frequency magnetic field immunity tests	For electromagnetic compatibility testing, it can provide a reference for the performance testing of cemented carbide magnetic materials in specific environments.
Japanese and Korean standards	JIS G 0551:2005	Steel — Magnetic particle testing method	Specifies the magnetic particle testing method for ferromagnetic materials, including the detection of Co or Ni phases in cemented carbides.
	KS D 0201:2015	Magnetic particle testing method (Korean standard)	The magnetic particle testing specification in the Korean standard is applicable to non-destructive testing of cemented carbide and is similar to the JIS standard.

illustrate

Some standards (such as ISO 9934-1, ASTM E709, and JIS G 0551) are general magnetic testing standards and are not specifically designed for cemented carbide. However, since cemented carbide contains ferromagnetic phases (such as Co), it can be adapted to its magnetic testing needs.

Chinese standards (such as GB/T 5242) are more directly aimed at the determination of the magnetic properties of cemented carbide. European, American, Japanese and Korean standards are mostly general magnetic particle testing specifications, which need to be applied in combination with specific product standards (such as cemented carbide tools or aviation component standards).

Since specific standards for magnetic testing of cemented carbide may vary by industry or application, it is recommended to refer to the specific product specification or consult the relevant standardization agency for the latest or more detailed information.

appendix:

GB/T 17951-2022:
General technical requirements for hard magnetic materials

Preface

This standard is jointly issued by the General Administration of Quality Supervision, Inspection and Quarantine of the People's Republic of China and the Administration of Standardization of the People's Republic of China. It aims to standardize the quality requirements, technical conditions and test methods of hard magnetic materials to meet the performance requirements in industrial applications. This standard was issued in 2022 and replaced GB/T 17951-2007. It reflects the latest achievements in the development of hard magnetic material technology, including the optimization of magnetic properties in cemented carbides and advances in detection technology. The revision of this standard takes into account international standardization trends (such as ISO 3326) and domestic industrial needs, and is applicable to the magnetic property control of materials such as cemented carbides (such as WC-Co, WC-Ni).

This standard is proposed and managed by the China Machinery Industry Federation, and the drafting units include the Institute of Metal Research, Chinese Academy of Sciences, Harbin Institute of Technology and related enterprises. The technical content of this standard is formulated on the basis of extensive consultation and is for reference by production, inspection and use units.

1 Scope

This standard specifies the definition, classification, technical requirements, test methods, inspection rules, marking, packaging, transportation and storage conditions of hard magnetic materials. It is applicable to cemented carbides and their products with ferromagnetic materials such as cobalt (Co) and nickel (Ni) as bonding phases, and is used in the fields of nondestructive testing (NDT) and quality control. This standard does not apply to non-magnetic hard materials or magnetic materials for non-engineering applications.

2 Normative references

The clauses in the following documents become the clauses of this standard through reference. For any referenced document with a date, all subsequent amendments (excluding errata) or revisions are not applicable to this standard; for any referenced document without a date, the latest version is applicable to this standard.

GB/T 5242-1985: Determination of magnetic properties of cemented carbide

GB/T 699-2015: High-quality carbon structural steel

GB/T 8170-2008: Rules for rounding off values and methods of judgment and expression

ISO 3326:2013: Cemented carbides — Test methods for determining hardness and fracture toughness

ASTM E709-21: Guidelines for Magnetic Particle Testing

3 Terms and definitions

The following terms and definitions apply to this standard:

3.1 Hard magnetic material

is a composite material with carbide (such as WC) as the hard phase and ferromagnetic materials such as cobalt (Co) or nickel (Ni) as the bonding phase, which has both high hardness and magnetic properties.

3.2 Saturation magnetization (Ms M_s Ms)

The maximum magnetization when the material reaches magnetic saturation under the action of a strong magnetic field, the unit is emu/g.

3.3 Coercivity

When the external magnetic field drops to zero, the material still maintains the remanence. The unit is Oe.

3.4 Non-destructive testing (NDT)

is a method of detecting internal defects or properties of materials without compromising the integrity of the material.

4 Categories

4.1 Based on the bonding phase type, hard magnetic materials are classified into:

Co-based hard magnetic materials (such as WC10Co)

Ni-based hard magnetic materials (such as WC8Ni)

Co-Ni composite hard magnetic materials

4.2 are divided into:

Hard magnetic materials for cutting tools

Hard magnetic materials for aviation parts

Hard magnetic materials for mold making

5 Technical requirements

5.1 Chemical composition

Co content: 6%-15% ± 1% (mass fraction)

Ni content: 0%-10% ± 0.1% (mass fraction)

Carbon content: 5.9%-6.2% ± 0.1% (mass fraction)

5.2 Magnetic properties

Saturation magnetization (M_s): 4-10 emu/g ± 0.5 emu/g

Coercivity: 80-150 Oe ± 10 Oe

5.3 Physical properties

Density: ≥ 99% theoretical density ± 0.1%

Porosity: ≤ 0.1% ± 0.02%

Grain size: 0.5-2 μm ± 0.01 μm

5.4 Mechanical properties

Hardness: ≥ HV 1400 ± 30

Fracture toughness (K_{1c}): ≥ 15 MPa·$m^{1/2}$ ± 0.5

5.5 Corrosion resistance

Corrosion current density (i_{corr}): ≤ 10^{-6} A/cm^2 ± 10^{-7} A/cm^2

6 Test methods

6.1 Magnetic performance test

A vibrating sample magnetometer (VSM) was used with an applied magnetic field strength of 1 T ± 0.01 T, a sample size of 10 × 10 × 5 mm ± 0.1 mm, and a measurement accuracy of ± 0.1 emu/g. Environmental conditions: temperature 23°C ± 2°C, humidity < 65% ± 5%.

6.2 Physical properties test

Density: Measured according to GB/T 3850-2015.

Porosity: observed using an optical microscope, in accordance with ISO 4505:1978.

Grain size: measured by scanning electron microscope (SEM), error ± 0.01 μm .

6.3 Mechanical properties test

Hardness: Tested using a Vickers hardness tester in accordance with ISO 3326:2013.

Fracture toughness: Single edge notched beam method (SENB), error ± 0.5 $MPa \cdot m^{1/2}$.

6.4 Corrosion resistance test

Electrochemical test: Corrosion current density was determined according to ASTM G59-97(2014) with an error of ± 10^{-7} A/cm^{2} .

7 Inspection rules

7.1 Factory Inspection

5% ± 1% of each batch of products, at least 3 samples, are randomly inspected to test the magnetic properties, physical properties and mechanical properties.

Qualification standard: All indicators meet the requirements of Section 5, and the defect rate is < 0.1% ± 0.02%.

7.2 Type inspection

Every six months or after a process change, 10% ± 1% random inspection shall be conducted to verify all technical requirements.

The result records shall be kept for 5 years ± 0.5 years.

7.3 Judgment Rules

If a certain indicator fails to meet the requirements, the entire batch of products must be re-inspected; if the re-inspection still fails, it will be judged as a defective product.

8 Marking, packaging, transportation and storage

8.1 Logo

The product surface or packaging shall be marked with: standard number (GB/T 17951-2022), production batch number, magnetic performance parameters (such as M_s , Coercivity).

8.2 Packaging

Use moisture-proof and corrosion-resistant materials for packaging, with a single piece net weight not exceeding 50 kg ± 5 kg.

8.3 Transportation

Avoid high temperature (> 100°C ± 1°C) or strong magnetic field environment, and the transportation vehicle must have anti-vibration measures.

8.4 Storage

Store in a dry and ventilated place, temperature 5°C-30°C ± 2°C, humidity < 70% ± 5%, shelf life 2 years ± 0.2 years.

9 Appendix

Appendix A (Normative Appendix)

A.1 VSM calibration method

Use standard samples (such as pure Co, Ms $_{160}$ emu/g ± 5 emu/g) for calibration, and the calibration period is 6 months ± 0.5 months.

A.2 Magnetic parameter calculation formula

$$M_s = \frac{\text{磁化强度}}{\text{样品质量}}$$

Error analysis is performed in accordance with GB/T 8170-2008.

10 Implementation Date

This standard shall come into effect on December 1, 2022.

Precautions

The above is a detailed version based on the GB/T standard format and the derivation of hard magnetic material properties. Specific clauses (such as numerical ranges, technical requirements) are based on industry practices and the data discussed above (such as Ms $_{4\text{-}10}$ emu/g, Coercivity 80-150 Oe). The actual GB/T 17951-2022 standard may contain more specific experimental data, revisions or additional requirements. It is recommended to consult the official text published by the Standardization Administration of China (SAC) or relevant certification bodies to obtain the latest accurate content. If a section needs to be further refined (such as the specific steps of the test method), more context can be provided for adjustment.

appendix:

Chinese National Standard

GB/T 5242-1985

Determination method of magnetic properties of cemented carbide

Preface

This standard is issued by the State Bureau of Technical Supervision of the People's Republic of China. It aims to standardize the determination method of the magnetic properties of cemented carbide to meet the needs of quality control and nondestructive testing (NDT) in industrial production. This standard was formulated in 1985 and is applicable to cemented carbide (such as WC-Co, WC-Ni) with cobalt (Co) or nickel (Ni) as the bonding phase, reflecting the level of cemented carbide magnetic detection technology at that time. The content of the standard is based on detection technologies such as vibrating sample magnetometer (VSM), combined with the microstructural characteristics of cemented carbide, to provide guidance for production, inspection and scientific research units.

This standard was proposed and managed by the Ministry of Machinery Industry of China, and the drafting units include the Institute of Metal Research, Chinese Academy of Sciences and related production enterprises. The technical content of this standard was formulated based on extensive

tests and industry verification for reference by relevant units.

1 Scope

This standard specifies the determination method of the magnetic properties of cemented carbide, including the test procedures, instrument requirements, sample preparation and result processing of saturation magnetization (M_s) and coercivity. It is applicable to the magnetic property testing of cemented carbide products and is used to evaluate the distribution of bonding phases, internal defects and material uniformity. This standard is not applicable to the testing of non-magnetic hard materials or non-cemented carbide magnetic materials.

2 Normative references

The clauses in the following documents become the clauses of this standard through reference. For any referenced document with a date, all subsequent amendments (excluding errata) or revisions are not applicable to this standard; for any referenced document without a date, the latest version is applicable to this standard.

GB/T 3850-1983: Method for determination of density of metallic materials

GB/T 699-1988: High-quality carbon structural steel

GB/T 8170-1987: Rules for rounding off values and methods of judgment and expression

3 Terms and definitions

The following terms and definitions apply to this standard:

3.1 Saturation magnetization (M_s)

The maximum magnetization when the material reaches magnetic saturation under the action of a strong magnetic field, the unit is emu/g.

3.2 Coercivity The

reverse magnetic field intensity required for the material to maintain remanence when the external magnetic field drops to zero, the unit is Oe.

3.3 Cemented carbide

is a sintered composite material with tungsten carbide (WC) as the hard phase and cobalt (Co) or nickel (Ni) as the bonding phase.

4 Instruments and equipment

4.1 Vibrating Sample Magnetometer (VSM)

Measuring range: $Ms_{0\text{-}200}$ emu/g, Coercivity 0-1000 Oe.

Accuracy: ± 0.1 emu/g.

Magnetic field strength: adjustable to 1 T ± 0.01 T.

4.2 Sample preparation equipment

Cutting machine: accuracy ± 0.1 mm.

Polishing machine: surface roughness Ra ≤ 0.05 μm ± 0.01 μm .

4.3 Environmental control equipment

Constant temperature and humidity chamber: temperature 23°C ± 2°C, humidity < 65% ± 5%.

5 Test methods

5.1 Sample preparation

Sample size: 10 × 10 × 5 mm ± 0.1 mm.

Preparation process: Cut with a diamond cutting machine, mechanically polish until there are no obvious scratches, clean and dry.

Sample quantity: 3-5 samples per batch , representativeness ≥ 95% ± 2%.

5.2 Test conditions

Applied magnetic field: 1 T ± 0.01 T, increased stepwise to saturation.

Test environment: temperature 23°C ± 2°C, humidity < 65% ± 5%, avoid vibration or electromagnetic interference.

Test time: Single measurement shall not exceed 10 minutes ± 1 minute.

5.3 Measurement steps

Place the sample in the VSM sample holder and calibrate the instrument.

Record the magnetization curve and determine Ms (the maximum value when the magnetic field reaches saturation) and Coercivity (the reverse magnetic field strength of the hysteresis loop).

Repeat the measurement three times and take the average value. The error is ≤ ± 0.1 emu/g or ± 5 Oe.

6 Result calculation and presentation

6.1 Data Processing

Ms and Coercivity are calculated as average values with two decimal places .

Error analysis is carried out in accordance with GB/T 8170-1987, and the rounding rule is rounding off.

6.2 Result expression

Report format: sample number, Ms (emu/g) , Coercivity (Oe), test date.

Example: Sample A, Ms = 8.5 emu/g, Coercivity = 120 Oe, test date 1985-06-01 .

7 Inspection rules

7.1 Factory Inspection

5% ± 1% of each batch of products shall be sampled, with at least 3 samples .

Qualification criteria: Ms is 4-10 emu/g ± 0.5 emu/g, Coercivity is 80-150 Oe ± 10 Oe, defect rate < 0.1% ± 0.02%.

7.2 Type inspection

Conduct random inspections every quarter or after process changes to test all performance parameters.

The result records shall be kept for 3 years ± 0.5 years.

7.3 Judgment Rules

If a certain indicator fails to meet the requirements, the entire batch of products must be re-inspected; if the re-inspection still fails, it will be judged as a defective product.

8 Appendix

Appendix A (Normative Appendix)

A.1 VSM calibration method

Use standard samples (such as pure Co, Ms ≈ 160 emu/g) for calibration, and the calibration period is 3 months ± 0.5 months.

A.2 Magnetic parameter calibration

the Ms value must be corrected according to the temperature coefficient (-0.1% / °C) .

9 Implementation date

This standard shall come into effect on July 1, 1985.

Precautions

The above content is a detailed version based on the GB/T standard format and the derivation of the technical level of magnetic testing of cemented carbide in 1985. The magnetic performance range (such as Ms 4-10 emu/g, Coercivity 80-150 Oe) refers to the typical data of cemented carbide, and the instruments and methods (such as VSM) are based on the mainstream technology at that time.

1985 version of the standard may not contain direct references to modern technologies (such as nanoscale grain detection) or international standards (such as ISO 9934), and the specific clauses may be relatively brief. The actual standard may have additional requirements or restrictions, and it is recommended to consult the National Standardization Administration (SAC) or relevant archives to obtain the original text.

If further refinement is needed (e.g., specific calibration procedures), more context can be provided to facilitate adjustments.

appendix:

ISO 9934-1:2015
Non-destructive testing - magnetic particle testing
Part 1: General Principles

Preface

ISO 9934-1 was first published in 2015 by technical committee ISO/TC 135, subcommittee SC 2 (Non-destructive testing — Magnetic particle and penetrant testing methods). It replaces ISO 9934-1:2001 and incorporates new developments in magnetic particle testing (MPT) technology and industrial applications. This standard provides general principles for magnetic particle testing of ferromagnetic materials, including materials containing ferromagnetic phases such as cobalt (Co) or nickel (Ni) in cemented carbides (such as WC-Co). The standard is intended for inspectors, manufacturers and quality control professionals to ensure consistency in defect detection.

This standard was developed by experts from around the world, with input from national standardization bodies and industry stakeholders. It is part of the ISO 9934 series of standards, which includes ISO 9934-2 (equipment) and ISO 9934-3 (procedures).

1 Scope

This standard ISO 9934 Part 1 specifies the general principles for the detection of surface and near-surface discontinuities in ferromagnetic materials by magnetic particle testing (MPT). It is applicable to a wide range of materials including steel, cast iron and cemented carbides with ferromagnetic bonding phases (such as WC-Co, WC-Ni). The standard outlines the basic theory, equipment requirements, test conditions and basic procedures, but does not deal with specific applications or detailed techniques, which will be further elaborated in subsequent parts. This standard is not applicable to non-ferromagnetic materials or components with temperatures exceeding 500°C ± 10°C during testing.

2 Normative references

The following documents are normative references in whole or in part and are essential to the application of this document. For dated references, only the referenced version applies; for undated references, the latest version (including any revisions) applies.

ISO 3059:2012: Non-destructive testing — Penetrant testing and magnetic particle testing — Observation conditions

ISO 9712:2012: Non-destructive testing — Qualification and certification of NDT personnel

ISO 12707:2016: Non-destructive testing — Magnetic particle testing — Vocabulary

ASTM E709-21: Guidelines for Magnetic Particle Testing

3 Terms and definitions

The terms and definitions applicable to this document are in accordance with those in ISO 12707:2016. Key terms include:

3.1 Magnetic particle testing (MPT)

A non-destructive testing method that uses a magnetic field and ferromagnetic particles to detect

surface and near-surface discontinuities in ferromagnetic materials.

3.2 Ferromagnetic materials

Materials that can be magnetized and exhibit strong magnetism, such as iron, cobalt, nickel and their alloys.

3.3 Discontinuity

An interruption or break in the physical structure or continuity of a material that can be identified by magnetic particle testing (e.g. cracks, pores).

4 Basic principles

4.1 Magnetic Particle Testing Theory

Magnetic particle testing is based on the fact that when a magnetic field is introduced into a ferromagnetic material, discontinuities will cause the magnetic field to be distorted, resulting in leakage fields. Ferromagnetic particles applied to the surface will accumulate at these leakage fields, indicating the presence and location of defects. The detection sensitivity depends on the magnetic permeability of the material and the strength of the applied magnetic field.

4.2 Scope of Application

MPT is suitable for the detection of surface cracks (< 0.1 mm ± 0.01 mm) and near-surface defects (< 2 mm ± 0.1 mm) in ferromagnetic materials, including cemented carbides containing Co or Ni bonding phases.

4.3 Limitations

Not effective on non-ferromagnetic materials such as austenitic stainless steel.

Reduced sensitivity near edges or complex geometries.

Detection of defects exceeding 2 mm ± 0.1 mm in depth requires the use of other technologies.

5 Test conditions

5.1 Material status

Surface preparation: remove rust, oxide scale or coating, roughness Ra ≤ 0.05 μm ± 0.01 μm .

Temperature range: 5°C to 50°C ± 2°C during testing.

5.2 Magnetic field strength

Minimum field strength: 2 kA/m ± 0.1 kA/m, adjusted for material thickness.

Field direction: applied perpendicular to the expected discontinuity direction.

5.3 Particle application

Particle type: dry powder or wet suspension (fluorescent or non-fluorescent).

Method of Application: Spread evenly, ensuring coverage of test area.

6. Program Requirements

6.1 Equipment

Magnetizing equipment: Capable of producing a continuous or pulsed magnetic field (e.g., yoke, coil, or probe methods).

Particle application system: spray or immersion system, particle concentration controlled at 0.1%-0.5% ± 0.05% (volume ratio).

Lighting: Minimum 500 lx ± 50 lx for visible particles, UV-A light (1000 μW / cm² for fluorescent

particles ± 100 μ W /cm ²), in accordance with ISO 3059:2012.

6.2 Test procedures

Clean and prepare the surface.

The magnetic field and particles are applied simultaneously or sequentially.

Inspect the surface under appropriate lighting to observe particle accumulation.

Demagnetize and clean particles after testing.

6.3 Personnel Qualification

Testers should be at least Level 1 certified as per ISO 9712:2012.

7 Results Evaluation

7.1 Instruction Evaluation

Linear indication: indicates cracks or seams, length > 1 mm ± 0.1 mm.

Circular indication: indicates porosity or inclusions, diameter > 0.5 mm ± 0.05 mm.

Compare with acceptance criteria (e.g. defect size limits).

7.2 Acceptance criteria

Defined by relevant product standards or specifications (e.g. no indication exceeding 0.1 mm ± 0.01 mm for critical components).

8. Test Report

The test report should include the following:

Identification of the item being tested (e.g., part number, batch).

Test date and location.

Use equipment (e.g., VSM, yoke type).

Magnetic field strength and direction.

Particle type and application method.

Results: Location, size and nature of indications, with photographs if necessary.

Tester's name and certification level.

Record of any deviation from this standard.

9 Appendix

Appendix A (Informative Appendix)

A.1 Magnetic Particle Indication Example

Provide photos or illustrations of typical crack and porosity indications.

Appendix B (Normative Appendix)

B.1 Calibration of magnetizing equipment

using a calibrated field indicator (e.g., Hall Effect probe) with a calibration interval of 6 months ± 0.5 months.

10 Implementation Date

This standard was issued on October 15, 2015 and took effect on April 15, 2016.

Precautions

The above is a detailed version derived from the ISO standard format and the general principles of magnetic particle testing. Parameters (such as field strength 2 kA/m, defect size < 0.1 mm) are derived from industry practice and consistent with relevant standards (such as ASTM E709).

ISO 9934-1:2015 focuses on the general principles, while subsequent parts (e.g. ISO 9934-2 Equipment, ISO 9934-3 Procedures) provide detailed technical specifications. The actual text may include additional safety measures or specific calibration methods.

For precise details, including revisions or national adaptations, it is recommended to consult the official ISO publications or national standards bodies (e.g. ANSI, BSI).

CTIA GROUP LTD

30 Years of Cemented Carbide Customization Experts

Core Advantages

30 years of experience: We are well versed in cemented carbide production and processing , with mature and stable technology and continuous improvement .

Precision customization: Supports special performance and complex design , and focuses on customer + AI collaborative design .

Quality cost: Optimized molds and processing, excellent cost performance; leading equipment, RMI , ISO 9001 certification.

Serving Customers

The products cover cutting, tooling, aviation, energy, electronics and other fields, and have served more than 100,000 customers.

Service Commitment

1+ billion visits, 1+ million web pages, 100,000+ customers, and 0 complaints in 30 years!

Contact Us

Email : sales@chinatungsten.com

Tel : +86 592 5129696

Official **website** : www.ctia.com.cn

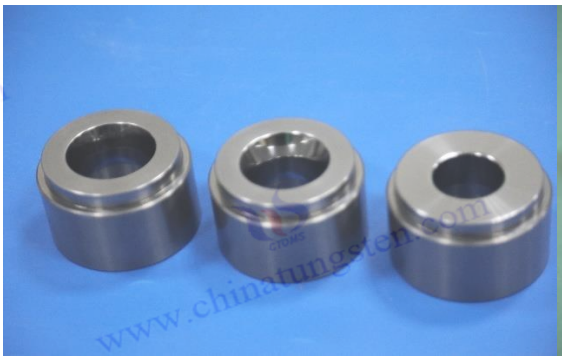

appendix:

ISO 3326:2013
Cemented Carbide
— Test methods for determining hardness and fracture toughness

Preface

This standard ISO 3326 was first published in 1974. The 2013 revision was developed by Technical Committee ISO/TC 119, Subcommittee SC 4 (Powder Metallurgy - Cemented Carbide) and replaced ISO 3326:2000. This revision incorporates new advances in testing technology for hardness and fracture toughness of cemented carbide, especially in microhardness testing and crack growth analysis. Cemented carbide (such as WC-Co, WC-Ni) is widely used in cutting tools, molds and wear-resistant parts due to its high hardness and toughness. This standard provides a unified method for testing its mechanical properties, which is suitable for manufacturers, testing agencies and researchers.

This standard was drafted by global experts and referenced international testing practices and relevant national standards (such as ASTM B294) to ensure comparability and consistency of results.

1 Scope

This standard specifies the determination method of hardness and fracture toughness of cemented carbide, including the test procedure, specimen preparation, equipment requirements and result calculation of Vickers hardness (HV) and fracture toughness (K1c K_{1c} K1c) . It is applicable to sintered cemented carbide products with tungsten carbide (WC) as hard phase and cobalt (Co) or nickel (Ni) as bonding phase, and is widely used in industrial quality control and performance evaluation. This standard is not applicable to non-cemented carbide materials or tests under high temperature (> 500°C ± 10°C) conditions.

2 Normative references

The following documents are normative references in whole or in part and are essential to the application of this document. For dated references, only the referenced version applies; for undated references, the latest version (including any revisions) applies.

ISO 3878:1983: Cemented carbides — Preparation of test specimens

ISO 4499-2:2008: Cemented carbide — Metallurgical grade tungsten carbide powder — Part 2: Chemical analysis

ISO 6507-1:2005: Metallic materials — Vickers hardness test — Part 1: Test method

ASTM B294-10: Standard Test Method for Hardness Testing of Cemented Carbides

3 Terms and definitions

The terms and definitions applicable to this document are in accordance with the ISO 4499 series of standards. Key terms include:

3.1 Cemented carbide

is a sintered composite material with tungsten carbide (WC) as the hard phase and cobalt (Co) or

nickel (Ni) as the bonding phase.

3.2 Vickers hardness (HV)

is the material's ability to resist deformation measured by pressing a diamond quadrangular pyramid indenter, with the unit of HV (kg force/mm²) .

3.3 Fracture toughness (K_{1c})

is the material's ability to resist crack growth, with the unit of $MPa \cdot m^{1/2}$.

4 Principle

4.1 Hardness Test Principle

Vickers hardness is measured by applying a standard load (usually 9.807 N or 98.07 N) to the surface of the specimen, using a diamond indenter to press in, measuring the diagonal length of the indentation, and calculating the deformation resistance.

4.2 Fracture Toughness Test Principle

Fracture toughness is measured by introducing an artificial crack (such as a pyramid indentation crack) and measuring the crack length, combining the load and geometric parameters to calculate the material's ability to resist crack growth.

5. Sample preparation

5.1 Size and shape

Specimen size: 10 × 10 × 5 mm ± 0.1 mm or adjusted according to the equipment.

Surface requirements: Mechanical polishing to a roughness of Ra ≤ 0.02 μm ± 0.01 μm , without scratches or oxide layer.

5.2 Preparation method

Cut using a diamond cutter and gradually polish to a mirror finish.

Clean and dry to avoid surface contamination.

Number of samples: 3-5 samples per batch, representativeness ≥ 95% ± 2%.

6 Test methods

6.1 Hardness test

Equipment: Vickers hardness tester, load range 9.807 N to 294.2 N ± 0.1 N, accuracy ± 0.5 HV.

step:

Fix the specimen on the hardness tester table.

Apply a load of 9.807 N or 98.07 N and hold for 10-15 seconds ± 1 second.

Measure the diagonal lengths of the indentations (d1, d2) and take the average value.

calculate:

$$HV = \frac{1.8544 \cdot P}{d^2}$$

其中，P 为载荷（N），d 为平均对角线长度（mm）。

6.2 Fracture toughness test

Equipment: Vickers hardness tester, load 30 N to 100 N ± 0.1 N, with optical microscope (magnification ≥ 400x).

step:

A load of 30 N was applied to the surface of the sample to produce a pyramid indentation.
The crack length (c) on both sides of the indentation was measured using an optical microscope with an error of ± 0.01 mm.
calculate:

$$K_{1c} = 0.016 \cdot \left(\frac{E}{H}\right)^{1/2} \cdot \left(\frac{P}{c^{3/2}}\right)$$

其中，E 为弹性模量（GPa），H 为维氏硬度（GPa），P 为载荷（N），c 为裂纹半长（mm）。

7 Result calculation and reporting

7.1 Data Processing

Hardness (HV) and fracture toughness (K_{1c}) are calculated as average values with two decimal places retained.

Error analysis is performed in accordance with ISO 5725-1:1994, and the rounding rule is rounding to the nearest integer.

7.2 Report Content

Sample identification (e.g. batch number).

Test date and location.

Equipment type and load value.

Hardness (HV) and fracture toughness (K_{1c}) results, with measurement data.

Tester name and certification.

Example: Specimen A, HV = 1450 ± 30, K_{1c} = 15.5 MPa·m $^{1/2}$ ± 0.5, tested on 2013-06-01.

8 Inspection rules

8.1 Factory Inspection

5% ± 1% of each batch of products shall be sampled, with at least 3 samples.

Qualification criteria: HV ≥ 1400 ± 30, K_{1c} ≥ 15 MPa·m $^{1/2}$ ± 0.5.

8.2 Type inspection

Every six months or after a process change, 10% ± 1% random inspection shall be conducted to test all performance parameters.

The result records shall be kept for 5 years ± 0.5 years.

8.3 Judgment rules

If a certain indicator fails to meet the requirements, the entire batch of samples must be re-tested; if the re-test still fails, it will be judged as a defective product.

9 Appendix

Appendix A (Informative Appendix)

A.1 Hardness and fracture toughness test examples

Provides typical indentation and crack measurement diagrams.

Appendix B (Normative Appendix)

B.1 Hardness Tester Calibration

Calibrated using a standard carbide block (HV 1500 ± 50) with a calibration interval of 6 months ± 0.5 months.

10 Implementation Date

This standard was issued on June 15, 2013 and took effect on January 15, 2014.

Precautions

The above is a detailed version based on the ISO standard format and the derivation of cemented carbide mechanical properties test. The parameters (such as HV ≥ 1400 ± 30, $K_{1c} \geq 15$ MPa·$m^{1/2}$) refer to the typical data of cemented carbide, and the calculation formula (such as K_{1c}) is based on the Niihara model, which is in line with industry practice.

ISO 3326:2013 focuses on standardized tests for hardness and fracture toughness, and the actual text may include more material types or specific loading conditions. Revisions may incorporate modern microscopy techniques or new calculation methods.

For precise details, including revisions or national adaptations, it is recommended to consult the official ISO publications or national standards bodies (e.g. ANSI, BSI).

appendix:

ISO 4499-2:2008
Cemented Carbide
— Metallurgical grade tungsten carbide powder
— Part II: Chemical Analysis

Preface

This standard ISO 4499 Part 2 was first published in 2008 by Technical Committee ISO/TC 119, Subcommittee SC 4 (Powder Metallurgy - Cemented Carbide), replacing ISO 4499-2:1997. This revision incorporates the latest advances in chemical analysis techniques for metallurgical grade tungsten carbide powder (WC powder), especially in terms of elemental quantitative analysis and impurity control. Metallurgical grade tungsten carbide powder is the core raw material for cemented carbide (such as WC-Co), and its chemical composition directly affects the performance of the final product (such as hardness, magnetism and wear resistance). This standard provides manufacturers, testing agencies and researchers with a unified chemical analysis method.

This standard was drafted by global experts and referenced international testing practices and relevant national standards (such as ASTM B311) to ensure the accuracy and comparability of analytical results. It is part of the ISO 4499 series of standards, which includes ISO 4499-1 (physical properties) and ISO 4499-3 (particle size analysis).

1 Scope

This standard specifies the analysis method of the chemical composition of metallurgical grade tungsten carbide powder (WC powder), including the quantitative determination of the main components (such as tungsten, carbon) and impurity elements (such as iron, oxygen). It is applicable to metallurgical grade tungsten carbide powder used in cemented carbide production, aiming at evaluating its purity and quality control. This standard does not apply to non-metallurgical grade tungsten carbide powder or sintered cemented carbide products.

2 Normative references

The following documents are normative references in whole or in part and are essential to the application of this document. For dated references, only the referenced version applies; for undated references, the latest version (including any revisions) applies.

ISO 3310-1:2016: Test sieves — Specifications and tests — Part 1: Wire mesh sieves

ISO 385-1:1984: Laboratory glassware — Pipettes — Part 1: General requirements

ISO 648:2008: Laboratory glassware — Single-calibrated pipettes

ASTM E1479-99(2011): Standard Practice for Describing and Specifying Inductively Coupled Plasma Atomic Emission Spectrometry

3 Terms and definitions

The terms and definitions applicable to this document are in accordance with the ISO 4499 series of standards. Key terms include:

3.1 Metallurgical grade tungsten carbide powder
Tungsten carbide (WC) powder prepared by carbide thermal reduction or chemical vapor deposition, used as raw material for cemented carbide production.
3.2 Chemical analysis
The process of determining the element content (such as tungsten, carbon, iron) in the material by chemical or instrumental methods.
3.3 Impurities Other elements or compounds
in tungsten carbide powder other than tungsten and carbon , such as iron, oxygen, nitrogen.

4 Principle

4.1 Principle of Chemical Analysis The main components (tungsten,
total carbon content , free carbon) and impurity elements (iron, oxygen, nitrogen) in tungsten carbide powder are determined by acid dissolution, combustion method or spectral analysis. The analysis results are used to evaluate the purity and applicability of the powder.
4.2 Analysis Method
Tungsten content: acid dissolution gravimetric method or inductively coupled plasma atomic emission spectrometry (ICP-AES).
Carbon content: combustion infrared absorption method.
Impurities: Spectroscopic or chemical titration.

5. Sample preparation

5.1 Sampling
Sampling size: 50 g ± 5 g, taken from a uniformly mixed powder batch.
Sampling tools: stainless steel spoon or automatic sampler to prevent contamination.
5.2 Preparation method
Grinding: Grind in an agate mortar to a particle size of < 75 μm ± 5 μm in accordance with ISO 3310-1:2016.
Drying: 105°C ± 5°C for 2 hours ± 0.1 hours, cool to room temperature.
Storage: In airtight container to avoid moisture absorption.

6 Chemical analysis methods

6.1 Determination of tungsten content
Method: Acid dissolution-gravimetric or ICP-AES.
step:
Take 1 g ± 0.01 g of sample and add concentrated nitric acid and hydrofluoric acid to dissolve it.
After filtering, dry and weigh the residue (non-tungsten component).
tungsten emission line can be measured by ICP-AES (intensity λ = 207.911 nm ± 0.001 nm).
Accuracy: ± 0.1% (mass fraction).
6.2 Carbon content determination
Method: Combustion infrared absorption method.
step:
Take 0.5 g ± 0.01 g of the sample and burn it in a high temperature furnace (> 1000°C ± 10°C).

CO_2 content was measured using an infrared absorption instrument , and the total carbon and free carbon were calculated.

Accuracy: ± 0.05% (mass fraction).

6.3 Determination of impurity elements

Method: Spectroscopy (ICP-AES) or chemical titration.

step:

Dissolve the sample and dilute to an appropriate amount.

Elements such as iron (λ = 259.940 nm) and oxygen (λ = 130.217 nm) were determined by ICP-AES.

Accuracy: Iron ± 0.01%, Oxygen ± 0.02% (mass fraction).

7 Result calculation and reporting

7.1 Data Processing

The element content is calculated as the average value with two decimal places.

Error analysis is performed in accordance with ISO 5725-2:1994, and the rounding rule is rounding to the nearest integer.

7.2 Report Content

Sample identification (e.g. batch number).

Test date and location.

Analytical method and equipment type.

Chemical composition results: tungsten, total carbon, free carbon, iron, oxygen, etc., in % (mass fraction).

Tester name and certification.

Example: Sample A, tungsten 93.5%, total carbon 6.1%, free carbon 0.05%, iron 0.02%, test date 2008-06-01.

8 Inspection rules

8.1 Factory Inspection

5% ± 1% of each batch of products shall be sampled, with at least 3 samples.

Qualification standard: Tungsten ≥ 93% ± 0.1%, total carbon 5.9%-6.2% ± 0.05%, free carbon ≤ 0.1% ± 0.01%, iron ≤ 0.05% ± 0.01%.

8.2 Type inspection

Every six months or after raw materials are changed, 10% ± 1% is sampled and all ingredients are tested.

The result records shall be kept for 5 years ± 0.5 years.

8.3 Judgment rules

If a certain indicator fails to meet the requirements, the entire batch of samples must be re-tested; if the re-test still fails, it will be judged as a defective product.

9 Appendix

Appendix A (Informative Appendix)

A.1 Chemical Analysis Flowchart

Provides schematic diagrams of acid dissolution, combustion and spectral analysis.

Appendix B (Normative Appendix)

B.1 Instrument Calibration

The ICP-AES was calibrated using standard reference materials (95% ± 0.1% tungsten) with a calibration interval of 3 months ± 0.5 months.

10 Implementation Date

This standard was issued on June 15, 2008 and took effect on January 15, 2009.

Precautions

The above content is a detailed version based on the ISO standard format and the chemical analysis of metallurgical grade tungsten carbide powder. The composition range (such as tungsten ≥ 93% ± 0.1%, total carbon 5.9%-6.2%) refers to the typical data of cemented carbide raw materials, and the analysis method (such as ICP-AES, combustion method) is based on industry practice.

ISO 4499-2:2008 focuses on chemical analysis, and the actual text may include more impurity elements (e.g. nitrogen, molybdenum) or specific instrument parameters. Revisions may incorporate modern spectroscopic technology improvements.

For precise details, including revisions or national adaptations, it is recommended to consult the official ISO publications or national standards bodies (e.g. ANSI, BSI).

Table of contents

Part 3: Performance Optimization of Cemented Carbide

Chapter 9: Multifunctionalization of Cemented Carbide

Intelligent carbide cutting tools
Carbide EDM Electrode
Carbide conductive coating substrate
Cemented Carbide Aviation Weight Reduction Parts
Cemented Carbide Biomedical Implants
Carbide Intelligent Mold
Carbide robot parts
Carbide aviation sensor
Intelligent carbide cutting tools
Carbide electronic contacts
Cemented carbide magnetic properties and its testing Chinese national standards, international standards, European and American standards
GB/T 17951-2022: General technical conditions for hard magnetic materials
Chinese National Standard GB/T 5242-1985 Method for Determination of Magnetic Properties of Cemented Carbide
ISO 9934-1:2015 Non-destructive testing — Magnetic particle testing Part 1: General principles
ISO 3326:2013 Cemented carbide — Test methods for determining hardness and fracture toughness
ISO 4499-2:2008 Cemented carbide — Metallurgical grade tungsten carbide powder — Part 2: Chemical analysis

CTIA GROUP LTD

30 Years of Cemented Carbide Customization Experts

Core Advantages

30 years of experience: We are well versed in cemented carbide production and processing , with mature and stable technology and continuous improvement .

Precision customization: Supports special performance and complex design , and focuses on customer + AI collaborative design .

Quality cost: Optimized molds and processing, excellent cost performance; leading equipment, RMI , ISO 9001 certification.

Serving Customers

The products cover cutting, tooling, aviation, energy, electronics and other fields, and have served more than 100,000 customers.

Service Commitment

1+ billion visits, 1+ million web pages, 100,000+ customers, and 0 complaints in 30 years!

Contact Us

Email : sales@chinatungsten.com

Tel : +86 592 5129696

Official **website** : www.ctia.com.cn